Extraction of Lower Alcohols using Novel Hydrophobic Deep Eutectic Mixtures: Synthesis, Phase Equilibria Experiments and Process Economics

A

Thesis

Submitted in

Partial Fulfillment of the

Requirements for the Degree of

DOCTOR OF PHILOSOPHY

By

Rupesh Verma

Supervised By

Prof. Tamal Banerjee

Department of Chemical Engineering

Indian Institute of Technology Guwahati

Guwahati – 781039, India

June, 2018

Dedicated

To

My guide and My Parents for

Their support and Encouragement

Throughout My Research Work

CERTIFICATE

It is certified that the work presented in the thesis entitled **"Extraction of Lower Alcohols using Novel Hydrophobic Deep Eutectic Mixtures: Synthesis, Phase Equilibria Experiments and Process Economics"**, by **Rupesh Verma** (Roll No. 126107014), Department of Chemical Engineering, Indian Institute of Technology Guwahati, has been carried out under my supervision and this work has not been submitted elsewhere for any other degree.

Date: 22/6/18

Prof. Tamal Banerjee
Department of Chemical Engineering
Indian Institute of Technology Guwahati
Guwahati – 781039, Assam, India

ACKNOWLEDGEMENT

It is my great privilege to sincerely thank several people who have supported me to complete my Doctoral Dissertation. At the foremost, I would like to express my sincere gratitude to my research advisor **Prof. Tamal Banerjee** for his invaluable guidance throughout my research work. He will always be the source of positive energy that generated my keen interest in research. His positive attitude, smiling face and kind nature encouraged me to make research as my passion. His motivational and inspiring quotes improved my thinking ability, problem solving ability and technical writing skills. I got the opportunity to improve my research skills and personality under his leadership.

I would like to thank my Doctoral Committee members, **Prof. G. Pugazhenthi** and **Prof. V. V. Goud,** Department of Chemical Engineering and **Prof. Manas Das**, Department of Mechanical Engineering. Their valuable inputs and evaluation during my research progress kept the flow of research work in the right direction.

I am indebted to **Prof. Dipankar Bandyopadhyay** for their research oriented teaching during my research work. I also thank **Prof. Bishnupada Mandal**, Head, Department of Chemical Engineering, for his administrative support. Furthermore, I would like to thank other Faculty and Staff members of Department of Chemical Engineering for their valuable support during my research.

My sincere thanks to **Prof. José Palomar Herrero** (Universidad Autónoma De Madrid, Spain) and **Prof. Tamal Banerjee** along with MHRD and IIT Guwahati for conducting GIAN course entitled "Integration of Molecular Design to Process Simulation for the Development of Industrial Chemical Products and Processes". It helped me to understand the concepts of ASPEN and Quantum Chemistry in greater details.

I am grateful to Central Instrument Facility **(CIF)** and Analytical Lab Facility, Department of Chemical Engineering for providing me the necessary support for sample analysis using Nuclear Magnetic Resonance (NMR), Thermogravimetric Analysis (TGA), Interfacial Rheometer, Karl Fischer Titrator etc. I would like to thank **Prof. Vimal Katiyar** Centre of Excellence for Sustainable Polymers **(CoE-SUSPOL)**, IIT Guwahati for providing Differential Scanning Calorimetry (DSC) analysis.

Without the help of Dr. Anand Bharti, Mood Mohan, Dr. Dharamashibhai V. Rabari, Debashis Kundu, Pyarimohan Dehury and Papu Kumar Naik, it would not have been possible to do my research work in such a short time.

I also thank my research group members Dr. Sanjukta Bhoi, Basudhrity Banerjee, Upasana Mahanta, Reema Biswas, Dhirendra Mishra, Janardan Singh, Abhigyan Malviya, Nikhil Kumar and Naubendu Paul for providing a co-operative research environment.

My sincere thanks to my friends Mr. Jitendra Singh Rawat, Mr. Rahul Patwa, Mr. Sunny Kumar, Mr. M. K. Fahad, Mr. Rahul Ramteke, Mr. Kishant Kumar, Mr. Spatak Rarotra, Mr. Abhik Bhattacharjee, Mr. Ranjeet Kumar, Mr. Bhaskar, Jyoti Medhi, Mr. Badri Vishal, Mr. Shravan Kumar, Mr. Awadh Kishor and many more for making my stay at IIT Guwahati memorable.

My sincere gratitude to **Prof. Nishith Verma, Prof. Ashok Khanna, Prof. Deepak Kunzru** from IIT Kanpur, **Prof. Ram Prasad, Prof. Subhash Sharma, Prof. A. K. Mishra, Prof. O. P. Rama** (Late), H.B.T.I. Kanpur and many more. My whole hearted gratitude goes to my **Dear Mother (Late)**, **Dear Father**, brothers, sister, wife Medhavi and my sweet daughter whose blessings and boundless patience kept my morale high during the research.

Above all I am thankful to GOD for giving me a wonderful and healthy life.

(Rupesh Verma)

SYNOPSIS

1. Introduction

The demand for energy is increasing proportionally together with the current population. In such a scenario, energy generation is the key to sustain such a fast pace development. Currently fossil fuel replenish nearly 80% of the energy demand globally. Hence there is a dire need to explore alternate energy sources in order to lessen the dependency upon the non-renewable fossil fuel which are very limited to cater future needs [1-3]. Lower alcohols are considered as potential replacement for conventional fuels. Lower alcohols such as ethanol, propanol and butanol are vital and very likely be preferred as renewable energy sources. Table 1 explores this fact that 1-butanol has a higher calorific value, higher hydrophobicity and lesser flammability than other alcohol fuels [4]. Qureshi et al. [3] described that butanol with a lower vapor pressure and higher flash point is also less corrosive. Biobutanol like butanol has also shown promising properties similar to gasoline. Thus lower alcohol such as primarily 1-butanol can hence be used as a renewable bio-fuel with little or no modification to the engine. One of the source of butanol is the Acetone-Butanol-Ethanol (ABE) fermentation where alcohol such as butanol exists as an azeotrope with the water rich phase.

In the chemical process, industrial separation of azeotropic mixtures is of great importance. Methods such as extraction, adsorption, pervaporation, gas striping and membrane separation have been used conventionally for separation of lower alcohols from the fermentation broth. Membrane separation and pervaporation are expensive due to low mass transfer rates and requirement of low pressure [3, 5-7]. Typically, butanol removal from fermentation broth by adsorption from the liquid phase can only be used in laboratory scale due to the small-capacity of adsorbents. The other option of 1-butanol removal is to use methods such as membrane reactors where the immobilization of microorganisms occurs in the membrane. On industrial scale, cell immobilized technique gives more disadvantages due to poor mechanical strength and an increase in mass transfer resistance.

One normally switches to liquid-liquid extraction when component separation (from a mixture of many components) cannot be achieved economically by other mass transfer operations such as distillation, evaporation and crystallization. Azeotropic distillation, extractive distillation and liquid−liquid extraction, which are three of the most important

industrial separation techniques for azeotrope breaking, involve the use of an extracting agent. In such a scenario, solvent extraction is a suitable operation particularly when the solvents possess simultaneously high affinity for alcohol and low solubility with water. An important aspect with these hydrobhobic solvents is their lower density than water, making separation easier. This prompted researchers to use these conventional solvents such as mesitylene and oleyl alcohol for the extraction of 1-butanol in particular and generate the thermodynamic phase equilibria data. However the conventional solvents even effective have lower efficiency and have issues with reusability. Further these solvents are volatile, flammable, non-biodegradable and hazardous for health as well as for the environment. Thus the extraction of lower alcohols by alternative hydrophobic solvents has been proposed and explored in the present thesis.

In the literature, two approaches to separate alcohol-water azeotrope mixture with alternative green solvents such as Ionic Liquids are reported. They are namely (a) hydrophilic ILs and (b) hydrophobic ILs. Hydrophilic ILs works in instances where there is concentrated feed mixture of 1-butanol and water [7-10]. However in many situations, separation from dilute feed stream becomes challenging. Also due to its high cost and nature of toxicity, cheaper and sustainable solvents are now desired. It is in these context that the synthesis of low cost hydrobhobic solvent is desired. Deep Eutectic Solvents (DESs) were introduced as analogues and alternative green solvents to the conventional ILs, with the advantage of easy preparation with high purities and low cost. By definition, DESs result from the establishment of specific interactions, mainly hydrogen bonds, between two compounds namely a Hydrogen Bond Donor (HBD) and a Hydrogen Bond Acceptor (HBA). This renders a new chemical entity with a melting point lower than that of the initial compounds.

Most of the DESs proposed so far in the open literature have a hydrophilic character and thus are unstable in water, leading to the separation of both components. In such a scenario, the choice of HBA and HBD is crucial . With respect to the hydrophobicity of the DES, DL-menthol is chosen as the common HBA. This is then varied with increasing chain number of organic acids or HBD namely Decanoic acid, Lauric acid, Myristic Acid and Plamitic Acid [11-12] (Figure 1). It should be noted that their toxicity are yet too documented, hence at this point we shall merely refer them as second generation IL's [11, 12]. The entire thesis is summarized as given in Figure S-1.

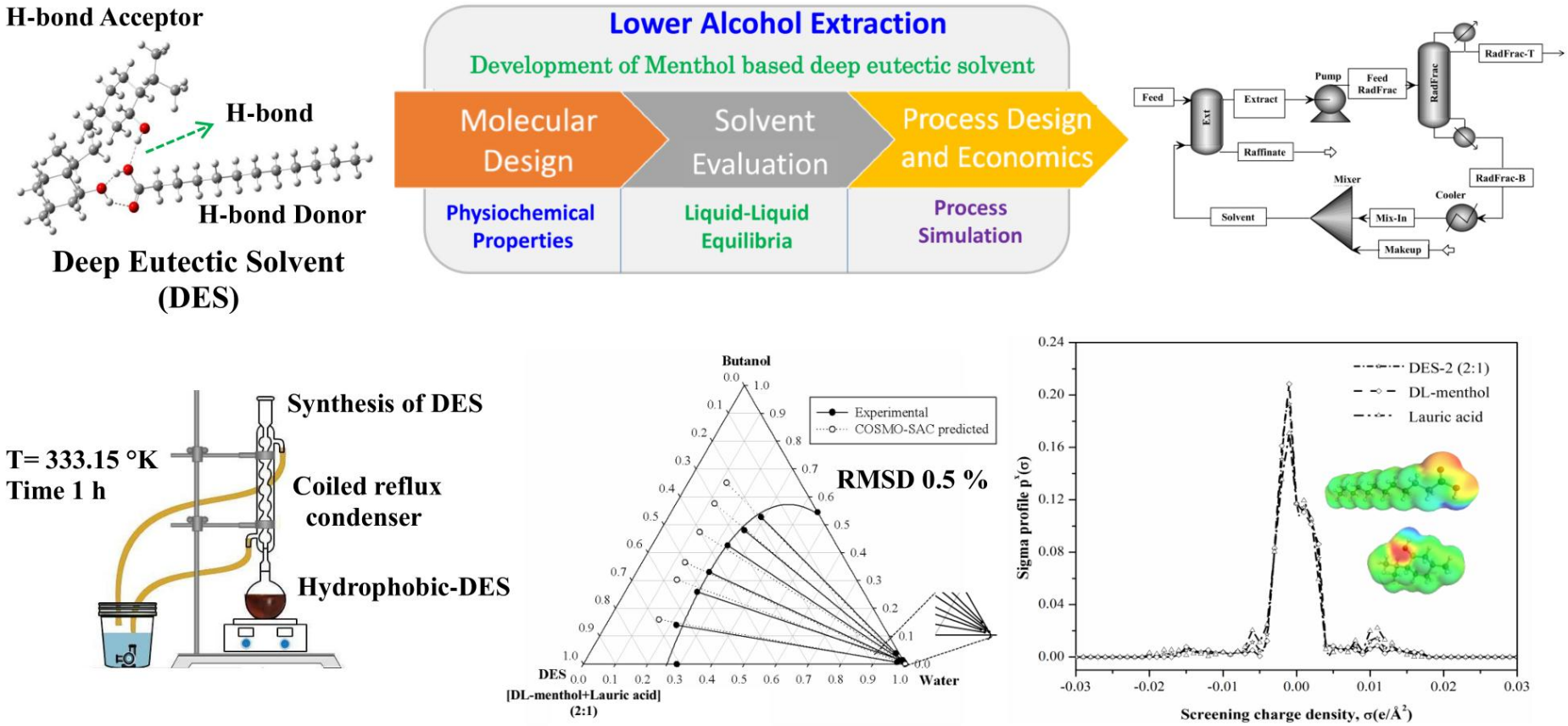

Figure S-1: Schematic of the Entire Thesis

The ensuing chapters within the thesis initially discusses the synthesis procedure and its physiochemical properties which includes thermal and water stability. Thereafter LLE measurement initially with conventional solvents (mesitylene and oleyl alcohol) and then later DES were performed. Here the feed points are chosen such that the concentrations of feed points are identical with ABE product concentration. The following sections summarizes the key objective of this thesis:

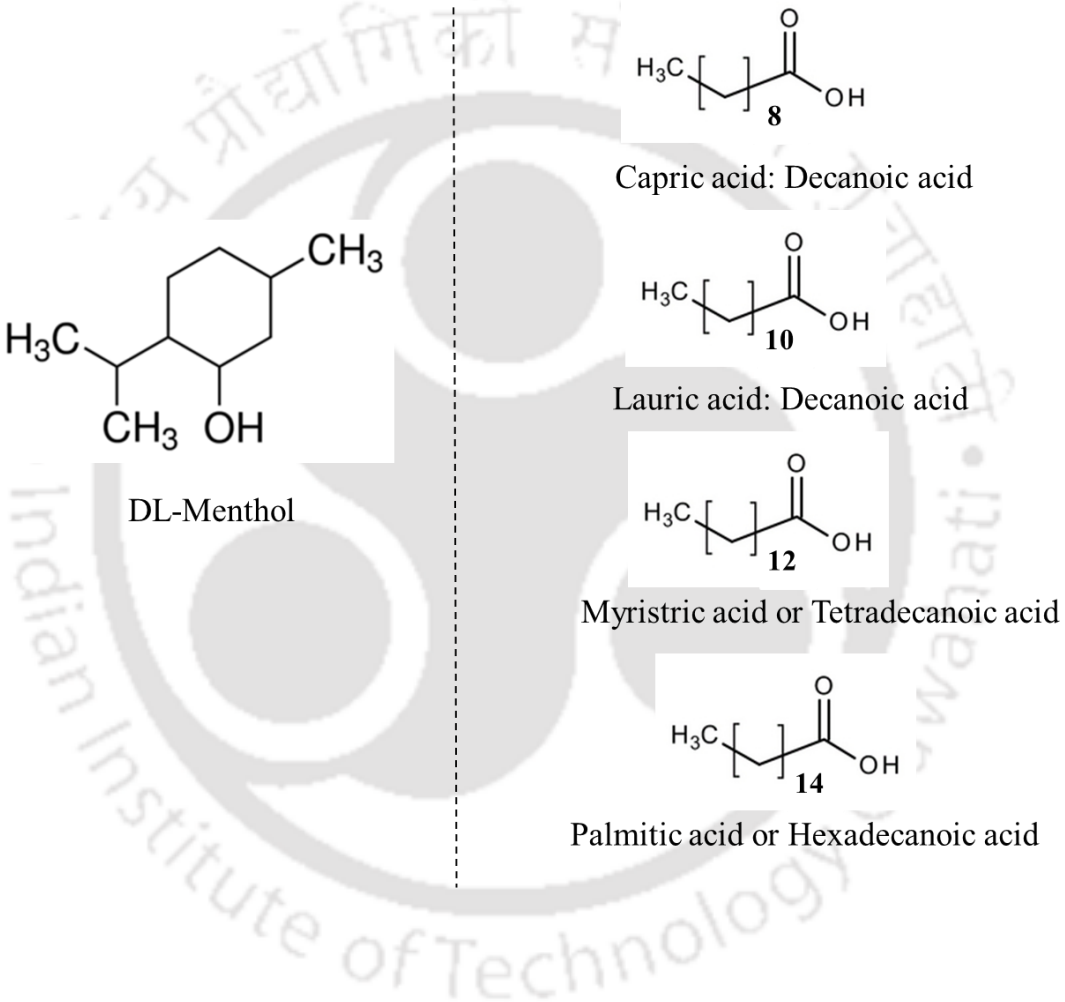

Figure 1: Structures of HBD (organic acids) and HBA (DL-menthol) used for DES synthesis

2. Evaluation of Mesitylene and Oleyl Alcohol as Conventional Solvents

Before proceeding for Deep Eutectic Solvents, the thesis first explores conventional solvents such as mesitylene and oleyl alcohol. The extraction of 1-butanol is reported from aqueous streams using low density solvents namely, mesitylene (ρ=0.864 gm/cm^3) and oleyl alcohol (ρ=0.849 gm/cm^3). The ternary Liquid-Liquid Equilibrium (LLE) studies for mesitylene (1) + 1-butanol (2) + water (3) and oleyl alcohol (1) + 1-butanol (2) + water (3)

were conducted to explain the effectiveness of the two solvents. A type-I phase behavior with a large immiscible region was observed at T = 298.15 K and p = 0.1 MPa. High values of selectivity ranging from 400-2500 for mesitylene and 750-6500 oleyl alcohol were observed. Distribution coefficient values higher than unity indicated an easier diffusion of 1-butanol from aqueous phase to extract phase. It also confirmed a lower solvent to feed ratio for separation of 1-butanol from water. ^{1}H NMR spectra indicated an aqueous rich phase free of solvent, while the contrary was observed in the solvent rich phase. Non-random two liquid (NRTL) and UNIversal QUAsichemical (UNIQUAC) models gave root mean square deviation (RMSD) in the range of 0.1-0.5% for both the systems. Further the predictions of the tie lines were also confirmed though the quantum chemical based COnductor like Screening MOdel Segment Activity Coefficients (COSMO-SAC) which gave RMSD in the range of 5%. Based on the selectivity values of 1-butanol at lower concentration, mesitylene was chosen as the recommended solvent for extraction. Thereafter a hybrid extraction process using Aspen Plus V8.8® was designed to carry out an optimized flowsheet concerning the recovery and recycle of 1-butanol and mesitylene respectively.

3. Synthesis of Menthol Based Deep Eutectic Solvents

The synthesis of hydrophobic DESs based on inorganic compound DL-Menthol and different organic acid (Figure 1) is reported [12-14]. As an example, one of the DES is synthesized by the addition of DL-menthol and Lauric acid (Dodecanoic Acid) with a molar ratios of 2:1 (Figure 2). In a similar manner, DL-menthol (HBA) and decanoic acid (HBA) are added in the molar ratio 1:1 for making decanoic acid based DES. Further DL-menthol (HBA) and Myristic acid (HBA) are added in the molar ratio 6:1 for making Myristic acid based DES. The chain length of the organic acid was further increased when DL-menthol (HBA) and Palmitic acid (HBA) are added in the molar ratio 12:1. Figure 3 shows the visual observation all the prepared DES along with the different molar ratio for synthesizing DES. In order to confirm the purity of the DES, the ^{1}H NMR spectra for all the DES was measured and validated to confirm the molar ratio of HBD to HBA. This further have ensured that the moiety indeed stays as a single component with a constant molar ratio. Physiochemical properties such as density, viscosity and thermo gravimetric (TG) studies were also made to evaluate the chemical and thermal stability.

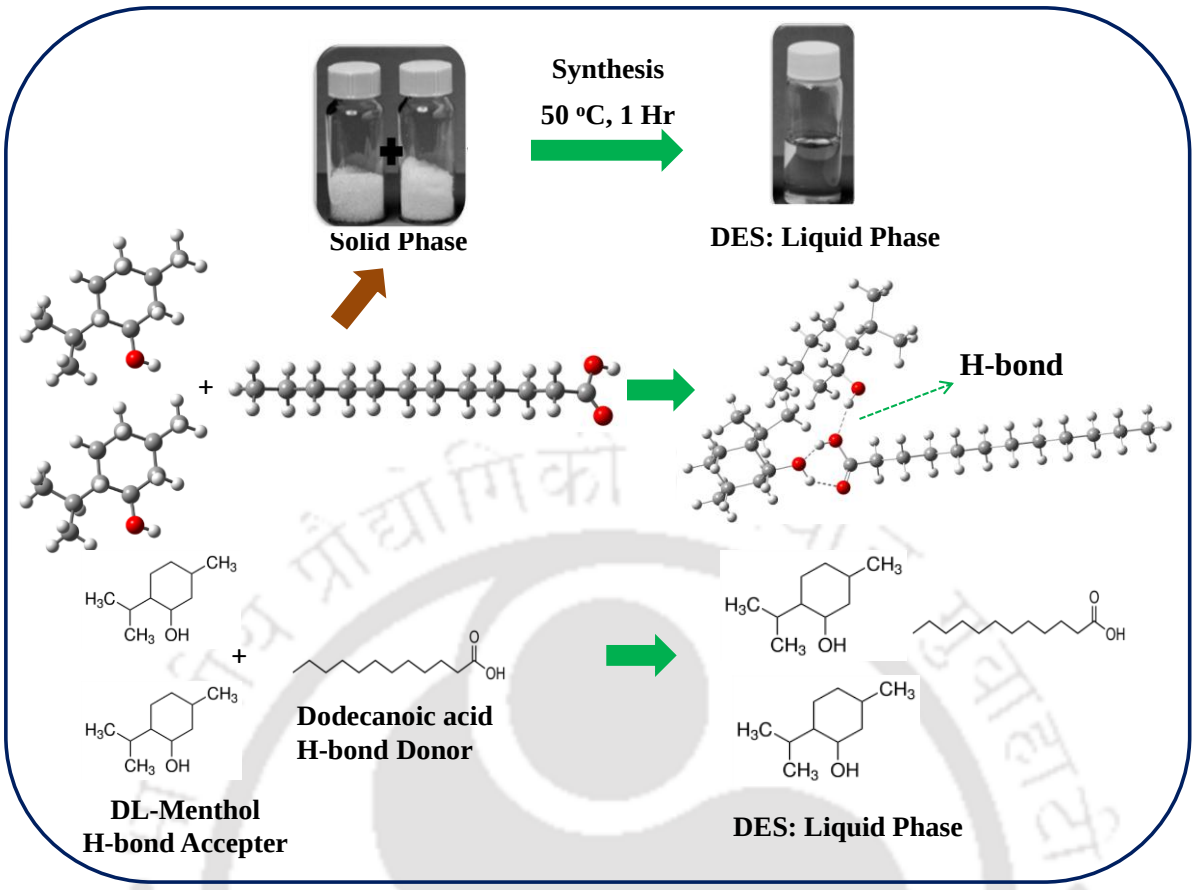

Figure 2: Deep Eutectic Solvent synthesis mechanism

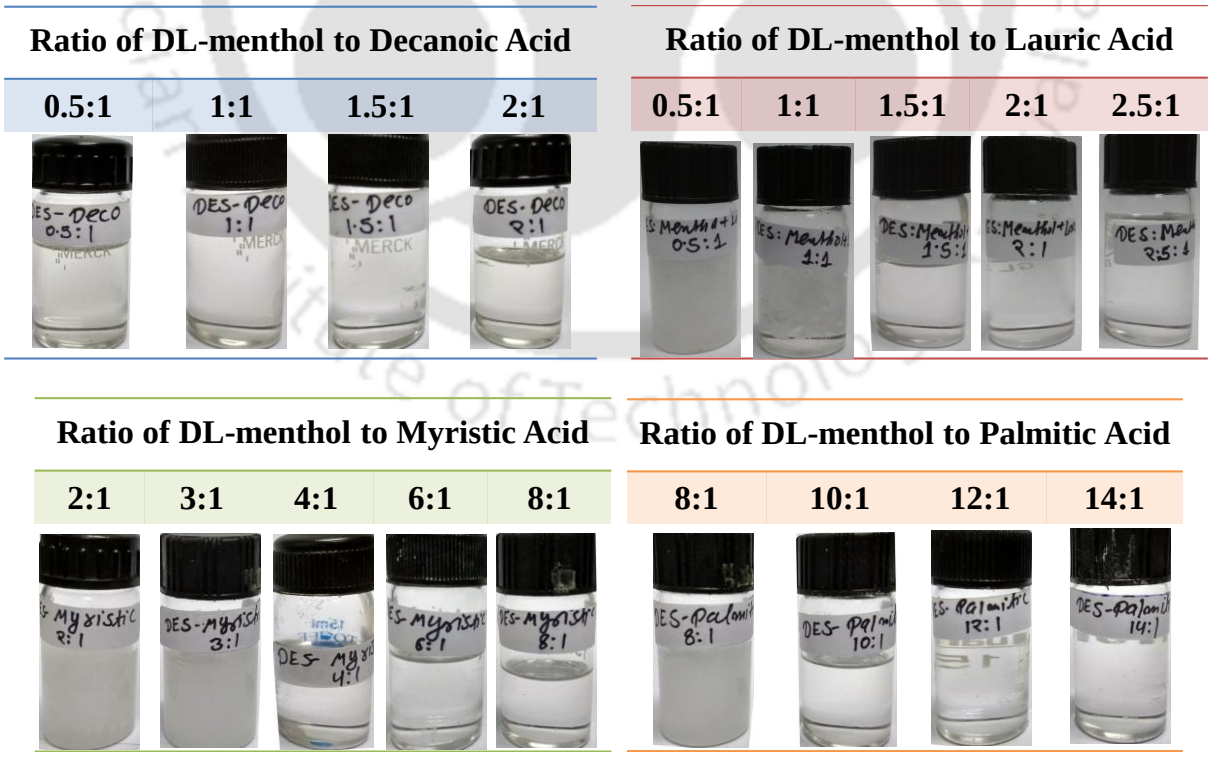

Figure 3: Formation of DES with different molar ratio of DL-menthol to Organic Acids (Decanoic/Lauric/Myristic/Palmitic).

All the DESs as synthesized have shown favorable solvation properties for both polar and nonpolar compounds [11, 15]. These are more stable at high temperature and/or in presence of chemicals and were found suitable for the extraction of inorganic and organic compounds [16-19].

4. Evaluation of Menthol based DES as Potential Solvents

After the successful synthesis, the current work then focusses on the synthesis and application of menthol (HBA) based hydrophobic deep eutectic solvent (DES) for the removal of lower alcohols from its aqueous solution. LLE (Liquid-Liquid Equilibria) experiments are then performed to evaluate the performance of the synthesized DES for the extraction of lower alcohols such as ethanol, 1-propanol and 1-butanol. LLE corresponding to the ternary systems of lower alcohols (1-butanol, Ethanol, Propanol) + hydrophobic DES + water are measured at T=298.15 K and p=1 bar [10]. The composition of the tie lines were evaluated using ^{1}H NMR analysis for both extract and raffinate phases. Thereafter the extraction efficiency of the DES is analyzed by determining the solute distribution coefficients and the selectivity values, and then comparing the same with existing solvents. Finally, the experimental LLE data for the systems were regressed using the excess Gibb's free energy thermodynamic model, Non Random Two Liquid (NRTL) model. Further the predictions of the tie lines were also confirmed though COnductor like Screening MOdel Segment Activity Coefficients (COSMO-SAC) model. The average root-mean-square deviations (RMSD) obtained were 1% and ~7% for NRTL and COSMO-SAC across all the systems.

5. Process Flow sheeting using ASPEN

The concluding section reports the scale up study that has been carried in ASPEN Plus. Here the hybrid Extraction-Distillation (Figure 4) process flow sheet for the comprehensive extraction of lower alcohols using both conventional solvent and DES were proposed [20-22]. In the hybrid extraction, extraction column operates at ambient temperature and pressure which implies that there is no requirement of additional energy. It hence provides significant savings in the operating cost as well as the total annual cost when compared to explicit extractive distillation. In the present case, feed is highly aqueous as butanol is less than 5 mole% (0.8 water and 0.2 butanol w/w). Extractive distillation will be not economical in these cases, as it will require a huge amount of steam to vaporize the water portion due to the fact that butanol has a higher boiling point. Hence hybrid

extraction−distillation system has been proposed in this work. In such a scenario, the entire water gets extracted from the raffinate phase of the extractor unit due to the LLE operation. This also reduces the energy consumption in the subsequent distillation column.An economic consideration with respect to Total Annual Cost (TAC) was also attempted and compared between the best DES and conventional solvent i.e. [DES: Menthol + Lauric Acid, Menthol + Decanoic Acid and Mesitylene] respectively. In our work the cost factor has been kept to a minimum by performing the simulation at 298.15 K and 1 atm pressure.

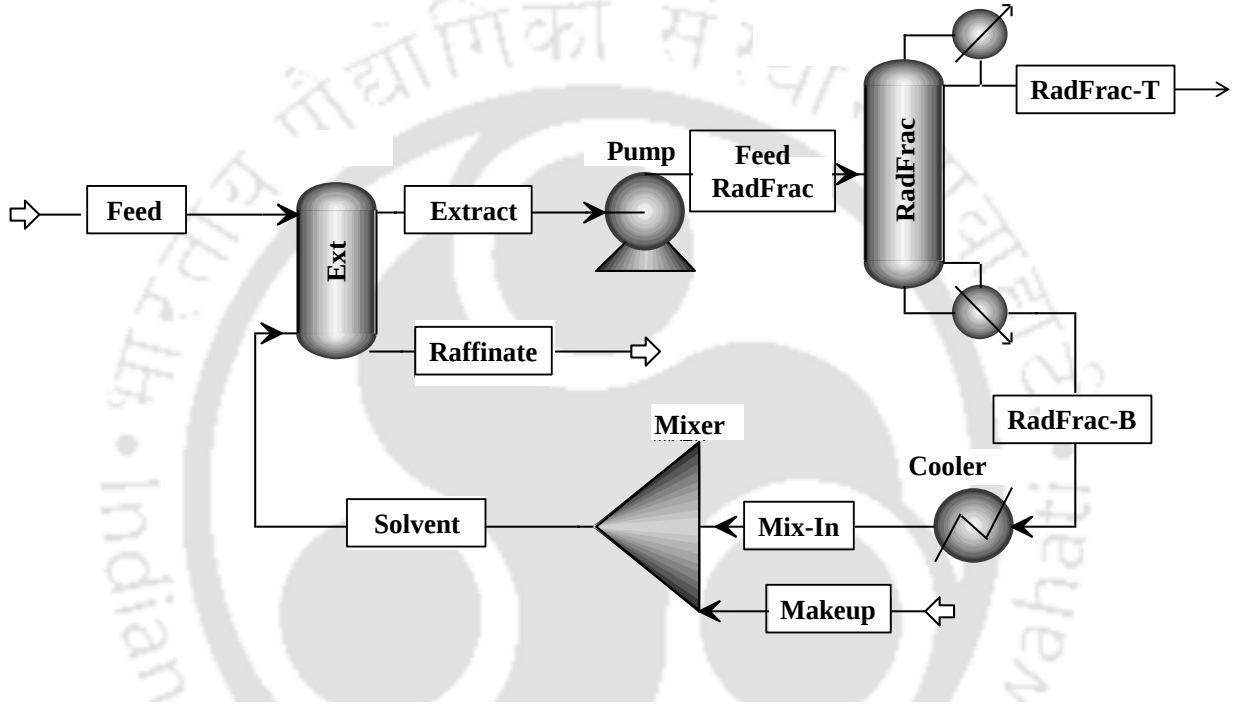

Figure 4: Hybrid Extraction-Distillation Process flow sheet for the separation of lower alcohols

A novel hybrid downstream process is hence proposed for the production of 1-butanol at the rate 5000 kg/hr (4.38×10^4 ton/yr). In the feed stream it is assumed that the feed is a mixture of 1-butanol and water has a flow rate 25000 kg/hr containing 0.2 w/w 1-butanol. NRTL thermodynamic model has been used for the simulation and the missing binary interaction parameters were regressed by UNIFAC or RPCES (Regression through Property Correlation and EStimation) model within ASPEN [20, 22].

In our work we have optimized the extractor (Ext) followed by the distillation column (RadFrac). Initially the sensitivity analysis was used in optimizing the extraction cost via optimization of number of stages in the extractor column [23] on the basis of f.o.b. purchase cost (Freight on board cost) using mesitylene/DES as solvent. Thereafter with optimized flowrate as in extractor, the optimization of the distillation column was performed

using two *DESIGN SPEC* namely: (a) fixing the mass fraction of 1-butanol in the distillate stream at 0.975; and (b) fixing the mass fraction of 1-butanol as 0.01 in the bottom stream. Thereafter the distillate rate followed by reflux ratio was varied as per established procedure. Taking into account the basis of economics and equipment sizing equations; the total annual cost, operating cost and capital cost have been calculated by varying the total number of stages in the distillation column.

References

1. W. Kaminski, E. Tomczak, A. Gorak: Biobutanol-production and purification methods. Atmosphere 2 (2011) 31-37
2. I.S. Maddox: The acetone-butanol-ethanol fermentation: recent progress in technology. Biotechnol. Genet. Eng. Rev. 7 (1989) 189-220
3. N. Qureshi, S. Liu, T. Ezeji: Cellulosic butanol production from agricultural biomass and residues: recent advances in technology, Advanced Biofuels and Bioproducts, Springer (2013)
4. X. Liu, H. Wang, Z. Zheng, J. Liu, R.D. Reitz, M. Yao: Development of a combined reduced primary reference fuel-alcohols (methanol/ethanol/propanols/butanols/n-pentanol) mechanism for engine applications. Energy 114 (2016) 542-558
5. W.J. Groot, H.S. Soedjak, P.B. Donck, R.G.J.M.V.d. Lans, K.C.A.M. Luyben, J.M.K. Timmer: Butanol recovery from fermentations by liquid-liquid extraction and membrane solvent extraction. Bioprocess Eng. 5 (1990) 203-216
6. S.H. Ha, N.L. Mai, Y.M. Koo: Butanol recovery from aqueous solution into ionic liquids by liquid–liquid extraction. Process Biochem. 45 (2010) 1899-1903
7. K. Kraemer, A. Harwardt, R. Bronneberg, W. Marquardt: Separation of butanol from acetone–butanol–ethanol fermentation by a hybrid extraction–distillation process. Comput. Chem. Eng. 35 (2011) 949-963
8. C.M. Neves, J.F. Granjo, M.G. Freire, A. Robertson, N.M. Oliveira, J.A. Coutinho: Separation of ethanol–water mixtures by liquid–liquid extraction using phosphonium-based ionic liquids. Green Chem. 13 (2011) 1517-1526
9. A. Pereiro, J. Araújo, J. Esperança, I. Marrucho, L. Rebelo: Ionic liquids in separations of azeotropic systems–A review. J. Chem. Thermodyn. 46 (2012) 2-28
10. A. Oudshoorn, L.A. van der Wielen, A.J. Straathof: Assessment of options for selective 1-butanol recovery from aqueous solution. Ind. Eng. Chem. Res. 48 (2009) 7325-7336

11. Q. Zhang, K.D.O. Vigier, S. Royer, F. Jérôme: Deep eutectic solvents: syntheses, properties and applications. Chem. Soc. Rev. 41 (2012) 7108-7146
12. C. Florindo, L. Branco, I. Marrucho: Development of hydrophobic deep eutectic solvents for extraction of pesticides from aqueous environments. Fluid Phase Equilib. 448 (2017) 135-142
13. B.D. Ribeiro, C. Florindo, L.C. Iff, M.A. Coelho, I.M. Marrucho: Menthol-based eutectic mixtures: hydrophobic low viscosity solvents. ACS Sustainable Chem. Eng. 3 (2015) 2469-2477
14. Y. Dai, J. van Spronsen, G.-J. Witkamp, R. Verpoorte, Y.H. Choi: Natural deep eutectic solvents as new potential media for green technology. Anal. Chim. Acta 766 (2013) 61-68
15. E.L. Smith, A.P. Abbott, K.S. Ryder: Deep eutectic solvents (DESs) and their applications. Chem. Rev. 114 (2014) 11060-11082
16. J.L. Anderson, D.W. Armstrong: Immobilized ionic liquids as high-selectivity/high-temperature/high-stability gas chromatography stationary phases. Anal. Chem. 77 (2005) 6453-6462
17. D. Rabari, N. Patel, M. Joshipura, T. Banerjee: Densities of six commercial ionic liquids: experiments and prediction using a cohesion based cubic equation of state. J. Chem. Eng. Data 59 (2014) 571-578
18. C.F. Poole, S.K. Poole: Extraction of organic compounds with room temperature ionic liquids. J. Chromatogr. A 1217 (2010) 2268-2286
19. C.P. Fredlake, J.M. Crosthwaite, D.G. Hert, S.N. Aki, J.F. Brennecke: Thermophysical properties of imidazolium-based ionic liquids. J. Chem. Eng. Data 49 (2004) 954-964
20. Y.C. Chen, K.L. Li, C.L. Chen, I.L. Chien: Design and Control of a Hybrid Extraction–Distillation System for the Separation of Pyridine and Water. Ind. Eng. Chem. Res. 54 (2015) 7715-7727
21. W.L. Luyben: Distillation design and control using Aspen simulation, John Wiley & Sons (2013)
22. K.I. Al-Malah: Aspen Plus: Chemical Engineering Applications, John Wiley & Sons (2016)
23. W.D. Seider, J. Seader, D.R. Lewin, S. Widagdo: Product and Process Design Principles: Synthesis, Analysis and Evaluation, Wiley (2010)

TABLE OF CONTENTS

Table of Contents

LIST OF FIGURES

LIST OF TABLES

Chapter 1

Introduction and Motivation

1.1. Introduction

The demand for energy is increasing proportionally with the current population. In such a scenario, energy generation is the key to sustain such a fast pace development. Currently fossil fuels replenish nearly 80% of the energy demand globally. Hence there is a dire need to explore alternate energy sources in order to lessen the dependency upon the non-renewable fossil fuels which are very limited to cater future needs [1-4]. Among them lower alcohols are considered as potential replacement for conventional fuels. Lower alcohols such as ethanol, propanol and 1-butanol are vital and are likely preferred as renewable energy sources. For e.g. 1-butanol has a higher calorific value, higher hydrophobicity and lesser flammability than other alcohol fuels [5]. Qureshi et al. [4, 6] described that 1-butanol with a lower vapor pressure and higher flash point is also less corrosive. Lower alcohols have also shown properties similar to gasoline. This implies that they can be used as a renewable bio-fuel with little or no modification to the engine. Table 1.1 shows the calorific values of lower alcohols compare to the gasoline and diesel. It has been observed lower alcohols have good calorific value, higher hydrophobicity and lesser flammability and can be used as an alternate source of energy [2, 7].

One of the sources of the lower alcohol i.e. primarily 1-butanol is the Acetone-Butanol-Ethanol (ABE) fermentation where alcohol such as 1-butanol exists as an azeotrope with the water rich phase. Hence its extraction from aqueous phase is essential. As a fuel, lower alcohols have shown promising properties which is similar on the line of gasoline [4, 8]. Available literature shows that alcohols have been conventionally used as blending components with gasoline. It should be noted that with increasing chain length of alcohols, the volatility, polarity and octane rating increases, while on the other hand it lessens the

corrosivene index. Thus it can be used as a substitute for gasoline without having to replace the existing technology [8, 9]. Higher heat of vaporization of these alcohols are another feature that facilitates the engine to start in cold weather. Therefore in the current work, the research work focuses on the enhancement of lower alcohols such as ethanol, butanol and propanol from its aqueous mixtures.

Table 1.1: A Comparison of Energy Content

Fuel name	Calorific value (Btu/gal)
Gasoline	114,800
Diesel	140,000
Menthol	55,600
Ethanol	76,100
Butanol	110,000

1.2. Separation of Lower Alcohols

In the chemical process, industrial separation of azeotropic mixtures is of great importance. Methods such as extraction, adsorption, pervaporation, gas striping and membrane separation have been used conventionally for separation of lower alcohols from the fermentation broth. Membrane separation and pervaporation are expensive due to low mass transfer rates and requirement of low pressure [1, 10-13].Typically, removal of lower alcohols from fermentation broth by adsorption from the liquid phase can only be used in laboratory scale due to the small-capacity of adsorbents [14]. The other option for removal of lower alcohols can be used such as membrane reactors where the immobilization of microorganisms occurs in the membrane. On industrial scale, cell immobilized technique gives more disadvantages due to poor mechanical strength and an increase in mass transfer resistance [2].

One normally switches to liquid-liquid extraction when component separation (from a mixture of many components) cannot be achieved economically by other mass transfer operations such as distillation, evaporation and crystallization. Azeotropic distillation, extractive distillation and liquid−liquid extraction, which are three of the most important industrial separation techniques for azeotrope breaking, involves the use of an extracting agent. In such a scenario, solvent extraction is a suitable operation particularly when the solvents possess simultaneously high affinity for alcohol and low solubility with water. An important aspect with these hydrobhobic solvents is its comparable density difference when compared to water, making separation easier. Further solvent extraction is a suitable operation particularly when the solvents possess simultaneously high affinity for butanol and low solubility with water .This prompted researchers to use different solvents such as organic and green hydrobhobic solvents, [2, 15, 16] for the extraction of lower alcohols.

From past literature, hydrobhopic Ionic Liquids (IL's) have been known to be perform better for the extraction of lower alcohols [17, 18]. On the other hand, hydrophilic ILs works in instances where there is a concentrated feed mixture of 1-butanol and water [10, 19-21]. However in many situations, separation from dilute feed stream becomes challenging. It is in these context that the synthesis of low cost hydrobhobic solvent is desired. Due to the high cost and nature of toxicity, cheaper and sustainable solvents are now been explored. At present there are two commercial bio-butanol plants operational: one in China while other bio-butanol plant is operational in Brazil.

1.3. Deep Eutectic Solvents (DESs)

Other than Ionic Liquids and conventional solvents, not much literature has been cited with respect to the newly developed novel green solvents namely Deep Eutectic Solvents (DESs) which are currently known to cheaper, sustainable and also easy to synthesis. DES

were introduced as analogues and alternative green solvents to the conventional ILs, with the advantage of easy preparation with high purities and low cost. Figure 1.1 shows the different properties of DES as green solvent. Examples of applications of DESs include such as solvents for green processing, purification processes, heat transfer fluids and storage media [22, 23]. Due to the interesting properties of DES, primarily their low ecological foot print and their attractive price, research on these solvents has been exponentially growing in the last few years [24-26]. The present thesis thereby attempted to adopt these solvents for the extraction of lower alcohols. Figure 1.2 shows that DES can be widely used for various applications in diverse areas [27].

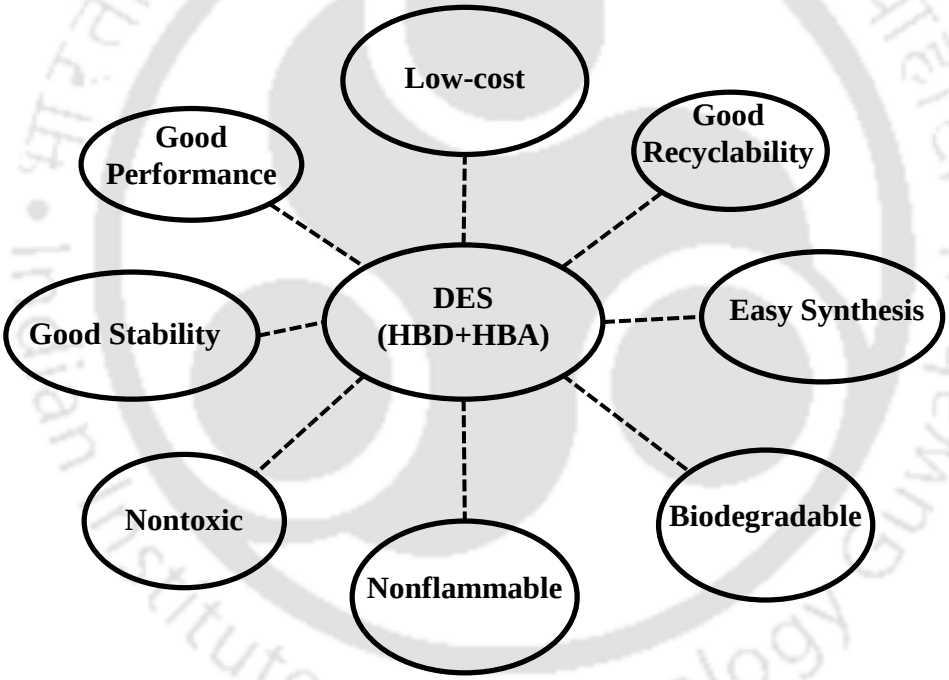

Figure 1.1: Physicochemical properties of Deep Eutectic Solvents (DESs) as green solvent (HBD: Hydrogen Bond Donor, HBA: Hydrogen Bond Acceptor)

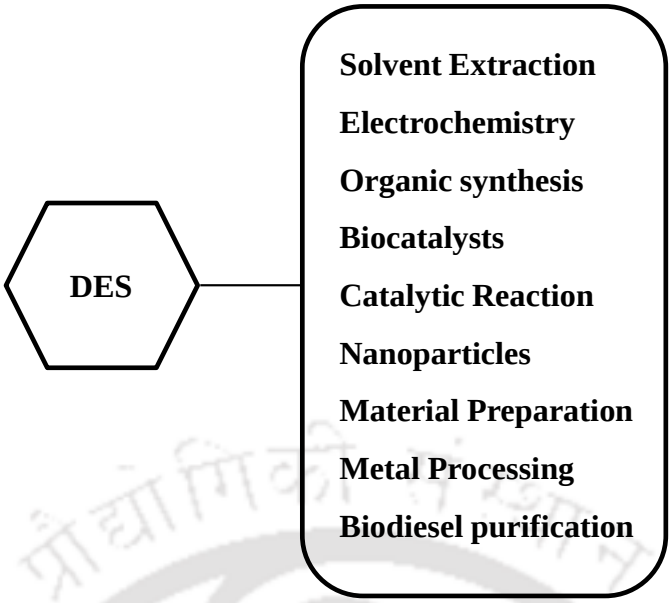

Figure 1.2: Applications of Deep Eutectic Solvents (DESs)

By definition, DESs result from the establishment of specific interactions, mainly hydrogen bonds, between two compounds namely a Hydrogen Bond Donor (HBD) and a Hydrogen Bond Acceptor (HBA). This renders a new chemical entity with a melting point lower than that of the initial compounds. Most of the DESs proposed so far in the open literature have a hydrophilic character and thus are unstable in water, leading to the separation of both components. In such a scenario, the choice of HBA and HBD is crucial [28-31]. It should be noted that their toxicity are yet to be too documented, hence at this point we shall merely refer them as a potential substitute for IL's [25, 27] .

Figure 1.3 shows the schematic for the synthesis of DES. It clearly shows that DES is mixture of two compounds in a certain molar ratio such that it remains in liquid phase at ambient temperature [22, 32]. Eutectic point occurs where the freezing point is found to be minimum. The reason behind the significant depression of freezing point is because of the hydrogen bond formation and the lowering of the Gibb's Free Energy between the two compounds A and B [32, 33]. In the present study, which is also detailed in chapter 2, DL-menthol (compound A) is the inorganic salt and is used as a Hydrogen Bond Acceptor

(HBA). On the other hand organic acids compounds (B) such as Decanoic, Lauric, Myristic and Palmitic acids are used as H-bond donor (HBDs) [22, 34].

In brief, Figure 1.4 shows the synthesis of a menthol-based hydrophobic deep eutectic solvent (DES) for the removal of lower alcohols from its aqueous solutions. The DES is synthesized by the addition of the Hydrogen bond acceptor (HBA: DL-menthol) combined with hydrogen bond donor [HBD: organic acid (Lauric acid)] with a molar ratio of 2:1 [34]. Once the choice of DES or the combination of HBA and HBD is made, we then initiate its effectiveness by measuring the Liquid−Liquid Equilibria experiments for the separation of lower alcohol (ethanol, propanol and butanol) and water. The LLE measurements have been described in chapter 3.

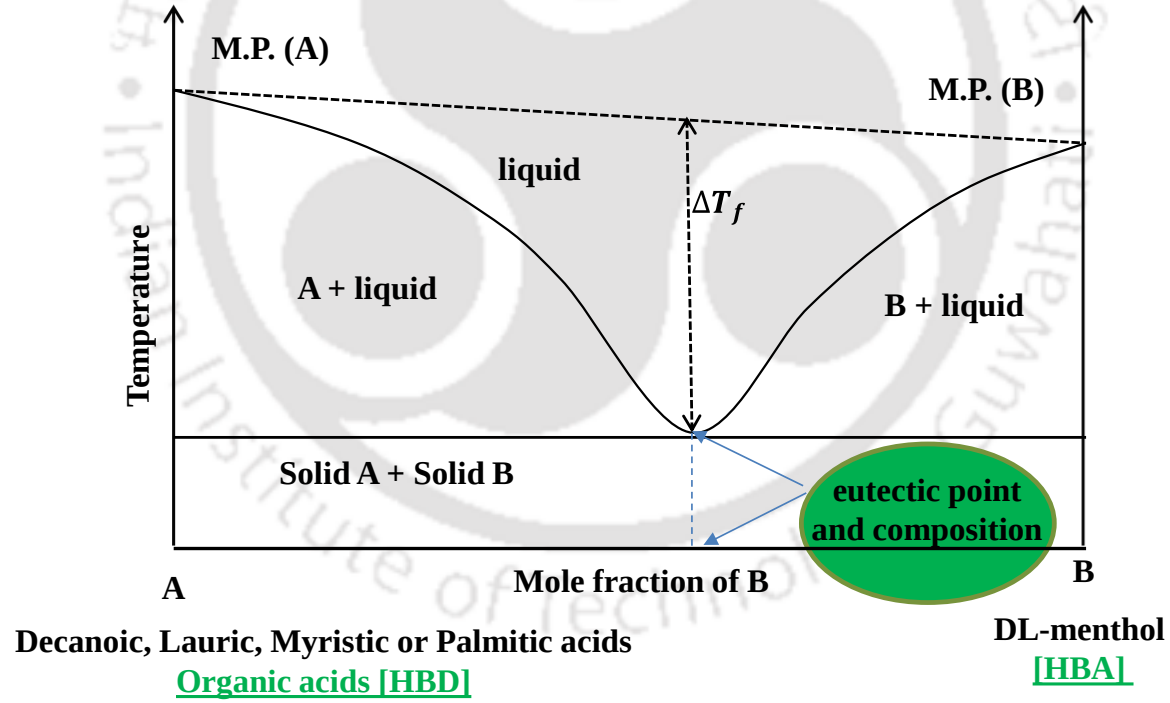

Figure 1.3: Schematic for the eutectic point representation on a two component phase diagram (MP: Melting Point)

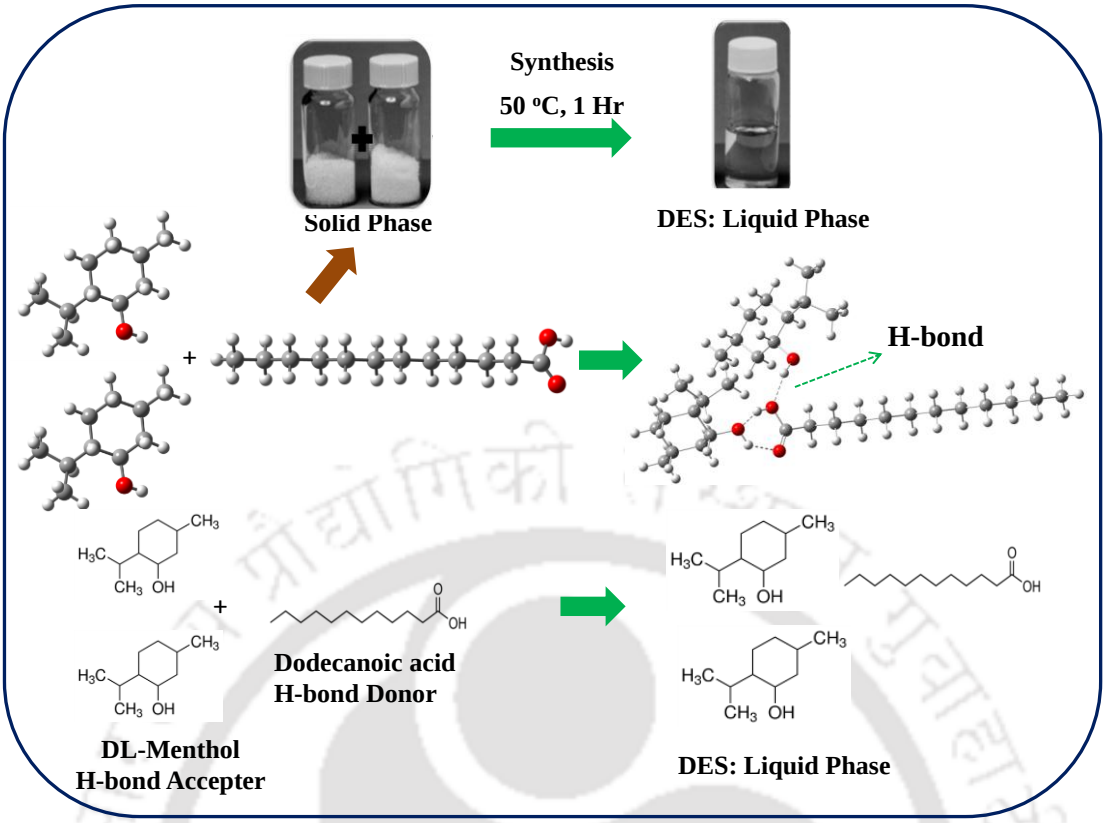

Figure 1.4: Typical structures of the DL-Menthol and Dodecanoic acid used for syntheses

1.4. Scale-up using Hybrid Extraction–Distillation

Once the Liquid−Liquid Equilbria results are available, a need of scale-up for the separation of lower alcohols needs to be adopted. Commercial software such as ASPEN Plus V8.8. helps us in understanding the process economics of separation of lower alcohols for the optimal design. Figure 1.5 shows the Hybrid Extraction-Distillation Process flow sheet for one such separation of lower alcohols from aqueous mixture. This is inline with an earlier work [35] where the hybrid separation processes is found to be an effective tool for reducing the energy intensive step of distillation. Hybrid separation processes can be effective for reducing the demand of energy [35], as previous authors [19, 36] have concluded that the solvent mesitylene can be used efficiently for the separation of 1-butanol from ABE fermentation products. This further needs to be compared with a conventional solvent [19].

ASPEN Plus V8.8® professional simulator (Bedford, Massachusetts) has been used for optimizing the whole flow sheet (Figure 1.5). Feed stream (FEED) is assumed as a mixture of 1-butanol and water. Initially this has been used on traditional solvent such as mesitylene. Thereafter excess Gibb's Free Energy such as NRTL has been used for the simulation and regression of missing binary interaction parameters through UNIFAC model or R_PCES (Regression Property Correlation and EStimation) [37, 38]. In brief, the overall flow sheet consists of a liquid–liquid extractor (Extractor, EXT-COL) and a component separator (Distillation, DST-COL). A total condenser has been used in the distillation column. The distillate, DIST from the distillation column contains higher proportion of butanol and solvent. Hence as solvent is lost here, some makeup solvent (MAKE-UP) is added in the mixture for recycle. This is added to the bottom (BOT) stream which is cooled from the distillation column and added with the makeup solvent. Thereafter the entire solvent is again fed back to the extractor (EXT-COL).

The operating conditions for the process design should be selected in order to lessen cost while respecting the requirement of an elevated purity of the raffinate (RAFFINATE) and an increasing yield for the alcohol in the extract phase (EXTRACT). All the flowsheets have been described and explained in chapter 4.

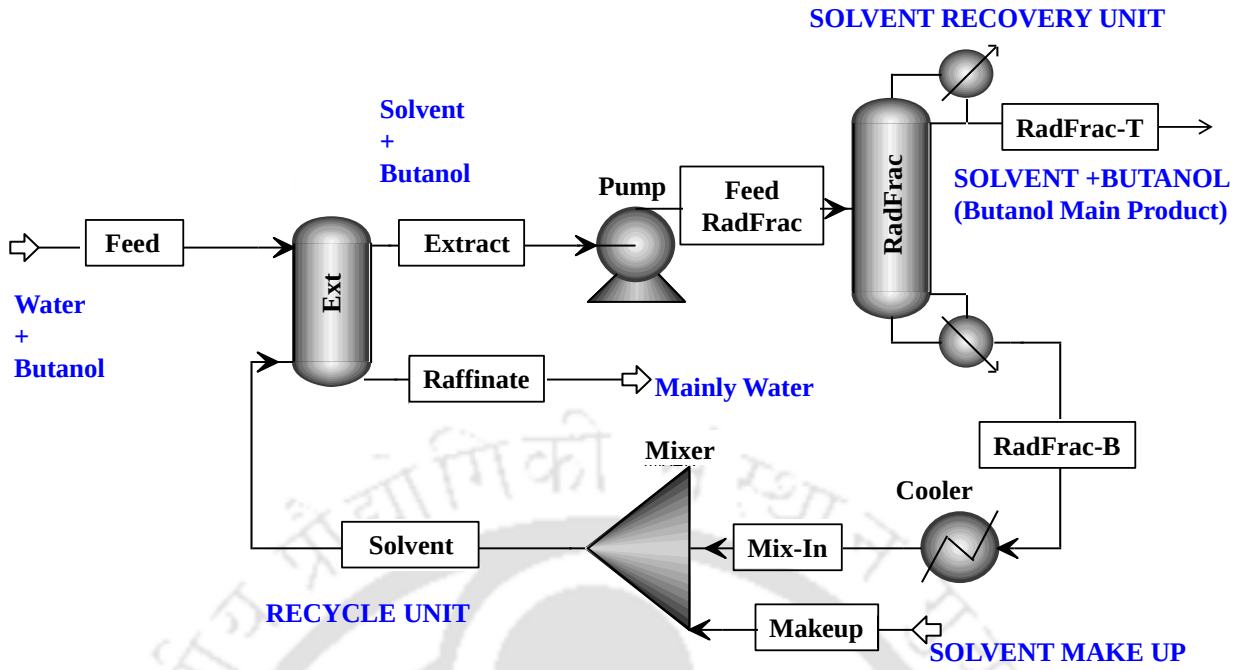

Figure 1.5: Hybrid Extraction-Distillation Process flow sheet for the separation of lower alcohols from aqueous mixture

1.5. Thesis Objectives

Following are the key objectives in the current thesis:

(a) Synthesis and Characterization of novel DES using DL-menthol as Hydrogen Bond Acceptor (HBA) and Organic acids such as Capric, Lauric, Myristic and Palmitic acids as Hydrogen Bond Donor (HBD)

(b) Measurement and validation of Liquid−Liquid Equilibria (LLE) with conventional solvents such as mesitylene and oleyl alcohol and compare their efficiency with the synthesized hydrophobic DESs as per (a).

(c) Initiate a Hybrid Extraction-Distillation Process Flow sheet for the Comprehensive Extraction of Lower alcohols from aqueous phase in ASPEN Plus using a combination of Extractor, Distillation Column and a Solvent Recovery Unit.

1.6. Structure of the thesis

This thesis initially describes the investigation of conventional solvents and also reports the synthesis of new class of solvents namely DESs. Thereafter it reports the ternary LLE of DES (1) + Alcohol (2) + Water (3) systems. Finally a hybrid Extraction-Distillation via ASPEN Plus is proposed for the scale up of such solvents. The entire thesis is divided into following chapters as follows:

Chapter 2 reports the synthesis of hydrophobic DESs based on organic salt such as DL-Menthol and organic acids with increasing chain length. This also includes the measurements of physical properties such as density and viscosity. Further the hydrophobicity of DES is also confirmed with deionized water.

Chapter 3 describes and compares the LLE performance using both conventional solvents (mesitylene, oleyl alcohol) and hydrophobic DESs based on DL-Menthol. Here the feed mixture is taken as mixture of lower alcohols (ethanol, propanol and butanol) and water. In these experiments the DES were prepared by mixing DL-menthol with each of the organic acid. The organic acids with increasing chain length namely, lauric acid, decanoic acid, palmitic acid and myristic acid were used in this thesis. Here the feed points are chosen such that the concentrations of feed points are identical with ABE product concentration. Liquid−Liquid Equilibrium data for the ternary systems contain, solvent (Mesitylene/oleyl alcohol/DESs) (1) + water (2) + lower alcohols (ethanol/propanol/butanol) (3) are measured and reported by ternary tie line plots. The experimental equilibrium data was correlated with the Gibb's Free energy models such as Non-Random Two-Liquid (NRTL) and UNIversal QUAsi Chemical (UNIQUAC). Further the quantum chemical based COSMO-SAC model was also adopted to predict the extract (DES rich phase) and raffinate (Water rich phase) composition. The regressed binary interaction parameters generated in the modeling was then used in the process optimization flowsheet such as ASPEN in the next chapter. Thus an

attempt was made in this chapter to transform laboratory data into process design at industrial scale.

Chapter 4 reports the scale up study that has been carried out using commercial software, ASPEN Plus V8.8, Here the hybrid Extraction-Distillation Process Flow sheet for the comprehensive extraction of lower alcohols using both conventional solvent and DESs were proposed. This consists of an extractor column and a distillation column for the solvent recovery analysis. It gives information regarding temperature, pressure and composition of the mixtures with respect to both VLE and LLE. An economic consideration with respect to Total Annual Cost (TAC) was also attempted and compared between the best DES and conventional solvent i.e. [DES: DL-menthol + Organic acid] and Mesitylene respectively.

Chapter 5 concludes the discussion on these novel hydrobhopic solvents and initiates the way forward which includes future corrections.

References

1. J. Marszałek, W. Kamiński: Concentration of butanol-ethanol-acetone-water using pervaporation. Proc. ECOpole 6 (2012) 31-36
2. W. Kaminski, E. Tomczak, A. Gorak: Biobutanol-production and purification methods. Atmosphere 2 (2011) 31-37
3. I.S. Maddox: The acetone-butanol-ethanol fermentation: recent progress in technology. Biotechnol. Genet. Eng. Rev. 7 (1989) 189-220
4. N. Qureshi, S. Liu, T. Ezeji: Cellulosic butanol production from agricultural biomass and residues: recent advances in technology, Advanced Biofuels and Bioproducts, Springer (2013)
5. X. Liu, H. Wang, Z. Zheng, J. Liu, R.D. Reitz, M. Yao: Development of a combined reduced primary reference fuel-alcohols (methanol/ethanol/propanols/butanols/n-pentanol) mechanism for engine applications. Energy 114 (2016) 542-558
6. N. Qureshi, I.S. Maddox, A. Friedl: Application of continuous substrate feeding to the ABE fermentation: relief of product inhibition using extraction, perstraction, stripping, and pervaporation. Biotechnol. Prog. 8 (1992) 382-390

7. D. Rabari, T. Banerjee: Biobutanol and n-propanol recovery using a low density phosphonium based ionic liquid at T= 298.15 K and p= 1atm. Fluid Phase Equilib. 355 (2013) 26-33
8. D. Antoni, V.V. Zverlov, W.H. Schwarz: Biofuels from microbes. Appl. Microbiol. Biotechnol. 77 (2007) 23-35
9. W.M. Haynes: CRC handbook of chemistry and physics, CRC press (2014)
10. A. Chapeaux, L.D. Simoni, T.S. Ronan, M.A. Stadtherr, J.F. Brennecke: Extraction of alcohols from water with 1-hexyl-3-methylimidazolium bis (trifluoromethylsulfonyl) imide. Green Chem. 10 (2008) 1301-1306
11. L.Y.G. Chavez, C.M. Garsia, B. Schuur, A.B.D. Haan: Biobutanol recovery using nonfluorinated task-specific ionic liquids. Ind. Eng. Chem. Res. 51 (2012) 8293-8301
12. A. Pereiro, J. Araújo, J. Esperança, I. Marrucho, L. Rebelo: Ionic liquids in separations of azeotropic systems–A review. J. Chem. Thermodyn. 46 (2012) 2-28
13. F.M.F. Vallana, L.A. Holland, K.R. Seddon: A New Technique for Studying Vapour–liquid Equilibria of Multi-Component Systems. Aust. J. Chem. 69 (2016) 1240-1246
14. K. Bhola, J.J. Varghese, L. Dapeng, Y. Liu, S.H. Mushrif: Influence of Hubbard U Parameter in Simulating Adsorption and Reactivity on CuO: Combined Theoretical and Experimental Study. J. Phys. Chem. C 121 (2017) 21343-21353
15. A.P. Abbott, G. Capper, D.L. Davies, R.K. Rasheed, V. Tambyrajah: Novel solvent properties of choline chloride/urea mixtures. Chem. Comm. (2003) 70-71
16. E.L. Smith, A.P. Abbott, K.S. Ryder: Deep eutectic solvents (DESs) and their applications. Chem. Rev. 114 (2014) 11060-11082
17. D. Rabari, T. Banerjee: Experimental and theoretical studies on the effectiveness of phosphonium-based ionic liquids for butanol removal at T= 298.15 K and p= 1 atm. Ind. Eng. Chem. Res. 53 (2014) 18935-18942
18. D.V. Rabari: Experimental, Modelling and Optimization Insights for the Enhancement of Butanol Production using Phosphonium based Ionic Liquids, Ph. D. Thesis, I.I.T., Guwahati, (2015)
19. K. Kraemer, A. Harwardt, R. Bronneberg, W. Marquardt: Separation of butanol from acetone–butanol–ethanol fermentation by a hybrid extraction–distillation process. Comput. Chem. Eng. 35 (2011) 949-963
20. C.M. Neves, J.F. Granjo, M.G. Freire, A. Robertson, N.M. Oliveira, J.A. Coutinho: Separation of ethanol–water mixtures by liquid–liquid extraction using phosphonium-based ionic liquids. Green Chem. 13 (2011) 1517-1526

21. L.Y. Garcia-Chavez, C.M. Garsia, B. Schuur, A.B. de Haan: Biobutanol recovery using nonfluorinated task-specific ionic liquids. Ind. Eng. Chem. Res. 51 (2012) 8293-8301
22. B.D. Ribeiro, C. Florindo, L.C. Iff, M.A. Coelho, I.M. Marrucho: Menthol-based eutectic mixtures: hydrophobic low viscosity solvents. ACS Sustainable Chem. Eng. 3 (2015) 2469-2477
23. Y. Dai, J. van Spronsen, G.-J. Witkamp, R. Verpoorte, Y.H. Choi: Natural deep eutectic solvents as new potential media for green technology. Anal. Chim. Acta 766 (2013) 61-68
24. Q. Zhang, K.D.O. Vigier, S. Royer, F. Jérôme: Deep eutectic solvents: syntheses, properties and applications. Chem. Soc. Rev. 41 (2012) 7108-7146
25. D. Carriazo, M.C. Serrano, M.C. Gutiérrez, M.L. Ferrer, F. del Monte: Deep-eutectic solvents playing multiple roles in the synthesis of polymers and related materials. Chem. Soc. Rev. 41 (2012) 4996-5014
26. D. Carriazo, M.C. Serrano, M.C. Gutiérrez, M.L. Ferrer, F. del Monte: Deep Eutectic Solvents Playing Multiple Roles in the Synthesis of Porous Carbon Materials, Applications of Ionic Liquids in Polymer Science and Technology, Springer (2015)
27. N.R. Mirza, N.J. Nicholas, Y. Wu, S. Kentish, G.W. Stevens: Estimation of normal boiling temperatures, critical properties, and acentric factors of deep eutectic solvents. J. Chem. Eng. Data 60 (2015) 1844-1854
28. A. Mohsenzadeh, Y. Al-Wahaibi, A. Jibril, R. Al-Hajri, S. Shuwa: The novel use of deep eutectic solvents for enhancing heavy oil recovery. J. Pet. Sci. Eng. 130 (2015) 6-15
29. P.K. Naik, P. Dehury, S. Paul, T. Banerjee: Evaluation of Deep Eutectic Solvent for the selective extraction of toluene and quinoline at T= 308.15 K and p= 1 bar. Fluid Phase Equilib. 423 (2016) 146-155
30. N.R. Rodriguez, J. Ferre Guell, M.C. Kroon: Glycerol-Based Deep Eutectic Solvents as Extractants for the Separation of MEK and Ethanol via Liquid–Liquid Extraction. J. Chem. Eng. Data 61 (2016) 865-872
31. M. Mohan, P.K. Naik, T. Banerjee, V.V. Goud, S. Paul: Solubility of glucose in tetrabutylammonium bromide based deep eutectic solvents: Experimental and molecular dynamic simulations. Fluid Phase Equilib. 448 (2017) 168-177

32. T. Phaechamud, S. Tuntarawongsa, P. Charoensuksai: Evaporation behavior and characterization of eutectic solvent and ibuprofen eutectic solution. AAPS PharmSciTech 17 (2016) 1213-1220

33. H.G. Morrison, C.C. Sun, S. Neervannan: Characterization of thermal behavior of deep eutectic solvents and their potential as drug solubilization vehicles. Int. J. Pharm. 378 (2009) 136-139

34. C. Florindo, L. Branco, I. Marrucho: Development of hydrophobic deep eutectic solvents for extraction of pesticides from aqueous environments. Fluid Phase Equilib. 448 (2017) 135-142

35. R.B. Eldridge, A.F. Seibert, S. Robinson, J. Rogers: Hybrid separations/distillation technology. Research opportunities for energy and emissions reduction, Univ. of Texas, Austin, TX (United States) (2005)

36. S. Pierucci, G.B. Ferraris: 20 European Symposium on Computer Aided Process Engineering. Comput.-Aided Chem. Eng. 28 (2010) 1-1342

37. K.I. Al-Malah: Aspen Plus: Chemical Engineering Applications, John Wiley & Sons (2016)

38. Y.C. Chen, K.L. Li, C.L. Chen, I.L. Chien: Design and Control of a Hybrid Extraction–Distillation System for the Separation of Pyridine and Water. Ind. Eng. Chem. Res. 54 (2015) 7715-7727

Chapter 2

Experimental and Computations Details

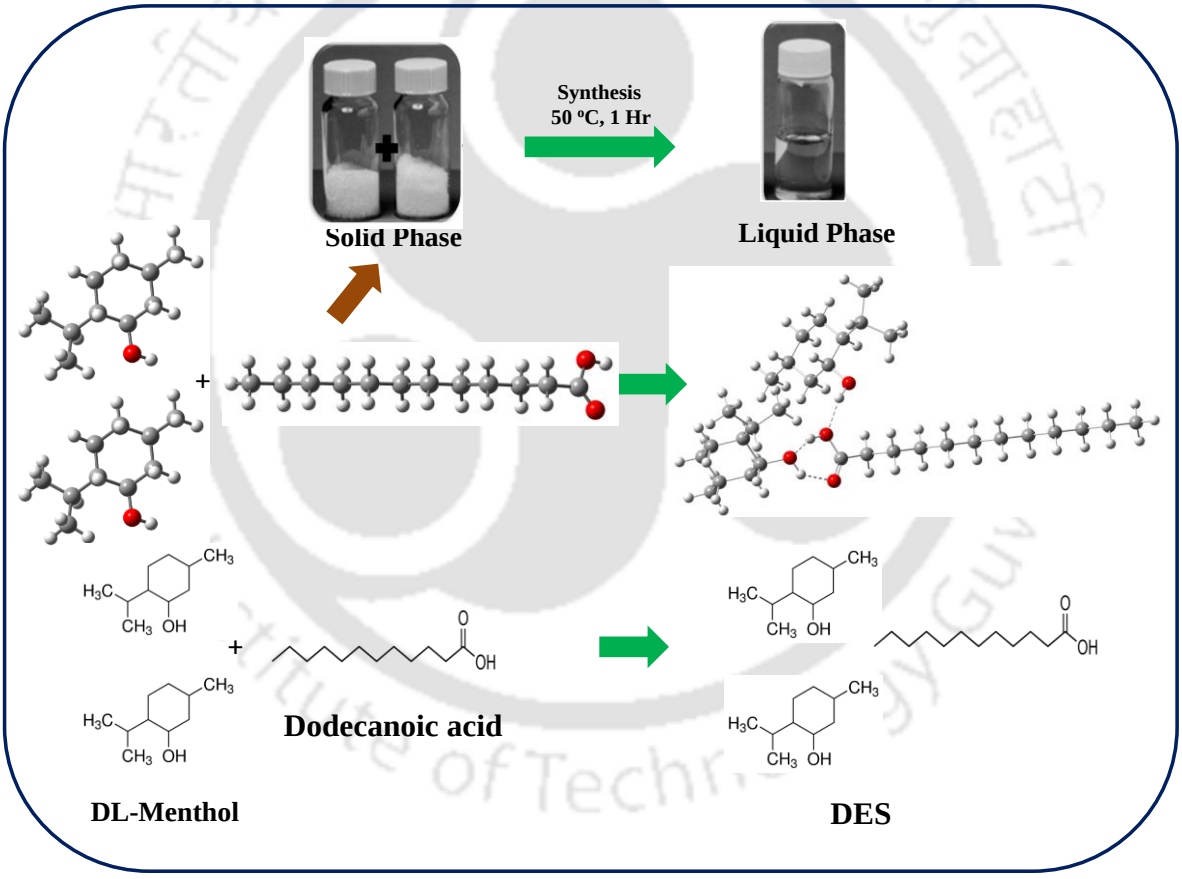

2.1. Introduction

The concept of DES was first introduced by Abbott et al., [1]. It was introduced as analogues and alternative green solvents to the conventional ILs, with the advantage of easy preparation with high purities and low cost. DESs have low melting point and low lattice energy due to its large, nonsymmetrical ions [2, 3]. DES have recently received a great interest in diverse fields including liquid-liquid extraction due to their unique solvation properties. Recently DESs have been used as azeotrope breakers for the liquid-liquid extraction of lower alcohols [4]. Most of the DESs proposed so far in the open literature have a hydrophilic character and thus are unstable in water. In such a scenario, the choice of HBA and HBD is crucial.

With respect to the hydrophobicity of the DES, in the current work, DL-menthol and organic acids have been chosen as HBA and HBD respectively [5-11]. In the present study organic acids and DL-menthol based DESs have been proposed for the extraction of lower alcohols such as ethanol, 1-propanol and 1-butanol. These DESs are known to have favorable solvation properties for polar and nonpolar compounds [2, 3, 5]. They are more stable at high temperature and/or in presence of chemicals and are suitable for the extraction of inorganic and organic compounds [6-9] . It is a well-known fact that chloride-ion based DESs produce a higher charge density resulting in a higher fraction of active site for initiating hydrogen bonding. It should also be noted that the chloride ion is responsible for the corrosion of reactor vessels when heated at high temperatures. This is due to the fact that at high temperature it can underdo hydrolysis thereby corroding the vessel surface. Thus DESs consisting of halogen or halogen containing anions such as $[AlCl_4]$, $[PF_6]$, $[BF_4]$, $[CF_3SO_3]$ and $[(CF_3SO_2)_2N]$ do indeed limit their ‘greenness’. Overall the presence of halogen atoms is known to cause serious concerns if the hydrolysis stability of the anion is poor or if a thermal processing and recycle is desired [10] . In both the cases additional operations are required to avoid the liberation of toxic and corrosive HF or HCl into the environment. Thus from an industrial point of view halogen containing DES are generally not recommended even though they have higher selectivity as well as distribution coefficient. Further it is also reported that the anionic part or the HBD of DES generally plays an important role in the thermal stability. For e.g. in the case of Ionic Liquid (IL), organic anions have higher thermal stability than those based on inorganic anions [11] . Figure 2.1 shows the molecular structures of different

compounds as used for synthesizing DES. Here organic acids are used as hydrogen bond donors (HBD) and DL-menthol as the inorganic salt which acts as a hydrogen bond acceptor (HBA)

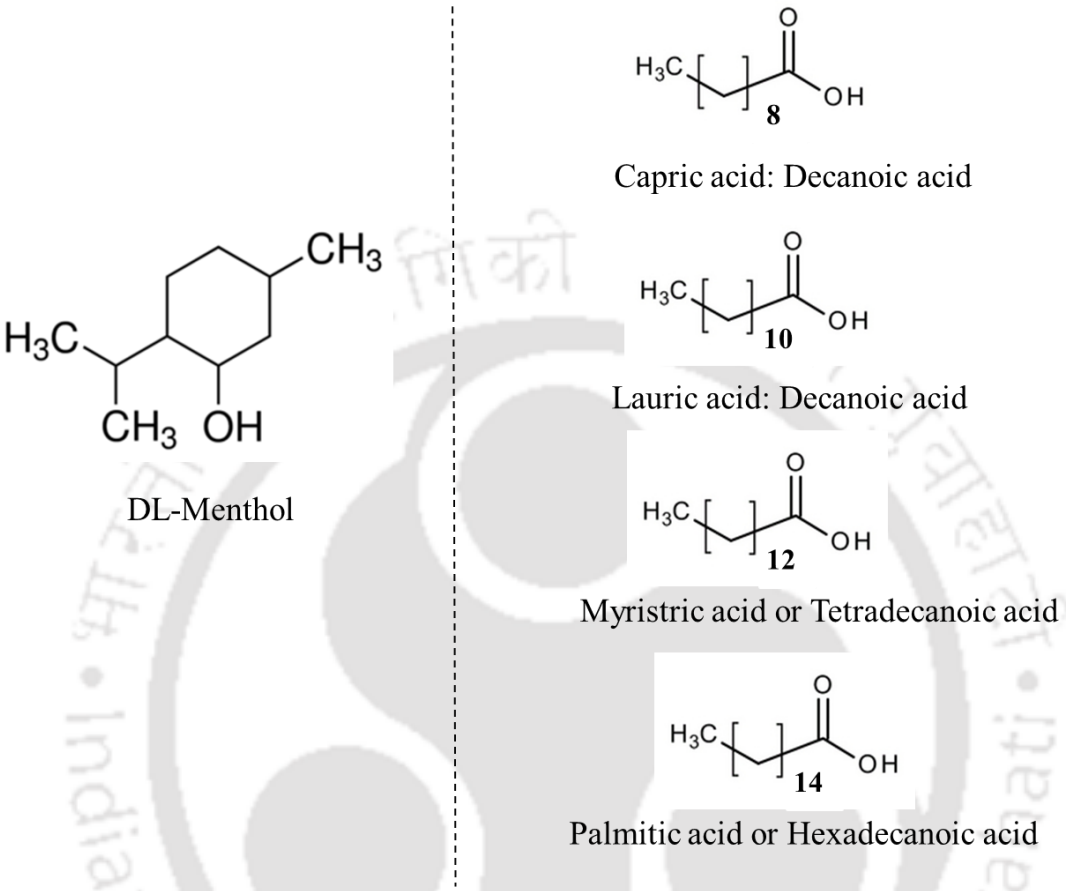

Figure 2.1: Structures of the HBA (DL-menthol), and HBD (Organic acids) used for DES syntheses along with their boiling points

The present study discusses the synthesis of four types of DESs abbreviated as DES-1 to DES-4 respectively .These are given below:

1. DES based on DL-menthol and Capric acid (Decanoic acid)
2. DES based on DL-menthol and Lauric acid (Dodecanoic acid)
3. DES based on DL-menthol and Myristic acid (Tetradecanoic acid)
4. DES based on DL-menthol and Palmitic acid (Hexadecanoic acid)

All the above synthesized DESs (namely: DES-1 to DES-4) will be used to measure the LLE with lower alcohols from their aqueous phase. Before we start the synthesis procedure, a need is felt geometrically optimize these structures [12, 13]. This will help us in selecting the molar ratio of HBD and HBA .It should be noted that not all ratio will give us a

eutectic point or a liquid phase. It is those points or in other words the lowest temperature which needs to be computed in such a manner that a liquid phase of DES co-exist. This can be initiated through quantum chemical calculations and adopting a statistical based approach. Hence the COSMO-SAC (Conductor like Screening Model Segment Activity Coefficient model) is adopted. The detailed methodology of COSMO and COSMO-SAC was already available in the earlier work by Lin et al. [14] and Klamt et al. [15], hence this is not discussed here. The applications of COSMO-SAC is well known and is documented in areas especially distillation, extraction and absorption [14-21]. Once the optimum ratio is known we shall then proceed for the experiments. The discussion herewith starts with the geometry optimization followed by COSMO-SAC predictions.

In order to confirm the effect of ratio of HBD to HBA preliminary attempts have been devised to predict the same through COSMO-SAC model. This is essentially a solid-liquid equilibrium (SLE) problem where the simplified form is given by Eq. 2.1 as below [22-24].

$$\ln\left(x_s^L \gamma_s^L\right) = -\frac{\Delta_{fus}H_s}{RT_{s,fus}}\left(1-\frac{T_{s,fus}}{T}\right) \tag{2.1}$$

Where $\Delta_{fus}H_s$ and $T_{s,fus}$ are the heat of fusion and melting temperature of the pure solute respectively. T (K) is the equilibrium temperature, *R* the ideal gas constant, x_s^L is the mole fraction of solute (decanoic/lauric/ myristic /palmitic) in liquid phase i.e. DL-menthol. Here DL-menthol is considered as the liquid phase as it has the lowest boiling point (Figure 2.2). γ_s^L is the activity coefficient of the solute (decanoic / lauric / myristic / palmitic) in the liquid phase i.e. DL-menthol. The right hand side of Eq. 2.1 requires the pure components parameters of the solid solute (decanoic / lauric / myristic / palmitic) only. The pure component parameters (melting point and heat of fusion) are obtained as per the literature given in Table 2.1.

Table 2.1: Melting properties of compounds for COSMO-SAC based eutectic point calculations

Name of the Comp.	T_m (K)	ΔH_f (kJ/mole)	Reference
Menthol	308.8	11000	Corvis et al.[25]
Decanoic Acid	304.75	27500	Pontes et al.[26], Matos et al.[27, 28]
Lauric acid	317.48	37830	Pontes et al.[26], Matos et al.[27, 28]
Myristic Acid	327.03	41290	Pontes et al. [26], Matos et al.[27, 28]
Palmitic Acid	336.84	51020	Pontes et al.[26]

In order to benchmark the COMSO-SAC predictions, eutectic point for the system Choline Chloride and 1-ethyl-3-methylimidazolium chloride [C_2mim]Cl as available earlier by Fernandez et al. [29] was chosen. As seen from Figure 2.2 the COMSO-SAC prediction correctly reproduced the experimental data. Using the same methodology we shall now proceed with DES.

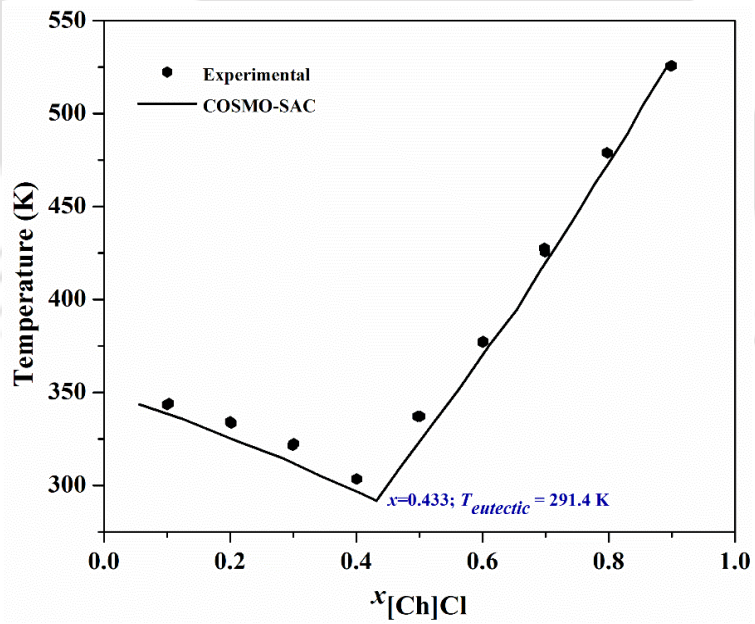

Figure 2.2: COSMO-SAC Prediction of Eutectic Point and Temperature for Choline Chloride and [C_2mim]Clbenchmarking System [29]

The eutectic point of the DES-1 is predicted at x=0.5, where x corresponds to the mole fraction of Decanoic acid (Figure 2.3). This essentially implies a molar ratio of 0.5/0.5

(HBA:HBD) or 1 which is the same as adopted in the experimental synthesis. This ratio therefore corresponds to the working liquid temperature of the DES.

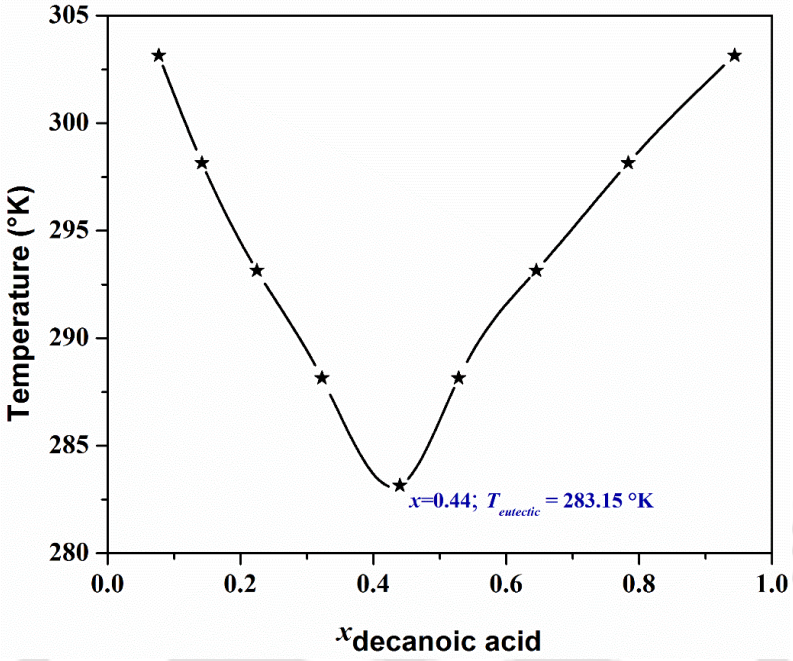

Figure 2.3: COSMO-SAC Prediction of Eutectic Point and Temperature for DES-1 (DL-menhol and Decanoic acid)

Table 2.2 shows the COSMO-SAC predication and experimental validation for the eutectic compositions and corresponding temperatures for the DL-menthol and Decanoic acid based DES.

Table 2.2: Coordinates of the Eutectic points as predicted and validated with COSMO-SAC model

System	Experimental		COSMO-SAC	
	$x_{[Ch]Cl/DL\text{-}menthol}$	T / K	$x_{[Ch]Cl/DL\text{-}menthol}$	T / K
[Ch]Cl + [Emim]Cl	0.430*	295.0	0.433	291.40
DL-menthol + Decanoic acid	0.500**	284.7	0.660	283.15

*Fernandez et al.[29]; **refers to the current work

Thus based on the COSMO-SAC predictions of the eutectic point, the appropriate mole ratio of HBA:HBD is chosen. This corresponds to a mole ratio of 1 for DL-menthol:Decanoic acid. With the obtained ratio we shall now discuss the synthesis procedure in the ensuing section.

2.2. Experimental Details

2.2.1. Synthesis of Deep Eutectic Solvents

The DESs selected here are mixture of DL-menthol and organic acids in such a manner that it remains as a stable liquid at the room temperature [30, 31].

2.2.2. Materials

Table 2.3 shows the compound name, solubility, purity and source of the chemicals used in the present study. Purities of ethanol, propanol, 1-butanol, lauric acid and DL-menthol were confirmed by ^{1}H NMR spectroscopy. The analysis of their^{1}H NMR peaks indicated negligible impurities. The NMR solvent, Dimethyl sulfoxide-d6 (DMSO-d6 ≥ 99.8%) supplied by Merck, Germany was used as received. All chemicals were of analytical grade and were used without further purification.

Table 2.3: Compound name, solubility, purities and source of the chemicals used in the work

Sl. No.	Compound Name	Solubility in water (g/lit)	M.P. (°C)	B.P. (°C)	Density* (g/cc)	Purity*	Source
1.	DL-menthol	0.420	34-36	214.6	0.890	≥95%	Sigma Aldrich, Germany
2.	Capric or Decanoic acid	0.062	29-32	268.7	0.893	≥98%	Tokyo Chemical Industry, Japan
3.	Lauric acid or Dodecanoic acid	0.059	43-45	298.9	1.007	≥99%	Merck, Germany
4.	Myristic acid or Tetradecanoic acid	0.022	54-57	326.0	0.862	≥99%	Tokyo Chemical Industry, Japan
5.	Palmitic acid or Hexadecanoic acid	0.00004	62-66	352.0	0.853	≥97%	Tokyo Chemical Industry, Japan

*This work; **as per Manufacturer

2.3. Synthesis of Menthol based DES

2.3.1. DES-1 or DL-menthol and Decanoic acid

DL-menthol (HBA) and decanoic acid (HBA) are added in the molar ratio of 1:1 in a flat-bottom flask which is fitted with a reflux condenser for 1 h at 50 °C with magnetic

stirring until a clear liquid is formed. After keeping it undisturbed for 6 hrs the unreacted phase was separated. Vacuum was then applied to the DES phase so as to remove the other impurities including the starting reactants. For reducing the water content and volatile compounds of DES to negligible values, a vacuum was applied at T = 60 °C for at least 48 h. This was also performed on DES samples prior to the LLE measurements. Thereafter the synthesized DES was evaluated for its purity using ^{1}H NMR spectra.

A600 MHz NMR spectrometer (Make: Bruker) was used for the ^{1}H NMR of DES samples to measure the peak areas of the distinct types of hydrogen nuclei. Based on the theory of NMR, the area under the curve is proportional to the number of hydrogen for the referred component. Figure 2.4 reports the ^{1}H NMR spectra of the synthesized DESs (DL-menthol: organic acids) along with the peak assignment. The reference peak for the NMR solvent namely DMSO-D6 has been recorded at 2.5 ppm. The concentration of other components are calculated by Eq. 2.2 given as :[24]

$$x_i = \frac{H_i}{\sum_{i=1}^{n} H_i} \tag{2.2}$$

Here H_i denotes the peak area of single hydrogen of component 'i' and x_i the mole fraction of component 'i'.

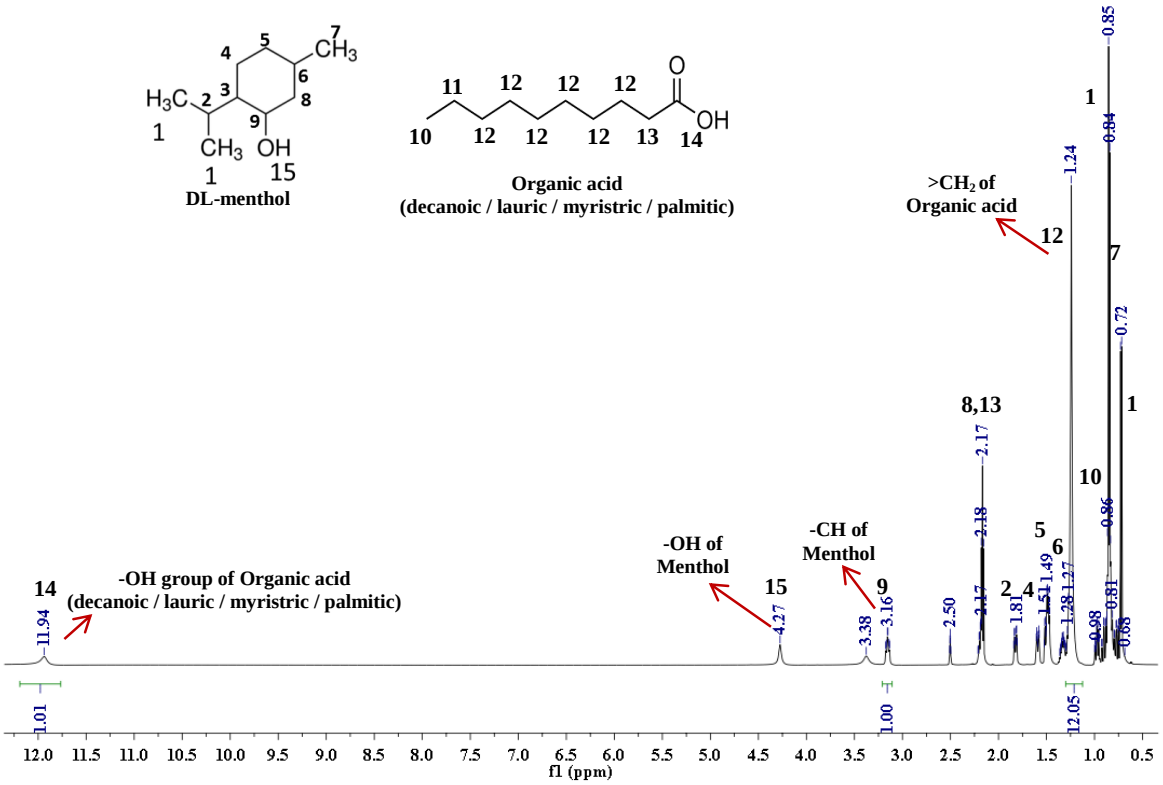

Figure 2.4: ^{1}H NMR spectra of synthesized DL-menthol and organic acid based DESs

As observed from ^{1}H NMR spectra of synthesized pure DES (Figure 2.5), the molar ratio of -OH group in DL-menthol (peak number 15) is equal to the -OH group (peak number 14) of decanoic acid. In another conformation, -CH group of DES (peak number 9) has an area of unity, while peak 12 resembling 12-H atoms of Decanoic acid has an area of 12. So an effective contribution of a single hydrogen atom of Decanoic acid is 1 (i.e 12/12). Hence the ratios of DL-menthol (1.0) and Decanoic acid (0.5) are in the molar ratio of 1:1.

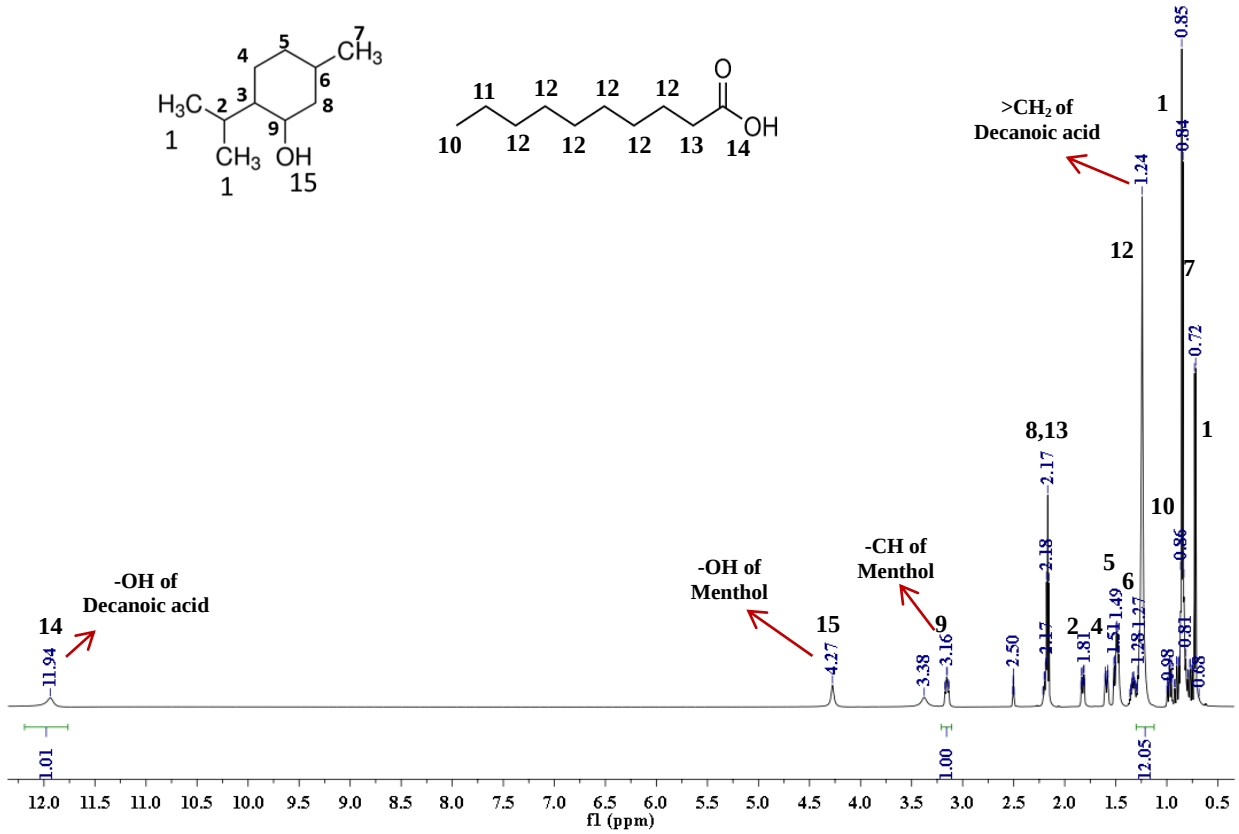

Figure 2.5: ^{1}H NMR spectra of synthesized DL-menthol and decanoic acid based DES

Additionally we have also attempted to synthesize molar ratios of 0.5:1, 1.5:1 and 2:1 for the synthesis of DL-menthol + Decanoic acid as shown in the visual conservation (Figure 2.6). It is clearly seen that for all the ratios, a clear transparent liquid formed. This also agrees with the reported literature and also our own COSMO-SAC predictions where the composition (1:1) have been used for synthesizing the similar DES [30, 31].

Ratio of DL-menthol to Decanoic Acid			
0.5:1	**1:1**	**1.5:1**	**2:1**
			

Figure 2.6: Formation of DES with different molar ratio of DL-menthol to Decanoic acid.

As the DES are essentially needs to be used in the aqueous rich phase, it stability with water is tested by mixing it with equal volume of water. The NMR spectra for pure DES and water rich phase are shown in the Figures 2.7 - 2.8. For analyzing the hydrophobic nature of DES-1, two parts water and one part of DES by weight were added in 15 mL size bottle. Shaking was performed with a magnetic stirrer for 30 min. Thereafter the mixture was kept for 12 h for equilibrium. The samples were drawn from both the water rich (lower phase) and the DES rich (upper phase) for ^{1}H NMR. Figure 2.7 represents the ^{1}H NMR spectra of upper phase (solvent rich-phase) which clearly shows an absence of water.Figure 2.8 shows the ^{1}H NMR of the washed sample repeatedly after four times. The spectra clearly reflects an absence of DES in the bottom phase (aqueous rich-phase) even after repeated washing. It implies that the synthesized DES-1 is close to be termed hydrophobic in nature.

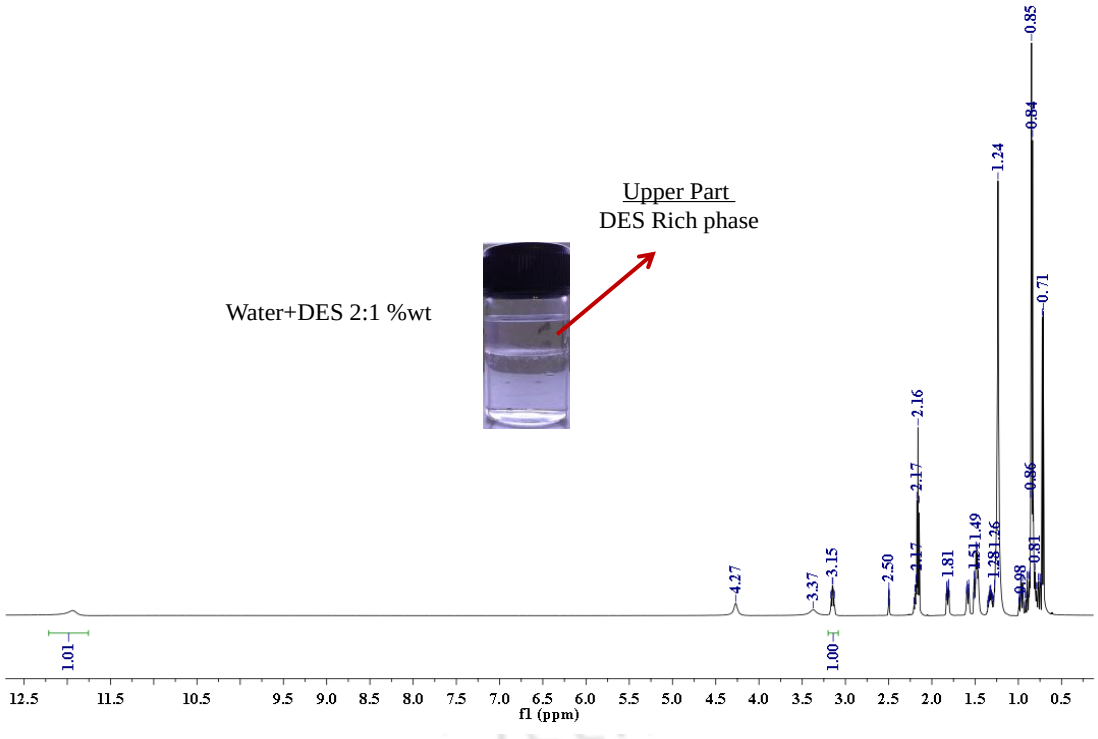

Figure 2.7: ^{1}H NMR analysis of DES-rich phase in water

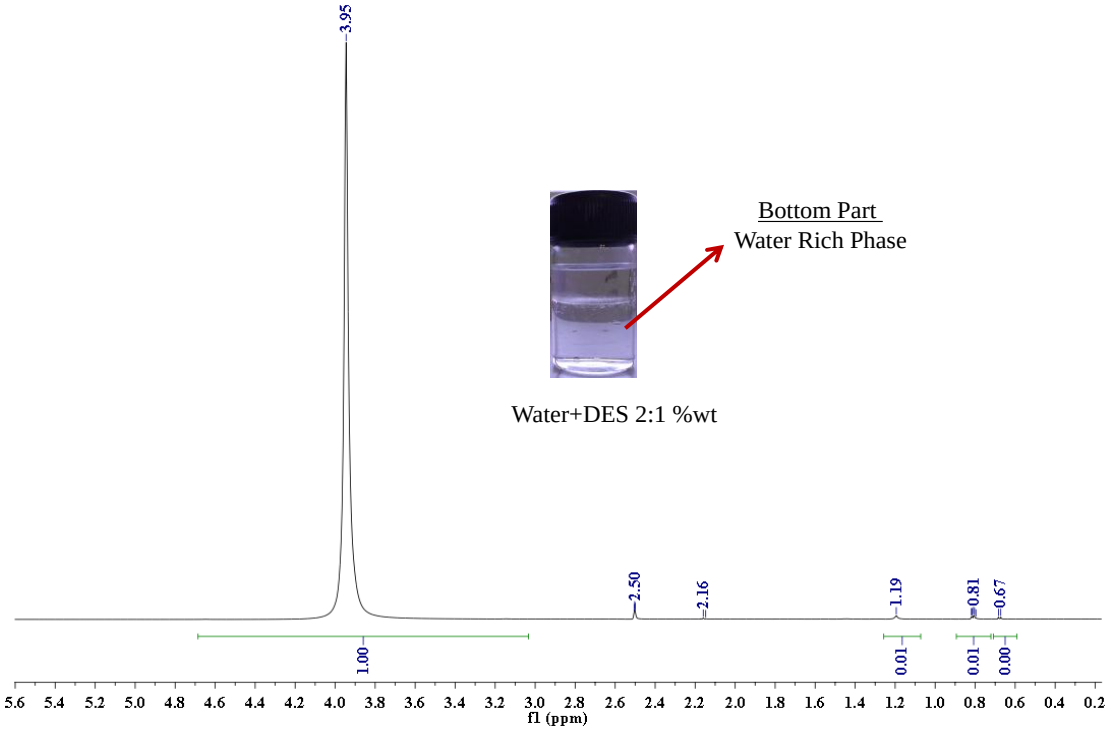

Figure 2.8: ^{1}H NMR analysis of water rich phase

2.3.2. DES-2 or DL-menthol and Lauric acid

Lauric acid is another organic acid having longer carbon chain as compared to decanoic acid. The COSMO-SAC predicted was found to be at x=0.311 where x corresponds to the mole fraction of lauric acid. This essentially implies a molar ratio of 0.689/0.311 ~2 (HBA:HBD). Hence this has been adopted in the experimental evaluation. Further as can be seen from Figure 2.9, the eutectic point is obtained at T = 283.15 K by COSMO-SAC predictions. This also agrees with the reported literature, where the ratio of 2:1 have been used for synthesizing the decanoic and lauric acid based DES respectively [30, 31]. This corresponds to a mole ratio of 2 (0.667/0.333) for DL-menthol:Lauric acid. The eutectic composition for DES-2 is given in Table 2.4. DL-menthol is combined with Lauric acid with a molar ratio of 2:1 and synthesized in a similar manner as discussed for DES-1.

.

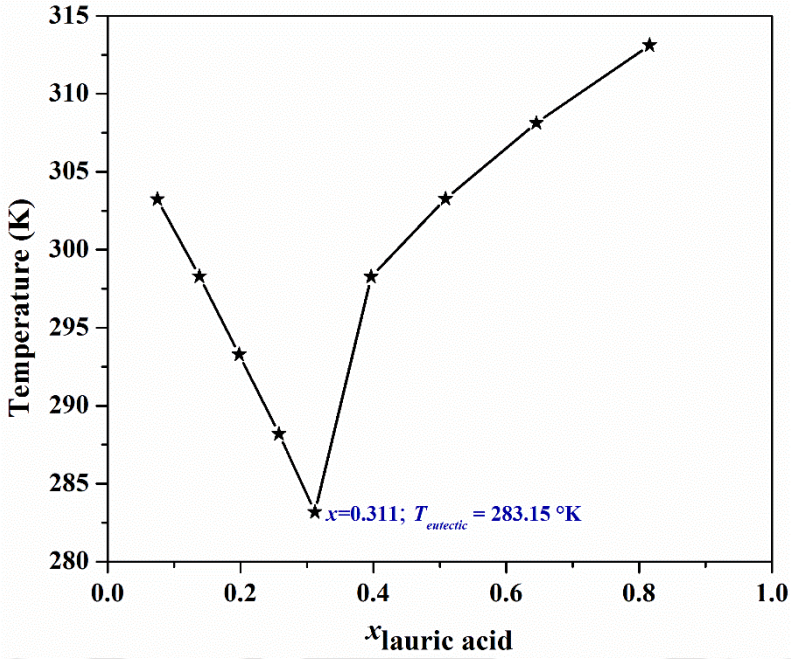

Figure 2.9: COSMO-SAC Prediction of Eutectic Point and Temperature for DES-2 (DL-menhol and Lauric acid)

Table 2.4: Coordinates of the Eutectic points as predicted and validated with COSMO-SAC model

System	Experimental		COSMO-SAC	
	$x_{DL\text{-}menthol}$	T / K	$x_{DL\text{-}menthol}$	T / K
DL-menthol + Lauric acid	0.667	288.19	0.689	283.15

Figure 2.10 shows the ^{1}H NMR of pure synthetized hydrophobic DES-2. The concentration of other components in each phase is again calculated by Eq. 2.2 [24] as discussed in section 2.3.1. As observed from ^{1}H NMR spectra of synthesized pure DES, the molar ratio of -OH group in DL-menthol (peak number 15) is twice than that of the corresponding -OH group (peak number 14) of Lauric acid. In another conformation, -CH group of DES (peak number 9) has an area of unity, while peak 12 resembling 16-H atoms of Lauric acid has an area of 8. So an effective contribution of a single hydrogen atom of Lauric acid is 0.5 (i.e. 8/16). Hence the ratios of DL-menthol (1.0) and Lauric acid (0.5) are in the molar ratio of 2:1.

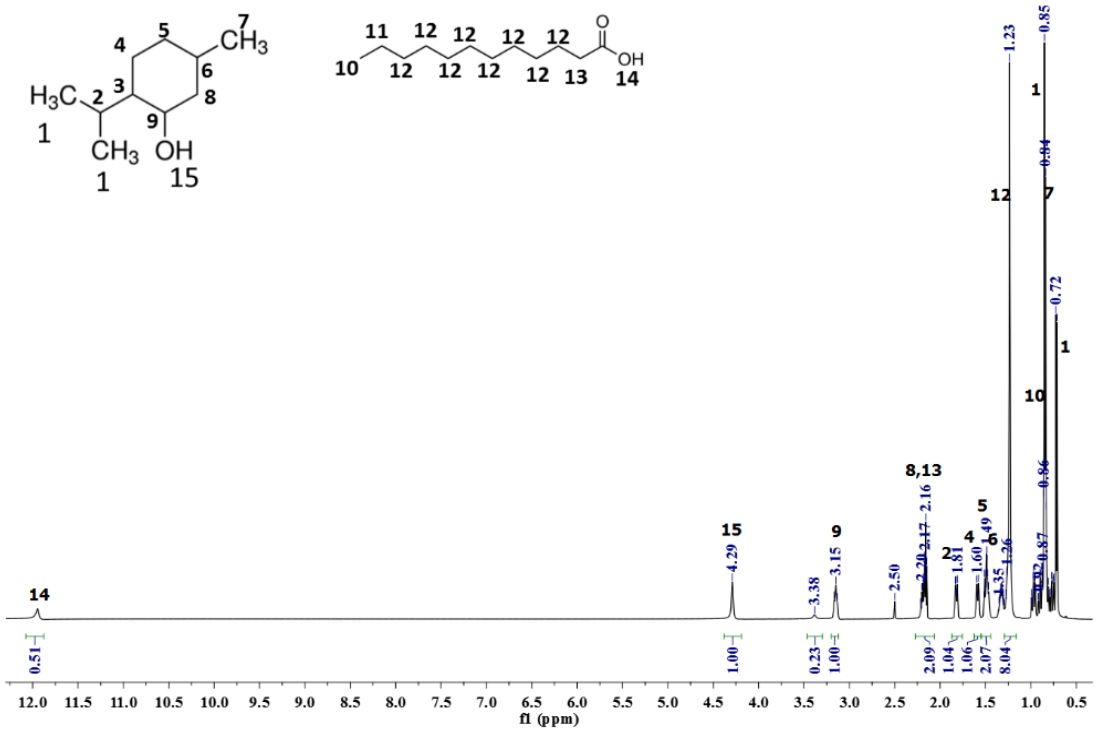

Figure 2.10: ^{1}H NMR spectra of synthesized DL-menthol and lauric acid based DES-2

In order to confirm the COSMO-SAC predictions, we have also attempted to synthesize molar ratios of 0.5:1, 1:1, 1.5:1 and 2.5:1 for the synthesis of DL-menthol + Lauric acid as shown in the visual observation (Figure 2.11). It is clearly seen that the ratio's below 1:1 posses crystal formation. This diminishes as the mole ratio increases or we go towards the left of Figure 2.11.

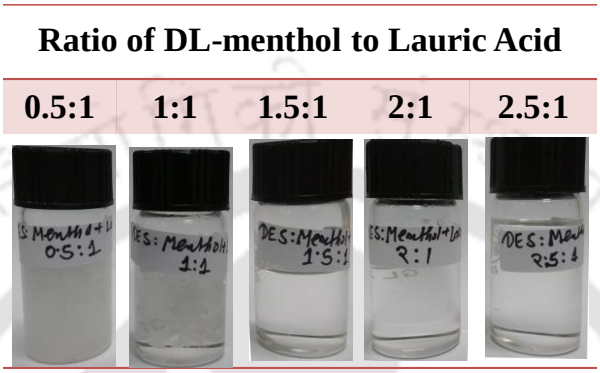

Figure 2.11: Formation of DES-2 with different molar ratio of DL-menthol to Lauric acid.

For the water stability, the NMR spectrum of washed DES is shown in Figure 2.12 and Figure 2.13. The NMR spectra clearly shows an absence of water in the upper phase (solvent rich-phase). NMR spectra of bottom part (aqueous rich-phase) again clearly reflects an absence of DES even after repeated washing. It implies that the synthesized DES-2 is also hydrophobic in nature.

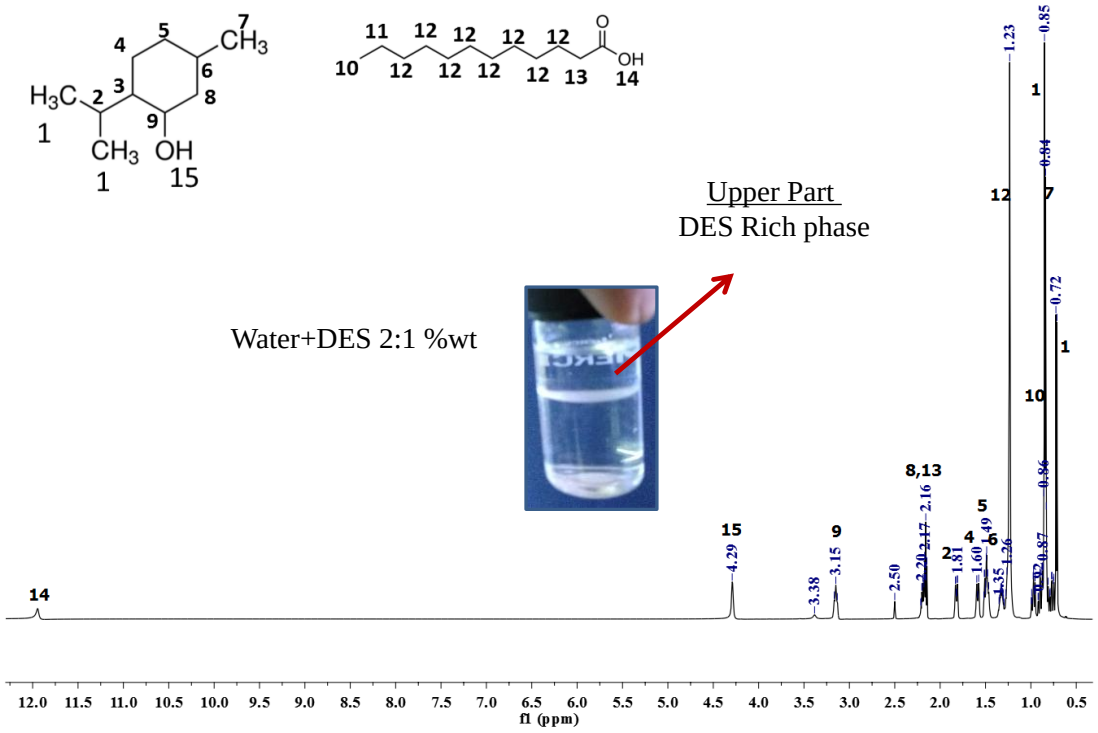

Figure 2.12: ^{1}H NMR analysis of DES-2 rich phase in water

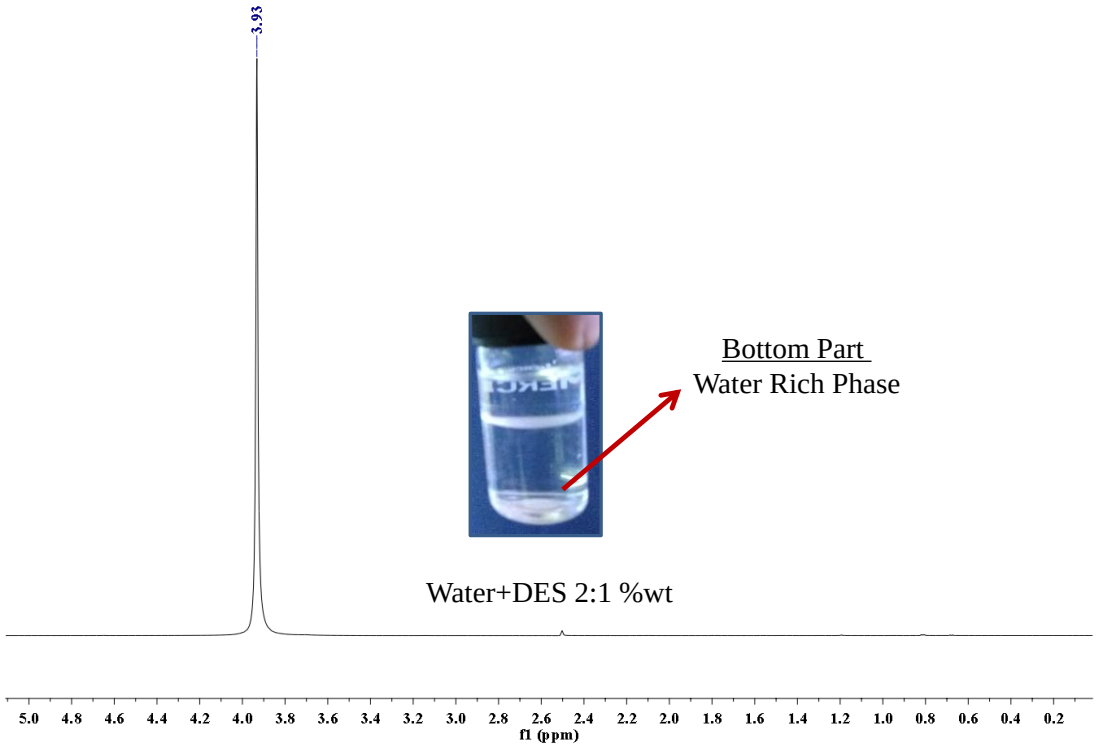

Figure 2.13: ^{1}H NMR analysis of water rich phase

2.3.3. DES-3 or DL-menthol and Myristic acid

In a similar manner, DL-menthol and myristic acid based hydrobhobic DES was synthesized in the present study. From the prediction, the eutectic point (Figure 2.14 and Table 2.5) corresponds to a mole ratio of four for DL-menthol + Myristic acid (0.802/0.198).

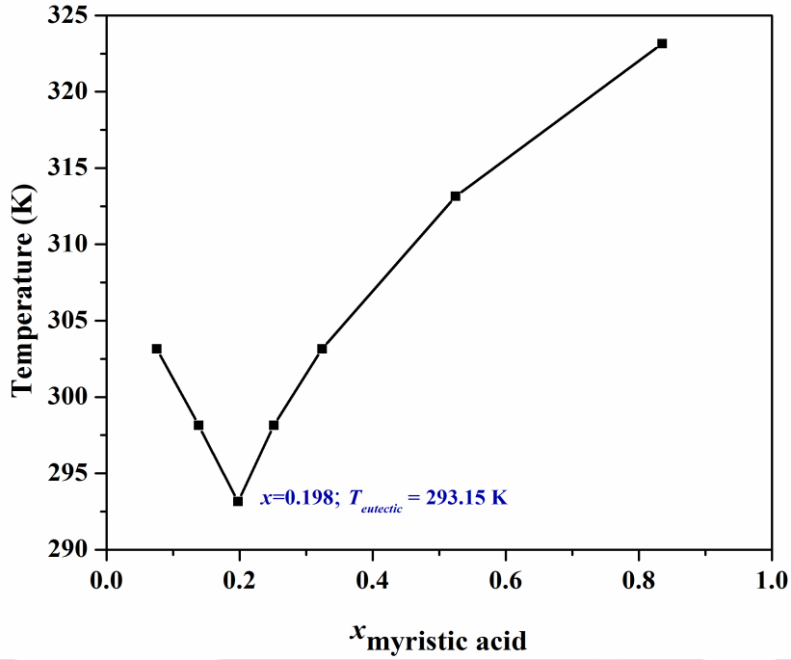

Figure 2.14: COSMO-SAC Prediction of Eutectic Point and Temperature for DES-3 (DL-menthol and Myristic acid)

Table 2.5: Coordinates of the Eutectic points as predicted and validated with COSMO-SAC model

System	Experimental		COSMO-SAC	
	$x_{DL\text{-}menthol}$	T / K	$x_{DL\text{-}menthol}$	T / K
DL-menthol + Myristic acid	0.802	292.4	0.802	293.15

Figure 2.15 depicts the ^{1}H NMR of pure synthesized myristic based DES. As observed from ^{1}H NMR spectra of synthesized pure DES (Figure 2.15), the molar ratio of -OH group in DL-menthol (peak number 15) is four times than that of the corresponding -OH group (peak number 14) of myristic acid.

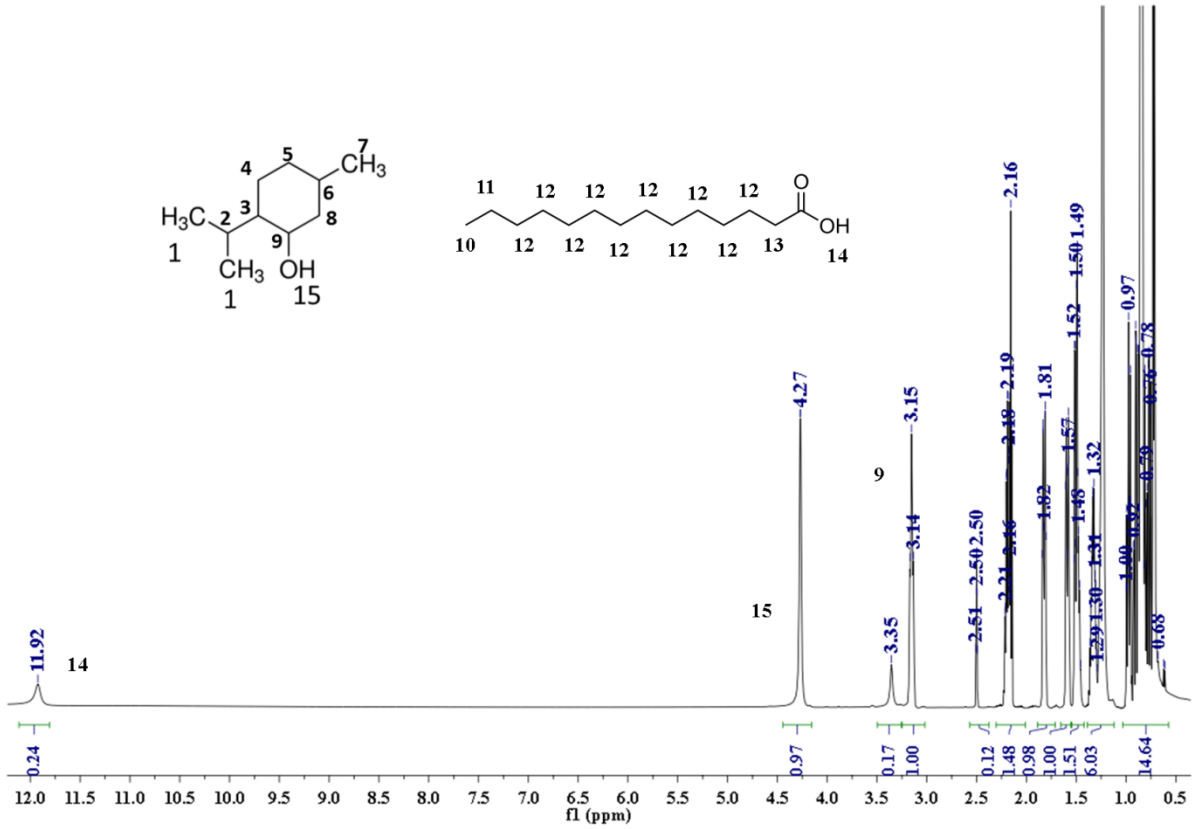

Figure 2.15: ^{1}H NMR Spectra of synthesized DL-menthol and myristic acid based DES

As before the water stability was checked by mixing equal volume of DES and water and washed repeatedly for four cycles. Figures 2.16 - 2.17 show ^{1}H NMR spectra of washed DES-3, to check the hydrophobicity of DES-3. The NMR spectra clearly shows an absence of water in the upper phase (solvent rich-phase, Figure 2.16). Further NMR spectra of bottom part (aqueous rich-phase, Figure 2.17) clearly reflects an absence of DES even after repeated washing. It implies that the new synthesized DES-3 is also hydrophobic in nature.

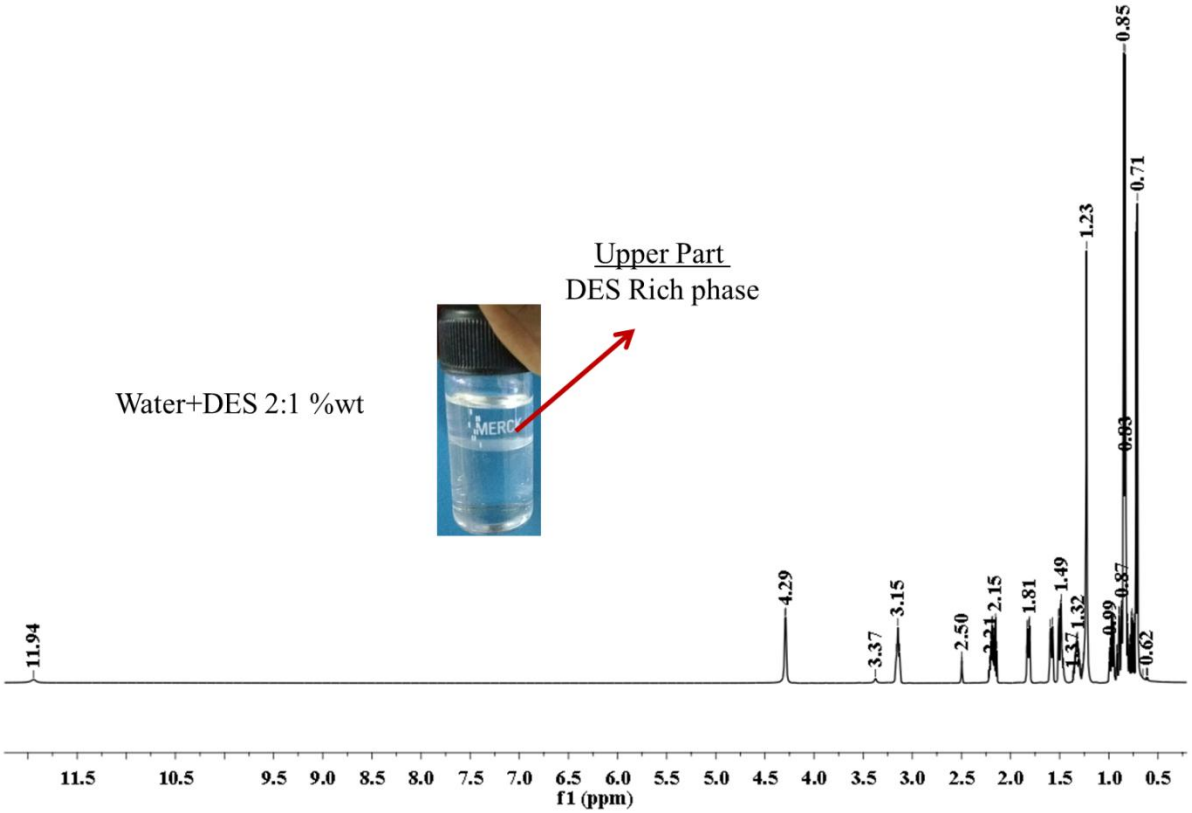

Figure 2.16: ^{1}H NMR analysis of DES-3 rich phase in water

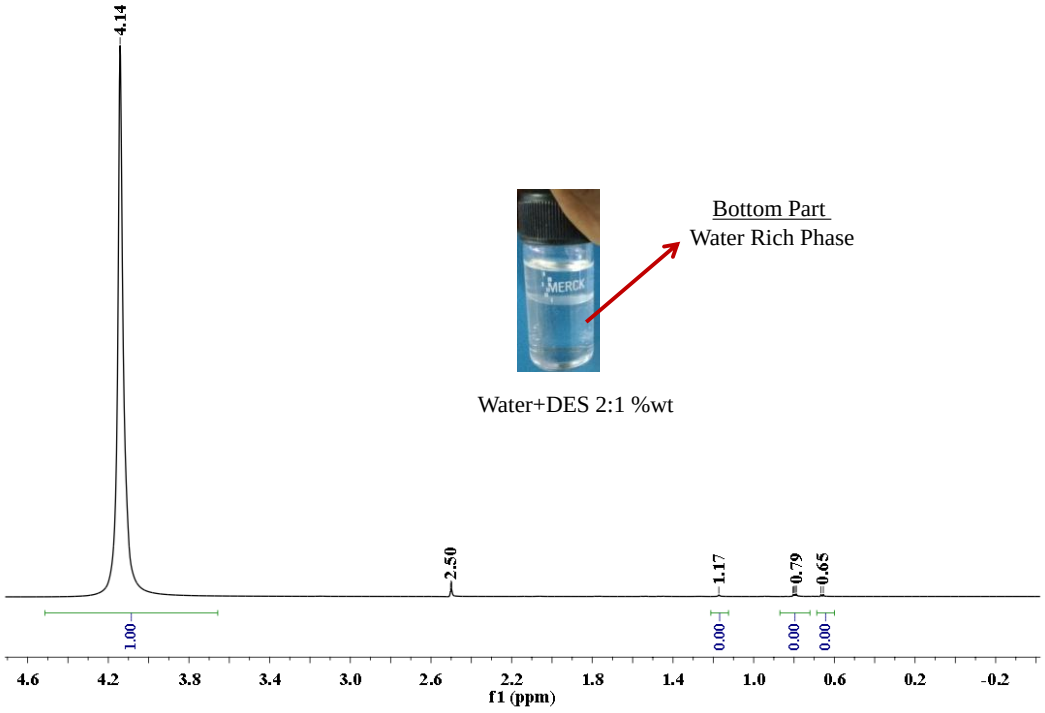

Figure 2.17: ^{1}H NMR analysis of water rich phase

We have also attempted to synthesize molar ratios of 2:1, 3:1, 4:1, 6:1 and 8:1 for the synthesis of DL-menthol + Myristic acid as shown in the visual observation (Figure 2.18). This was to validate further the COSMO-SAC predictions. It is clearly seen that the ratio's below 3:1 shall have crystal formation on account of higher Gibb's free energy. This diminishes as the mole ratio increases or we go towards the left side of Figure 2.18.

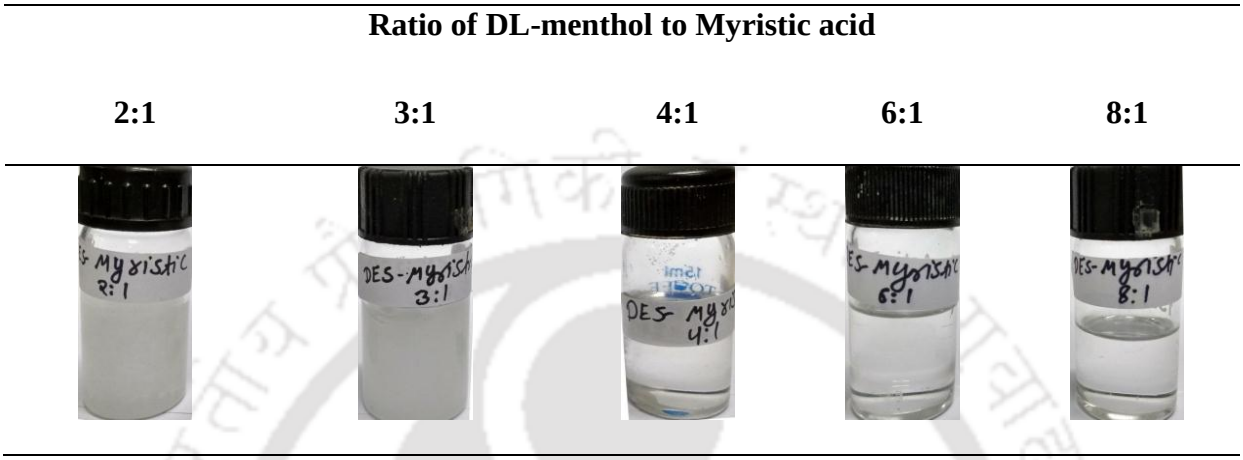

Figure 2.18: Formation of DES-3 with different molar ratio of DL-menthol to Myristic acid.

2.3.4. DES-4 on DL-menthol and Palmitic acid

The DES namely DL-menthol and Palmitic acid corresponds to a mole ratio of 12 (0.923/0.081). A higher ratio may be primarily due to the enhanced and longer chain of the organic acid leading to higher steric hindrance. Here both DL-menthol (HBA), and Palmitic acid (HBD) were again mixed in a similar manner as discussed in section 2.3.1, until a clear liquid was formed (Figure 2.19 and Table 2.6). The temperature was again maintained 50 °C for first 15 min and then after 80 °C for 1 h. In this case synthesis temperature is maintained at 80 °C because the melting point of Palmitic acid is around 62-66 °C (Table 2.3).

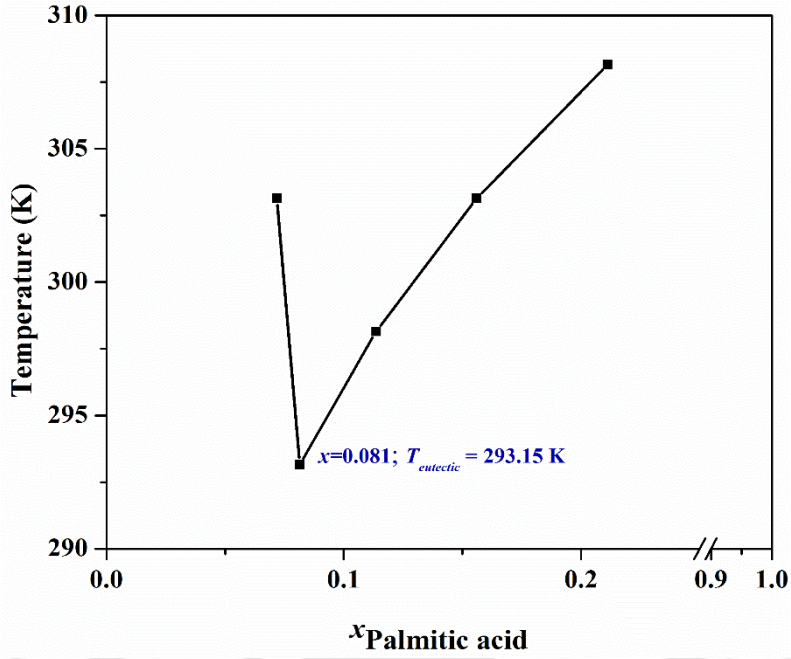

Figure 2.19: COSMO-SAC Prediction of Eutectic Point and Temperature for DES-1 (DL-menhol and Palmitic acid)

Table 2.6: Coordinates of the Eutectic points as predicted and validated with COSMO-SAC model

System	Experimental		COSMO-SAC	
	$x_{DL\text{-}menthol}$	T / K	$x_{DL\text{-}menthol}$	T / K
DL-menthol + Palmitic acid	0.923	296.31	0.887	288.16

Figure 2.20 shows the ^{1}H NMR spectra of synthetized DES. The reference peak for the NMR solvent namely DMSO-D6 has been recorded at 2.5 ppm. The concentration of other components in each phase was then calculated by Eq. 2 [24], as described in section 2.3.1. As observed from ^{1}H NMR spectra of synthesized pure DES, the molar ratio of -OH group in DL-menthol (peak number 15) is twelve times than that of the corresponding -OH group (peak number 14) of palmitic acid.

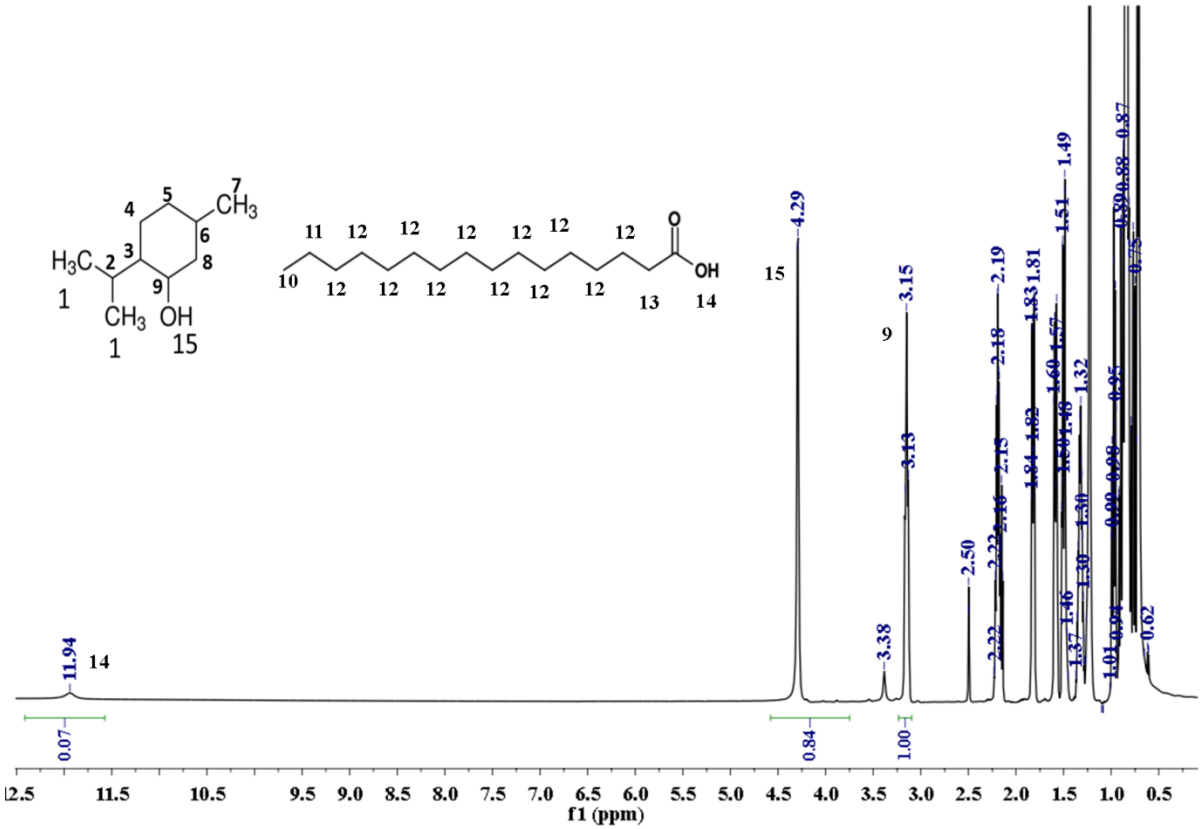

Figure 2.20: ^{1}H NMR Spectra of Synthesized DL-menthol and palmitic acid based DES-4

For water stability analysis, Figure 2.21 and Figure 2.22 depicts the ^{1}H NMR of the washed sample repeatedly after four times so as to check their hydrophobicity. The NMR spectra clearly reflects an absence of DES in the bottom phase (aqueous rich-phase, Figure 2.22) even after repeated washing. It implies that the new synthesized DES-4 is also hydrophobic in nature.

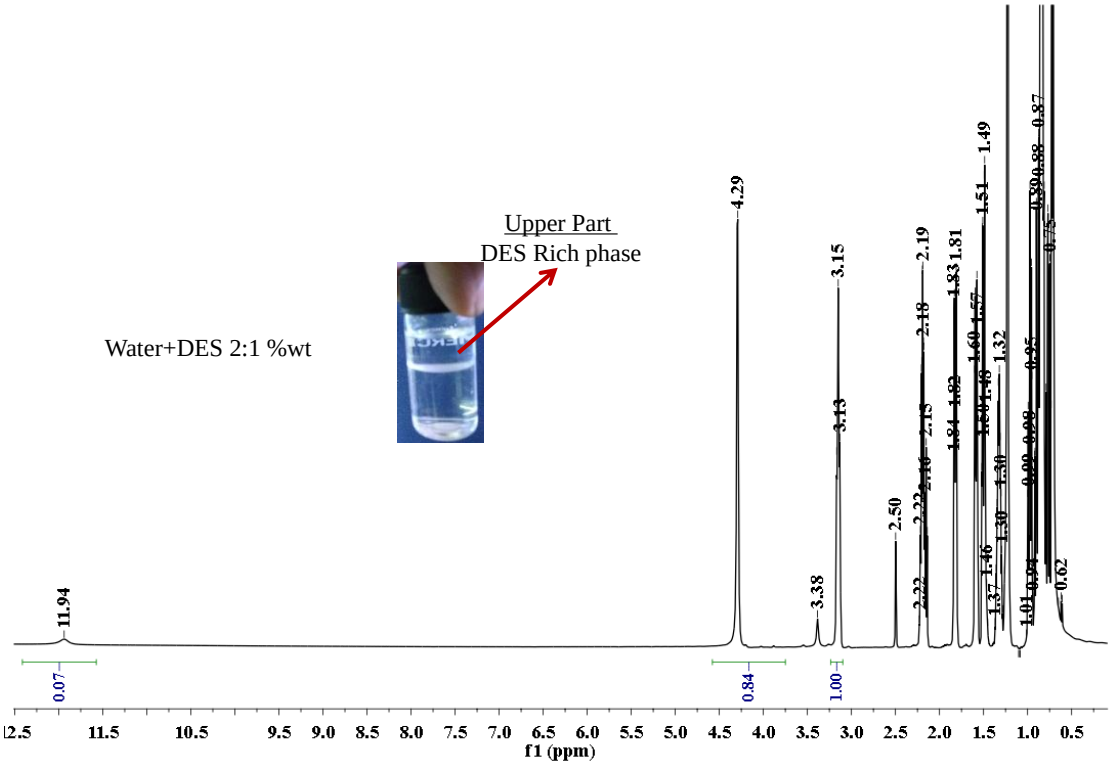

Figure 2.21: ^{1}H NMR analysis of DES-4 rich phase in water

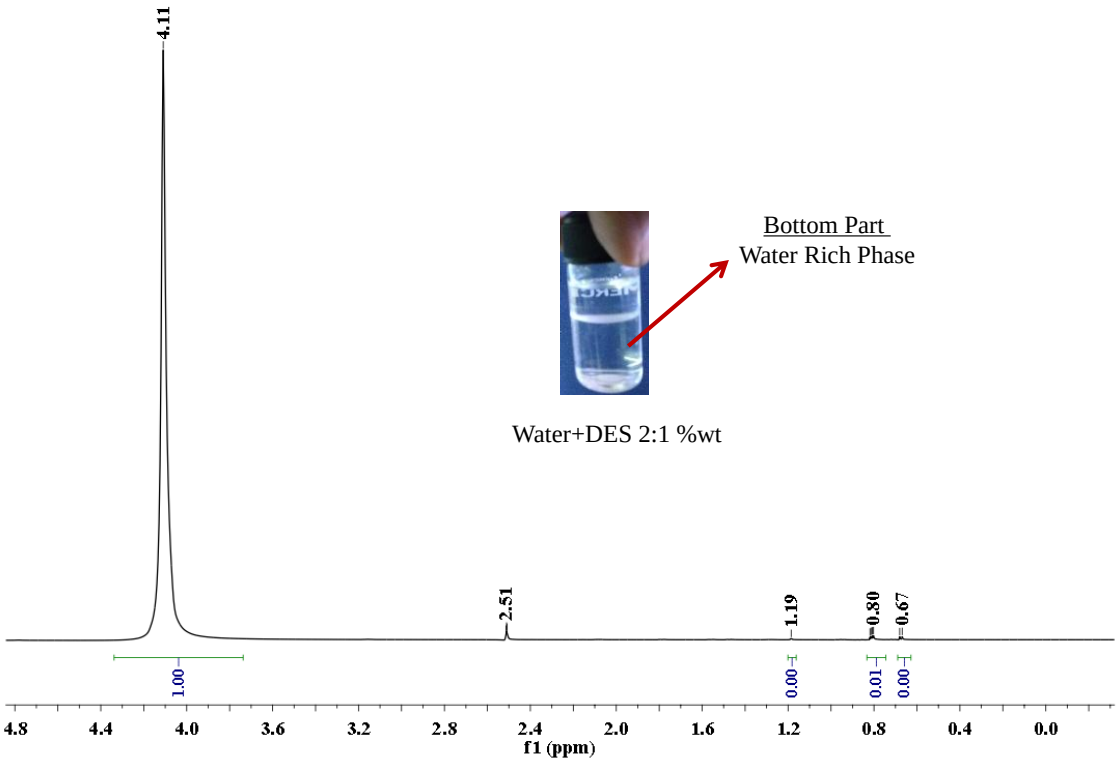

Figure 2.22: ^{1}H NMR analysis of water rich phase

We have also attempted to synthesize molar ratios of 8:1, 10:1, 12:1 and 14:1 for the synthesis of DL-menthol + Palmitic acid as shown in the visual observation (Figure 2.23). It is clearly seen that the ratio's below 8:1 shall have crystal formation, while 10:1 is not found to be stable for a long period of time. However ratio's greater than 10:1 increases this stability and gives a clear solution. For economical reason, ratio's higher than 12:1 has been avoided.

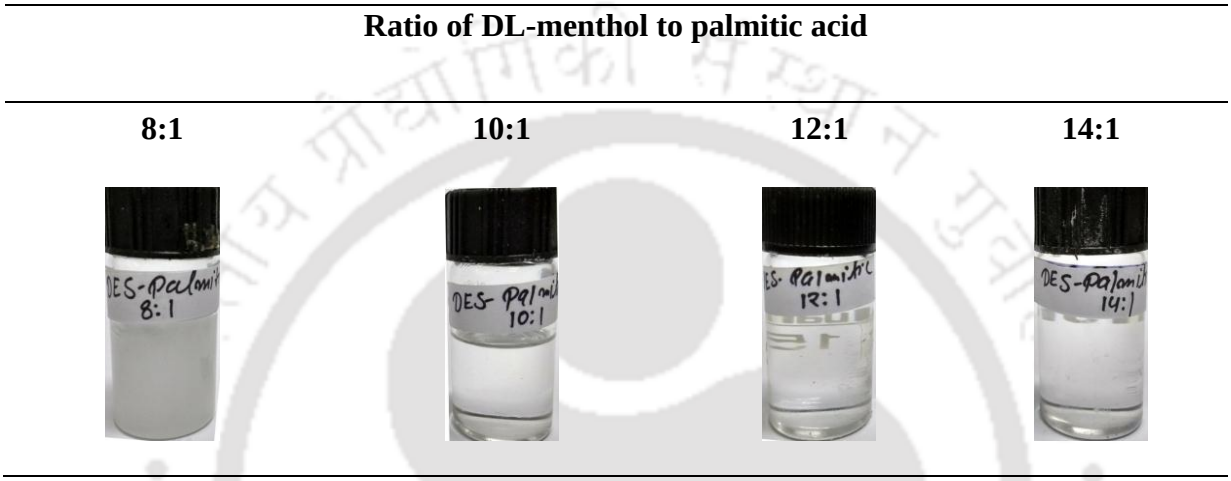

Figure 2.23: Formation of DES-4 with different molar ratio of DL-menthol to Palmitic acid.

2.4. Physicochemical Properties of DES

The next step relates to the measurement of the physicochemical properties of DESs [31] Economically, physicochemical properties play a very important role in designing the process equipment, piping and pumping.

2.4.1. Density and Viscosity

The density and viscosity were measured in the temperature range 293.15 - 353.15 K. Table 2.7 shows the physicochemical properties namely density and viscosity at different temperature of DES-1. These are also compared with experimental densities [19-20]. The density of all the solvents and DES were measured by a DMA 4500 M densitometer (Anton Paar Make) with a relative expanded uncertainty of 0.003. The viscosity of DESs were measured by an interfacial rheometer (Model: Physica MCR301, Anton-Paar Make) with a relative expanded uncertainty of 0.033.Figure 2.24 shows the density of the all synthesized

DESs in the temperature range 293.15-353.15 K. As observed, the density of the DES decreases as the chain of carbon atom increases. The order of the density is found to follow the order given below:

DES-1 (DL-menthol + Decanoic acid) > DES-2 (DL-menthol + Lauric acid) > DES-3 (DL-menthol + Myristic acid) > DES-4 (DL-menthol + Palmitic acid)

Table 2.7: The Experimental Density and Viscosity Data of Pure DL-menthol and Lauric acid based DES at p = 1 atm and Different Temperatures[a]

Temperature (K)	Density (g cm^{-3})[b]		Viscosity (mPa)[b]	
	Present work	Lit[19-20]	Present work	Lit[19-20]
293.15	0.8971	0.9002	21.810	29.689
303.15	0.8898	0.8930	12.500	16.957
313.15	0.8826	0.8857	7.657	10.527
323.15	0.8753	0.8780	5.112	7.057
333.15	0.8678	0.8703	3.623	4.872
343.15	0.8603	0.8631	2.670	3.599
353.15	0.8526	0.8549	2.088	2.650
AAD	0.003		2.84	

[a]The standard uncertainty u are $u\,(T)$ = 0.1 K, $u\,(p)$ = 1 kPa;[b]the relative expanded uncertainty U are $U_r(\rho)$ = 0.003, and $U_r(\eta)$ = 0.033; $AAD = \sum_{i=n}^{n} \frac{|w_i^{cal} - w_i^{exp}|}{n}$

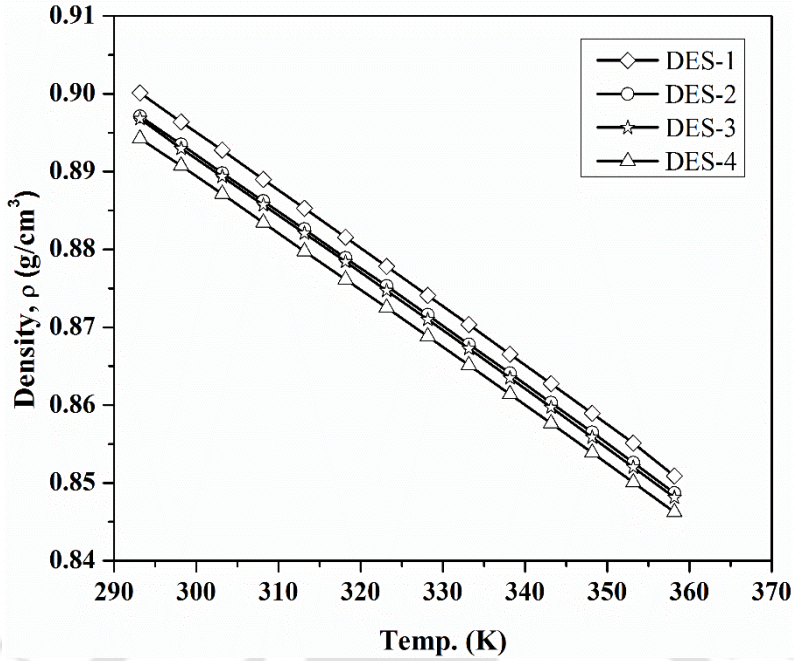

Figure 2.24: Density of DL-menthol based DESs at different temperatures

The density values of the studied DESs were fitted as a function of temperature by a linear relationship as follows:

$$\rho = a + bT \quad (2.3)$$

Where ρ is the density, T is temperature, *a* and *b* are the fitting parameters for the DES molar ratio under consideration. An interesting observation is that the density of all the DES is less than that of water implying easier separation with aqueous systems.

Figure 2.25 shows the viscosity of all DESs from *T*= 293.15-363.15 K. The viscosities of DESs have been found to be contrary to the density pattern as per the following order:

DES-1 (DL-menthol + Decanoic acid) < DES-2 (DL-menthol + Lauric acid) < DES-3 (DL-menthol + Myristic acid) < DES-4 (DL-menthol + Palmitic acid)

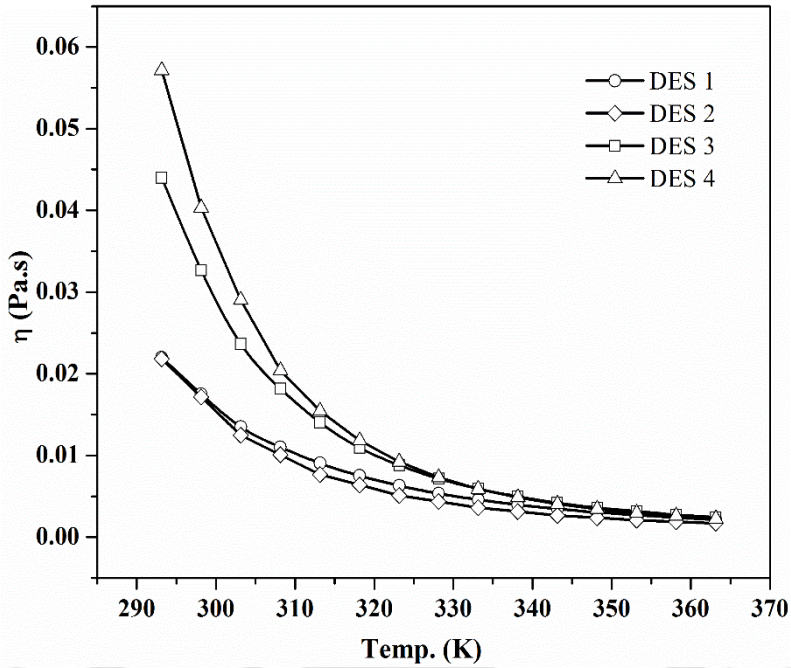

Figure 2.25: Viscosity of DL-menthol based DESs at different temperatures.

Table 2.8 shows the density and viscosity of DESs at T = 298.15 K and p = 1 atm. It clearly shows that density and viscosity show an opposite trend for the DESs especially with increasing length of carbon chain in organic acid [31]. This implies that decanoic acid based DES may be adopted as the suitable DES when used in a hybrid extraction system, as the aqueous rich phase being the heavier phase may be easy to separate This has been discussed separately in chapter 4. Thus lower the viscosity of decanoic acid based DES, higher the mass transfer of lower alcohol into the solvent phase.

Table 2.8: Properties of DL-menthol and organic acid based synthesized hydrophobic DESs at T= 298.15 K and p = 1 atm

Molecular Compound	Density (g/cm^3)	Viscosity (Pa.s)
DES-1 (Decanoic acid:DL-menthol)	0.8964	0.0163
DES-2 (Lauric acid:DL-menthol)	0.8935	0.0172
DES-3 (Myristic acid:DL-menthol)	0.8930	0.0327
DES-4 (Palmitic acid:DL-menthol)	0.8907	0.0403

2.4.2. Thermal Analysis

Thermal properties via DSC (Model: TGA/DSC1 Star System, Make: Mettler Toledo, Switzerland) and TGA (Model: TG 209 F1 Libra, Make: NETZSCH instrument, Germany) [27, 28] are conducted on the synthesized DES.

2.4.2.1 Differential Scanning Calorimetry (DSC)

The solid-liquid phase transition was measured from 243.15 K to 323.15 K with a heating and cooling rate of 5 K/min. The condensation in the furnace was avoided with the use of dry nitrogen as purge gas. The flow rate of the purge gas was kept at 60 ml/min. Indium with a melting point of 429.75 K was used as a standard for calibration. Samples of DES and DL-menthol ranging from 5-10 mg were then transferred to aluminium DSC pan and hermetically sealed so as to prevent its vaporization. The uncertainty in the melting point temperature obtained by calculation of the standard deviation of three consecutive measurements for the same sample was found to be better than ±1 K.

Figure 2.26 shows the DSC plots of the DES based on DL-menthol and Lauric acid or DES-2 and the starting compounds. DES-2 possesed a melting point (15 ^{o}C), which is lower than that of DL-menthol (35.30 ^{o}C), and lauric acid (46.28 ^{o}C). It is to be noted that DL-menthol presents two melting point namely 28.31 °C and 35.3 °C. This is primarily due to its polymorphs α and β. This closely agrees with the results of both Florindo et al. [30] and Rebiero et al. [31] where the corresponding value of 27 °C and 34 °C were obtained.

Figure 2.27: shows the DSC plots for DES-1 to DES-4. The melting point of the DESs are found to be in the increasing order as given by: DES-1 (DL-menthol + Decanoic acid) < DES-2 (DL-menthol + Lauric acid) < DES-3 (DL-menthol + Myristic acid) < DES-4 (DL-menthol + Palmitic acid). Overall the melting point tends to increase with the length of organic acids.

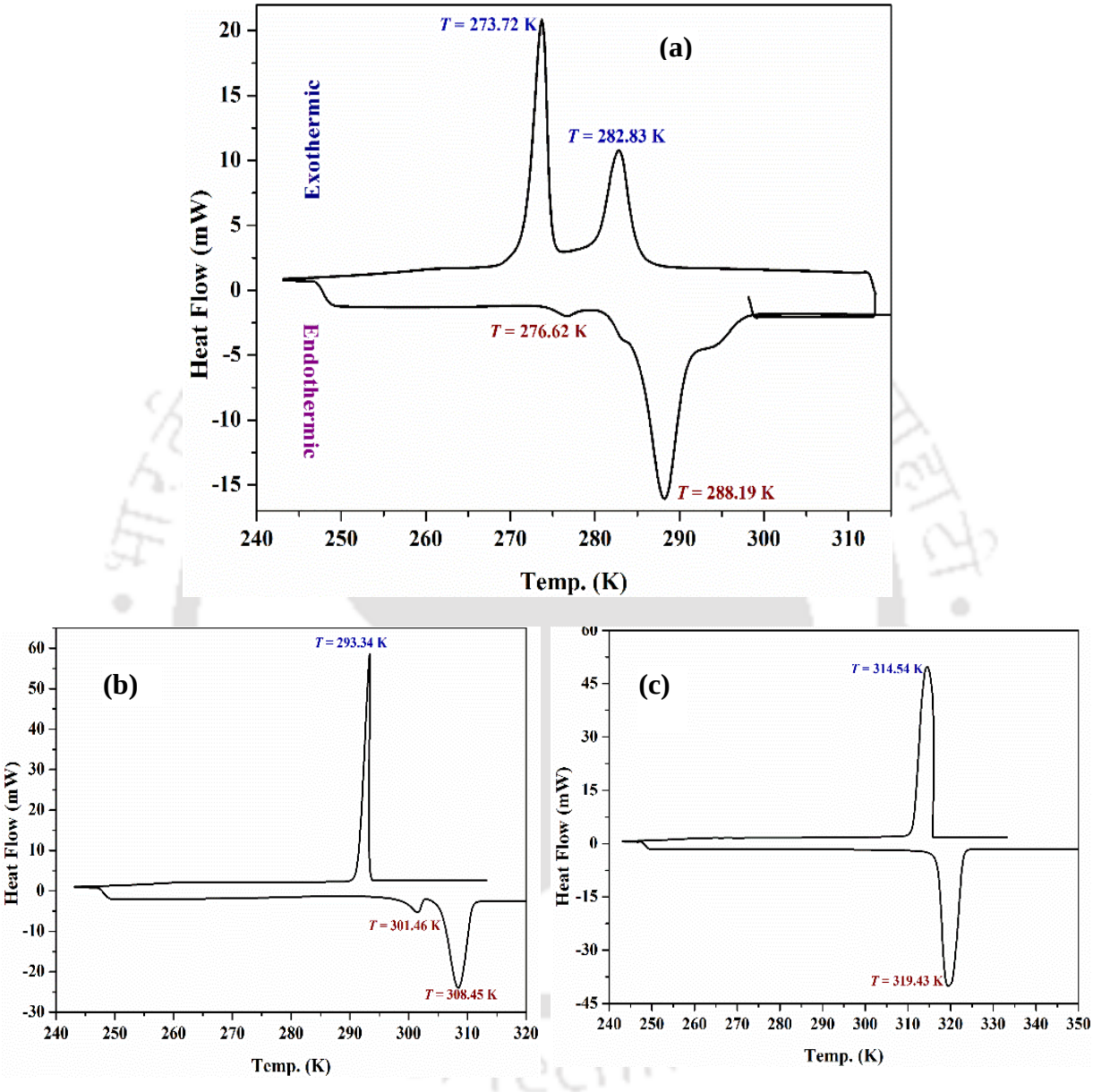

Figure 2.26: Differential Scanning Calorimetry (DSC) for (a) DES-2: DL-menthol and Lauric acid (b) DL-menthol and (c) Lauric acid

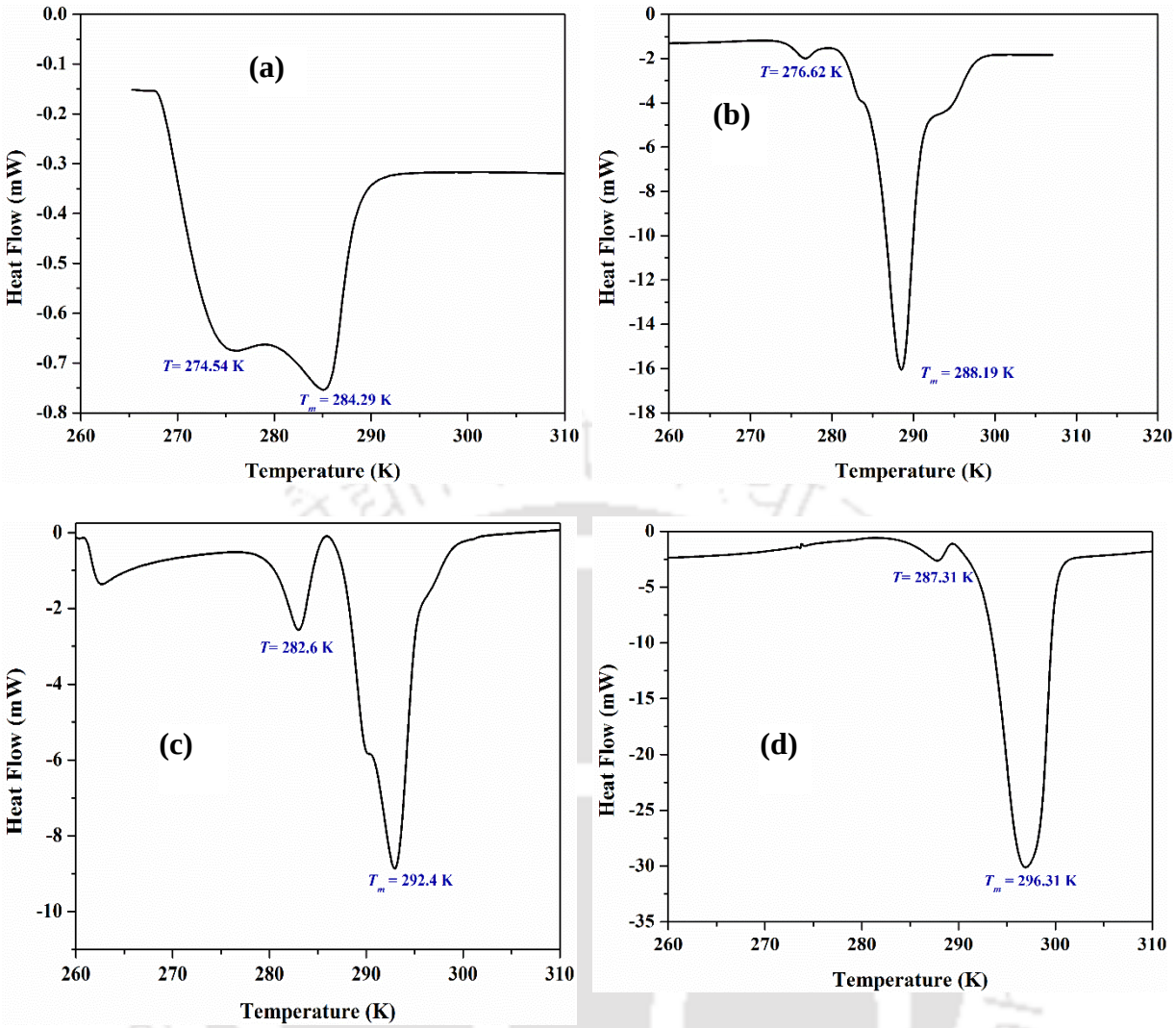

Figure 2.27: Differential Scanning Calorimetry (DSC) of Menthol basedDESs: (a) DES-1 (b) DES-2 (c) DES-3 and (d) DES-4

2.4.2.2 Thermogravimetric Analysis (TGA)

Once the melting point is established, the thermal stability also needs to be elucidated. Overall the TGA has been used to measure the respective eutectic mixture decomposition temperature (T_{dec}). TGA analysis was performed on a NETZSCH make, TGA instrument (TG 209 F1 Libra®, Germany)under an inert atmosphere by continuously purging with N_2 gas at a flowrate of 40 ml/min. ~10 mg of sample was loaded with the heating rate of 10 K/min over the temperature range 303.15-673.15 K. Figure 2.28 and Table 2.9 shows the TGA for all the DESs. It has been observed that decanoic acid based DES shows good thermal stability as compared to other DESs. By looking at the TGA of the starting material namely DL-menthol and lauric acid, it can be said the stability of the DES-2 lies in between them.

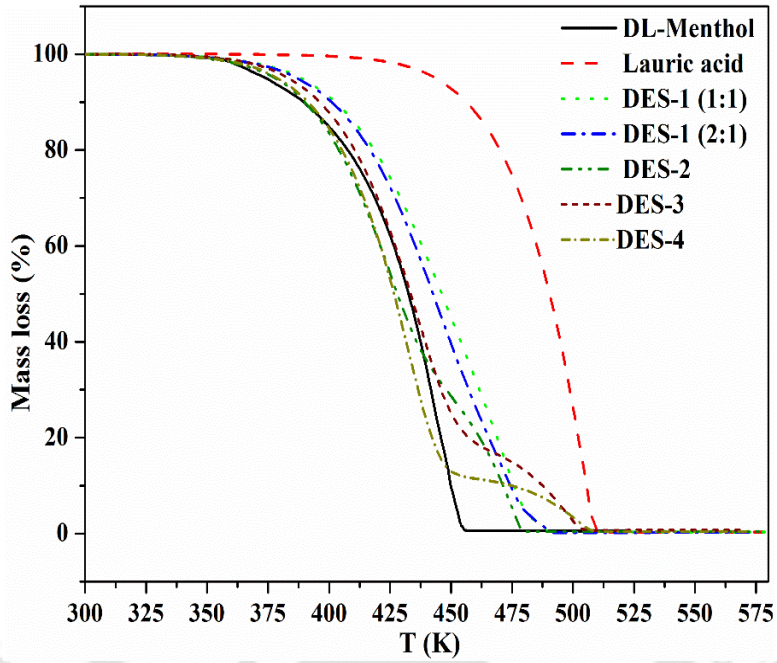

Figure 2.28: ThermoGravimetric Analysis (TGA) for menthol based DESs.

Table 2.9: Thermal properties of studied eutectic mixtures: Decomposition temperature (T_{dec}) and normal melting temperature (T_m).

Compound Name	T_m (K)	T_{deg} (K)
Pure compounds		
DL-menthol	307.15-309.15	309.15
Capric acid or Decanoic acid	302.15-305.15	305.15
Lauric acid or Dodecanoic acid	316.15-318.15	318.15
Myristic acid or Tetradecanoic acid	327.15-330.15	330.15
Palmitic acid or Hexadecanoic acid	335.15-339.15	339.15
Eutectic Mixture		
DES1 (DL-menthol:Decanoic acid)	284.19	498.15
DES2 (DL-menthol:Lauric acid)	288.19	504.15
DES3 (DL-menthol:Myristic acid) 4:1	292.32	518.15
DES4 (DL-menthol:Palmitic acid) 12:1	296.49	541.15

2.5. Quantum Calculations

After a thorough analysis of its physiochemical properties, a need it felt to evaluate the effectiveness of both HBA and HBD through quantum chemical method such as COSMO-SAC.One way is to evaluate the sigma profile of the HBA and HBD and then analyze its donor and acceptor groups. In the COSMO system, sigma profile describes the local polarity of molecular surface and determines the interaction energies of the molecular surface. A cut-off region for hydrogen bond donor (σ_{HB}<−0.0082 e/Å^2) and hydrogen bond acceptor (σ_{HB}>+0.0082 e/Å^2) is adopted for hydrogen bond donors and acceptors respectively. This means that the profile lying in the left side of σ_{HB} will have the ability to donate its hydrogen atom for hydrogen bonding while profile lying in the right side of σ_{HB} will have the ability to accept the incoming hydrogen atom or entity for hydrogen bonding.

2.5.1. Geometry Optimization of HBD and HBA

The initial structures of DL-menthol and organic acids were drawn using the molecule visualizer Gauss View 5.0.

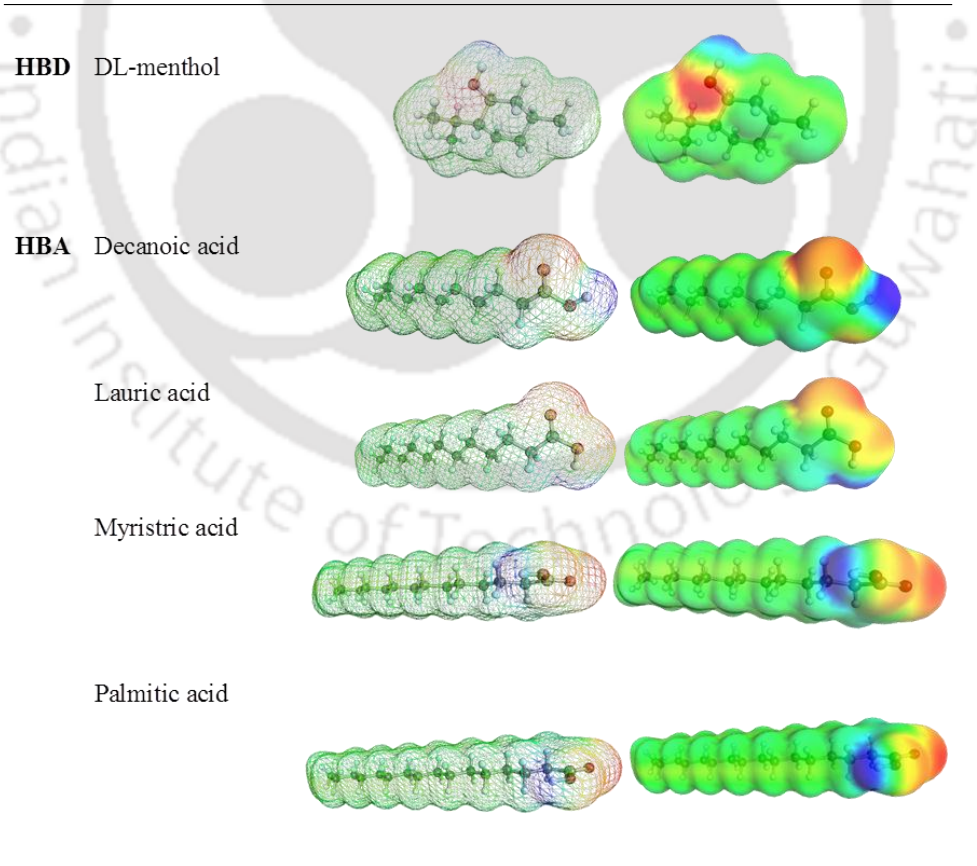

Figure 2.29: COSMO surfaces of Organic acids (HBD) and DL-menthol (HBA) molecules used for DES syntheses.

The geometry optimization was carried out using the DFT theory B3LYP along optimized structure with 6-31G* basis set. The COSMO file was generated by BVP86/TZVP/density functional theory (DFT) level of theory [32]. Gaussian 09 was used to generate the above procedure or also termed as COSMO file initiation. Figure 2.29 shows COSMO surfaces for DL-menthol (HBA), decanoic acid, lauric acid, myristic acid and palmitic acid as HBD molecules. Surfaces color indicates screening charge density with its respective magnitude.The middle column of Figure 2.29 shows the segmented regions. While the blue regions have negative screening charge values, green regions indicates neutral and red region positive values. For e.g. the oxygen in both menthol and organic acid shows a red region which implies that the charges developed are positive in nature. This is true as the COSMO induced screening charges are opposite in nature to its inherent charge. Using the same analogy, the green regions consists of the hydrogens while the blue region is due to the presence of hydrogen atoms.

2.5.2. Sigma Profile of HBA and HBD

Sigma profile for the hydrogen bond donor (HBD) and acceptor (HBA) regions are shown in Figure 2.31. DL-menthol does not have any appreciable acceptors in the left side of the profile which indicates that it is the HBD or the organic acid which is responsible for the bonding with the incoming molecules. This is evident as a small hump lies in the right side of σ_{HB} cut off. This is primarily due to the oxygen atoms of the organic acid which is negatively charged. Overall a similar trend is also seen when combining the HBD and HBA profile i.e the DES profile (Figure 2.32). For the COSMO file the global adjustable parameter used here were surface area of the segment (a_{eff} =6.32 Å^2), misfit energy interaction constant [α' = 8419 kcal Å^4/(mol e^2)], the cutoff for hydrogen-bonding interaction (σ_{HB} =0.0084 e/Å^2), and hydrogen-bonding interaction constant [c_{HB}= 75,006 kcal Å^4/(mol e^2)].

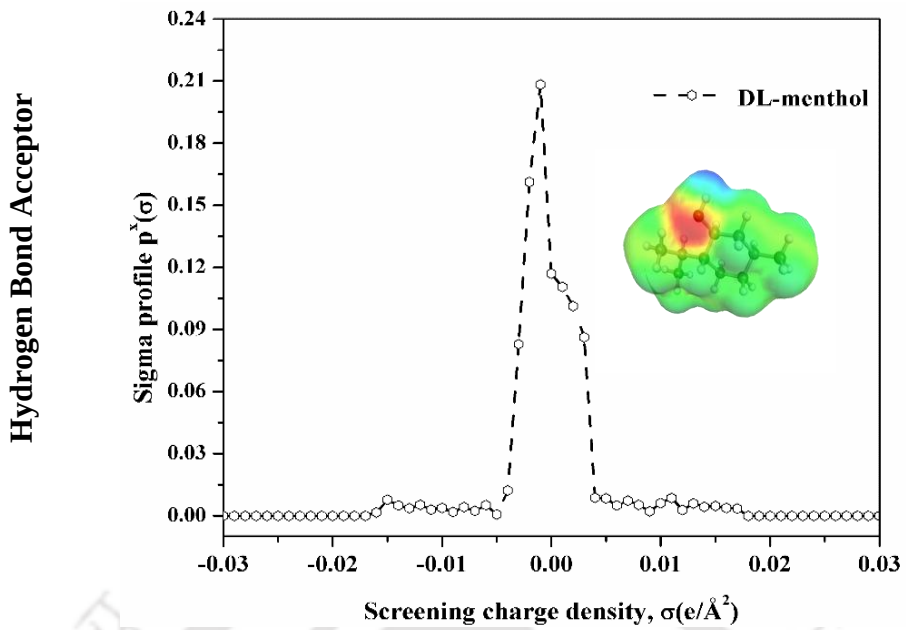

Figure 2.30: Sigma profile and COSMO segmented surface of HBD and HBA molecules

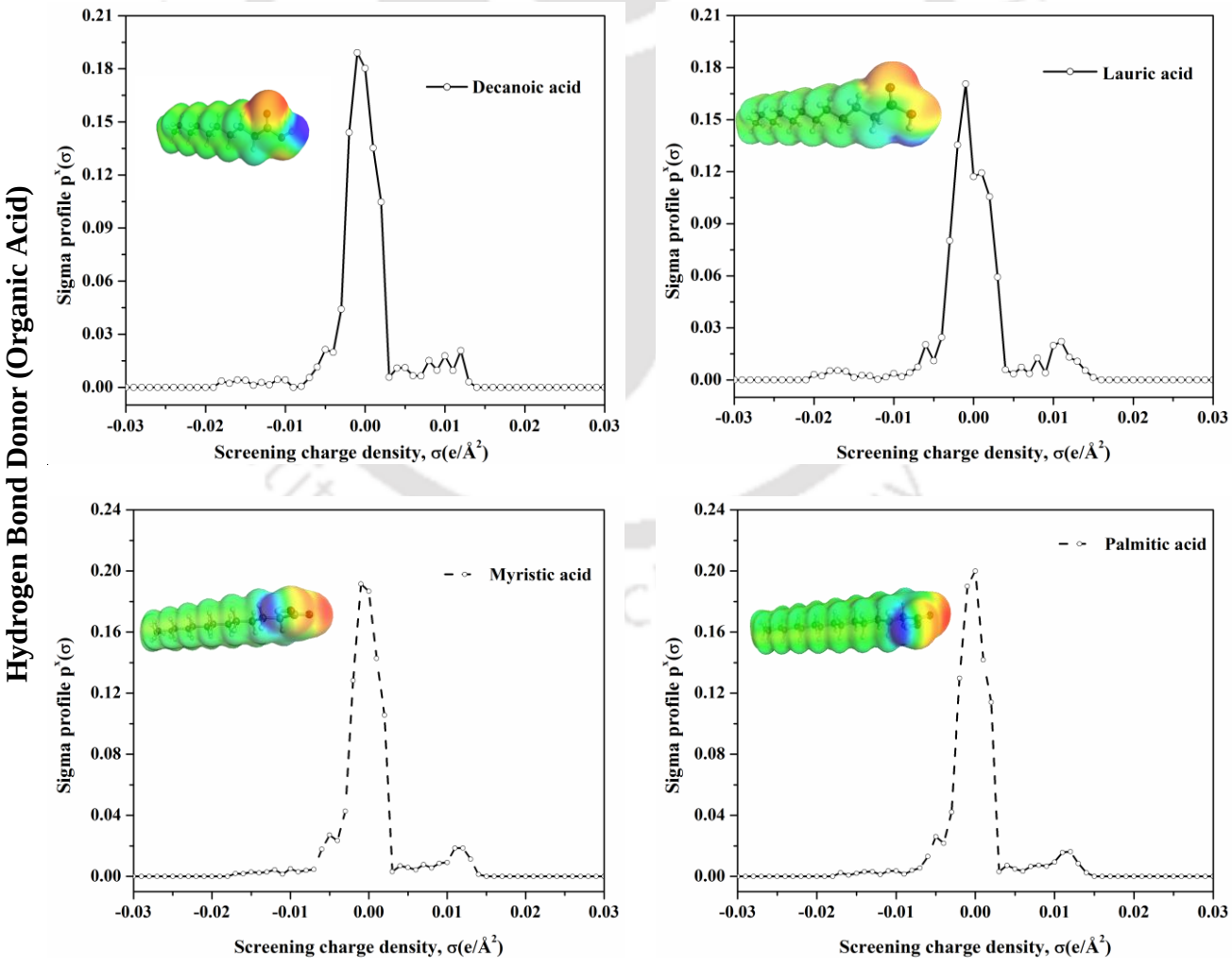

Figure 2.31: Sigma profile and COSMO segmented surface of HBD and HBA molecules

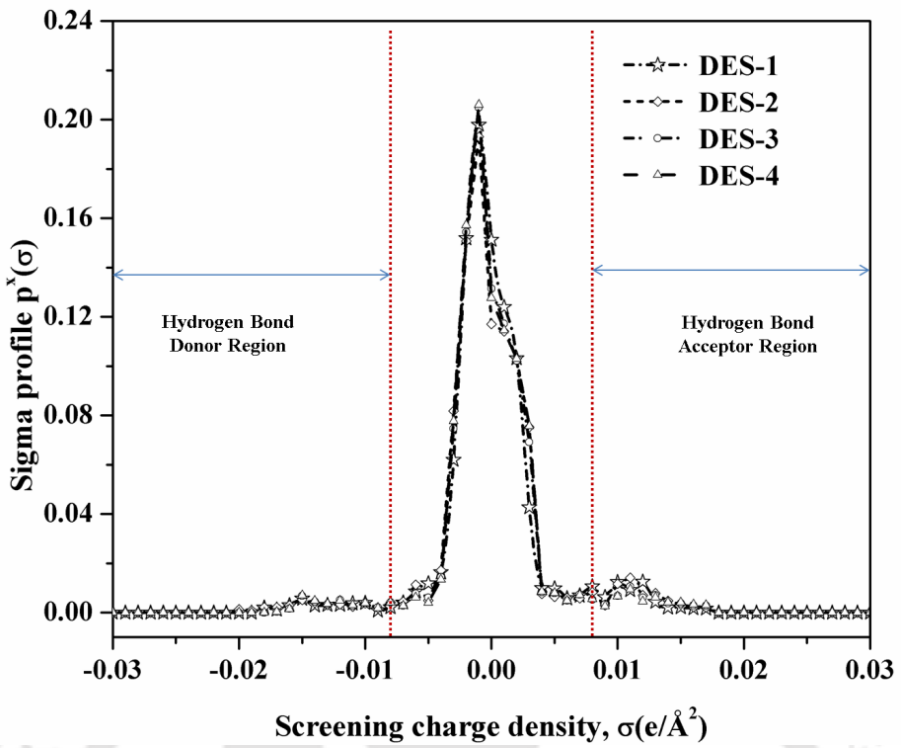

Figure 2.32: COSMO segmented surface for the Menthol based DES

After a thoroughly evaluation of the pure component properties, we shell now move towards its evaluation as solvent in the form of LLE measurement in the next chapter.

References

1. A.P. Abbott, G. Capper, D.L. Davies, R.K. Rasheed, V. Tambyrajah: Novel solvent properties of choline chloride/urea mixtures. Chem. Comm. (2003) 70-71
2. A. Abo-Hamad, M. Hayyan, M.A. AlSaadi, M.A. Hashim: Potential applications of deep eutectic solvents in nanotechnology. Chem. Eng. J. 273 (2015) 551-567
3. E.L. Smith, A.P. Abbott, K.S. Ryder: Deep eutectic solvents (DESs) and their applications. Chem. Rev. 114 (2014) 11060-11082
4. A.S. Gouveia, F.S. Oliveira, K.A. Kurnia, I.M. Marrucho: Deep eutectic solvents as azeotrope breakers: liquid–liquid extraction and COSMO-RS prediction. ACS Sustainable Chem. Eng. 4 (2016) 5640-5650

5. A. Mohsenzadeh, Y. Al-Wahaibi, A. Jibril, R. Al-Hajri, S. Shuwa: The novel use of deep eutectic solvents for enhancing heavy oil recovery. J. Pet. Sci. Eng. 130 (2015) 6-15
6. P.K. Naik, P. Dehury, S. Paul, T. Banerjee: Evaluation of Deep Eutectic Solvent for the selective extraction of toluene and quinoline at T= 308.15 K and p= 1 bar. Fluid Phase Equilib. 423 (2016) 146-155
7. N.R. Rodriguez, J. Ferre Guell, M.C. Kroon: Glycerol-Based Deep Eutectic Solvents as Extractants for the Separation of MEK and Ethanol via Liquid–Liquid Extraction. J. Chem. Eng. Data 61 (2016) 865-872
8. M. Mohan, P.K. Naik, T. Banerjee, V.V. Goud, S. Paul: Solubility of glucose in tetrabutylammonium bromide based deep eutectic solvents: Experimental and molecular dynamic simulations. Fluid Phase Equilib. 448 (2017) 168-177
9. C.P. Fredlake, J.M. Crosthwaite, D.G. Hert, S.N. Aki, J.F. Brennecke: Thermophysical properties of imidazolium-based ionic liquids. J. Chem. Eng. Data 49 (2004) 954-964
10. P. Wasserscheid, R. van Hal, A. Bösmann: 1-n-Butyl-3-methylimidazolium ([bmim]) octylsulfate—an even 'greener'ionic liquid. Green Chem. 4 (2002) 400-404
11. B. Tang, W. Bi, M. Tian, K.H. Row: Application of ionic liquid for extraction and separation of bioactive compounds from plants. J. Chromatogr. B 904 (2012) 1-21
12. P. Elavarasan, K. Kondamudi, S. Upadhyayula: Synthesis of antioxidants: Green chemistry route. Int. J. Chem. Sci 8 (2010) 578-584
13. P.N. Amaniampong, Q.T. Trinh, J.J. Varghese, R. Behling, S. Valange, S.H. Mushrif, F. Jérôme: Unraveling the mechanism of the oxidation of glycerol to dicarboxylic acids over a sonochemically synthesized copper oxide catalyst. Green Chem. (2018)
14. S.-T. Lin, S.I. Sandler: A priori phase equilibrium prediction from a segment contribution solvation model. Ind. Eng. Chem. Res. 41 (2002) 899-913
15. A. Klamt: Conductor-like Screening Model for Real Solvents: A New Approach to the Quantitative Calculation of Solvation Phenomena. J. Phys. Chem. 99 (1995) 2224-2235
16. C.-M. Hsieh, S.I. Sandler, S.-T. Lin: Improvements of COSMO-SAC for vapor–liquid and liquid–liquid equilibrium predictions. Fluid Phase Equilib. 297 (2010) 90-97
17. R. Fingerhut, W.-L. Chen, A. Schedemann, W. Cordes, J.r. Rarey, C.-M. Hsieh, J. Vrabec, S.-T. Lin: Comprehensive Assessment of COSMO-SAC Models for Predictions of Fluid-Phase Equilibria. Ind. Eng. Chem. Res. 56 (2017) 9868-9884

18. W.-L. Chen, C.-M. Hsieh, L. Yang, C.-C. Hsu, S.-T. Lin: A Critical Evaluation on the Performance of COSMO-SAC Models for Vapor–Liquid and Liquid–Liquid Equilibrium Predictions Based on Different Quantum Chemical Calculations. Ind. Eng. Chem. Res. 55 (2016) 9312-9322
19. D. Kundu, T. Banerjee: Multicomponent vapor–liquid–liquid equilibrium prediction using an a priori segment based model. Ind. Eng. Chem. Res. 50 (2011) 14090-14096
20. A. Bharti, T. Banerjee: Enhancement of bio-oil derived chemicals in aqueous phase using ionic liquids: Experimental and COSMO-SAC predictions using a modified hydrogen bonding expression. Fluid Phase Equilib. 400 (2015) 27-37
21. S.-T. Lin, L.-H. Wang, W.-L. Chen, P.-K. Lai, C.-M. Hsieh: Prediction of miscibility gaps in water/ether mixtures using COSMO-SAC model. Fluid Phase Equilib. 310 (2011) 19-24
22. J.M. Prausnitz, R.N. Lichtenthaler, E.G. de Azevedo: Molecular thermodynamics of fluid-phase equilibria, Pearson Education (1998)
23. S. Bhoi, D. Dey, T. Banerjee, K. Mohanty: Solid–liquid equilibria predictions for the dissolution of brown coal in ionic liquids using a continuum solvation model. Fuel Process. Technol. 126 (2014) 112-121
24. M. Mohan, V.V. Goud, T. Banerjee: Solubility of glucose, xylose, fructose and galactose in ionic liquids: Experimental and theoretical studies using a continuum solvation model. Fluid Phase Equilib. 395 (2015) 33-43
25. Y. Corvis, P. Négrier, S. Massip, J.-M. Leger, P. Espeau: Insights into the crystal structure, polymorphism and thermal behavior of menthol optical isomers and racemates. CrystEngComm 14 (2012) 7055-7064
26. P.V. Pontes, E.A. Crespo, M.A. Martins, L.P. Silva, C.M. Neves, G.J. Maximo, M.D. Hubinger, E.A. Batista, S.P. Pinho, J.A. Coutinho: Measurement and PC-SAFT modeling of solid-liquid equilibrium of deep eutectic solvents of quaternary ammonium chlorides and carboxylic acids. Fluid Phase Equilib. 448 (2017) 69-80
27. F.C. de Matos, M.C. da Costa, A.J. de Almeida Meirelles, E.A.C. Batista: Binary solid–liquid equilibrium systems containing fatty acids, fatty alcohols and triolein by differential scanning calorimetry. Fluid Phase Equilib. 404 (2015) 1-8
28. F.C. de Matos, M.C. da Costa, A.J. de Almeida Meirelles, E.A.C. Batista: Binary solid–liquid equilibrium systems containing fatty acids, fatty alcohols and trilaurin by differential scanning calorimetry. Fluid Phase Equilib. 423 (2016) 74-83

29. L. Fernandez, L.P. Silva, M.A. Martins, O. Ferreira, J. Ortega, S.P. Pinho, J.A. Coutinho: Indirect assessment of the fusion properties of choline chloride from solid-liquid equilibria data. Fluid Phase Equilib. 448 (2017) 9-14

30. C. Florindo, L. Branco, I. Marrucho: Development of hydrophobic deep eutectic solvents for extraction of pesticides from aqueous environments. Fluid Phase Equilib. 448 (2017) 135-142

31. B.D. Ribeiro, C. Florindo, L.C. Iff, M.A. Coelho, I.M. Marrucho: Menthol-based eutectic mixtures: hydrophobic low viscosity solvents. ACS Sustainable Chem. Eng. 3 (2015) 2469-2477

32. R. Biswas, A. Malviya, T. Banerjee, P. Ghosh, S.M. Ali: Alkali Metal Ion Partitioning with Calix [4] arene-benzo-crown-6 Ionophore in Acidic Medium: Insights from Experiments, Statistical Mechanical Framework, and Molecular Dynamics Simulations. J. Phys. Chem. B 122 (2018) 2102-2112

Chapter 3

Liquid-Liquid Extraction of Lower Alcohols using Conventional Solvents and Hydrophobic Deep Eutectic Solvent

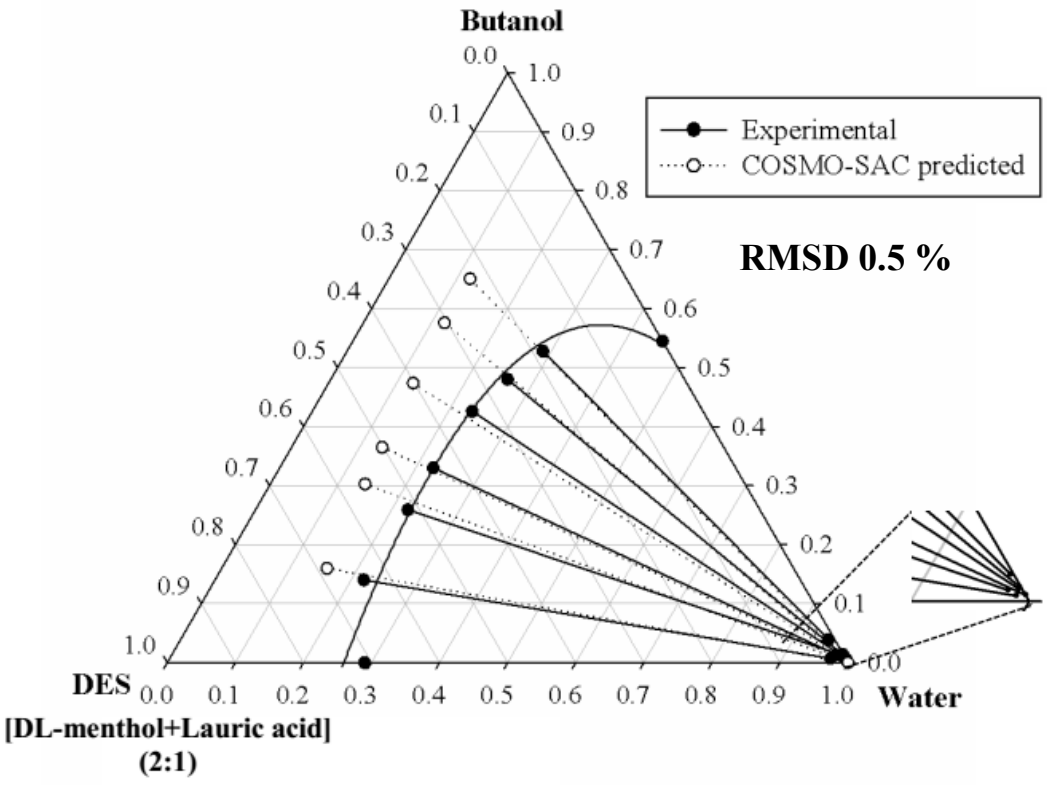

3.1. Introduction

As mentioned earlier distillation is not considered economical as the difference of boiling point of ethanol (78.37 ^{o}C), 1-propanol (97 ^{o}C) and 1-butanol (117.7 ^{o}C) are almost similar to that of water (100 ^{o}C) [1]. Azeotropic distillation, extractive distillation and liquid−liquid extraction, which are three of the most important industrial separation techniques for azeotrope breaking involve the use of an extracting agent. One normally switches to liquid-liquid extraction when component separation (from a mixture of many components) cannot be achieved economically by other mass transfer operations such as distillation, evaporation and crystallization. Solvent extraction is a suitable operation particularly when the solvents possess simultaneously high affinity for alcohol and low solubility with water. A good solvent is required in our case to extract the lower alcohol into extract stream and reject the water in the raffinate outlet stream. Measurement and validation of Liquid−Liquid Equilibria (LLE) is thus a necessary step for evaluating these solvents. In this chapter we shall first obtain the LLE with conventional solvents such as mesitylene and oleyl alcohol and then compare their efficiency with the synthesized hydrophobic DESs.

In the present chapter the extraction of 1-butanol from aqueous stream using low density conventional solvents namely, mesitylene (0.864 gm/cm^3) and oleyl alcohol (0.849 gm/cm^3) is discussed. Thereafter DL-menthol based low density hydrophobic DESs as synthesized in chapter 2 are used for the extraction of lower alcohols (ethanol/1-propanol/1-butanol). In the subsequent sections we have reported the ternary systems, namely, (a) mesitylene (1) + 1-butanol (2) + water (3); (b) oleyl alcohol (1) + 1-butanol (2) + water (3) and (c) DES-1/DES-2/DES-3/DES-4 (1) + ethanol/1-propanol/1-butanol (2) + water (3) at T =298.15-303.15 K and p=1 atm.

3.2. Chemicals and Materials

Table 3.1 shows the chemicals used for the LLE in the present study along with their purities. Purities of mesitylene, oleyl alcohol, ethanol, 1-propanol and 1-butanol were confirmed by ^{1}H NMR spectroscopy where the analysis of peaks indicated negligible impurities. The NMR solvent, Dimethyl sulfoxide-d6 (DMSO-d6 ≥99.8%) supplied by Merck, Germany was used as received. All chemicals were of analytical grade and were used without further purification. In order to check its purity, the densities were measured by

Anton Paar Density Meter (DMA 4500 M) so as to compare the manufacturer specification. Further the viscosities were also measured by a viscometer (Anton Paar Phsica MCR301). The water content of mesitylene, oleyl alcohol and synthesized DESs were measured by Karl Fischer Titrator (870 KF Titrino plus). As discussed in chapter 2, the measured densities of all the chemicals were within ±1% of their literature values.

Table 3.1: Compound name, solubility, purities and source of the chemicals used for LLE in the present study.

Sl. No.	Compound Name	Solubility in water (g/lit.)	B.P. (°C)	Chemical Purity (vol. %)	Sources
1. 1	Mesitylene	0.420	214.6	≥99.0	Sigma Aldrich, Germany
2.	Oleyl alcohol	0.059	298.9	≥99.0	Otto Chemie Pvt Ltd
3.	Ethanol	infinite	78.24	≥99.9%	Merck, Germany
4.	1-Propanol	infinite	98	≥99%	Merck, India
5.	1-Butanol	75	117.7	≥99%	Merck, India
6.	Chloroform-d	NA		≥99.8	Merck, India
7.	Dimethyl sulfoxide-d_6	NA		≥99.8	Merck, India

NA: Not Available

Figure 3.1 shows the structure of conventional solvents such as mesitylene, oleyl alcohol used for the LLE of lower alcohols in the present study. Mesitylene and oleyl alcohol are nowadays commercially used for extraction of alcohols [2]. Mesitylene is a derivative of benzene which is produced from coal tar and thus is easily available. However on the other side it is known as a pollutant or VOC when combusted. The extraction experiments if considered at ambient conditions, can reduce the harmful effects of mesitylene, thereby approving their use as potential solvents. On the contrary the other solvent, oleyl alcohol is eco-friendly in nature and also occurs naturally in fish oils. It is known to be completely hydrophobic in nature. Looking at the hydrophobic nature of both the solvents, a need is thus felt to evaluate the effectiveness for extraction by measuring the LLE data with 1-butanol and water.

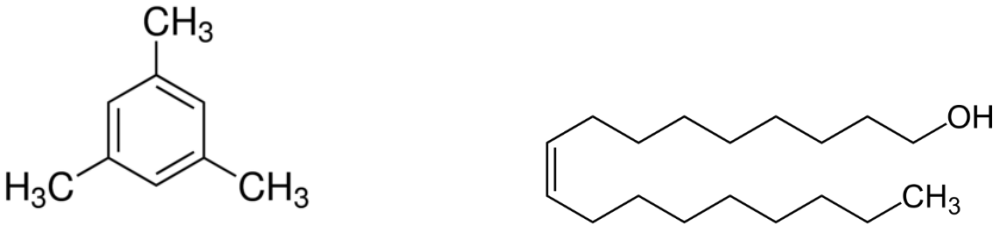

(a) (b)

Figure 3.1: Structures of organic compounds such as, (a) Mesitylene and (b) Oleyl alcohol

3.3. Separation using Mesitylene and Oleyl Alcohol

3.3.1. Experimental Procedure and Composition Analysis

For each experiment known quantities of components were added in 15-30 ml size glass vial. Feed compositions were prepared in such a way that the mixtures of solvent, lower alcohols (ethanol/1-propanol/1-butanol) and water formed heterogeneous regions. The sample bottles were kept inside the incubator shaker (Daihan Lab Tech, China), with the set temperature of 298.15-303.15 K (uncertainty of ± 0.01 K) at 200 rpm for 6 h. After the shaking, the mixture was kept for 24 h so as to ensure equilibrium of the two phases. The composition of the tie lines were evaluated using ^{1}H NMR analysis for both extract (solvent rich) and raffinate (water rich) phases.

For a mixture containing more than two components, the composition analysis by calibration methods like density and refractive index are difficult. The composition analysis can be carried out by Nuclear Magnetic Resonance (NMR) spectroscopy [3]. ^{1}H NMR spectroscopy is a characterization technique that is based on magnetic properties of the proton (^{1}H). ^{1}H nuclei in magnetic field absorb and re-emit electromagnetic radiation. The magnetic properties of hydrogen atom affect the amount of radiated energy. ^{1}H NMR characterization is thus easier for the mixture of multiple compounds. The reliability of the NMR method was checked using known compositions of binary (alcohol + solvent) and ternary mixtures which gave an uncertainty range of ±0.001. For experimental uncertainty, we have also triplicated few experiments. The measured results were found to be in good agreement with the actual compositions with an uncertainty level of ±0.001.Hence in the present study ^{1}H NMR has been used to calculate the mole fraction of LLE compounds.

^{1}H NMR spectroscopy were performed on two clear transparent phases namely solvent rich phase (upper layer) and water rich phase (lower layer).Para film has been used on

the cap of NMR tube to avoid any evaporation losses. For ^{1}H NMR analysis, samples were collected from each phase using syringe for composition analysis. The experiments were performed with a help of Hamilton Syringes of 0.1 mL. Sample of 0.1 ml from each phase was mixed with 0.5 ml of NMR solvent DMSO-d_6 or $CDCl_3$ in a NMR tube (thrift grade, Sigma Aldrich). Reference peak for each ^{1}H NMR solvent, namely DMSO-d_6 (2.5 ppm) and $CDCl_3$ (7.27 ppm) were recorded. Peaks from each ^{1}H NMR sheet were then used for the calculation of mole fraction of each component in respective phase. Due to short time response, the syringes, even though they had to cross the upper phase contamination were not observed. This has been further checked with known binary mixtures by subsequently recording their ^{1}H NMR. Equilibrium was confirmed when two successive sample concentrations gave the same molar concentration at the desired temperature.

3.3.2. Measurement of Liquid−Liquid Equilibria

Peaks from each ^{1}H NMR sheet were then used for the calculation of mole fraction of each component in respective phase. In extract phase (Figure 3.2), three independent hydrogen atoms (>CH-) at ~6.95 ppm was considered to quantify mesitylene. Similarly, in case of oleyl alcohol (Figure3.4), two independent hydrogen atoms at ~5.34 ppm quantified oleyl alcohol. The methyl group (-CH_2-) having a peak at ~3.75 ppm was considered as the corresponding peak for 1-butanol. Due to the shifting of the peak in the mixture [4], water shows a peak at ~5.0 ppm in $CDCl_3$ solvent. In raffinate phase (Figure 3.3), three independent hydrogen displayed peak at ~6.79 ppm, which was considered to quantify mesitylene. Similarly, in case of oleyl alcohol two independent hydrogen atoms at ~4.77 ppm was considered to quantify oleyl alcohol (Figure 3.5). Methyl group (-CH_2-) having a peak at ~3.40 ppm was again considered as the reference for computing the concentration of 1-butanol. As before water shows a peak at ~3.97 ppm [5] in DMSO-d_6. The concentrations of each individual component [6, 7] were then calculated by Eq. (3.1) as given below

$$x_i = \frac{H_i}{\sum_{i=1}^{n} H_i} \tag{3.1}$$

Where, H_i = the peak area of a single hydrogen for sample (s) and x_i = the mole fraction of component in the mixture. Since used solvents are hydrophobic in nature, mole fraction of solvent in aqueous phase was limited to 0.001 - 0.002. The corresponding mole fraction of water in solvent rich phase or extract phase was also found to be 0.089 - 0.066. In all the

systems, type I LLE behavior has been observed. NMR spectra for raffinate phase is found to be almost free of solvent but predominantly water (Figure 3.3 and Figure 3.5). From this it can be confirmed that the points of raffinate phase lie in the extreme corner of the binary axis of water and 1-butanol. The LLE experimental data for the systems, mesitylene (1) + 1-butanol (2) + water (3) and oleyl alcohol (1) + 1-butanol (2) + water (3) are reported in Table 3.2 and Table 3.3 respectively.

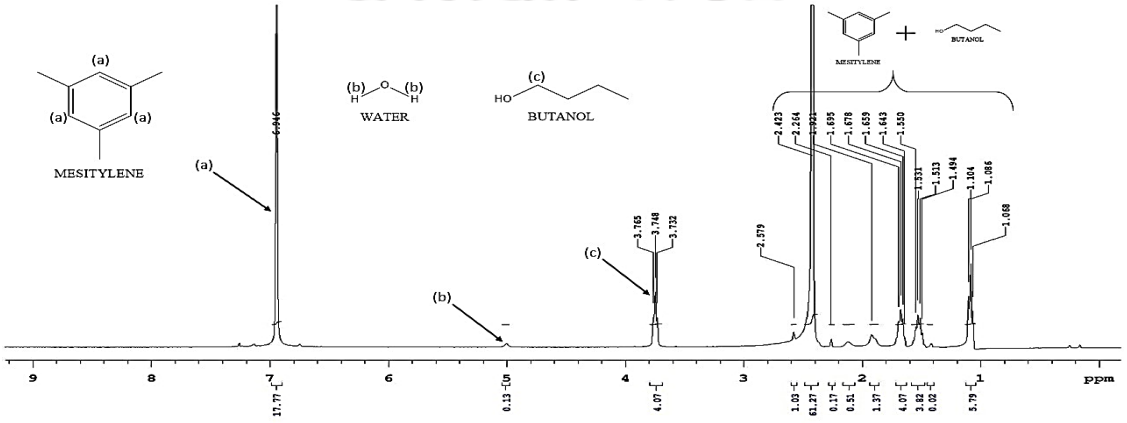

Figure 3.2: ^{1}H NMR spectra for extract phase of mesitylene (1) + 1-butanol (2) + water (3) system.

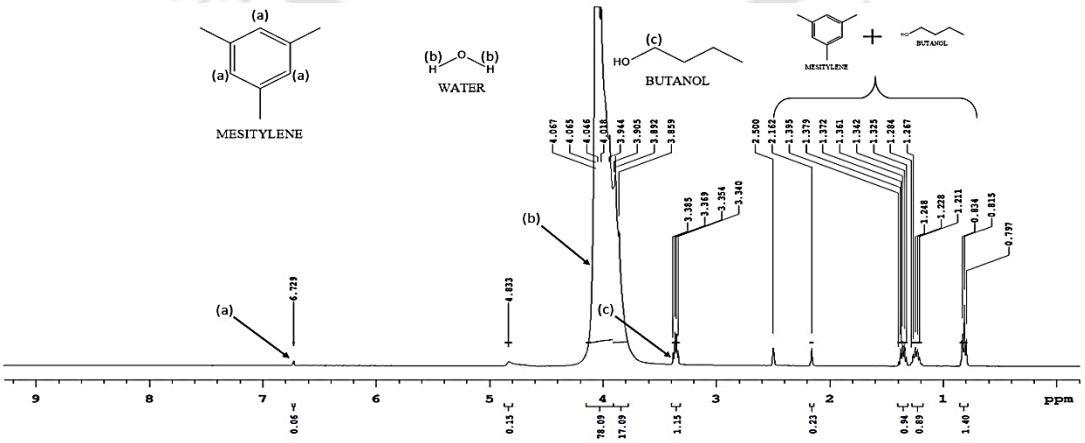

Figure 3.3: ^{1}H NMR spectra for raffinate phase of mesitylene (1) + 1-butanol (2) + water (3) system.

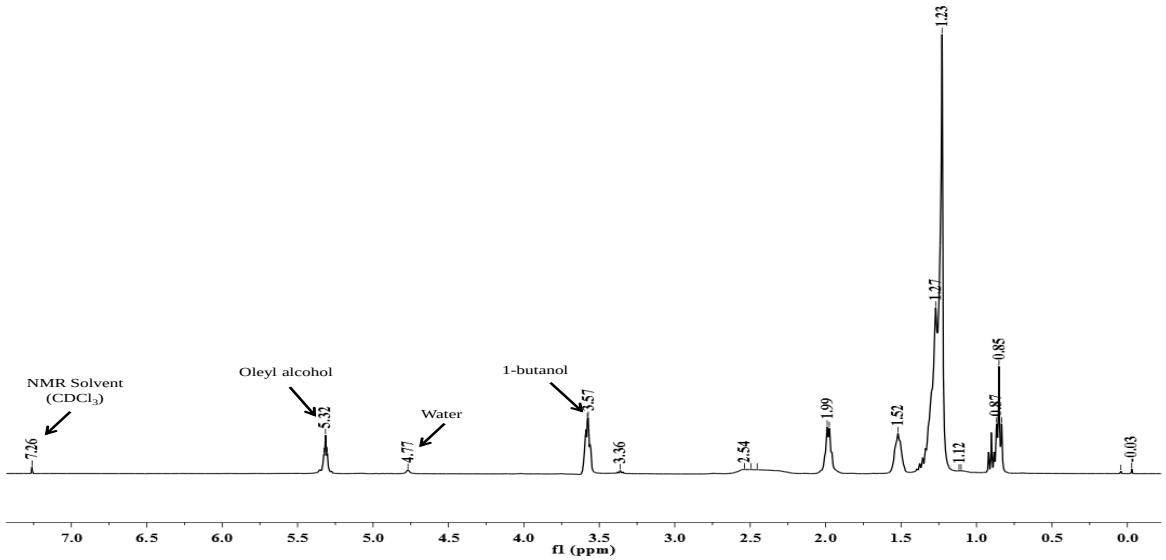

Figure 3.4: ^{1}H NMR spectra for extract phase of oleyl alcohol (1) + 1-butanol (2) + water (3) system.

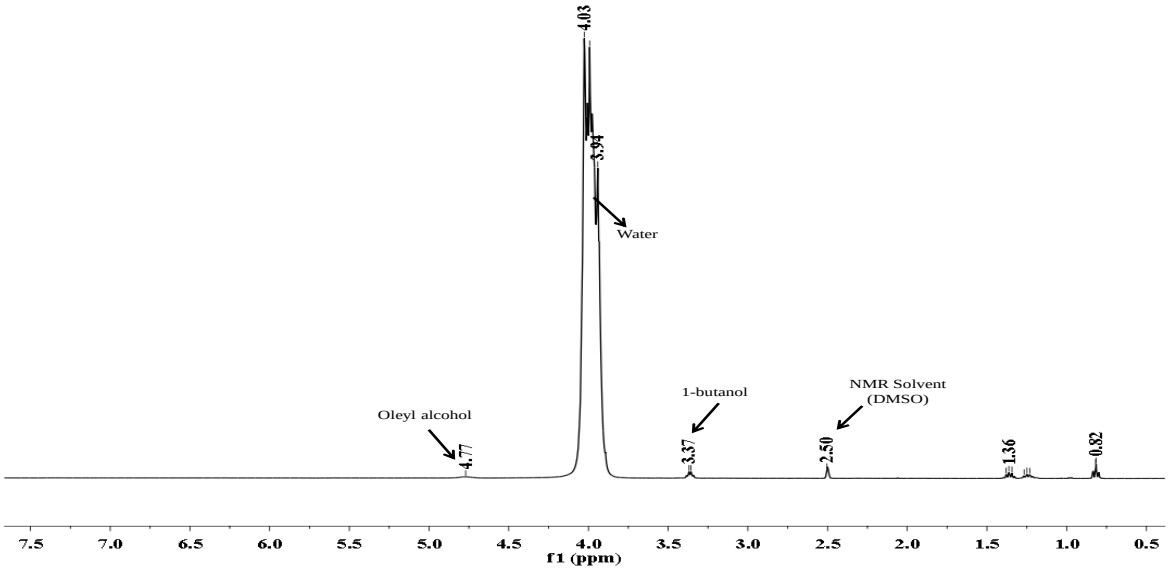

Figure 3.5: ^{1}H NMR spectra for raffinate phase of oleyl alcohol (1) + 1-butanol (2) + water (3) system.

3.3.3. Measurement of distribution coefficient (β) and selectivity (S)

The distribution coefficient (β) and selectivity (S) of 1-butanol [8] are calculated using Eqs. (3.2) and (3.3) as follows:

$$\beta_{alc} = \frac{x_{alc}^{DES}}{x_{alc}^{Water}} \tag{3.2}$$

$$S = \beta_{acl} \Big/ \beta_{water} \tag{3.3}$$

Here x_{alc} and x_w are the mole fractions of alcohol and water respectively. The superscripts DES and water represents the extract (E) and raffinate (R) phase, respectively. Higher values of selectivity indicate a better ability for the extraction of 1-butanol from water. The distribution coefficient refers to the amount of solvent (mesitylene and oleyl alcohol) used to effect the separation. Table 3.2 and Table 3.3 also shows the comparison of distribution coefficient (β) and selectivity (S) for the extraction of 1-butanol at lower concentrations using mesitylene and oleyl alcohol as an extraction solvent respectively. It reports a value close to infinity and ~6367 for mesitylene and oleyl alcohol respectively.

Table 3.2: Experimental tie line data [7] for Mesitylene (1) + 1-Butanol (2) + Water (3) at T = 298.15 K and p = 1 atm.

Extract phase			Raffinate phase			$\beta_{1\text{-butanol}}$	Selectivity (S)
$x_{\text{mesitylene}}$	$x_{1\text{-butanol}}$	x_{water}	$x_{\text{mesitylene}}$	$x_{1\text{-butanol}}$	x_{water}		
0.927	0.073	0.000	0.000	0.012	0.988	6.2	-
0.823	0.177	0.000	0.000	0.011	0.989	16.7	-
0.738	0.254	0.008	0.001	0.012	0.988	21.3	2591.2
0.645	0.330	0.025	0.000	0.011	0.989	28.9	1126.6
0.576	0.397	0.026	0.000	0.008	0.992	50.6	1913.6
0.496	0.446	0.059	0.000	0.014	0.986	32.5	542.6
0.427	0.497	0.077	0.001	0.013	0.986	37.6	481.7
0.373	0.529	0.098	0.000	0.013	0.987	39.5	398.9

Standard uncertainties are u(T) = 0.01 K, u(x) = 0.001

Table 3.3: Experimental tie line data [7] for Oleyl alcohol (1) + 1-Butanol (2) + Water (3) at T= 298.15 K and p = 1 atm.

Extract phase			Raffinate phase			$\beta_{1\text{-butanol}}$	Selectivity (S)
x_{OA}	$x_{1\text{-butanol}}$	x_{water}	x_{OA}	$x_{1\text{-butanol}}$	x_{water}		
0.656	0.317	0.027	0.001	0.003	0.996	105.7	3780.7
0.662	0.297	0.041	0.002	0.002	0.996	148.5	3226.7
0.694	0.256	0.050	0.001	0.003	0.997	85.3	1891.8
0.628	0.339	0.033	0.001	0.002	0.997	169.5	6367.7
0.747	0.218	0.035	0.002	0.001	0.997	218.0	6932.6
0.751	0.196	0.053	0.001	0.001	0.998	196.0	2956.4
0.816	0.118	0.066	0.000	0.002	0.997	59.0	777.1

Standard uncertainties are $u(T)$ = 0.01 K, $u(x)$ = 0.001

We shall now focus the effectiveness of the menthol based DES which has been described in chapter 2.

3.4. Separation of Lower Alcohols (LLE) using Hydrophobic DESs

Extraction of lower alcohols was also carried out by synthesized hydrophobic DESs as per details given in chapter 2. The LLE was also conducted in a similar manner as discussed in section 3.3.1 (for conventional solvents). Initially we have compared our estimated uncertainty with similar experimental work such as those of LLE measurements with ionic liquid [9] and other DES [10] and have found them to be reliable. Common to all the experiments, for equilibrium, samples were withdrawn at different time intervals to check their uniformity. Subsequently their concentrations in both the phases were determined by ^{1}H NMR. All the LLE for the ternary systems namely, DES (1) + lower alcohol (2) + water (3), were measured at T =303.15 K and atmospheric pressure.

3.4.1. Extraction of Lower alcohols by DL-menthol and Decanoic acid based hydrophobic DES

The LLE for the ternary systems namely, DES-1 (1) + 1-ethanol (2) + water (3), DES-1 (1) + 1-propanol (2) + water (3) and DES-1 (1) + 1-butanol (2) + 1-water (3) were measured at T =303.15 K and atmospheric pressure. The experimental tie line data are reported in Tables 3.6-3.8 for ethanol, 1-propanol and 1-butanol respectively in terms of mole fraction in the extract and raffinate phase. The compositions have been obtained after the ^{1}H NMR analysis as discussed in section 3.3.2. Figure 3.6 shows the ^{1}H NMR spectra of the extract phase for the system: DES-1 (1) + 1-propanol (2) + water (3). The peaks referred in the composition analysis for DES in extract phase was the >CH- grouping from DL-menthol at 3.15 ppm. In the extract phase the spectra of water gets merged with the -CH_2- attachment of 1-butanol which is at ~3.4 ppm. In such a scenario suitable equations were formed to evaluate the water and alcohol composition separately by using peak information from the -CH_2-OH peak of alcohols at ~1.4 ppm. In order to ensure correct water content in the extract phase, the compositions were confirmed through a Karl Fisher Titrator (MetroOhm 787 KF Titino). The uncertainty of the method for water determination was 0.01 wt %. Water exhibited a dominant peak at 4 ppm (Figure 3.7) in the raffinate rich phase. Considering triplicate runs performed in each point, it was determined that the uncertainty in the water content was always lower than 0.03 % w/w. Tables 3.4-3.5 show algebraic procedure for computing mole fraction in extract and raffinate phase from ^{1}H NMR data respectively.

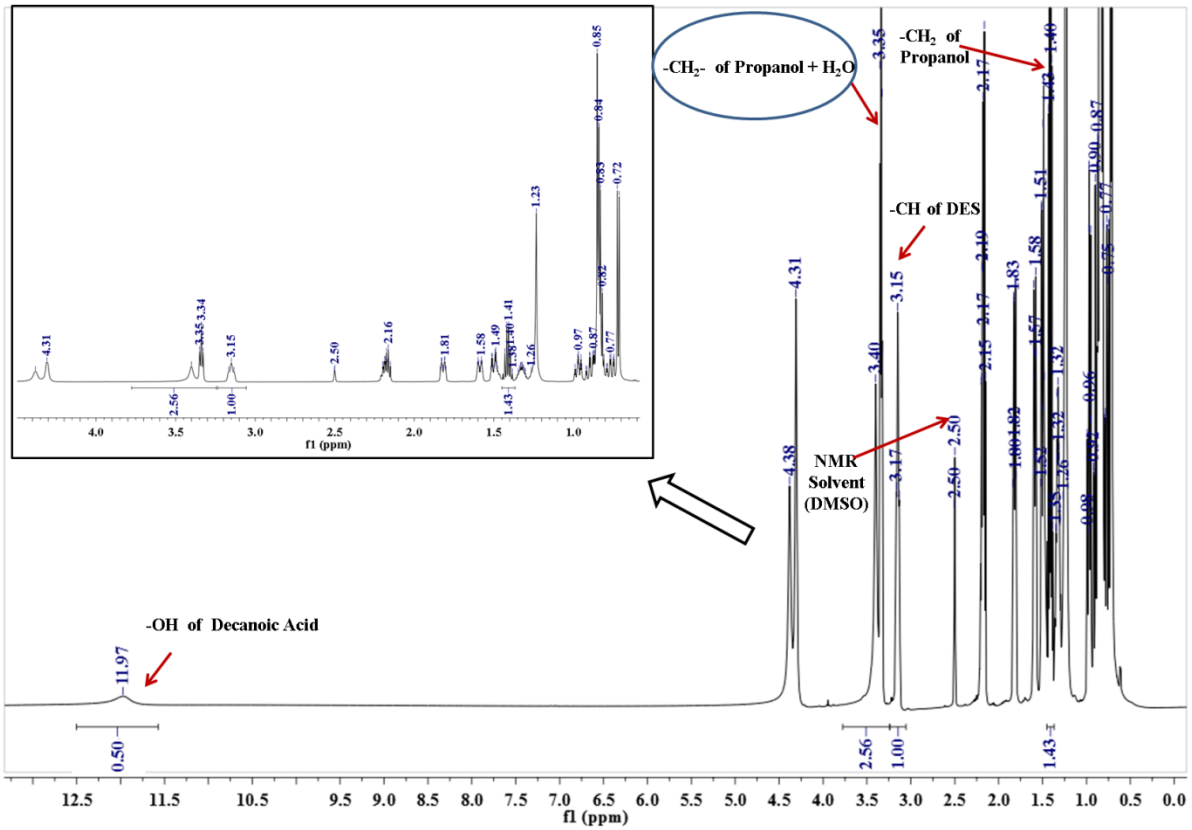

Figure 3.6: Typical ^{1}H NMR Spectra of DES rich phase

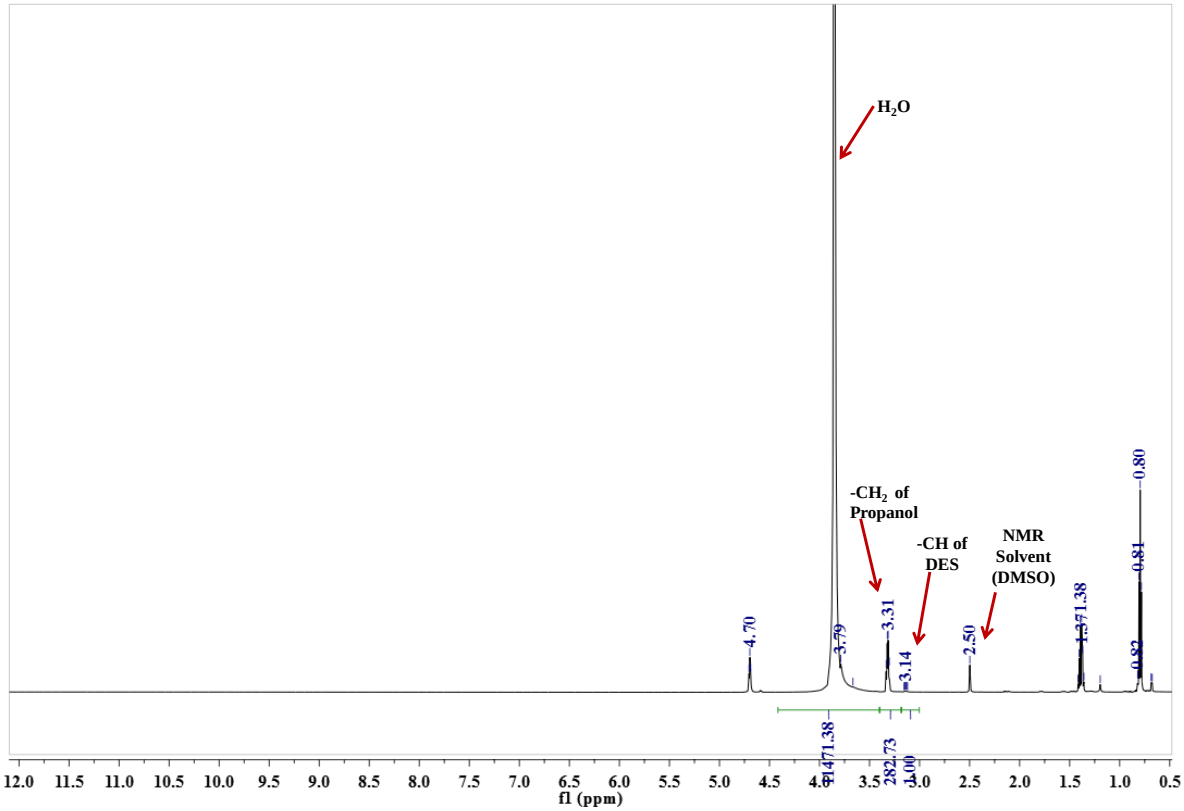

Figure 3.7: Typical ^{1}H NMR Spectra of aqueous rich phase

Table 3.4: Algebraic procedure for computing mole fraction in extract phase from ^{1}H NMR data

Compound name	Corresponding peak	Peak Position* (PPM)	Corresponding Area	Area due to single atom of H	Mole Fraction
DES	>CH- of DES	3.14	1	1	0.438
H_2O	-CH_2- of 1-propanol (attached with –OH group of 1- propanol) + H_2O	3.35	2.56 (four Hydrogen atoms)	0.565	0.248
1-propanol	-CH_2- of 1-propanol	1.40	1.43 (two hydrogen atoms)	0.715	0.314
			Sum	2.28	1

*As per Figure 3.6

Table 3.5: Algebraic procedure for computing mole fraction in raffinate phase from ^{1}H NMR data

Compound name	Corresponding chosen peak	Peak Position* (PPM)	Corresponding Area	Area due to single atom of H	Mole Fraction
DES	>CH- of DES	3.14	1	0.00017	0
H_2O	2H of H_2O	3.85	11471.38	5735.69	0.976
1-propanol	-CH_2- of 1-propanol	3.31	282.73	141.365	0.024
			Sum	5878.055	1

*As per Figure 3.7

Tables 3.6-3.8 reports the distribution ratio, which is the ratio of the concentration of alcohols in the DES phase to the concentration in the aqueous phase. Another important descriptor namely the distribution coefficient (β) and selectivity (S) are calculated using equations as given in section 3.3.3. Large value of distribution coefficient is desirable since it indicates lesser solvent require for particular degree of separation [11].

Among the alcohols high values of selectivity were reported for 1-butanol (Table 3.8). This indicates that the DES-1 has a preferential ability to extract 1-butanol when compared to ethanol and propanol. In general, the separation factor decreases as the concentration of alcohol in the feed increases. This is primarily due to the reduction of the two-phase region when the concentration of alcohol increases. This indicates the fact that the separation capacity of the solvent is reduced. A similar pattern is also seen for the distribution

coefficient which refers to the amount of solvent required for the desired separation. As the DES is hydrophobic in nature, the mole fraction is limited to negligible in the raffinate phase.

Table 3.6: Experimental LLE Data for the ternary system, DES-1 (1) + Ethanol (2) + Water (3) at T = 303.15 K and p = 1 atm

Extract phase			Raffinate phase				
x_{DES} [DL-menthol+ Decanoic acid] (1:1)	$x_{ethanol}$	x_{water}	x_{DES}	$x_{ethanol}$	x_{water}	$\beta_{ethanol}$	Selectivity (S)
0.604	0.177	0.219	0.000	0.042	0.958	4.214	18.435
0.525	0.241	0.234	0.002	0.059	0.939	4.085	16.391
0.379	0.347	0.274	0.002	0.084	0.914	4.131	13.780
0.291	0.416	0.293	0.001	0.13	0.869	3.200	9.491
0.176	0.5	0.324	0.004	0.175	0.821	2.857	7.240

Standard uncertainties are $u(T)$ = 0.01 K, $u(x)$ = 0.001

Table 3.7: Experimental LLE Data for the ternary system, DES-1 (1) + 1-Propanol (2) + Water (3) at T = 303.15 K and p = 1 atm

Extract phase			Raffinate phase				
x_{DES} [DL-menthol+ Decanoic acid] (1:1)	$x_{1\text{-propanol}}$	x_{water}	x_{DES}	$x_{1\text{-propanol}}$	x_{water}	$\beta_{propanol}$	Selectivity (S)
0.503	0.228	0.269	0	0.012	0.988	19.000	69.784
0.386	0.323	0.291	0	0.025	0.975	12.920	43.289
0.29	0.414	0.296	0	0.036	0.964	11.500	37.453
0.212	0.485	0.303	0	0.046	0.954	10.543	33.196
0.107	0.551	0.342	0.001	0.064	0.935	8.609	23.537

Standard uncertainties are $u(T)$ = 0.01 K, $u(x)$ = 0.001

Table 3.8: Experimental LLE Data for the ternary System, DES-1 (1) + 1-Butanol (2) + Water (3) at T = 303.15 K and p = 1 atm

Extract phase			Raffinate phase				
x_{DES} [DL-menthol+ Decanoic acid] (1:1)	$x_{1\text{-butanol}}$	x_w	x_{DES}	$x_{1\text{-butanol}}$	x_w	$\beta_{1\text{-butanol}}$	Selectivity (S)
0.669	0.144	0.187	0.001	0.002	0.997	72.000	383.872
0.577	0.236	0.187	0	0.007	0.993	33.714	179.028
0.471	0.288	0.241	0	0.005	0.995	57.600	237.809
0.29	0.391	0.319	0	0.007	0.993	55.857	173.875
0.21	0.46	0.33	0.001	0.008	0.991	57.500	172.674
0.149	0.528	0.323	0.001	0.012	0.987	44.000	134.452
0.113	0.582	0.305	0.002	0.015	0.983	38.800	125.050

Standard uncertainties are $u(T)$ = 0.01 K, $u(x)$ = 0.001

3.4.2. Extraction of Lower alcohols by DL-menthol and Lauric acid based hydrophobic DES

The LLE for the ternary systems namely, DES-2 (1) + 1-ethanol (2) + water (3), DES-2 (1) + 1-propanol (2) + water (3) and DES-2 (1) + 1-butanol (2) + water (3) were measured at T =303.15 K and p=1 atm. The experimental tie line data are reported in Tables 3.9-3.11, for ethanol, 1-propanol and 1-butanol respectively in terms of mole fraction for the extract and raffinate phase. The compositions have been obtained by ^{1}H NMR analysis as discussed in the previous section for decanoic based DES or DES1. Tables 3.9-3.11 give information about the distribution ratio and selectivity as discussed in section 3.3.3. Among the alcohols high values of selectivity and distribution ratio were reported for 1-butanol(Table 3.11). This indicates that the DES-2 has a preferential ability to extract 1-butanol when compared to ethanol and 1-propanol.

Table 3.9: Experimental LLE Data for the ternary system, DES-2 (1) + Ethanol (2) + Water (3) at T = 303.15 K and p = 1 atm

Extract phase			Raffinate phase				
x_{DES} [DL-menthol+Lauric acid] (2:1)	$x_{ethanol}$	x_{water}	x_{DES}	$x_{ethanol}$	x_{water}	$\beta_{ethanol}$	Selectivity (S)
0.702	0.080	0.218	0.000	0.044	0.956	1.818	7.973
0.639	0.130	0.231	0.002	0.043	0.955	3.023	12.499
0.478	0.275	0.247	0.003	0.082	0.915	3.354	12.423
0.388	0.302	0.310	0.002	0.101	0.897	2.990	8.652
0.336	0.334	0.330	0.001	0.117	0.882	2.855	7.630
0.236	0.406	0.358	0.001	0.159	0.840	2.553	5.991

Standard uncertainties are u(T) = 0.01 K, u(x) = 0.001

Table 3.10: Experimental LLE Data for the ternary system, DES-2 (1) + 1-Propanol (2) + Water (3) at T = 303.15 K and p = 1 atm

Extract phase			Raffinate phase				
x_{DES} [DL-menthol+Lauric acid] (2:1)	$x_{1\text{-propanol}}$	x_{water}	x_{DES}	$x_{1\text{-propanol}}$	x_{water}	$\beta_{propanol}$	Selectivity (S)
0.671	0.128	0.201	0.002	0.006	0.992	21.333	105.287
0.581	0.186	0.233	0.003	0.014	0.983	13.286	56.051
0.491	0.276	0.233	0.001	0.025	0.974	11.040	46.150
0.439	0.313	0.248	0.000	0.024	0.976	13.042	51.325
0.267	0.430	0.303	0.004	0.038	0.958	11.316	35.777
0.330	0.381	0.289	0.002	0.034	0.964	11.206	37.379

Standard uncertainties are u(T) = 0.01 K, u(x) = 0.001

Table 3.11: Experimental LLE Data for the ternary System, DES-2 (1) + 1-Butanol (2) + Water (3) at T = 303.15 Kand p = 1 atm

Extract phase			Raffinate phase				
x_{DES} [DL-menthol+Lauric acid] (2:1)	$x_{1\text{-butanol}}$	x_w	x_{DES}	$x_{1\text{-butanol}}$	x_w	$\beta_{1\text{-butanol}}$	Selectivity (S)
0.651	0.150	0.199	0.022	0.007	0.971	21.43	104.56
0.517	0.269	0.214	0.001	0.012	0.987	22.41	103.39
0.434	0.310	0.256	0.000	0.006	0.994	51.66	200.61
0.330	0.381	0.289	0.003	0.012	0.985	31.75	108.21
0.260	0.480	0.260	0.001	0.014	0.985	34.28	129.89
0.184	0.508	0.308	0.009	0.039	0.952	13.02	40.26

Standard uncertainties are $u(T)$ = 0.01 K, $u(x)$ = 0.001

3.4.3. Extraction of Lower alcohols by DL-menthol and Myristic acid based hydrophobic DES

The LLE for the ternary systems namely DES-3 (1) + 1-ethanol (2) + water (3), DES-3 (1) + 1-propanol (2) + water (3) and DES-3 (1) + 1-butanol (2) + water (3) were measured at T =303.15 K and atmospheric pressure. The experimental tie line data are reported in Tables 3.12-3.14, for ethanol, 1-propanol and 1-butanol respectively in terms of mole fraction for the extract and raffinate phase. The compositions have been obtained after the ^{1}H NMR analysis as discussed in the previous section. Tables 3.12-3.14 give information about the distribution ratio and selectivity as discussed in section 3.3.3. Among the alcohols high values of selectivity were again reported for 1-butanol (Table 3.14). This indicates that the DES-3 has a preferential ability to extract 1-butanol when compared to ethanol and 1-propanol.

Table 3.12: Experimental LLE Data for the ternary system, DES-3 (1) + Ethanol (2) + Water (3) at T = 303.15 K and p = 1 atm

Extract phase			Raffinate phase				
x_{DES} [DL-menthol+ Myristic acid] (4:1)	$x_{ethanol}$	x_{water}	x_{DES}	$x_{ethanol}$	x_{water}	$\beta_{ethanol}$	Selectivity (S)
0.609	0.08	0.311	0.002	0.021	0.977	3.810	11.968
0.542	0.142	0.316	0.000	0.042	0.958	3.381	10.250
0.418	0.264	0.318	0.002	0.083	0.915	3.181	9.152
0.307	0.338	0.355	0.003	0.127	0.87	2.661	6.522
0.225	0.373	0.402	0.002	0.16	0.838	2.331	4.860

Standard uncertainties are u(T) = 0.01 K, u(x) = 0.001

Table 3.13: Experimental LLE Data for the ternary system, DES-3 (1) + 1-Propanol (2) + Water (3) at T = 303.15 K and p = 1 atm

Extract phase			Raffinate phase				
x_{DES} [DL-menthol+ Myristic acid] (4:1)	$x_{1\text{-propanol}}$	x_{water}	x_{DES}	$x_{1\text{-propanol}}$	x_{water}	$\beta_{propanol}$	Selectivity (S)
0.662	0.1	0.238	0.003	0.005	0.992	20.000	83.361
0.576	0.187	0.237	0.002	0.013	0.985	14.385	59.784
0.437	0.332	0.231	0.001	0.027	0.972	12.296	51.740
0.319	0.42	0.261	0.001	0.056	0.943	7.500	27.098
0.234	0.467	0.299	0.001	0.085	0.914	5.494	16.795

Standard uncertainties are u(T) = 0.01 K, u(x) = 0.001

Table 3.14: Experimental LLE Data for the ternary System, DES-3 (1) + 1-Butanol (2) + Water (3) at T = 303.15 K and p = 1 atm

Extract phase			Raffinate phase				
x_{DES} [DL-menthol+ Myristic acid] (4:1)	$x_{1\text{-butanol}}$	x_{water}	x_{DES}	$x_{1\text{-butanol}}$	x_{water}	$\beta_{1\text{-butanol}}$	Selectivity (S)
0.63	0.149	0.221	0.003	0.003	0.994	49.667	223.388
0.537	0.227	0.236	0.003	0.005	0.992	45.400	190.834
0.395	0.345	0.26	0.003	0.009	0.988	38.333	145.667
0.305	0.414	0.281	0.003	0.012	0.985	34.500	120.934
0.232	0.463	0.305	0.0038	0.0152	0.981	30.461	97.973
0.197	0.482	0.321	0.001	0.012	0.987	40.167	123.503

Standard uncertainties are u(T) = 0.01 K, u(x) = 0.001

3.4.4. Extraction of Lower alcohols by DL-menthol and Palmitic acid based hydrophobic DES

The LLE for the ternary systems namely, DES-4 (1) + ethanol (2) + water (3), DES-4 (1) + 1-propanol (2) + water (3) and DES-4 (1) + 1-butanol (2) + water (3) were measured at T =303.15 K and atmospheric pressure. The experimental tie line data are reported in Tables 5-7, for ethanol, propanol and 1-butanol respectively in terms of mole fraction for the extract and raffinate phase. The compositions have been obtained after the ^{1}H NMR analysis as discussed in the previous section. Tables 3.15-3.17 give information about the distribution ratio and selectivity as discussed in section 3.3.3. Among the alcohols high values of selectivity were again reported for 1-butanol (Table 3.17).

Table 3.15: Experimental LLE Data for the ternary system, DES-4 (1) + Ethanol (2) + Water (3) at T = 303.15 Kand p = 1 atm

Extract phase			Raffinate phase				
x_{DES} [DL-menthol+ Palmitic acid] (12:1)	$x_{ethanol}$	x_{water}	x_{DES}	$x_{ethanol}$	x_{water}	$\beta_{ethanol}$	Selectivity (S)
0.652	0.074	0.274	0.007	0.015	0.978	4.933	17.609
0.575	0.135	0.29	0.002	0.043	0.955	3.140	10.339
0.45	0.259	0.291	0.003	0.084	0.913	3.083	9.674
0.359	0.338	0.303	0	0.152	0.848	2.224	6.223
0.305	0.379	0.316	0.003	0.205	0.792	1.849	4.634

Standard uncertainties are $u(T)$ = 0.01 K, $u(x)$ = 0.001

Table 3.16: Experimental LLE Data for the ternary system, DES-4 (1) + 1-Propanol (2) + Water (3) at T = 303.15 Kand p = 1 atm

Extract phase			Raffinate phase				
x_{DES} [DL-menthol+ Palmitic acid] (12:1)	$x_{propanol}$	x_{water}	x_{DES}	$x_{propanol}$	x_{water}	$\beta_{propanol}$	Selectivity (S)
0.653	0.115	0.232	0.004	0.015	0.981	7.667	32.418
0.576	0.187	0.237	0.001	0.028	0.971	6.679	27.362
0.459	0.316	0.225	0.002	0.043	0.955	7.349	31.192
0.348	0.377	0.275	0.001	0.055	0.944	6.855	23.530
0.243	0.453	0.304	0.001	0.065	0.934	6.969	21.412

Standard uncertainties are $u(T)$ = 0.01 K, $u(x)$ = 0.001

Table 3.17: Experimental LLE Data for the ternary System, DES-4 (1) + 1-Butanol (2) + Water (3) at T = 303.15 Kand p = 1 atm

Extract phase			Raffinate phase				
x_{DES} [DL-menthol+ Palmitic acid] (12:1)	$x_{1\text{-butanol}}$	x_w	x_{DES}	$x_{1\text{-butanol}}$	x_w	$\beta_{1\text{-butanol}}$	Selectivity (S)
0.61	0.115	0.275	0.002	0.006	0.992	19.167	69.139
0.558	0.179	0.263	0.0024	0.0106	0.987	16.887	63.374
0.457	0.291	0.252	0.001	0.014	0.985	20.786	81.246
0.329	0.394	0.277	0.0015	0.021	0.9775	18.762	66.209
0.261	0.453	0.286	0.001	0.026	0.973	17.423	59.275
0.203	0.494	0.303	0.001	0.034	0.965	14.529	46.274

Standard uncertainties are $u(T)$ = 0.01 K, $u(x)$ = 0.001

Overall the results indicates that DES-1 has a preferential ability to extract 1-butanol when compared to ethanol and 1-propanol among all the DESs studied. This implies that the extraction is favoured with a lower chain of organic acid. However one does not go for DES less than organic acid chain length of 10 (or decanoic acid: $C_{10}H_{20}O_2$) as the DES itself becomes unstable in water. Let us now have a look at the ternary diagrams and also relate the experiments with the NRTL and UNIQUAC predictions in the ensuing sections.

3.5. Thermodynamic Modelling

3.5.1. Prediction of Tie lines by NRTL and UNIQUAC model

Once the LLE data are available, we can then use these data to regress the binary interaction parameters in NRTL and UNIQUAC models. There are two ways used for predicting the NRTL and UNIQUAC model in this thesis. For mesitylene and oleyl alcohol we have used NRTL and UNIQUAC interaction parameters as available in the ASPEN-LLE database [12, 13]. On the contrary for the DES based systems we have used our in house regression using Genetic Algorithm [14-16] as it requires the addition of both HBA and HBD in required proportion as against mesitylene or oleyl alcohol which are single molecules.

Both the methods can be used interchangbly. The binary parameters $a_{ij,}$ $b_{ij,}$ $c_{ij,}$ d_{ij} and e_{ij} are unsymmetrical. The ASPEN physical property system has a large number of built-in binary parameters for the UNIQUAC model. These binary parameters have been regressed using VLE or LLE ASPEN data bank. ASPEN built in model parameters, ASPEN-LLE database [12, 13] have been used for the binary pairs where it is available. In case of missing parameters, the NRTL model parameters were estimated via UNIFAC group contribution method in ASPEN Plus itself [13] using "R-PCES", which means utilizing Property Constant EStimation (PCES) regression. PCES provides the Bondi method for estimating the R and Q parameters for UNIFAC functional groups. The ASPEN Plus physical property system then uses these parameters in the UNIFAC, Dortmund UNIFAC, and Lyngby UNIFAC model. The Bondi method here requires the molecular structure as an input. It should be noted that the binary NRTL interaction parameters for mesitylene-butanol has been carried out by R-PCES regression (Table 3.18). In a similar manner binary UNIQUAC interaction parameters were predicted for mesitylene-butanol pairs (Table 3.19) [12, 13, 17].

The binary interaction model parameters used in the current work given in Table 3.18 and 3.19 [12, 13].

NRTL Model: In ASPEN Plus simulation software the following equation has been defined to calculate the activity coefficient and binary interaction parameters

$$\ln \gamma_i = \frac{\sum_{j=1}^{n} x_j \tau_{ji} G_{ji}}{\sum_{k=1}^{n} x_k G_{ki}} + \sum_{j=1}^{n} \frac{x_j G_{ij}}{\sum_{k=1}^{n} x_k G_{kj}} \left[\tau_{ij} - \frac{\sum_{m=1}^{n} x_m \tau_{mj} G_{mj}}{\sum_{k=1}^{n} x_k G_{kj}} \right] \quad (3.4)$$

Where $G_{ij} = \exp(-\alpha_{ij} \tau_{ij})$;; $\tau_{ij} = a_{ij} + \left(\frac{b_{ij}}{T}\right) + e_{ij} \ln T$

$\alpha_{ij} = c_{ij}$

$\tau_{ii} = 0$

$G_{ii} = 0$

Here *a*, *b*, *c*, *d* and *e* are the binary interaction parameters as listed in ASPEN.

UNIQUAC Model: The model is given as [17]:

$$\ln \gamma_i = \ln\left(\frac{\Phi_i}{x_i}\right) + \frac{z}{2} q_i \ln\left(\frac{\theta_i}{\Phi_i}\right) - q_i' \ln t_i' - q_i' \sum_{j=1}^{c} \frac{\theta_i' \tau_{ji}}{r_i'} + l_i + q_i' - \frac{\Phi_i}{x_i} \sum_{j=1}^{c} x_j l_j \quad (3.5)$$

Where

$\theta_i = \frac{q_i x_i}{q_T}$ $\quad q_T = \sum_k q_k x_k$ $\quad \theta_i' = \frac{q_i' x_i}{q_T'}$ $\quad q_T' = \sum_k q_k' x_k$

$\Phi_i = \frac{r_i x_i}{r_T}$ $\quad r_T = \sum_k r_k x_k$ $\quad l_i = \frac{z}{2}(r_i - q_i) + 1 - r_i$

$t_i' = \sum_{k=1}^{c} \theta_k' \tau_{ki}$ $\quad \tau_{ij} = \exp\left(a_{ij} + \frac{b_{ij}}{T} + c_{ij} \ln T + d_{ij} T + \frac{e_{ij}}{T^2} \right)$ $\quad z = 10$

Table 3.18: NRTL binary interaction model parameters used in the current work*

Component i	mesitylene	mesitylene	water
Component j	water	1-butanol	1-butanol
Source	ASPEN-LLE	UNIFAC	ASPEN-LLE
a_{ij}	-3.73	0	90.53
a_{ji}	10.25	0	204.24
b_{ij}	2542.78	488.69	-4983.16
b_{ji}	-66.04	87.21	-9291.70
c_{ij}	0.2	0.30	0.2
d_{ij}	0	0	0
e_{ij}	0	0	-12.06
e_{ji}	0	0	-30.58

*ASPEN Plus – NRTL model

Table 3.19: UNIQUAC binary interaction model parameters used in this work*

Component i	mesitylene	mesitylene	Water
Component j	water	1-butanol	1-butanol
Source	ASPEN-LLE	UNIFAC	ASPEN-LLE
a_{ij}	2.89	0	6.63
a_{ji}	-1.37	0	-70.97
b_{ij}	-1881.48	-307.46	-16.49
b_{ji}	67.88	106.57	3132.83
c_{ij}	0	0	-1.32
c_{ji}	0	0	10.63
d_{ij}	0	0	0
d_{ji}	0	0	0
e_{ij}	0	0	0
e_{ji}	0	0	0

*ASPEN Plus – UNIQUAC model

With respect to the NRTL and UNIQUAC predicted tie lines as evident from Figures 3.8-3.12, all of them exhibits a type-I LLE behavior. Further from the NMR spectra the

raffinate phase of all the systems are almost free of solvent and mostly contain water. It should be noted that the due to the baseline correction of the NMR spectra, concentration lower than 0.001 are very difficult to obtain. This usually signifies the uncertainty levels of the NMR spectra. In all the alcohols, the raffinate phase lies on the extreme corner of binary axis of water-1-butanol and water–propanol. Further a negligible amount of alcohol is present in the raffinate phase after extraction. From Figure 3.8, it can be observed that the points are nearer to 100%, i.e. water which indicates that the entire 1-butanol is transferred to extract phase. It also confirms a higher distribution coefficient due to a large difference of 1-butanol concentration in both the phases.

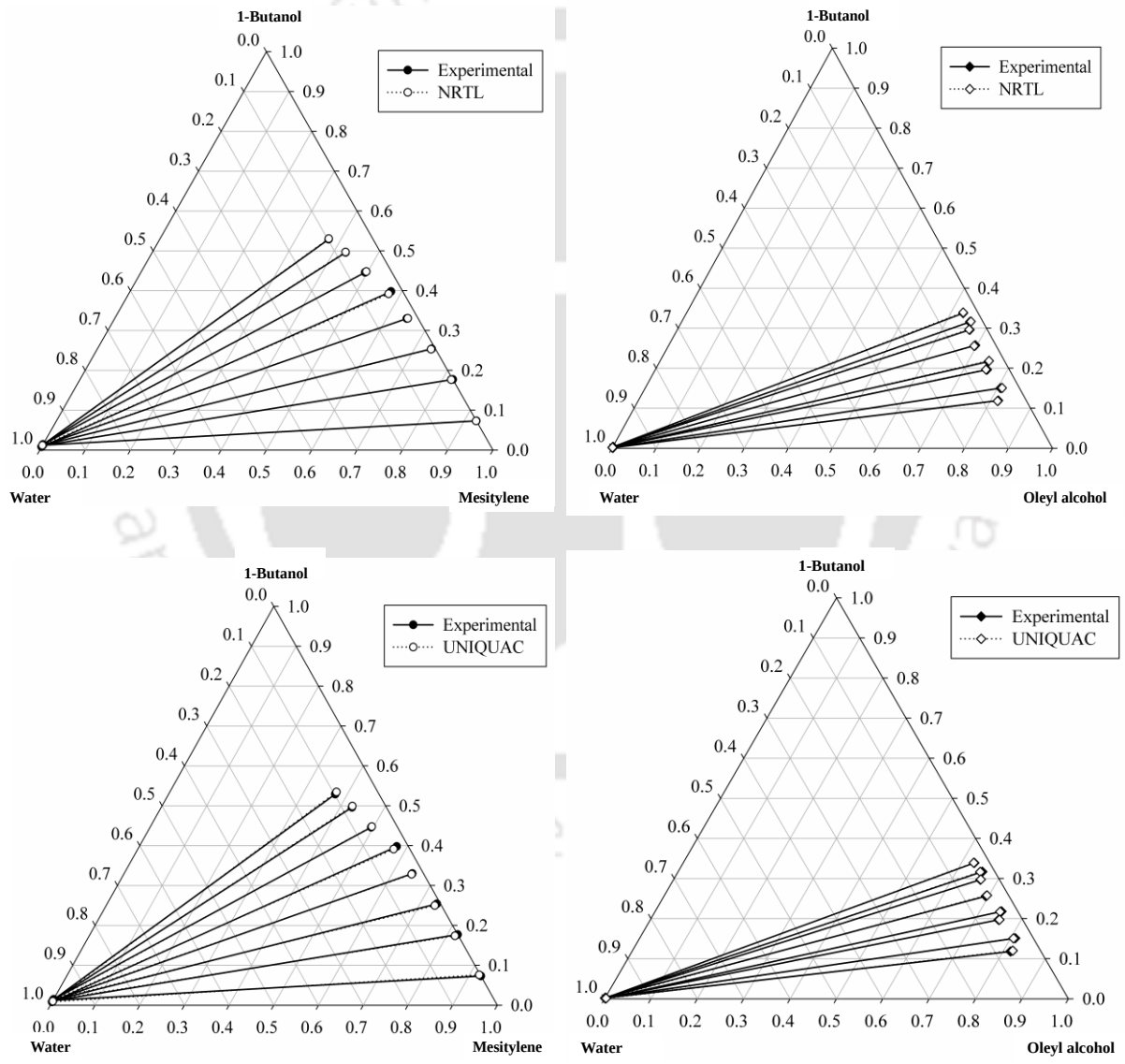

Figure 3.8: Experimental and NRTL/UNIQUAC predicted tie lines for the ternary system using ASPEN Plus: mesitylene/oleyl alcohol (1) + 1-butanol (2) + water (3) system at T = 298.15 K and p = 1 atm.

3.5.2. Prediction of Tie lines by NRTL and UNIQUAC model for DESs

The reliability of experimental data of DESs was checked via NRTL [18] and UNIQUAC [15, 16] model both with our in-house implementation and ASPEN Plus [12, 13, 17] prediction. Let us first discuss the implementation of NRTL and UNIQUAC model as per our earlier work [14, 15, 19].

3.5.3. Algorithm for Prediction of LLE through NRTL/UNIQUAC model

Initially we compute the feed concentration of component *i* (z_i) from experimental concentration of component *i* in both phases.

$$z_i = \frac{x_i^I + x_i^{II}}{2} \tag{3.6}$$

Here x_i^I and x_i^{II} are the mole fraction of component *i* in phases *I* (Extract) and *II* (Raffinate), respectively. Thereafter we predict the activity coefficient of component *i* (γ_i) in both phases by NRTL/UNIQUAC model (Eqs. 3.4-3.5) with the help of the objective function in GA (Eq. 3.14). Overall the LLE equation is represented as:

$$\hat{x}_i^I \gamma_i^I = \hat{x}_i^{II} \gamma_i^{II} \tag{3.7}$$

Where $\hat{x}_i^I$ and $\hat{x}_i^{II}$ are the mole fraction of component *i* in phases *I* and *II* predicted by NRTL/UNIQUAC, respectively.

We then compute the distribution coefficient of component *i* (K_i) from activity coefficient of component *i*.

$$\frac{x_i^I}{x_i^{II}} = \frac{\gamma_i^{II}}{\gamma_i^I} = K_i \tag{3.8}$$

Thereafter we solve the Isothermal flash algorithm for extract to feed (Ψ) ratio.

$$f(\Psi) = \sum \frac{z_i (1 - K_i)}{1 + \Psi (K_i - 1)} = 0 \tag{3.9}$$

subject to,

$$F z_i = L_1 x_i^I + L_2 x_i^{II} \tag{3.10}$$

and $$\Psi = L_1 / F \tag{3.11}$$

Here F, L_1 and L_2 represent the flow rate of the feed, extract and raffinate phases respectively. If Eq. 3.9 is converged then we go ahead else we go back to Eq. 3.8, and invoke GA toolbox for new set of binary interaction parameters (τ_{ij}/τ_{ji} or $A_{ij}/A_{ji)}$. Finally we calculate the mole fractions in both phases as:

$$x_i^I = \frac{z_i}{1 + \Psi (K_i - 1)} \tag{3.12}$$

$$x_i^{II} = K_i x_i^I \tag{3.13}$$

A suitable minimization process using GA as per our earlier work [14, 15] is carried out with the objective function given in Eq. 3.14. The obtained binary interaction parameters are given in Tables 3.8-3.11. A detailed methodology is given in our earlier work [6, 18, 20, 21] and is not discussed here.

$$\text{Maximize}: \quad F_{\left(\begin{array}{l}\text{with respect to } A_{ij} \\ \text{where } i,j=1,2,3 \\ \text{and } j \neq i\end{array}\right)} = -\sum_{k=1}^{m}\sum_{l=I}^{II}\sum_{i=1}^{c} w_{ik}^l \left(x_{ik}^l - \hat{x}_{ik}^l\right)^2, \quad w_{ik}^l = 1 \tag{3.14}$$

The goodness of the fit was predicted by the root mean square deviation (RMSD) which is defined as per the following equation [22]:

$$RMSD = \left(-\frac{F}{2mc}\right)^{1/2} = \left[\sum_{k=1}^{m}\sum_{i=1}^{c}\sum_{l=I}^{II} \frac{\left(x_{ik}^l - \hat{x}_{ik}^l\right)^2}{2mc}\right]^{1/2} \tag{3.15}$$

Where, m refers to the number of tie lines and c refers to the number of components (viz. 3 for the present system). Here x_{ik}^l and $\hat{x}_{ik}^l$ are the experimental and predicted values of composition (mole fraction) for component i in the k^{th} tie line for phase l, respectively. It should be noted that the parameters τ_{ij} from Eq. 3.5 are merely regressed parameters for NRTL model. It has no physical interpretation.

From the previous work of Singh et al. [14] and Sahoo et al. [19] for aqueous systems it was observed that the objective function remains asymptotically flat when population size and generation greater than 100 and 200 respectively is chosen, Therefore *population size* of 100 and *number of generations* as 200 is adopted in this current work. GA was required as

the objective function is highly convex in nature with the result that traditional optimization algorithms fail.

Figures 3.9-3.12 reports and compares the NRTL and UNIQUAC predictions for all the DES namely DES1 (Figure 3.9), DES2 (Figure 3.10), DES3 (Figure 3.11) and DES4 (Figure 3.12). From all the figures it can be observed that the points are nearer to 100%, i.e. water which indicates that the entire 1-butanol is transferred to extract phase as compared to ethanol and 1-propanol. It also confirms a higher distribution coefficient due to a large difference of 1-butanol concentration in both the phases. The binary interaction parameters (A_{ij}) are also given in Tables 3.20-3.23.

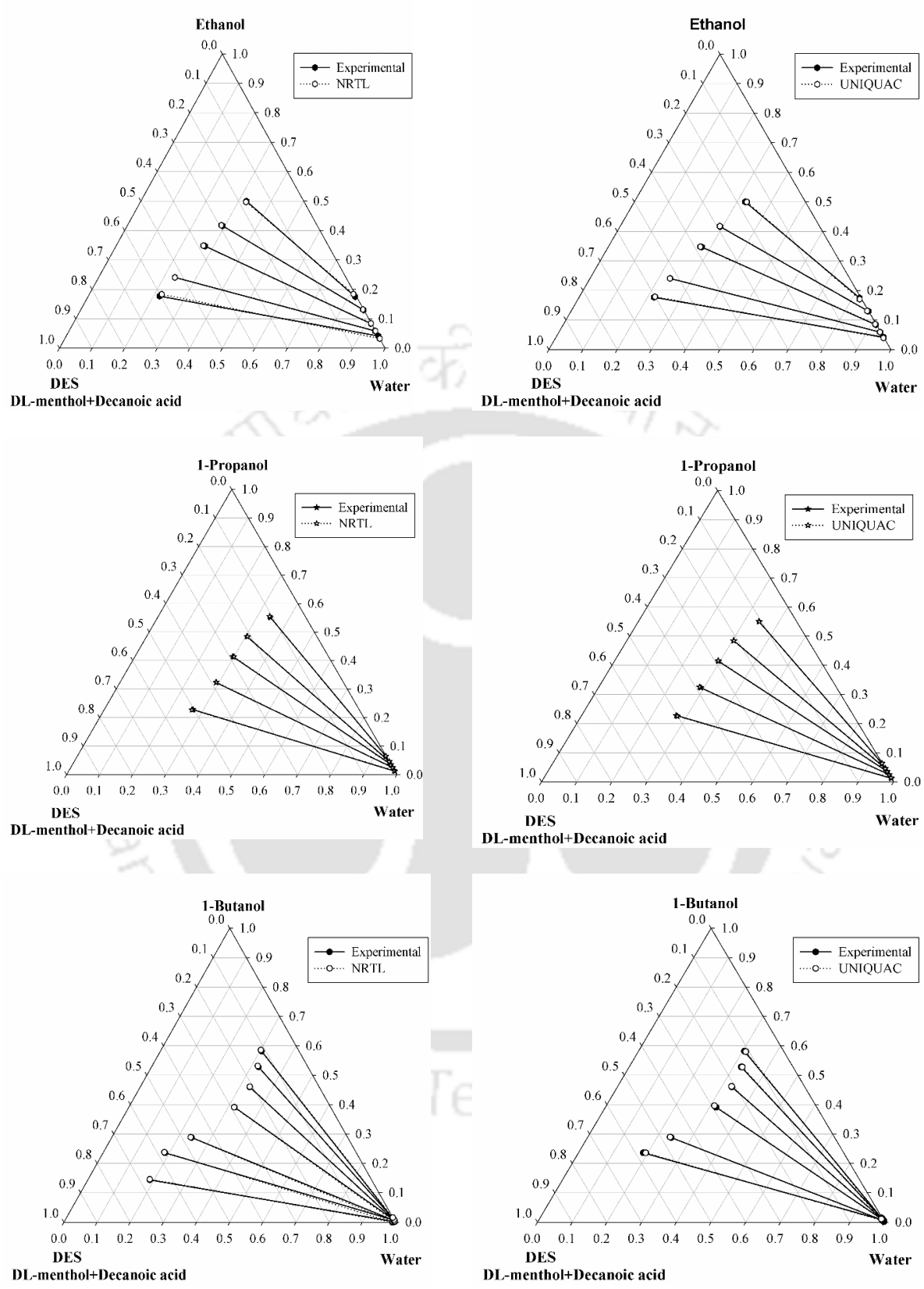

Figure 3.9: Experimental and NRTL/UNIQUAC predicted tie lines for the ternary system DES-1 (1) + Ethanol/1-propanol/1-butanol (2) + water (3) system at T = 303.15 K and p = 1 atm.

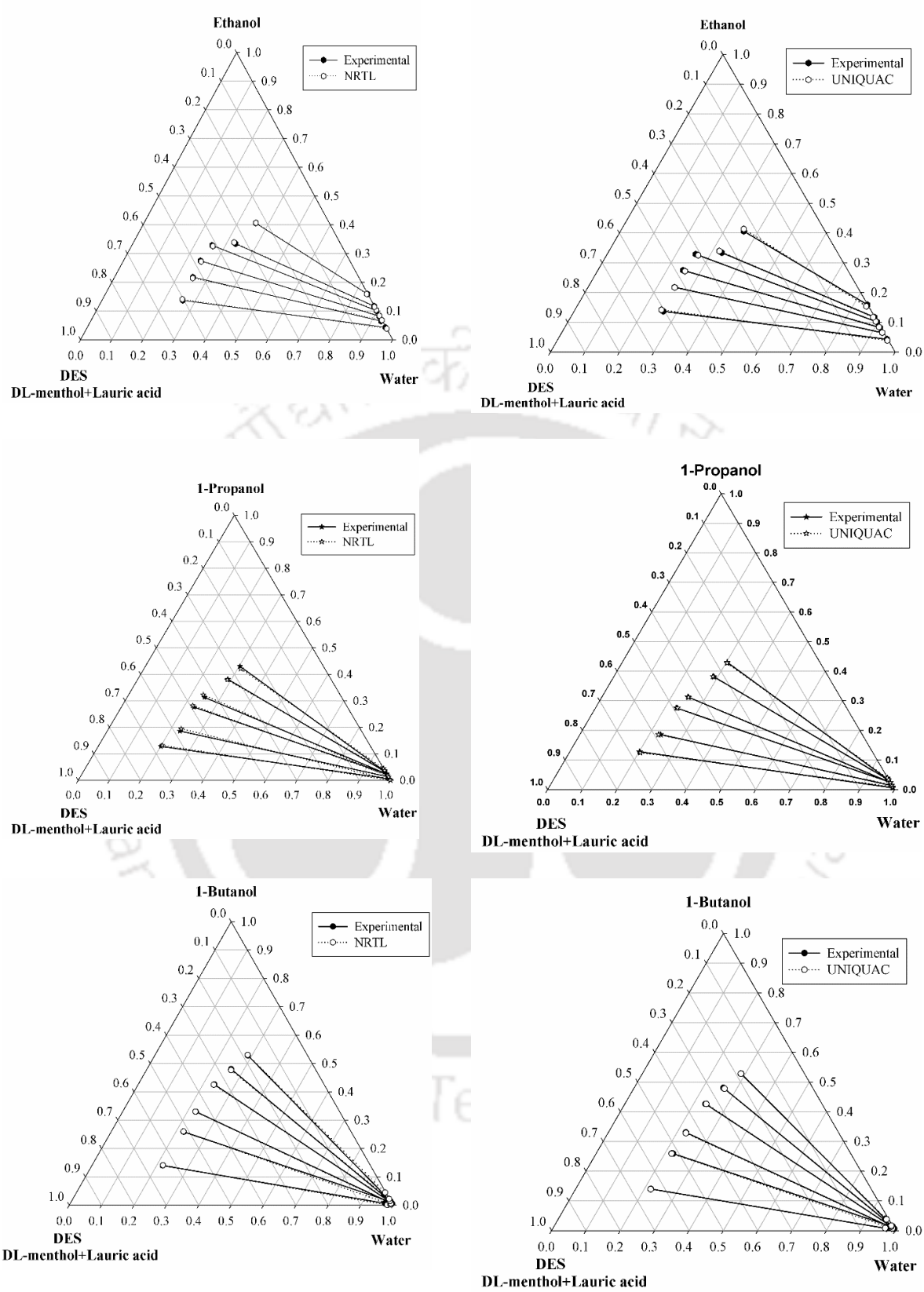

Figure 3.10: Experimental and NRTL/UNIQUAC predicted tie lines for the ternary system DES-2 (1) + Ethanol/1-propanol/1-butanol (2) + water (3) system at T = 303.15 K and p = 1 atm.

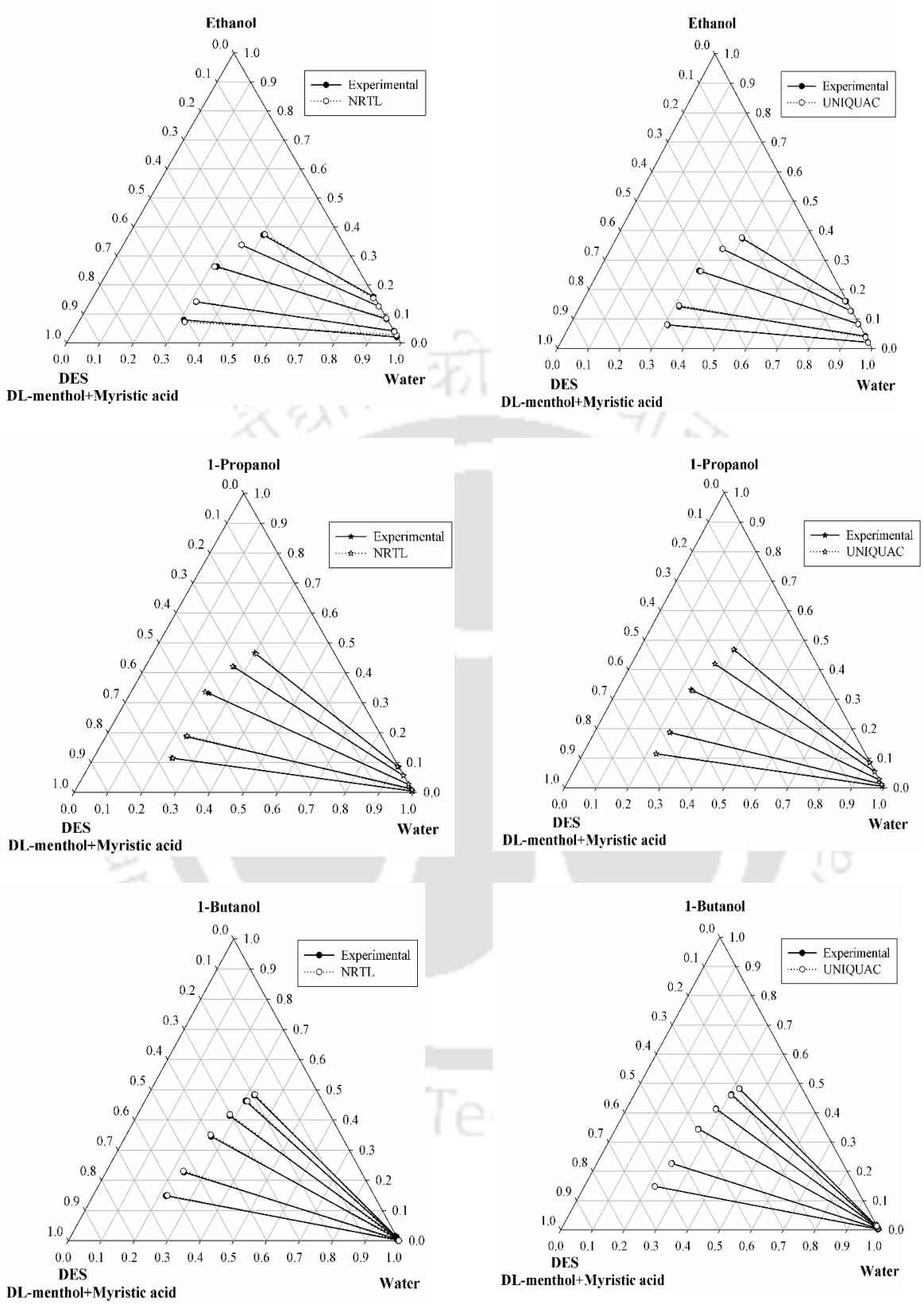

Figure 3.11: Experimental and NRTL/UNIQUAC predicted tie lines for the ternary system DES-3 (1) + Ethanol/1-propanol/1-butanol (2) + water (3) system at T = 303.15 K and p = 1 atm.

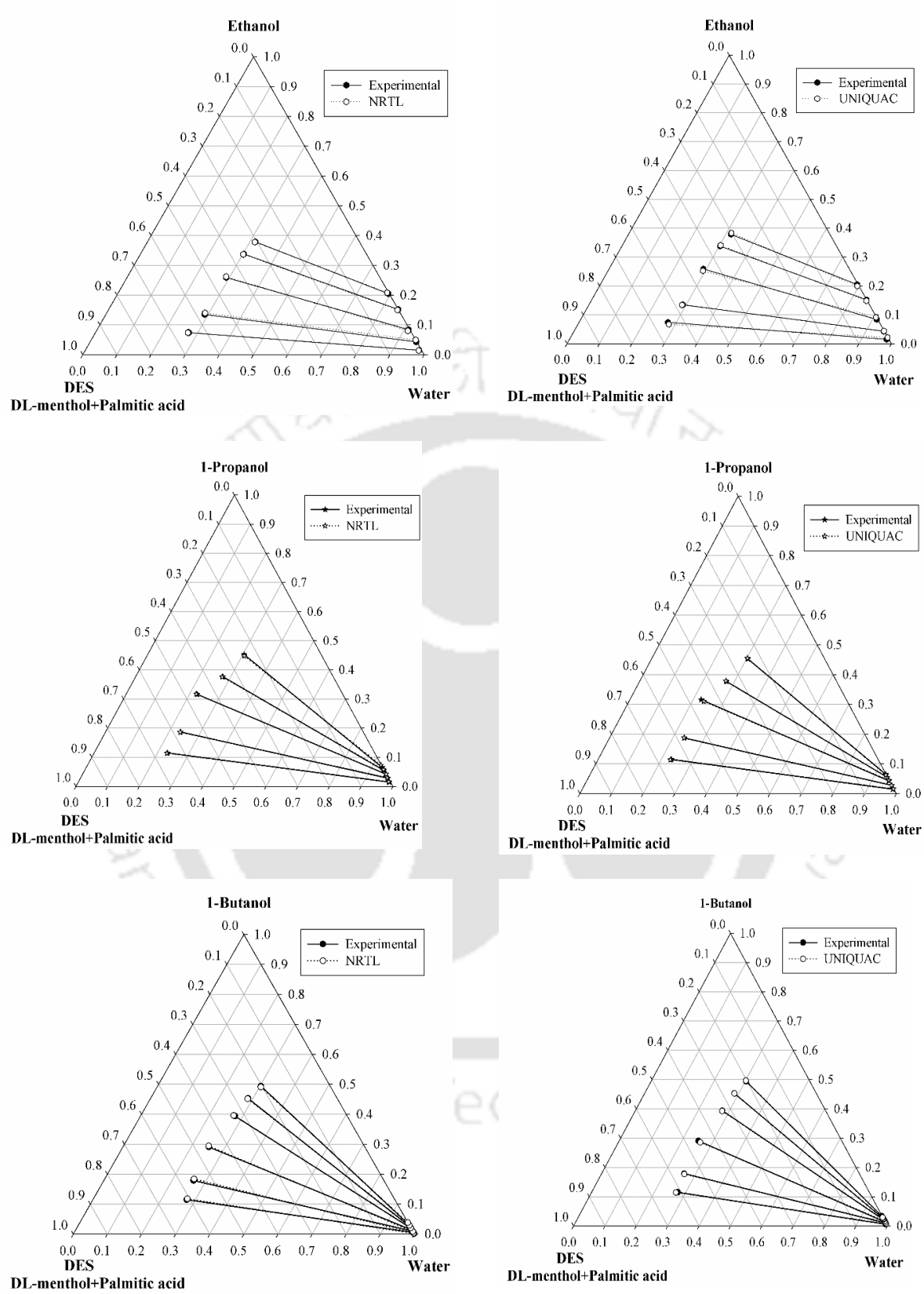

Figure 3.12: Experimental and NRTL/UNIQUAC predicted tie lines for the ternary system DES-4 (1) + Ethanol/1-propanol/1-butanol (2) + water (3) system at T = 303.15 K and p = 1 atm.

Table 3.20: NRTL and UNIQUAC interaction parameters for ternary systems at T=303.15 K and p=1 atm.

i-j	NRTL Model Parameters				UNIQUAC Model Parameters			
	τ_{ij}	τ_{ji}	F[a]	%RMSD[b]	A_{ij}/K	A_{ji}/K	F[a]	%RMSD[b]
DES-1 (1) + Ethanol (2) + Water (3)								
1-2	19.00	12.83			370.23	155.04		
1-3	2.53	0.38	-2.1×10^{-4}	0.26	383.05	28.753	-6.4×10^{-4}	0.463
2-3	1.14	6.57			693.6	250.82		
DES-1 (1) + 1-Propanol (2) + Water (3)								
1-2	2.77	6.94			213.16	215.89		
1-3	15.76	-1.52	-0.9×10^{-4}	0.17	533.8	344.31	-1.4×10^{-4}	0.219
2-3	17.22	2.62			525.02	-174.43		
DES-1 (1) + 1-Butanol (2) + Water (3)								
1-2	3.94	3.91			325.15	111.01		
1-3	-0.82	3.81	-1.1×10^{-4}	0.29	595.65	427.73	-3.4×10^{-4}	0.55
2-3	0.90	-6.54			826.97	-117.76		

[a]Calculated by Eq. 3.14; [b]Calculated by Eq. 3.15

Table 3.21: NRTL and UNIQUAC interaction parameters for ternary systems at T=303.15 K and p=1 atm.

i-j	NRTL Model Parameters				UNIQUAC Model Parameters			
	τ_{ij}	τ_{ji}	F[a]	%RMSD[b]	A_{ij}/K	A_{ji}/K	F[a]	%RMSD[b]
DES-2 (1) + Ethanol (2) + Water (3)								
1-2	5.76	13.53			615.09	205.37		
1-3	-0.06	6.64	-1.0×10^{-4}	0.44	363.57	82.259	-7.1×10^{-4}	0.52
2-3	12.34	17.97			671.51	427.11		
DES-2 (1) + 1-Propanol (2) -Water (3)								
1-2	5.00	-5.45			284.29	311.34		
1-3	4.75	8.79	-1.5×10^{-4}	0.24	344.1	101.7	-2.1×10^{-4}	0.65
2-3	11.80	19.21			622.97	44.661		
DES-2 (1)-1-Butanol (2)-Water (3)								
1-2	3.27	19.68			189.75	146.09		
1-3	-4.66	15.58	-1.1×10^{-4}	0.39	733.31	533.39	-5.7×10^{-4}	0.55
2-3	3.69	2.99			776.37	-273.94		

[a]Calculated by Eq. 3.14; [b]Calculated by Eq. 3.15

Table 3.22: NRTL and UNIQUAC interaction parameters for ternary systems at T=303.15 K and p=1 atm.

i-j	NRTL Model Parameters				UNIQUAC Model Parameters			
	τ_{ij}	τ_{ji}	F[a]	%RMSD[b]	A_{ij}/K	A_{ji}/K	F[a]	%RMSD[b]
				DES-3 (1) + Ethanol (2) + Water (3)				
1-2	1.62	19.63			-22.355	266.2		
1-3	13.92	1.86	-2.1×10^{-4}	0.26	297.97	397.92	-3.8×10^{-4}	0.35
-3	8.23	-1.11			466.02	-301.54		
				DES-3 (1) + 1-Propanol (2) + Water (3)				
1-2	1.56	11.44			-211.95	303.21		
1-3	12.10	-2.60	-1.3×10^{-4}	0.21	490.04	85.252	-5.0×10^{-4}	0.41
2-3	12.09	18.79			525.38	-515.47		
				DES-3 (1) + 1-Butanol (2) + Water (3)				
1-2	14.34	9.73			314.73	569.69		
1-3	13.48	3.23	-1.2×10^{-4}	0.19	314.98	698.01	-1.8×10^{-4}	0.71
2-3	17.46	2.27			453.59	-246.86		

[a]Calculated by Eq. 3.14; [b]Calculated by Eq. 3.15

Table 3.23: NRTL and UNIQUAC interaction parameters for ternary systems at T=303.15 K and p=1atm.

i-j	NRTL Model Parameters				UNIQUAC Model Parameters			
	τ_{ij}	τ_{ji}	F[a]	%RMSD[b]	A_{ij}/K	A_{ji}/K	F[a]	%RMSD[b]
DES-4 (1) + Ethanol (2) + Water (3)								
1-2	2.26	11.06			326.25	433.69		
1-	20.00	2.18	-1.71×10^{-4}	0.29	505.94	998.96	-3.2×10^{-4}	0.75
2-3	17.18	-0.27			399.3	-86.571		
DES-4 (1)-1 + 1-Propanol (2) + Water (3)								
1-2	19.97	20.00			232.48	317		
1-3	3.02	1.04	-2.7×10^{-4}	0.30	463.98	169.59	-9.87×10^{-4}	0.57
2-3	2.48	6.50			517.71	13.666		
DES-4 (1)-1 + 1-Butanol (2) + Water (3)								
1-2	2.93	8.17			152.85	395.49		
1-3	-0.13	-2.69	-4.51×10^{-4}	0.35	377.82	58.647	-4.7×10^{-4}	0.39
2-3	19.01	14.02			394.97	76.301		

[a]Calculated by Eq. 3.14; [b]Calculated by Eq. 3.15

3.5.4. LLE Predictions using COSMO-SAC Model

Quantum-chemical based solvation models such as COSMO-SAC [15, 23] is another pathway which provides an alternative mean of predicting activity coefficients and other thermodynamic properties using a statistical mechanical framework. This is based on the COSMO (**CO**nductor like **S**creening **MO**del) continuum model and its variants or statistical mechanical framework such as COSMO-SAC (**CO**nductor like **S**creening **M**odel- **S**egment **A**ctivity **C**oefficient) as proposed by Lin and Sandler [24]. These determine liquid phase nonideality using molecular interactions derived from quantum chemical solvation calculation. An advantage of COSMO based models over UNIFAC is that it can distinguish between isomers

because molecules are drawn with respect to their specific conformal structures before performing optimization. This is followed by COSMO calculations in quantum chemistry optimization packages such as Gaussian 09 [25]. It is a known fact that quantum chemical information in different conformers influences the activity coefficient calculations. The methodology and equations are already available in our published literature [16, 26] and hence is not discussed here.

The COSMO files once generated are then used to generate the sigma profile [16, 24, 27, 28] of the molecules. This is then used in the statistical framework namely SAC or Segment Activity Coefficient (SAC) [16] in order to obtain the activity coefficient. The activity coefficients predicted with the modified Rashford Rice Algorithm (section 3.5.3) to generate the tie lines. This solves the isofugactiy problem. Assuming the process to occur isothermally, the compositions of the extract and raffinate phases are calculated using a flash algorithm as described by the modified Rashford-Rice Algorithm section. The details of the calculation is similar to the one given in Section 3.5.3 (Algorithm for prediction of LLE through NRTL/UNIQUAC model) and also described in our earlier work [16, 26].The COSMO-SAC predicted ternary tie lines are then compared with experimental tie lines for all the systems using COSMO-SAC (Figure 3.13-3.17) model. In our case we have obtained similar results with both our in-house COSMO-SAC and the one implemented in ASPEN Plus V8.8.We shall refer the COSMO-SAC predictions in ASPEN as "COSMO-ASPEN" in the future text. We have followed our model in the case of ternary systems representing lauric acid based DES (DES-2), while the remaining have been predicted by ASPEN Plus. We shall initially discuss lauric acid based ternary system using our own model and also compare the same with ASPEN. Thereafter we shall discuss conventional and other DES solvents with prediction from ASPEN.

3.5.5. COSMO-SAC Predictions for DES-2 (Lauric Acid Based System)

The first step for a COSMO based scheme is to obtain an accurate geometry optimized structure of the molecules (water, alcohol, DL-menthol, Lauric Acid) in gas phase. The geometry optimization was carried out at B3LYP using 6-31G* basis set with Gaussian 09, from at least three initial geometries of each complex systems. The geometries were drawn by Gauss View 5.0 [29] visualization package. Further details including COSMO file generation is as per section 2.5. For DL-menthol which has equal contribution from both *dextro and levo* stereoisomer, the

geometries for each stereoisomer were obtained by the *modreduntant* option in Gaussian09 [25]. Frequency analysis was carried out of each complex at the same level of theory. Absence of imaginary vibrational frequencies determines the true energy minimum structures. For the COSMO-SAC calculation, BVP86 functional with SVP basis set and density fitting basis set DGA1 are used. While calculating the Coulomb interaction, the density fitting basis set expands the density in a set of atom-centred functions. Thus for a medium sized system, a performance gain in terms of accuracy in molecular structure and relative energies are achieved. The COSMO files once generated were then used to generate the sigma profile of the molecules, which were then used in the statistical framework namely Segment Activity Coefficient (SAC) to obtain the activity coefficient. The activity coefficients were then used with the modified Rashford Rice Algorithm to generate the tie lines as per section 3.5.3. Table 3.24 shows the universal COSMO-SAC parameters used namely effective area, cut-off value for hydrogen bonding interaction and constant for hydrogen bonding interaction [27].

Table 3.24: COSMO-SAC parameters used for DES2 (Lauric Acid) based prediction

Name	Value	Unit
effective area (a_{eff})	7.5	$Å^2$
cutoff value for hydrogen bonding interaction (σ_{hb})	0.0084	$e/Å^2$
constant for hydrogen bonding interaction (c_{hb})	85580	$(Kcal/mol)(Å^4/e^2)$

For the sigma profile calculation of DES, a molar ratio was used for DL-menthol (HBA) and lauric acid (HBD) molecule respectively. The sigma profile of DL-menthol was taken as the average of *dextro and levo* isomers ($p_{HBA}(\sigma)$). The charge distribution for such a DES will then be the algebraic sum of the sigma profiles calculated separately [30]. It takes the form:

$$p_{DES}(\sigma) = p_{HBA}(\sigma) + p_{HBD}(\sigma) = f_{HBA}\, p_{HBA}(\sigma) + f_{HBD}\, p_{HBD}(\sigma) \tag{3.16}$$

$$p_{HBA}(\sigma) = p_{MTBP}(\sigma) + p_{Br}(\sigma) \tag{3.17}$$

Here $p_{HBA}(\sigma)$ and $p_{HBD}(\sigma)$ are the sigma profile of the components of DES, namely the HBD and HBA. f_{HBA} and f_{HBD} are the mole ratio's that have been adopted in the experimental work

(chapter 2). The sigma profile of DES is then normalized so that it would appear as the sigma profile of a single molecule. Using both the NRTL and COSMO-SAC models, the average Root Mean Square Deviation (RMSD) values obtained were 1% and 7% respectively. NRTL model is expected to agree with a higher accuracy when compared to COSMO-SAC model owing to its regression from experimental data. The COSMO-SAC model is predictive in nature where the only input required is the optimized molecular structure and the temperature. The ternary tie lines for DES2 have been depicted for both COSMO-ASPEN (Figure 3.13(a)) and our in-house COSMO-SAC code (Figure 3.13(b)).

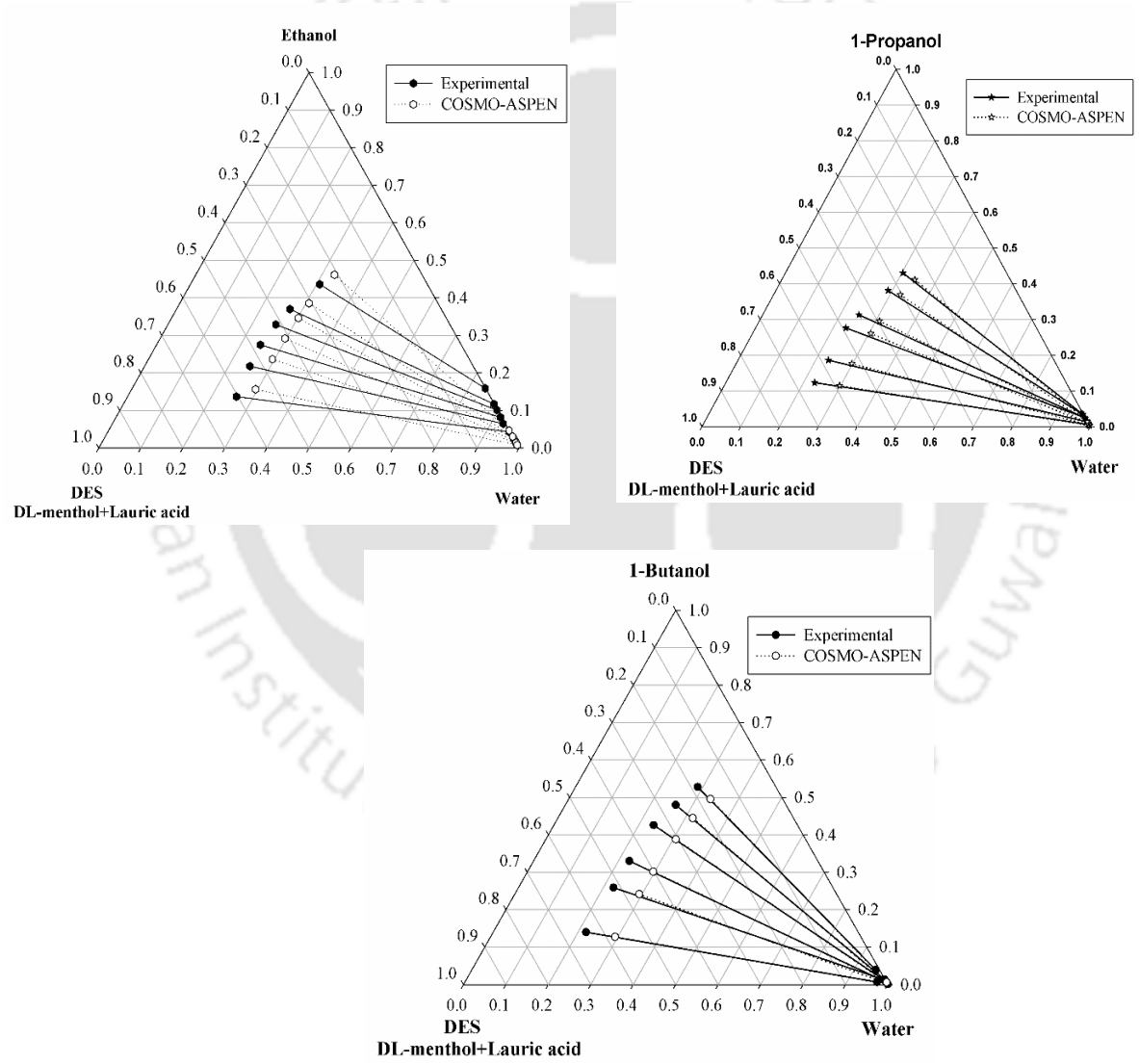

Figure 3.13 (a): Experimental and COSMO-ASPEN predicted tie lines for the ternary system: DES-2 (1)-alcohol (2)-water (3) at 303.15 K and 1 atm.

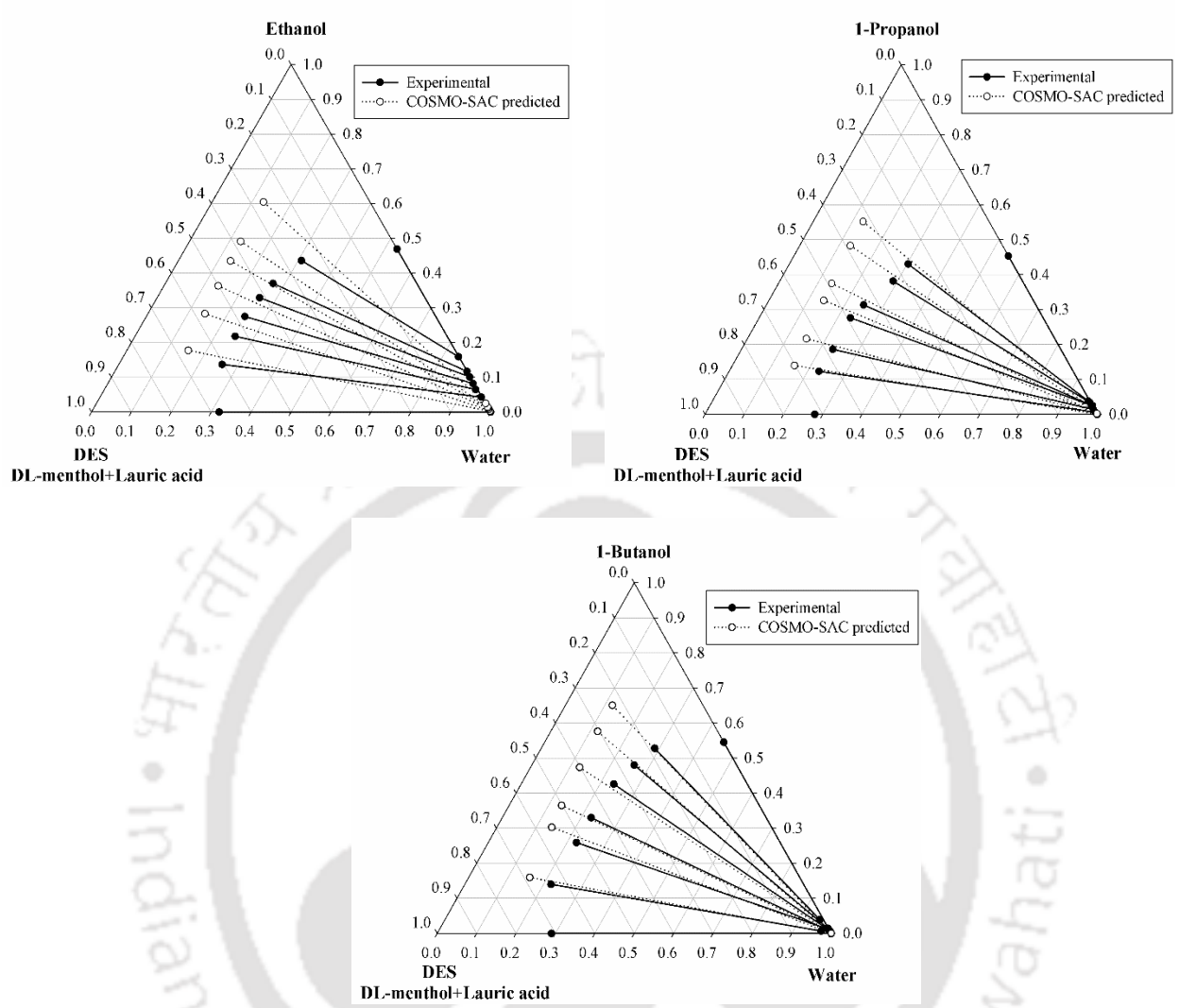

Figure 3.13 (b): Experimental and COSMO-SAC predicted tie lines for the ternary system: DES-2 (1)-alcohol (2)-water (3) at 303.15 K and 1 atm.

It can be seen that the average RMSD % for predictions using COSMO-ASPEN and our in-house COSMO-SAC model are 3.64, 2.51, 2.21 and 8.75, 7.71, 5.83 for ethanol, 1-propanol and 1-butanol, respectively. Due to the lower RMSD in COSMO-ASPEN, the same have been used for the remaining systems. Thereafter the remaining systems are predicted using COSMO-ASPEN and depicted for mesitylene and oleyl alcohol (Figure 3.14), while for DES: DES-1 (Figure 3.15), DES-3 (Figure 3.16) and DES-4 (Figure 3.17).In all the systems the tie lines are having positive slope with DES1 giving the highest slope. Hence DES-1 may be recommended as potential solvent. The goodness of fit is usually measured by Root Mean Square Deviation

(RMSD) as discussed in section 3.5.3. Table 3.25 show the RMSD obtained via COSMO-SAC model using COSMO-ASPEN for all the solvents used in the present study.

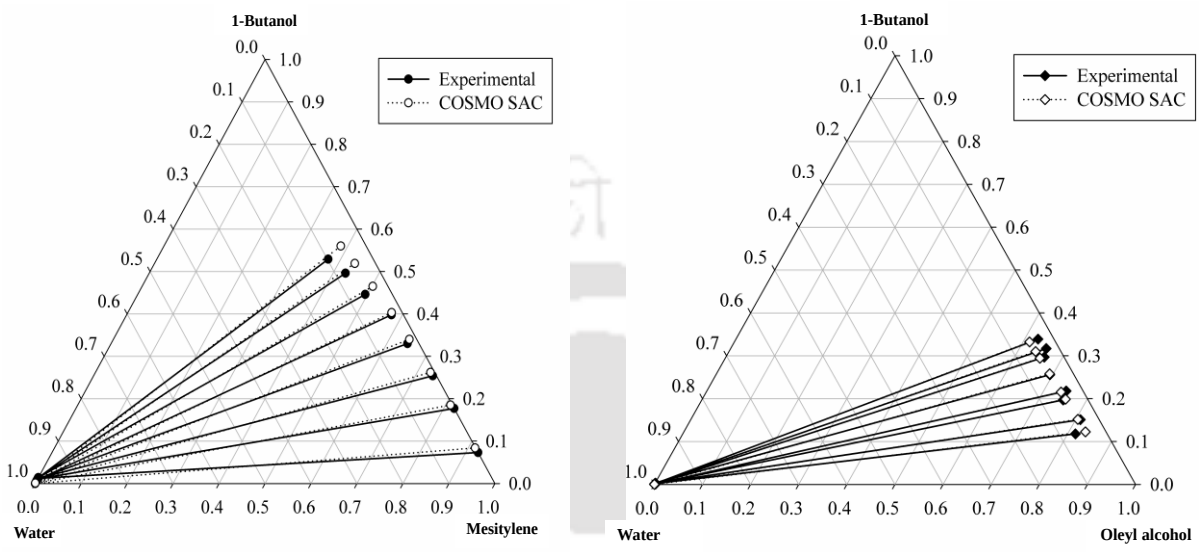

Figure 3.14: Experimental and COSMO-SAC predicted tie lines for the ternary system: mesitylene/Oleyl alcohol (1) + 1-butanol (2) + water (3) system at T = 303.15 K and p = 1 atm (Experimental results from [7]).

3.5.6. Prediction for DES-1, DL-menthol and Decanoic acid based DES

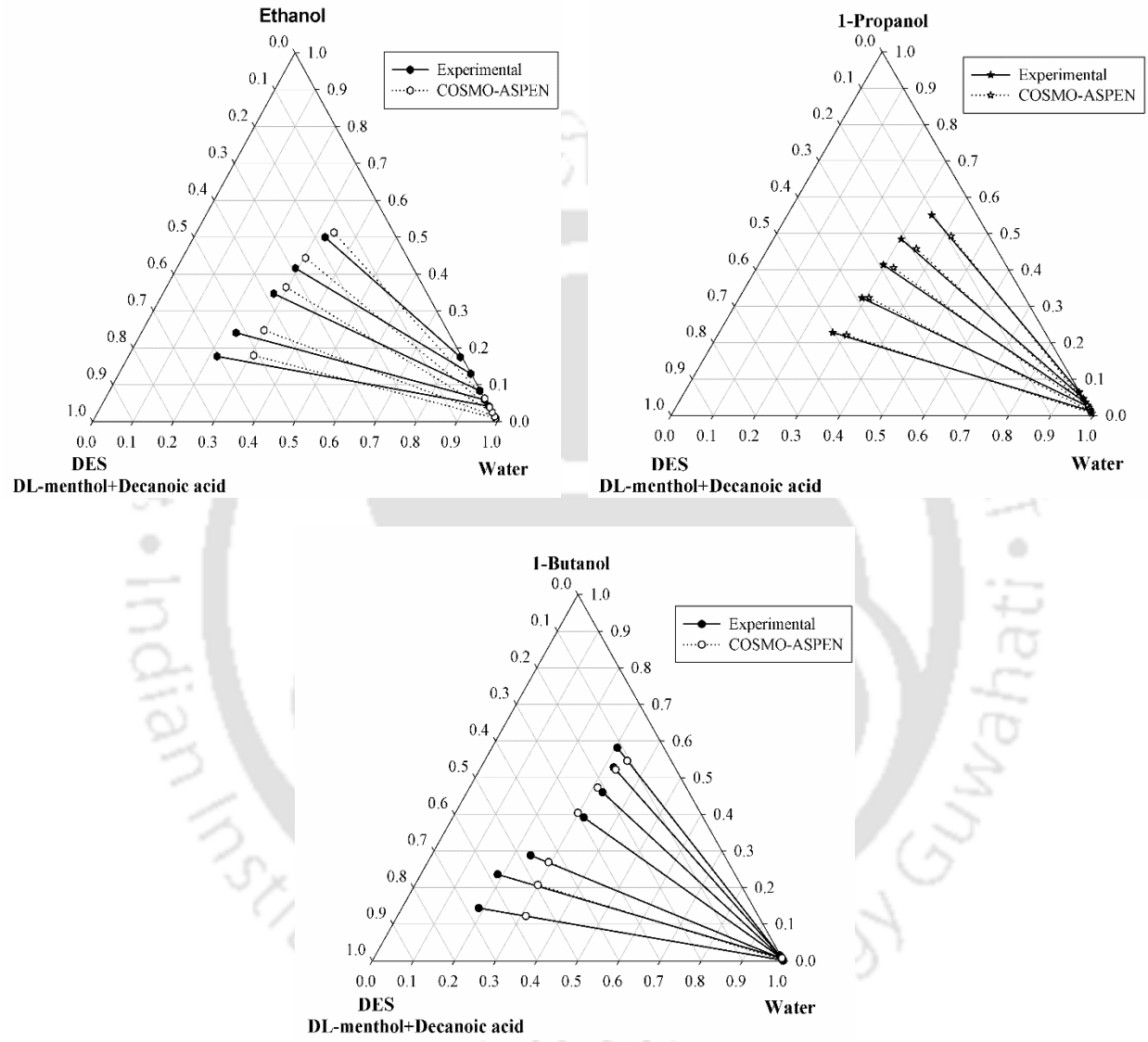

Figure 3.15: Experimental and COSMO-SAC predicted tie lines for the ternary system: DES-1 (1)-alcohol (2)-water (3) at 303.15 K and 1 atm.

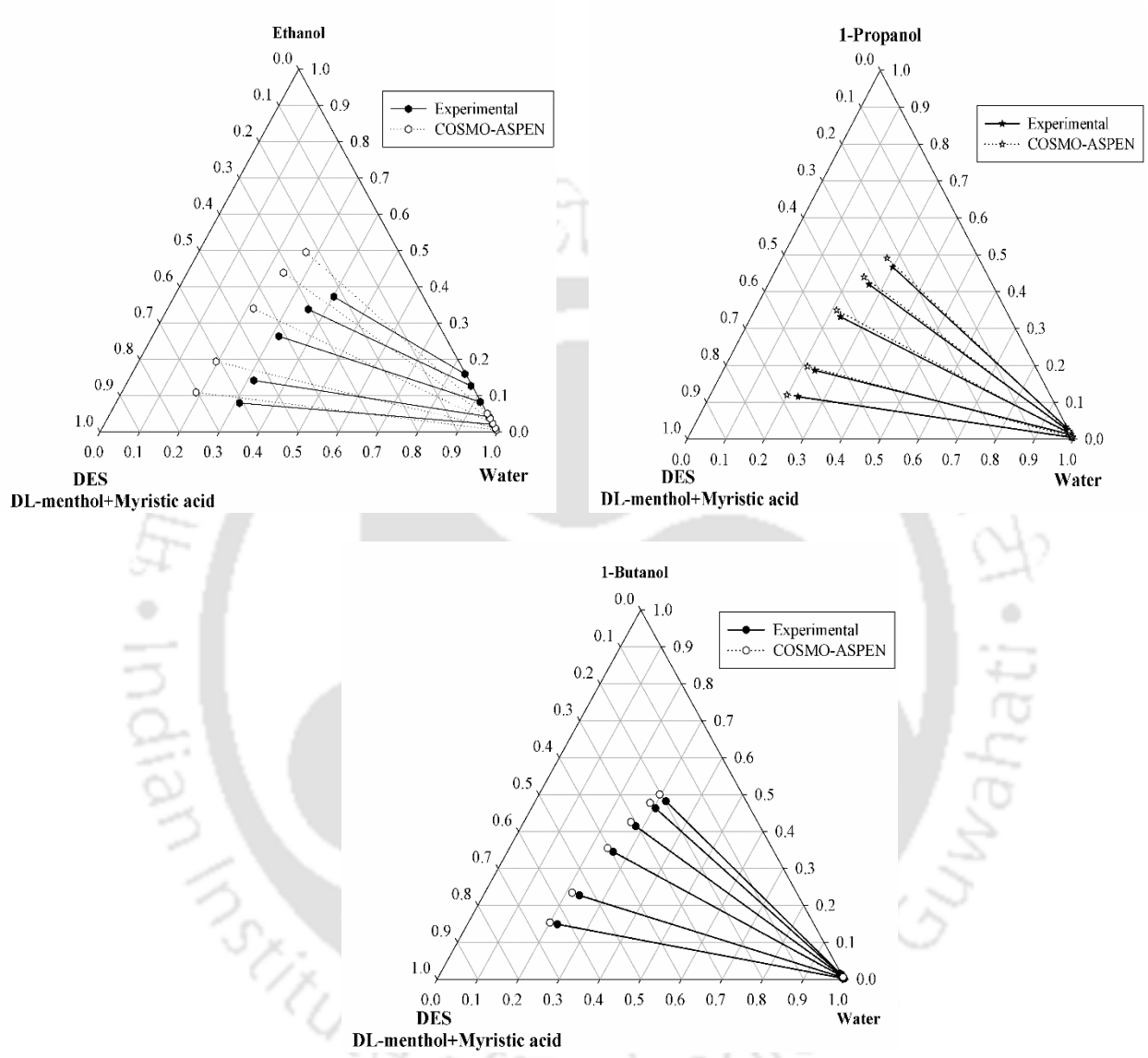

Figure 3.16: Experimental and COSMO-SAC predicted tie lines for the ternary system: DES-3 (1)-alcohol (2)-water (3) at 303.15 K and 1 atm.

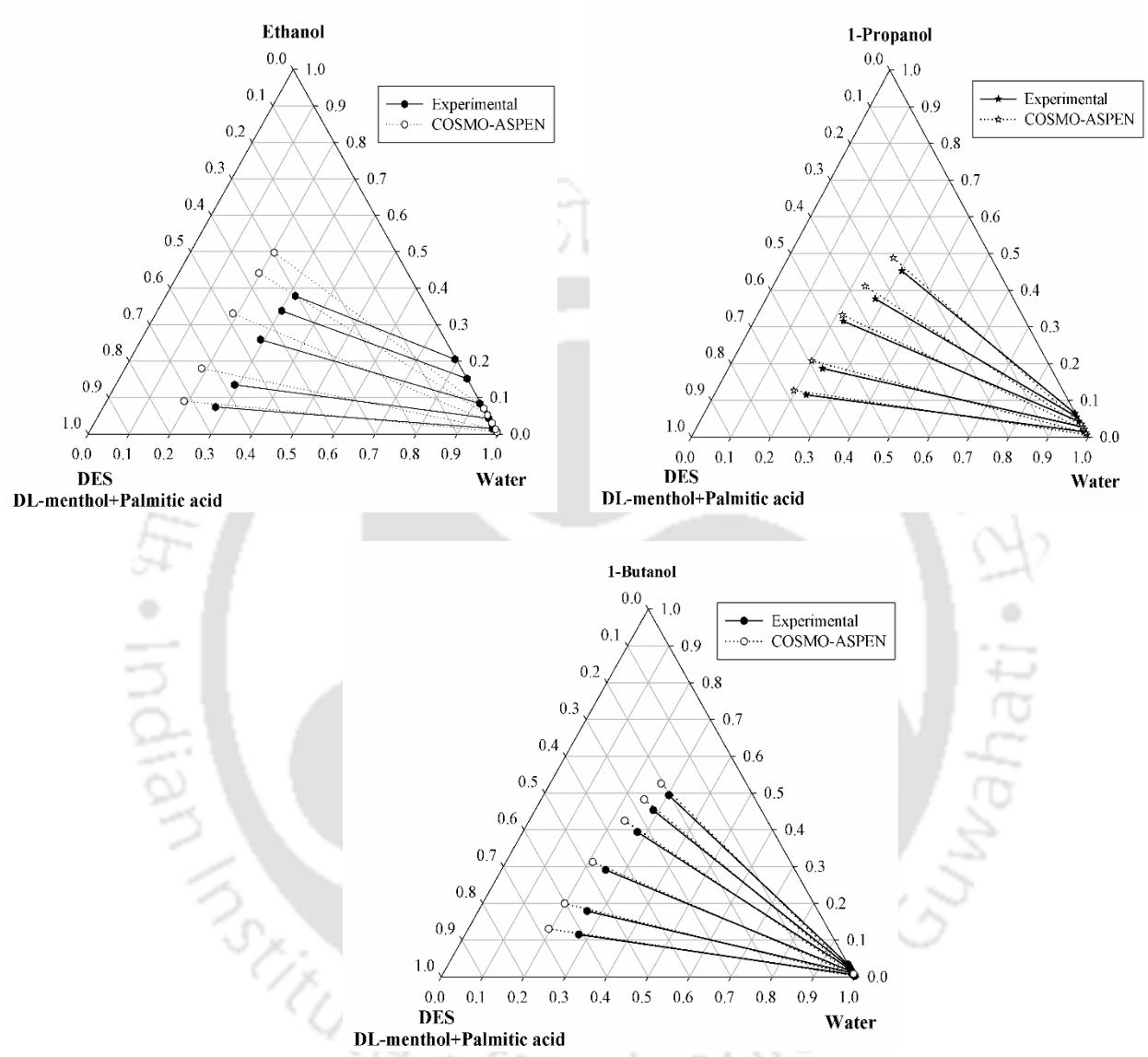

Figure 3.17: Experimental and COSMO-SAC predicted tie lines for the ternary system: DES-4 (1)-alcohol (2)-water (3) at 303.15 K and 1 atm.

Table 3.25: RMSD obtained via COSMO-SAC model using COSMO-ASPEN

	DES-1	DES-2	DES-3	DES-4	Mesitylene	Oleyl alcohol
Ethanol	0.053	0.036	0.05	0.052	-	-
1-propanol	0.01	0.025	0.01	0.016	-	-
1-butanol	0.008	0.022	0.008	0.021	0.014	0.0083

Overall the NRTL, UNIQUAC and COSMO-SAC models gave Root Mean Square Deviation (RMSD) values as (0.21%, 0.34% and 1.34%); and (0.16%, 0.21% and 0.83%) for the systems mesitylene (1) + 1-butanol (2) + water (3) and oleyl alcohol (1) + 1-butanol (2) + water (3) respectively. Overall RMSD of DES-1 to DES-4 for NRTL, UNIQUAC and COSMO-SAC are reported in Tables 3.20-3.23 and Table 3.25 respectively. It has been observed that among the NRTL, UNIQUAC and COSMO-SAC models, the average root mean square deviation (RMSD) values obtained were lesser than unity for NRTL and UNIQUAC models. This is expected as in NRTL [18] the interaction parameters have been regressed using the experimental data, while for COSMO-SAC [15, 18] this is predicted using a statistical mechanical framework.

Figure 3.18 and Figure 3.19 show the distribution coefficient and selectivity of the solvents used in the present study for the extraction of 1-butanol. It has been observed that decanoic acid based DES gave the highest selectivity as well as distribution coefficient among all DES. However it is worth mentioning that the distribution coefficient and selectivity for both oleyl alcohol and mesitylene are greater than either DES. Hence the choice may or can be directed towards DES if the economics namely amount of solvent flow and the capital cost is less. This is exactly been attempted in chapter 4.

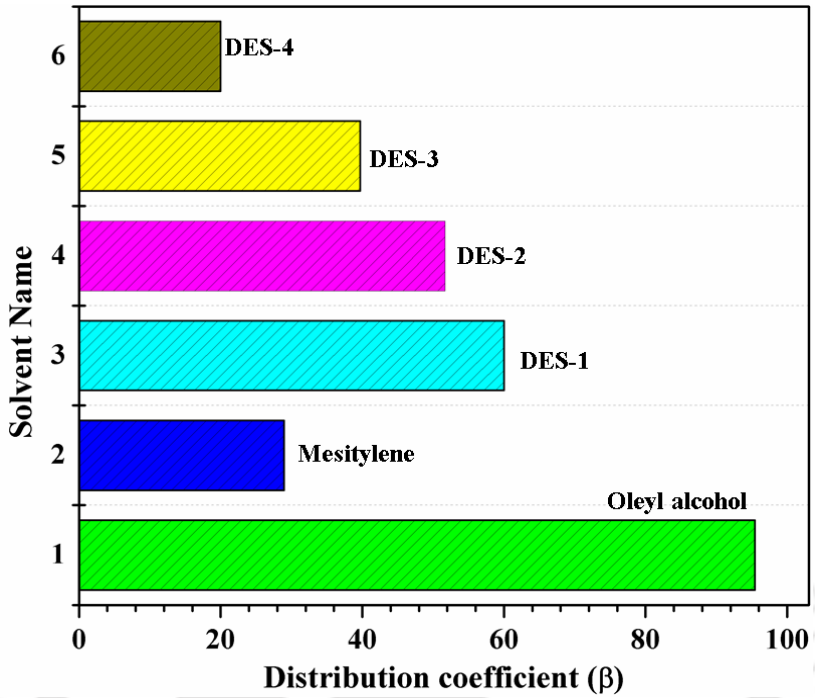

Figure 3.18: Distribution coefficient of the solvents for 1-butanol extraction.

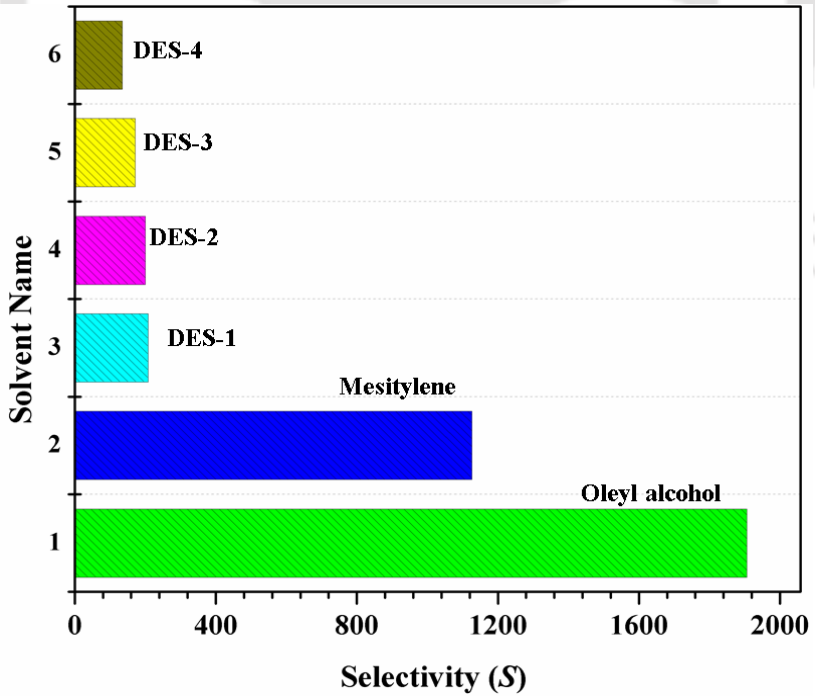

Figure 3.19: Selectivity of solvents for 1-butanol extraction.

3.6. Comparison of Selectivity and Distribution Ratios

In order to further explore the role of the hydrophobic character of the extractant, a comparison has been conducted with both reported DES and the Ionic Liquids in Tables 3.26-3.28, for ethanol, propanol and 1-butanol respectively. It is clear that the selectivities for choline chloride and tetramethylammonium chloride as Hydrogen Bond Acceptor [31] are comparable to our DES which is based on DL-menthol. A comparison with Ionic Liquids also points out to a similar fact in term of ethanol extraction as measured by Neves et al. [32] with trihexyl tetradecyl based phosphonium cations. On the contrary both the selectivities and distribution coefficient are larger for DES when compared to [BMIM][Tf_2N] for the case of propanol (Table 3.27) or 1-butanol (Table 3.28). In 1-butanol both the selectivities and distribution coefficient are larger than imidazolium[8], phosphonium[8] or morpholium based ionic liquids [33]. Looking at the distribution coefficients, it implies that the current DES will be beneficial as its will require a lower solvent to feed ratio for the same performance. In order to propose a technique for recovery of alcohols, the thermal stability of the DES mixtures needs to be ascertained so that distillation can be proposed to recover the alcohols. Table 3.28 reports a value close to infinity and ~6367 for mesitylene and oleyl alcohol respectively. This is higher than the previous reported work with ionic liquids such as 1-(2-hydroxyethyl)-2,3-dimethylimidozolium tetra fluoroborate (S=30) [34]. This is also higher than that reported for hydrophilic or hydrophobic ILs [35] and DES.

Table 3.26: Comparison of distribution coefficients and selectivities for ethanol extraction in aqueous media using conventional solvents, Ionic Liquids and DESs

System	Distribution Coefficient	Selectivity	References
DES-1 (DL-menthol/decanoic acid)	0.703	16.3	Present study
DES-2 (DL-menthol/lauric acid)	0.505	12.5	Present study
DES-3 (DL-menthol/myristic acid)	0.543	9.1	Present study
DES-4 (DL-menthol/palmitic acid)	0.52	9.6	Present study
DES [glycerol/choline chloride with molar ratios (4:1)]	0.811	21.9	Rodriguez et al.[31]
DES [glycerol/choline chloride with molar ratios (2:1)]	0.618	15.2	Rodriguez et al.[31]
DES [glycerol/tetramethylammonium chloride with molar ratios (4:1)]	0.643	13.3	Rodriguez et al.[31]
DES [glycerol/tetramethylammonium chloride with molar ratios (2:1)]	0.725	14.7	Rodriguez et al.[31]
[TDTHP][Phosph]*	0.83	5.1	Neves et al.[32]
[TDTHP][Deca]*	0.82	4.9	Neves et al.[32]
[TDTHP]Cl*	0.88	6.6	Neves et al.[32]
[TDTHP][CH_3SO_3]*	0.82	4.6	Neves et al.[32]
[TDTHP]Br*	0.70	8.4	Neves et al.[32]
[TDTHP][$N(CN)_2$]*	0.51	6.8	Neves et al.[32]
[TDTHP][Tf_2N]*	0.31	2.0	Neves et al.[32]
[BMIM][Tf_2N]*	0.15	7.5	Chafer et al.[36]

* Where Abbreviations:

[TDTHP][Phosph]: Tetradecyltrihexylphosphonium bis(2,4,4-trimethylpentyl) phosphinate

[TDTHP][Deca]: Tetradecyltrihexylphosphonium decanoate

[TDTHP]Cl: Tetradecyltrihexylphosphonium chloride

[TDTHP][CH_3SO_3]: Tetradecyltrihexylphosphonium methane sulfonate

[TDTHP]Br: Tetradecyltrihexylphosphonium bromide

[TDTHP][$N(CN)_2$]: Tetradecyltrihexylphosphonium dicyanimide

[BMIM][Tf_2N]: 1-butyl-1-methylpyrrolidinium bis(trifluoromethyl sulfonyl) imide

[TDTHP][Tf_2N]: Tetradecyltrihexylphosphonium bis(trifluoromethyl sulfonyl) imide

[Bmim][Tf_2N]: 1-butyl-1-methylpyrrolidinium bis(trifluoromethylsulfonyl)imide

Table 3.27: Comparison of distribution coefficients and selectivities for propanol extraction in aqueous media using conventional solvents, Ionic Liquids and DESs

System	Distribution Coefficient	Selectivity	References
DES-1	3.5	69.78	Present study
DES-2	1.95	56.05	Present study
DES-3	1.9	51.7	Present study
DES-4	2.2	31.19	Present study
[BMP][Tf_2N]*	0.37	19.8	Chafer et al.[37]
[TDTHP][Phosph]*	1.37	88.5	Bharti et al.[16]

*Where Abbreviations:

[Bmim][Tf_2N]: 1-butyl-1-methylpyrrolidinium bis(trifluoromethylsulfonyl)imide

[TDTHP][Phosph]:Tetradecyltrihexylphosphonium bis(2,4,4-trimethylpentyl)phosphinate

Table 3.28: Comparison of distribution coefficients and selectivities for 1-butanol extraction in aqueous media using conventional solvents, Ionic Liquids and DESs

System	Distribution Coefficient	Selectivity	References
Mesitylene	9.40	1913.6	Present study
Oleyl alcohol	19.88	6319.6	Present study
DES-1	10.6	237.8	Present study
DES-2	8.9	200.6	Present study
DES-3	5.94	145.67	Present study
DES-4	3.41	81.25	Present study
[$Im_{10,1}$][TCB]*	3.2	100	Heitmann et al.[8]
[$P_{6,6,6,14}$][TCB]*	2.0	500	Heitmann et al.[8]
[$Im_{8,1}$][FAP]*	0.8	420	Heitmann et al.[8]

[Im10,1][Tf_2N] *	5.7	90	Nann et al.[33]
[Mo10,1][TCB] *	4.8	70	Nann et al.[33]
[Mo10,1][Tf_2N] *	2.1	99.7	Nann et al.[33]
[Bmim][Pf_6] *	0.74	21.0	Ha et al. [35]
[Hmim][Pf_6] *	0.97	37.5	Ha et al. [35]
[Omim][Pf_6] *	1.11	49.2	Ha et al. [35]
[Bmim][Tf_2N] *	1.03	39.1	Ha et al. [35]
[Hmim][Tf_2N] *	1.25	66.1	Ha et al. [35]
[Omim][Tf_2N] *	1.37	78.9	Ha et al. [35]
[Hmim][TfO] *	0.90	2.6	Ha et al. [35]
[Omim][TfO] *	1.03	3.5	Ha et al. [35]
[Pmim][TfO] *	1.05	4.9	Ha et al. [35]
[HMIM]BF_4] *	0.90	3.9	Ha et al. [35]
[OMIM][BF_4] *	2.18	12.2	Ha et al. [35]
[Hmim][Tf_2N] *	1.11	120.0	Garcia et al. [38]
Cyphos 104*	9.21	55.0	Garcia et al. [38]
[MTOAOct] *	11.29	49.0	Garcia et al. [38]
[TDAMCH] *	8.49	130.0	Garcia et al. [38]
[TOAMNaph] *	21.00	274.0	Garcia et al. [38]

*
Where Abbreviations:

[$Im_{10,1}$][TCB]: (1-decyl-3-methyl-imidazolium tetracyanoborate)

[$P_{6,6,6,14}$][TCB]: (Trihexyltetradecylphosphonium tetracyanoborate)

[$Im_{8,1}$][FAP]: (1-decyl 3-methylimidazolium tris(pentafluoroethyl)trifluorophosphate)

[$Im_{10,1}$][Tf_2N]: (1-decyl-3-methyl-imidazolium bis(trifluoromethylsulfonyl)imide)

[$Mo_{10,1}$][TCB]: (4-decyl-4-methyl-morpholinium tetracyanoborate)

$[Mo_{10,1}][Tf_2N]$: (4-decyl-4-methyl-morpholinium bis(trifluoromethylsulfonyl)imide)

[Bmim][Tf_2N]: (1-butyl-1-methylpyrrolidinium bis(trifluoromethylsulfonyl)imide

[Hmim][Tf_2N]: Tetradecyltrihexylphosphonium bis(trifluoromethylsulfonyl)imide

[Omim][Tf_2N]: (1-butyl-1-methylpyrrolidinium bis(trifluoromethylsulfonyl)imide)

[Hmim][TfO]: 1-hexyl-3- methylimidazoliu trifluoromethanesulfonate

[Omim][TfO]: 1-methyl-3-octylimidazolium trifluoromethanesulfonate

[Pmim][TfO]: 1- phenylpropyl-3-methylimidazolium trifluoromethanesulfonate

[HMIM]BF_4]: 1-hexyl-3- methylimidazoliu tetrafluoroborate

[OMIM][BF_4]: 1-methyl-3-octylimidazolium tetrafluoroborate

[Hmim][Tf_2N]: 1-hexyl-3-methylimidazolium bis(trifluoromethylsulfonyl)imide

Cyphos 104: Tetradecyl(trihexyl) phosphonium bis-2,4,4-trimethylpentyl-phosphinate

[MTOAOct]: Methyltrioctylammonium octanoate

[TDAMCH]: Ttetrakis(decyl) ammonium 1-methyl-1-cyclohexanoate

[TOAMNaph]: Tetraoctylammonium 2-methyl-1-naphthoate

After successful thermodynamics modelling we shall now initiate a flowsheet to scale-up the laboratory scale data to an industrially feasible unit using Aspen Plus V8.8®. This will include optimization of the extractor and distillation unit and then coupling it to get the final TAC or the Total Annual Cost. This is exactly been discussed in chapter 4.

3.7. Summary

Improved mass transfer rates coupled with high separation efficiency was observed with mesitylene and oleyl alcohol for the separation of 1-butanol - water mixtures. Larger values of selectivity (399-2591) for both the conventional solvents indicate easier separation of 1-butanol from water. The raffinate phase from the experiment and simulation was found to comprise mainly water with mass composition as high as 99.9% w/w. Further the application of a hydrophobic deep eutectic and low-transition temperature mixture for the lower alcohol extraction has been investigated for the first time. Extraction of ethanol i.e. (5-40 mole%), propanol (5-30 mole%) and 1-butanol (10-50 mole%) from the aqueous solution was measured with the synthesized DESs and conventional solvents. The distribution coefficient and selectivity

were found to be much higher for 1-butanol as compared to ethanol and propanol. The ^{1}H NMR analysis depicted an absence of DES in the raffinate phase. This indicates that the DES does not contaminate the water phase, thereby enabling the ease of solvent recycling. The NRTL, UNIQUAC and COSMO-SAC model gave RMSD value for DES-1 to DES-4 in the range of 0.0026-0.0029, 0.0046-0.0075 and 0.036-0.053 respectively in case of ethanol; for DES-1 to DES-4: 0.0017-0.003, 0.0022-0.0065 and 0.01-0.025 respectively in case of 1-propanol; for DES-1 to DES-4: 0.0019-0.0035, 0.0039-0.0055 and 0.008-0.022 respectively in case of 1-butanol. It implies that NRTL model gave an excellent match with the experimental data and good prediction. Also, conventional solvents mesitylene and oleyl alcohol have been used for the separation of 1-butanol from their aqueous solution. Overall the slopes of the tie lines and the spread of two-phase region indicated higher separation as it covered a large part of the ternary plot.

References

1. S. Ishii, M. Taya, T. Kobayashi: Production of butanol by Clostridium acetobutylicum in extractive fermentation system. Journal of chemical engineering of Japan 18 (1985) 125-130
2. W. Kaminski, E. Tomczak, A. Gorak: Biobutanol-production and purification methods. Atmosphere 2 (2011) 31-37
3. R. Anantharaj, T. Banerjee: COSMO-RS based predictions for the desulphurization of diesel oil using ionic liquids: Effect of cation and anion combination. Fuel Process. Technol. 92 (2011) 39-52
4. X. Hu, J. Yu, H. Liu: Liquid− liquid equilibria of the system 1-(2-hydroxyethyl)-3-methylimidozolium tetrafluoroborate or 1-(2-hydroxyethyl)-2, 3-dimethylimidozolium tetrafluoroborate+ water+ 1-butanol at 293.15 K. J. Chem. Eng. Data 51 (2006) 691-695

5. H. Renon, J.M. Prausnitz: Local compositions in thermodynamic excess functions for liquid mixtures. AIChE journal 14 (1968) 135-144
6. M. Mohan, V.V. Goud, T. Banerjee: Solubility of glucose, xylose, fructose and galactose in ionic liquids: Experimental and theoretical studies using a continuum solvation model. Fluid Phase Equilib. 395 (2015) 33-43
7. P. Dehury: Liquid-Liquid Extraction and Conceptual Process Design for the Extraction of Lower Alcohols, M. Tech. Thesis, I.I.T., Guwahati, (2013)
8. S. Heitmann, J. Krings, P. Kreis, A. Lennert, W. Pitner, A. Górak, M. Schulte: Recovery of n-butanol using ionic liquid-based pervaporation membranes. Separation and purification technology 97 (2012) 108-114
9. S. García, M. Larriba, J. García, J.S. Torrecilla, F. Rodríguez: Liquid–liquid extraction of toluene from n-heptane using binary mixtures of N-butylpyridinium tetrafluoroborate and N-butylpyridinium bis (trifluoromethylsulfonyl) imide ionic liquids. Chem. Eng. J. 180 (2012) 210-215
10. A.S. Gonzalez, M. Francisco, G. Jimeno, S.L.G. de Dios, M.C. Kroon: Liquid–liquid equilibrium data for the systems {LTTM+ benzene+ hexane} and {LTTM+ ethyl acetate+ hexane} at different temperatures and atmospheric pressure. Fluid Phase Equilib. 360 (2013) 54-62
11. D.V. Rabari: Experimental, Modelling and Optimization Insights for the Enhancement of Butanol Production using Phosphonium based Ionic Liquids, Ph. D. Thesis, I.I.T., Guwahati, (2015)
12. Y.C. Chen, K.L. Li, C.L. Chen, I.L. Chien: Design and Control of a Hybrid Extraction–Distillation System for the Separation of Pyridine and Water. Ind. Eng. Chem. Res. 54 (2015) 7715-7727
13. K.I. Al-Malah: Aspen Plus: Chemical Engineering Applications, John Wiley & Sons (2016)
14. M.K. Singh, T. Banerjee, A. Khanna: Genetic algorithm to estimate interaction parameters of multicomponent systems for liquid–liquid equilibria. Comput. Chem. Eng. 29 (2005) 1712-1719

15. T. Banerjee, M.K. Singh, R.K. Sahoo, A. Khanna: Volume, surface and UNIQUAC interaction parameters for imidazolium based ionic liquids via polarizable continuum model. Fluid Phase Equilib. 234 (2005) 64-76
16. A. Bharti, D. Kundu, D. Rabari, T. Banerjee: Phase Equilibria in Ionic Liquid Facilitated Liquid–Liquid Extractions, CRC Press (2017)
17. W.L. Luyben, I.-L. Chien: Design and control of distillation systems for separating azeotropes, John Wiley & Sons (2011)
18. T. Banerjee, R.K. Sahoo, S.S. Rath, R. Kumar, A. Khanna: Multicomponent liquid− liquid equilibria prediction for aromatic extraction systems using COSMO-RS. Ind. Eng. Chem. Res. 46 (2007) 1292-1304
19. R.K. Sahoo, T. Banerjee, S.A. Ahmad, A. Khanna: Improved binary parameters using GA for multi-component aromatic extraction: NRTL model without and with closure equations. Fluid Phase Equilib. 239 (2006) 107-119
20. R. Anantharaj, T. Banerjee: Liquid–liquid equilibria for quaternary systems of imidazolium based ionic liquid+ thiophene+ pyridine+ iso-octane at 298.15 K: experiments and quantum chemical predictions. Fluid Phase Equilib. 312 (2011) 20-30
21. M. Mohan, T. Banerjee, V.V. Goud: Solid Liquid Equilibrium of Cellobiose, Sucrose, and Maltose Monohydrate in Ionic Liquids: Experimental and Quantum Chemical Insights. J. Chem. Eng. Data 61 (2016) 2923–2932
22. G.R. Harvianto, S.E. Kim, I.B. Jin, K.J. Kang, M. Lee: Liquid–Liquid Equilibria Data for the Quaternary System of Acetic Acid, Water, p-Xylene, and Ethyl Acetate at 313.15 K and 101.325 kPa. J. Chem. Eng. Data 61 (2015) 780-787
23. M.G. Freire, L.M. Santos, I.M. Marrucho, J.A. Coutinho: Evaluation of COSMO-RS for the prediction of LLE and VLE of alcohols + ionic liquids. Fluid Phase Equilib. 255 (2007) 167-178
24. S.-T. Lin, S.I. Sandler: A priori phase equilibrium prediction from a segment contribution solvation model. Ind. Eng. Chem. Res. 41 (2002) 899-913
25. M. Frisch, G.W. Trucks, H.B. Schlegel, G.E. Scuseria, Robb M. A., J.R. Cheeseman, G. Scalmani, V. Barone, B. Mennucci, G.A. Petersson, H. Nakatsuji, M. Caricato, X. Li, H.P. Hratchian, A.F. Izmaylov, J. Bloino, G. Zheng, J.L. Sonnenberg, M. Hada, M. Ehara, K. Toyota, R. Fukuda, J. Hasegawa, M. Ishida, T. Nakajima, Y. Honda, O. Kitao,

H. Nakai, M.T. Vreven, J.J. A, J.E. Peralta, F. Ogliaro, M. Bearpark, J.J. Heyd, E. Brothers, K.N. Kudin, V.N. Staroverov, T. Keith, R. Kobayashi, J. Normand, K. Raghavachari, A. Rendell, J.C. Burant, S.S. Iyengar, J. Tomasi, M. Cossi, N. Rega, J.M. Millam, M. Klene, J.E. Knox, J.B. Cross, V. Bakken, C. Adamo, J. Jaramillo, R. Gomperts, R.E. Stratmann, O. Yazyev, A.J. Austin, R. Cammi, C. Pomelli, J.W. Ochterski, R.L. Martin, K. Morokuma, V.G. Zakrzewski, G.A. Voth, P. Salvador, J.J. Dannenberg, S. Dapprich, A.D. Daniels, O. Farkas, J.B. Foresman, J.V. Ortiz, J. Cioslowski, D.J. Fox Gaussian 09 Revision B. 01, Gaussian, Inc, Wallingford, CT, DOI. (2010)

26. T. Banerjee, A. Ramalingam: Desulphurization and Denitrification of Diesel Oil Using Ionic Liquids: Experiments and Quantum Chemical Predictions, Elsevier (2015)
27. D. Kundu, T. Banerjee: Multicomponent vapor–liquid–liquid equilibrium prediction using an a priori segment based model. Ind. Eng. Chem. Res. 50 (2011) 14090-14096
28. A. Klamt: Conductor-like Screening Model for Real Solvents: A New Approach to the Quantitative Calculation of Solvation Phenomena. J. Phys. Chem. 99 (1995) 2224-2235
29. R. Dennington, T. Keith, J. Millam: GaussView, version 5. Semichem Inc., Shawnee Mission, KS (2009)
30. T. Banerjee, K.K. Verma, A. Khanna: Liquid–liquid equilibrium for ionic liquid systems using COSMO-RS: Effect of cation and anion dissociation. AIChE journal 54 (2008) 1874-1885
31. N.R. Rodriguez, J. Ferre Guell, M.C. Kroon: Glycerol-Based Deep Eutectic Solvents as Extractants for the Separation of MEK and Ethanol via Liquid–Liquid Extraction. J. Chem. Eng. Data 61 (2016) 865-872
32. C.M. Neves, J.F. Granjo, M.G. Freire, A. Robertson, N.M. Oliveira, J.A. Coutinho: Separation of ethanol–water mixtures by liquid–liquid extraction using phosphonium-based ionic liquids. Green Chem. 13 (2011) 1517-1526
33. A. Nann, C. Held, G. Sadowski: Liquid–liquid equilibria of 1-butanol/water/IL systems. Ind. Eng. Chem. Res. 52 (2013) 18472-18481
34. D.S. Abrams, J.M. Prausnitz: Statistical thermodynamics of liquid mixtures: a new expression for the excess Gibbs energy of partly or completely miscible systems. AIChE Journal 21 (1975) 116-128

35. S.H. Ha, N.L. Mai, Y.-M. Koo: Butanol recovery from aqueous solution into ionic liquids by liquid–liquid extraction. Process biochemistry 45 (2010) 1899-1903

36. A. Cháfer, J.D.l. Torre, A. Font, E. Lladosa: Liquid–Liquid Equilibria of Water+ Ethanol+ 1-Butyl-3-methylimidazolium Bis (trifluoromethanesulfonyl) imide Ternary System: Measurements and Correlation at Different Temperatures. J. Chem. Eng. Data 60 (2015) 2426-2433

37. A. Cháfer, J.D.l. Torre, E. Lladosa, J.P. Franco, M.P. Cumplido: Liquid–Liquid Equilibria of the Water + 1-Propanol + 1-Butyl-1-methylpyrrolidinium Bis(trifluoromethylsulfonyl)imide Ternary System: Study of the Ability of Ionic Liquid as a Solvent. J. Chem. Eng. Data 61 (2016) 4006-4012

38. L.Y. Garcia-Chavez, C.M. Garsia, B. Schuur, A.B. de Haan: Biobutanol recovery using nonfluorinated task-specific ionic liquids. Ind. Eng. Chem. Res. 51 (2012) 8293-8301

Chapter 4

Hybrid Extraction-Distillation Process Flow sheet for Extraction of Lower Alcohols with Deep Eutectic Solvent

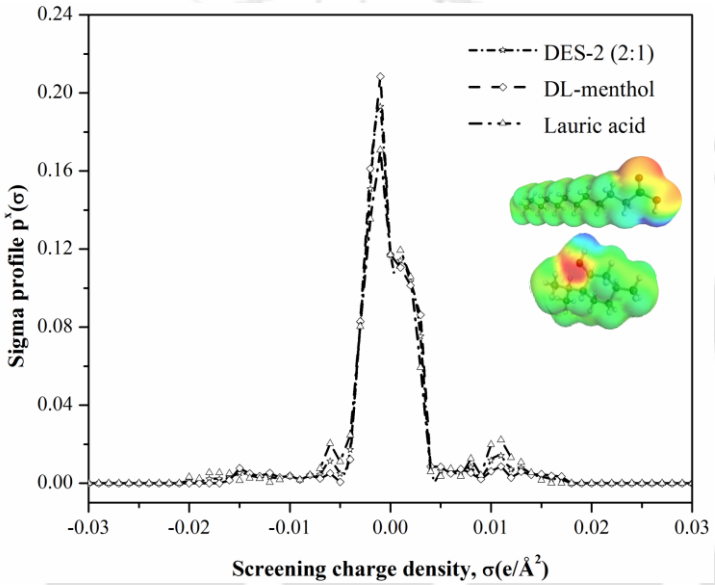

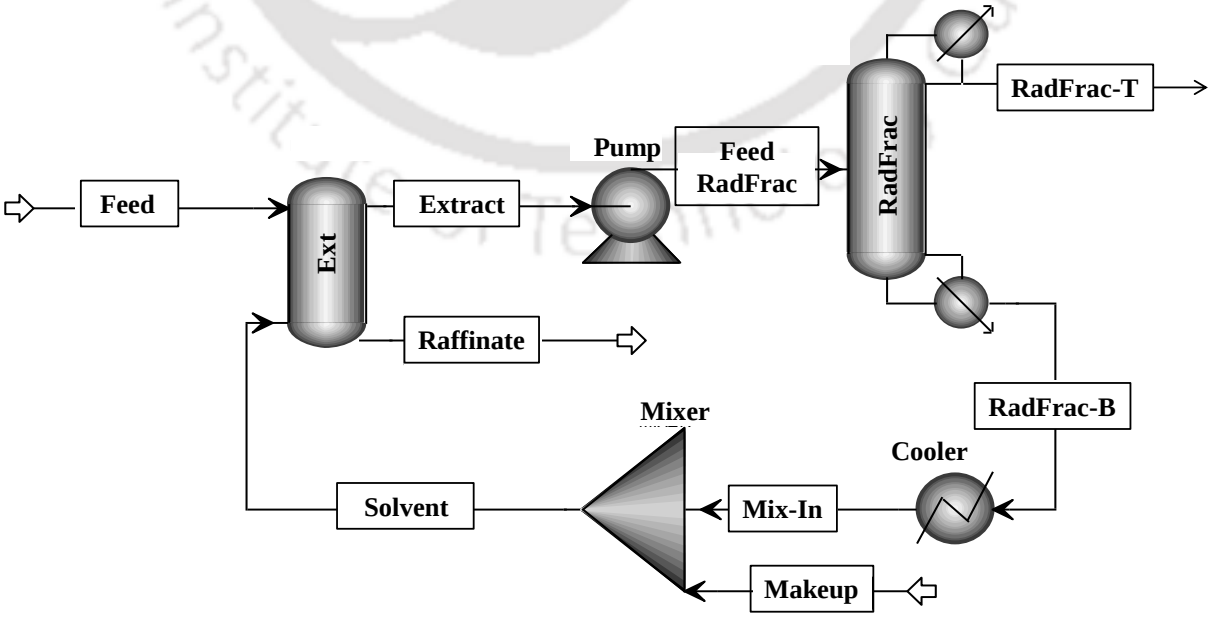

4.1. Introduction

Once the Liquid−Liquid Equilbria results are available, a need of scale-up for the separation of lower alcohols needs to be adopted. Commercial software such as ASPEN Plus V8.8 is conventionally used for understanding the process economics of any separation process. The separation of lower alcohols through a hybrid extraction system is already well known [1]. This is also inline with an earlier work [2] where the hybrid separation processes is found to be an effective tool for reducing the energy intensive step of distillation. In the hybrid extraction, extraction column operates at ambient temperature and pressure; which implies that there is no requirement of additional energy within the extractor column. It provides significant savings in the operating cost as well as the total annual cost when compared to explicit extractive distillation. Previous authors have assessed options for the selective 1-butanol recovery from aqueous solution making the separation economical and efficient [3, 4]. Technologies for butanol recovery integrated with fermentations [5, 6] are well explored. In another work,reduction in butanol inhibition by perstraction i.e utilization of concentrated lactose/whey permeate by *Clostridium acetobutylicum* was undertaken to enhance butanol fermentation economics. Further PDMS/ceramic composite membrane was also used for pervaporation separation of acetone–butanol–ethanol (ABE) aqueous solutions with an intensification step for the ABE fermentation process [7].

As discussed in previous chapters, the separation of lower chain alcohols from their aqueous phase is considered difficult because of azeotrope formation [8-10]. In our case, the feed is highly aqueous as 1-butanol is less than 5 mole% (0.8 water and 0.2 1-butanol w/w). From chapter 3, distillation is not considered an effective and economical step for such cases [3] as it will require a huge amount of steam to vaporize the water portion. This leads to a higher energy demand as 1-butanol has a higher boiling point. In such a scenario, the entire water gets extracted in the raffinate phase of the extractor. A similar strategy has been used by previous authors where the design and control of a Hybrid Extraction–Distillation system for the separation of pyridine and water was proposed and demonstrated [11, 12]. The flowsheet given below explains the entire sequential process optimization as per Figure 4.1 and Figure 4.2. This procedure shall remain the same for both conventional solvent such as mesitylene and new solvents i.e. DES. In

the present study the cost factor has been kept to a minimum by performing the simulation at 298.15-303.15 K and 1 atm pressure. For performing the solvent extraction process, a minimization of the production cost is necessary in order to recover the extracting solvent. Further this needs to be reused and recycled in the extraction flowsheet [12-14]. These aspects have been explained in the subsequent sections.

4.2. Simulation Details

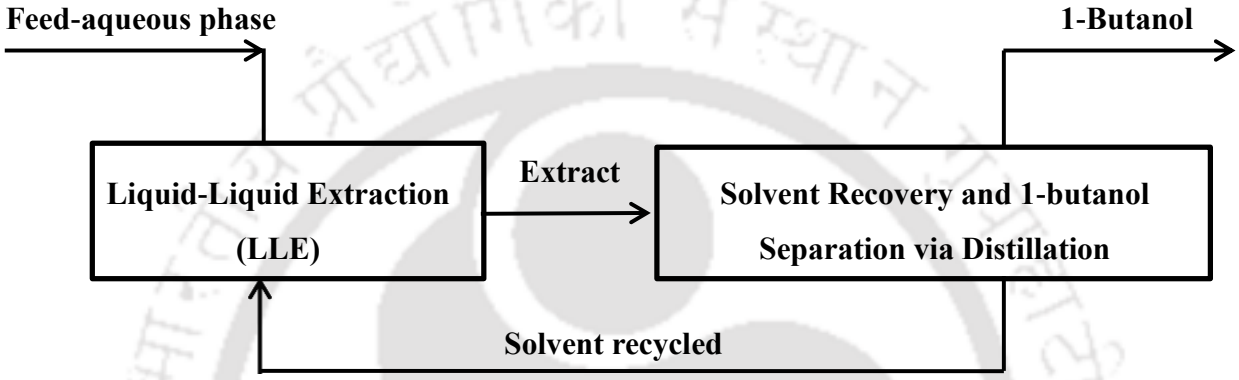

Figure 4.1: Sequential flow chart for optimization [3, 6]

Figure 4.2 shows the solution strategy for the extraction of 1-butanol using ASPEN Plus. The operating conditions for the extractor column will be used as p = 1 atm. and T = 25 ºC. The fresh feed composition in terms of mass fraction namely: water 0.8 (w/w) and 1-butanol 0.2 (w/w) is used in all the simulations. This is the same as per the reported LLE experiments and results in chapter 3. Non-random two-liquid model (NRTL) and COSMO-ASPEN thermodynamic model have been used in both conventional and DES solvent respectively. The missing binary interaction parameters were then evaluated with the R-PCES or UNIFAC tool of ASPEN. This has been earlier explained in chapter 3.

Initially the extractor column is designed for a recovery of 99.99% 1-butanol by keeping solvent flow rate as the manipulated variable. Optimization of number of stages in the extractor column is then selected on the basis of f.o.b. purchase cost (Freight on board cost). In the extractor, both *Design Spec* as well as *Sensitivity Analysis* tools of ASPEN have been used to optimize the solvent flow rate for a 99.9 w/w% recovery of 1-butanol. Within the extractor column, for a particular number of stages (i.e. 5, 6, 7, 8 etc.) the solvent flow rate is varied by applying *Design Spec* with 99.9% w/w. Thereafter for every stage, the f.o.b. purchase cost

(Freight on board cost) is computed and plotted. The stage number corresponding to the lowest f.o.b was then chosen as the number of stages for extractor. Once the number of stages is fixed, we adopt the *Sensitivity Analysis* tool to obtain the variation of solvent flow rate with butanol flow rate in the extract stream. With this we get an optimized flowrate of solvent (mesityene or DES).

In the distillation column, the same extract feed rate from extractor is used as a feed stream by increasing its pressure through a pump. In this column, the manipulated variables used are reflux ratio and distillate rate. *Design Spec* is then invoked by keeping a maximum purity of butanol in the distillate stream. Here both the reflux ratio and the butanol flow rate in distillate stream is varied from (0.01 to 100) and (1000 kg/hr to 6000 kg/hr) respectively while applying the *Design Spec*. The simulation is made to converge by varying the feed stage or the pump pressure. On similar lines the TAC of distillation column, which includes both capital (shell and heat exchange cost) and energy cost are also calculated by varying the number of stages in the distillation column. Optimum solutions obtained when the overall TAC (combined TAC of extractor and distillation column) is minimum.

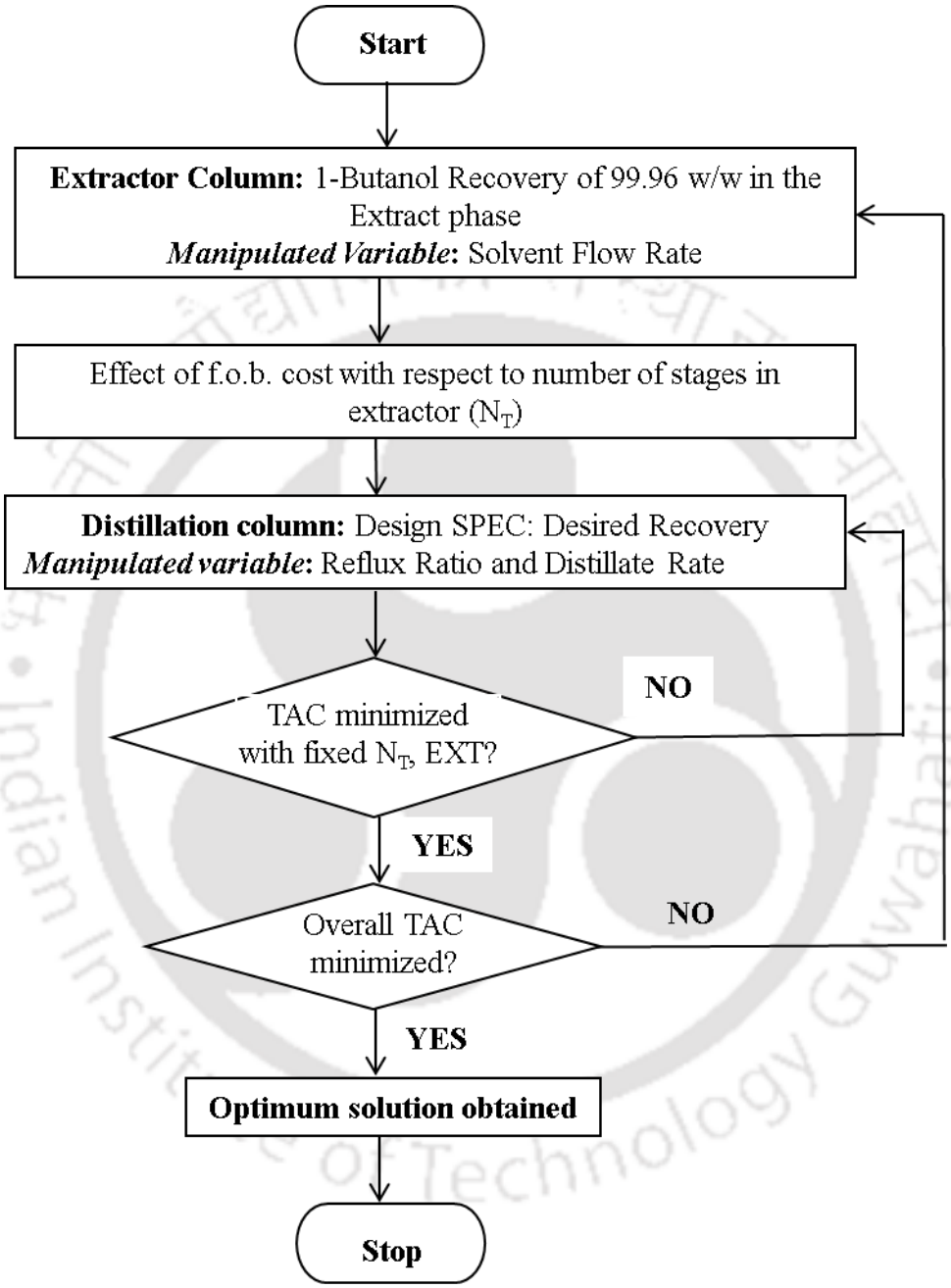

Figure 4.2: Solution Strategy for 1-butanol Extraction (EXT: Extractor; N_T=Number of stages)

4.3. Liquid-Liquid Extraction

Figure 4.3 shows the schematic of simple extractor used for liquid-liquid extraction (LLE). It shows the *Extract* and *Raffinate* phase as obtained from a LLE process. Separation efficiency of LLE mainly depends on solvent distribution coefficient, selectivity and recyclability [15]. The solvents which are considered are polar affects the extraction process by solvating the extracted complex in the extract phase. This tends to depend on the dielectric constant, dipole moment and hydrogen -bonding ability. We have not considered all these factors explicitly while simulating the same in ASPENone.

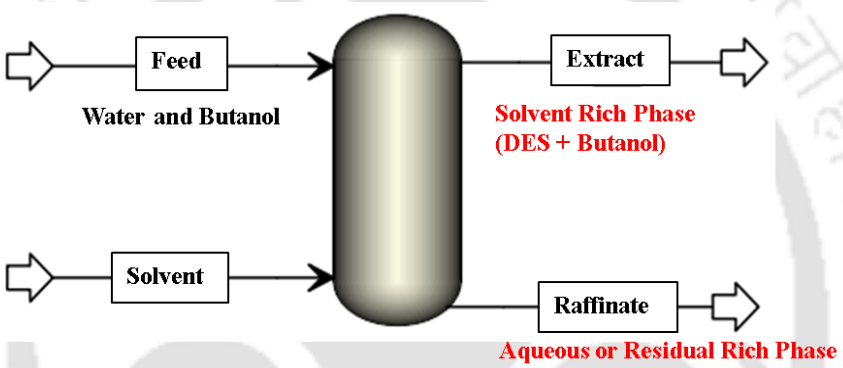

Figure 4.3: Extractor used for the Liquid-Liquid Extraction (LLE)

4.4. Hybrid Extraction-Distillation Unit

As discussed earlier, a hybrid downstream process (Figure 4.4) has also been proposed for the production of 1-butanol. Initially this has been used on traditional solvent such as mesitylene, thereafter it will be extended to all the four DES namely DES1, DES2, DES3 and DES4. Within ASPEN, the excess Gibb's Free Energy such as NRTL has been used for the simulation, while the regression of missing binary interaction parameters have been obtained by UNIFAC model or R-PCES (Regression Property Correlation and EStimation) [12, 16]. For defining the DES, the *PSEUDOCOMPONENT* mode using the sigma profile of the organic acid and DL-menthol have been used. The details and step wise procedure are explained in Appendix 4.1.

Feed stream (FEED) is assumed as a mixture of 1-butanol and water. The overall flow sheet consists of a liquid–liquid extractor EXT and a component separator (Distillation, RadFrac). A total condenser has been used in the distillation column. The distillate, RadFrac -T from the distillation column contains higher proportion of butanol and solvent. Hence as solvent is lost here, some makeup solvent (MAKE-UP) is added in the mixture for recycle. This is added to the bottom, RadFrac -B stream which is cooled from the distillation column and added with the makeup solvent. Thereafter the entire solvent is again fed back to the extractor (MIX-IN). The operating conditions for the process design should be selected in order to lessen cost while respecting the requirement of an elevated purity of the raffinate (RAFFINATE) and an increasing yield for the alcohol in the extract phase (EXTRACT).

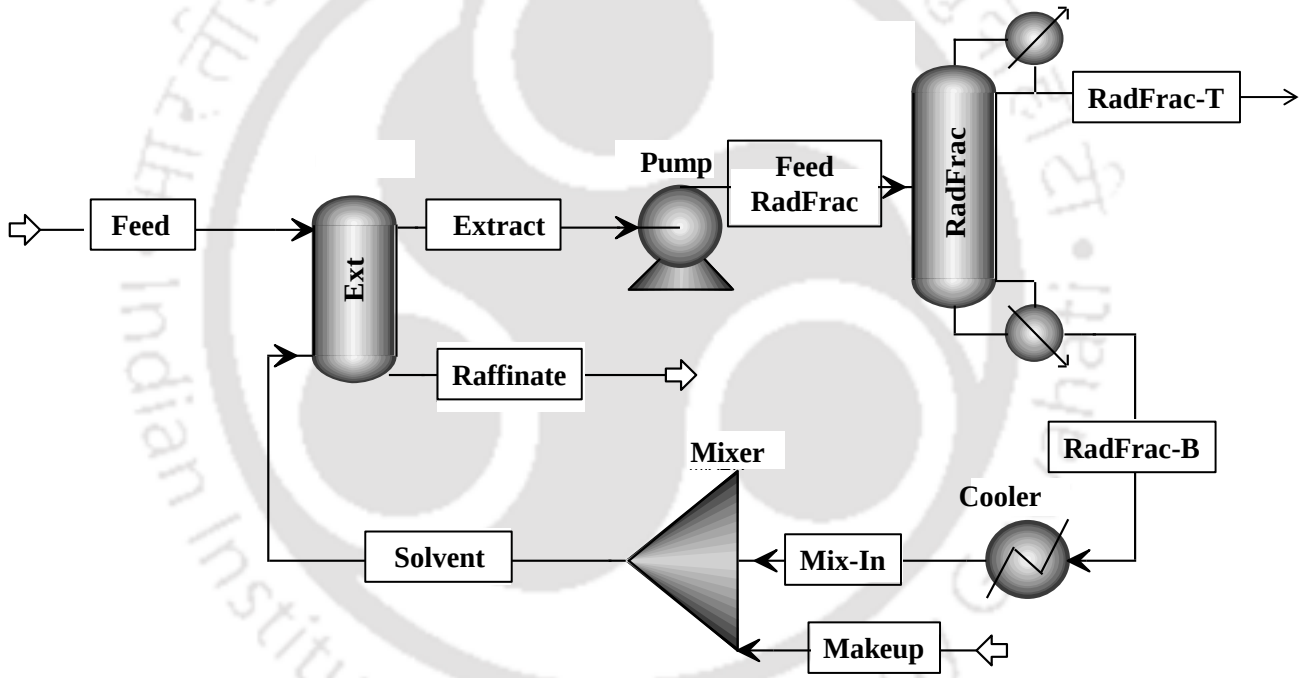

Figure 4.4: Hybrid Extraction-Distillation Process flow sheet for the separation of lower alcohols

4.4.1. 1-Butanol Production using Mesitylene

The overall flow sheet (Figure 4.7) thereby consists of a liquid–liquid extractor (Extractor) and a component separator (Distillation). Together the whole flow sheet was optimized where the operating conditions similar to the feed composition (0.2 w/w fraction 1-butanol) corresponding to the first tie line of the LLE data (Table 3.2, chapter 3) was used in this

study. The whole flowsheet has been proposed for the production of 1-butanol at the rate 5000 kg/hr (4.38×10^4 ton/yr). In the feed stream it is assumed that the feed which is the mixture of 1-butanol and water has a flow rate 25000 kg/hr containing 0.2 w/w 1-butanol.

4.4.2. Thermodynamic Modeling using NRTL and UNIQUAC model

ASPEN built in NRTL and UNIQUAC model parameters as available in ASPEN-LLE database [12, 16] have been used for the binary pairs.The missing binary pairs are regressed within ASPEN plus by UNIFAC or R-PCES model .The binary interaction parameters are available in chapter 3 and Tables 3.18-3.19.

4.4.3. Economics and equipment sizing

Table 4.1 shows the basis of economics and equipment sizing equations used for the present cost estimation. This shall be common to DES as well. The optimum diameter of distillation column is based on vapor velocity [1, 12]. For calculating the heat exchanger area, reboiler heat input, condenser heat removal (in MW), overall heat transfer coefficient and ΔT (i.e temperature difference of first and second stage for condenser; and last and second last stage for reboiler) are required. Reboiler and condenser heat duties mainly depends on the reflux ratio, as a higher reflux ratio requires a higher reboiler duty. The payback period here has been assumed to be three years for both mesitylene and DES. We shall now discuss the optimization of the extractor followed by the distillation column in case of mesitylene. The same shall be adopted for DES. This is again as per procedure discussed in Figure 4.1 and 4.2 (section 4.2).

Table 4.1: Economics and equipment sizing [1, 12, 13, 17, 18].

Parameter	Value
For Distillation Column	
Condenser $U = 0.852$ kW/(K m^2) $\Delta T = 8.953$ K Capital cost = $7296 \times (A_{condenser}$ in $m^2)^{0.65}$ $Q_{condenser} = (U \times A \times \Delta T)_{condenser}$ **Reboiler** $U = 0.568$ kW/(K m^2) $\Delta T = 22.197$ K Capital cost = $7296 \times (A_{reboiler}$ in $m^2)^{0.65}$ $Q_{reboiler} = (U \times A \times \Delta T)_{reboilerr}$	
TAC (Total Annual Cost)	capital cost/payback period + energy cost
Column vessel capital cost	17,640 × [diameter (D) in meters]$^{1.066}$ [length (L) in meters]$^{0.802}$
Energy Cost	4.7 $/GJ
For Extractor Tower	
Height (H)	N_T trays with 4 ft HETP plus additional 3 ft at the top and bottom separately
Diameter (D)	Calculations as per Seider et al. [13] with maximum liquid throughput = 120 $ft^3/h\text{-}ft^2$ and safety factor f = 0.6
Size factor (S) = $H_{actual} \times D^{1.5}$	
For Extractor: $Q_{total} = Q_{feed} + Q_{solvent}$	
Actual of Extractor = $(Q_{total}/120) \times (1/0.6)$	
$D_{Extractor} = (A_{actual}/\pi)^{0.5}$	
f.o.b. purchase cost, cost-iron = $250 \times (S)^{0.84}$	
f.o.b. purchase cost, stainless-steel = f.o.b. cast-iron × 2 × (410/394)	
Miscellaneous cost	
Pump capital cost = $C_p \times (1.8 + 1.5 \times F_p \times 2.4)$ $\log(C_P) = 3.5793 + 0.3208 \times \log(P) + 0.0285 \times \log(P)^2$ $F_p = 0.1682 + 0.3466 \times \log(Q) + 0.4841 \times \log(Q)^2$ Here: outlet pressure (P) in bar, duty (Q) in kW	
Cooling water Cost	0.16 $/GJ

4.4.4. Optimization of Extractor

Figure 4.5 depicts the sensitivity analysis, which eventually helps in optimizing the extraction cost. This is performed by optimizating the number of stages in the extractor column on the basis of f.o.b. purchase cost (Freight on board cost). The feed stream contains water 0.8 (w/w) and 1-butanol 0.2 (w/w) with a mass flow rate 25,000 kg/hr. The operating conditions for the extractor column used was p = 1 atm and T = 25 ^{o}C. The *Design Spec* (DS-1) configuration in Aspen Plus V8.8® has been invoked so as to achieve a recovery of 100% 1-butanol. This is performed by keeping the solvent flow rate as variable. Total number of stages has then been varied from 5 to 20 (Figure 4.5b) while at the same time computing f.o.b. Figure 4.5 depicts the f.o.b cost for each stage.

It has been observed that the f.o.b cost is minimum were the total number of stages is seven (Figure 4.5b). After the optimization of solvent flow rate for extractor, *selectivity analysis* tool has been used to optimize the solvent flow rate keeping the total number of stages as seven in the extractor. The solvent flow rate is then varied via *Design Spec* configuration (DS-1) and the subsequent f.o.b cost is calculated as per Table 4.1. Overall the sensitivity analysis shall provide us information with respect to 1-butanol recovery and solvent (mesitylene) flow rate for a fixed total number of stages in extractor. Figure 4.5c shows the sensitivity result i.e. 1-butanol recovery with solvent flow rate in the extract stream. Figure 4.5c also predicts the change in yield of butanol with solvent feed rate. It has been observed that a 76,000 kg/hr mesitylene flow rate is required for a full recovery i.e. 100% w/w of 1-butanol. In order to lessen the cost of solvent, the optimal solvent rate was kept at ~30000 kg/hr for a recovery of 0.99 w/w 1-butanol.

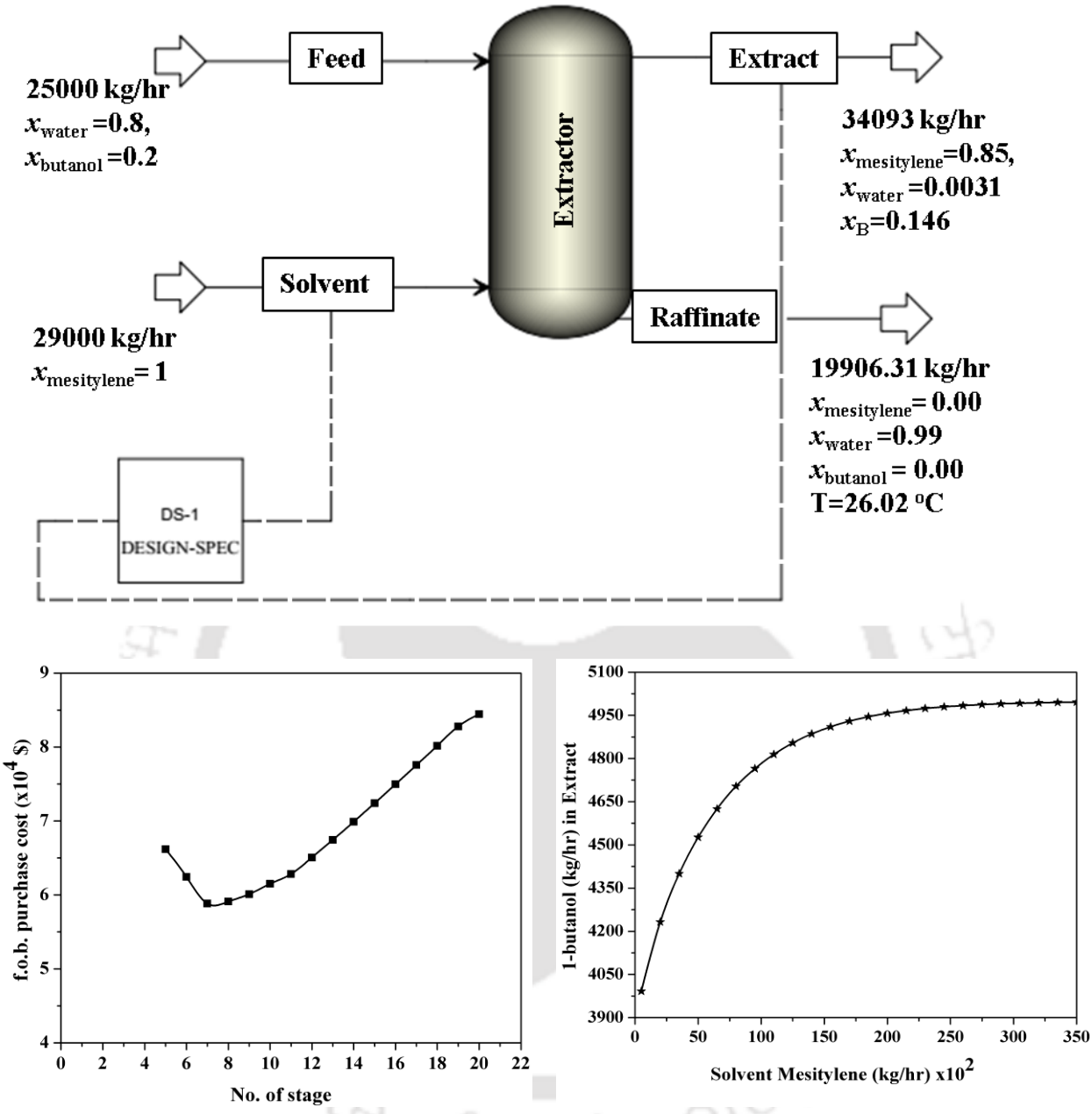

Figure 4.5: Optimal design flow-sheet for (a) liquid-liquid extraction of 1-butanol; (b) design spec (DS-1) for extractor; (c) sensitivity analysis for mesitylene flow rate

4.4.5. Optimization of Distillation Column

Once extraction is over, thereafter distillation column (RadFrac) has been used for the recovery of solvent (mesitylene) from 1-butanol in the extract stream, Here the feed input is the optimized extract flowrate as obtained in case of extraction (section 4.4.4).For optimizing the

distillation column, *DESIGN SPEC* have been used by ensuring the mass fraction of 1-butanol in the distillate stream to be 0.975, while at the same time and maintaining a mass fraction of 1-butanol as 0.01 in the bottom stream. The solvent recovered by distillation is then fed back to the extractor after cooling it to 25 ^{o}C. Thereafter the distillate rate followed by reflux ratio is varied as per Figure 4.2.

The total height of distillation column has been kept 20% more than the actual height, while the spacing between the two plates is 0.61 meter. Eq. 4.1 shows the height of the vessel required in case of the distillation column [1].

$$H = 1.2 \times 0.61 \times (N_T - 2) \tag{4.1}$$

Where $N_T - 2$ represent total number of stages minus one stage for condenser and one for reboiler. Figure 4.6 reports the TAC which includes both capital and energy cost. Here capital cost includes the shell and heat exchanger cost. It is found that lesser the number of stages, higher the reboiler heat duty which in turn increases the column diameter and heat exchanger areas. The basis of economics and equipment sizing equations used for the present cost estimation is already available in Table 4.1. The total annual cost, operating cost and capital cost have been calculated by varying the number of stages from 25 to 65 (Figure 4.6b and 4.6c). A minimum number of 42 stages have been obtained for this case with a reflux ratio of 2.19 at a TAC of 1.24×10^{6} \$/yr.

We shall invoke the approach of Luyben et al., [1, 19] where on the basis of TAC the optimum number of stages is selected. As observed, operating cost is continuously decreasing with increasing number of stages. Now, in the present simulation, reflux ratio (RR) is used to optimize the distillation column, hence the number of stages is considered optimum when the reflux ratio value is the least [20]. An increase in reflux ratio results in a decrease in column height, but on the other hand it leads to an increase of column diameter. This is due to the fact that a large quantity of liquid needs to recycled which necessitates a larger condenser, reboiler and reflux pump [1, 20]. This is the very reason that the fixed cost falls through a minimum and then again rises to infinity at total reflux ratio. At the minimum reflux ratio as per definition, an infinite number of stages are required. It implies fixed cost will be infinite but operating cost will be least in this case. Overall the heating and cooling requirement is found to increase directly with the reflux ratio, as evident in Figure 4.6b. Hence from Figure 4.6b, the number stage in the

distillation column is fixed at 48. This will also help us in obtaining an itemized equipment sizing and its related cost in the next section.

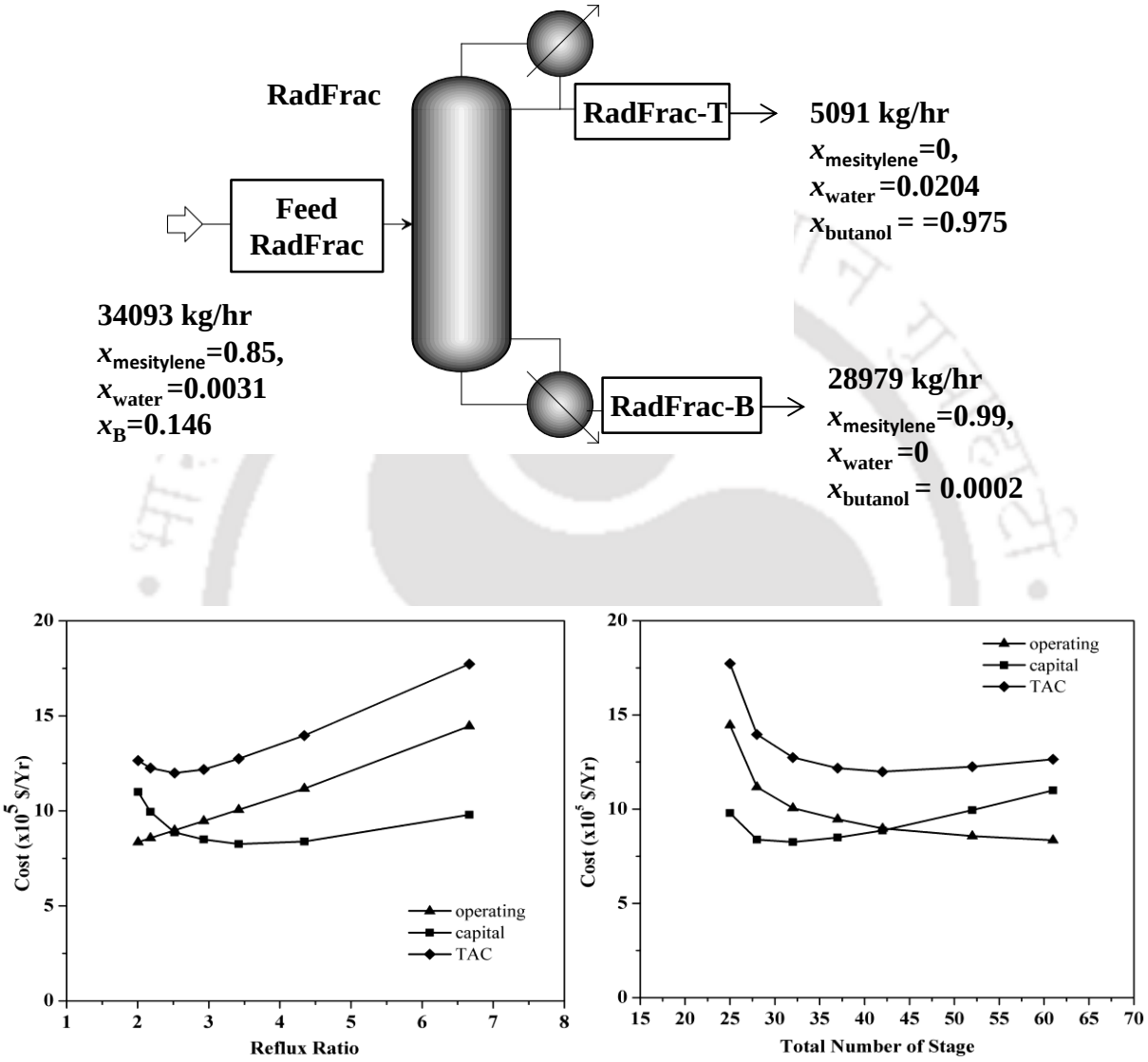

Figure 4.6: Optimal design flow-sheet for (a) Distillation of1-butanol and mesitylene; (b) Estimated cost (per year) vs total number of stage; (c) Estimated cost (per year) vs Reflux ratio

4.4.6. Recycle Solvent Stream

In the concluding part of mesitylene, the optimized flow rates from both extractor and distillation column has been connected as per Figure 4.7. The extraction column contains seven

equilibrium stages (section 4.4.4) and the distillation column posses forty eight stages (section 4.4.5). Mesitylene has been added as a make-up solvent for the material balance (Figure 4.7). More than 99% w/w of 1-butanol was extracted using mesitylene as a solvent with a weight fraction ~0.98 w/w. 1-butanol is recovered as a distillate product from the distillation column after the separation of the solvent by distillation. As before a total condenser has been used in the distillation column. The separated solvent from the distillation is recycled back to the extractor after cooling it to 25 ^{o}C. The final purity of 1-butanol from the distillate has been obtained as ~0.98 w/w, when using a fixed distillate and feed rate. It can be seen that the raffinate phase (in extractor) is dominated by water which is inline with our experimental results (Table 3.2 chapter 3), while the extract phase after solvent separation (via Distillation) consists mainly 1-butanol. Distillation of the extract stream gave a recovery of ~99% solvent which was then recycled back to the extractor column after cooling it to 25 °C.

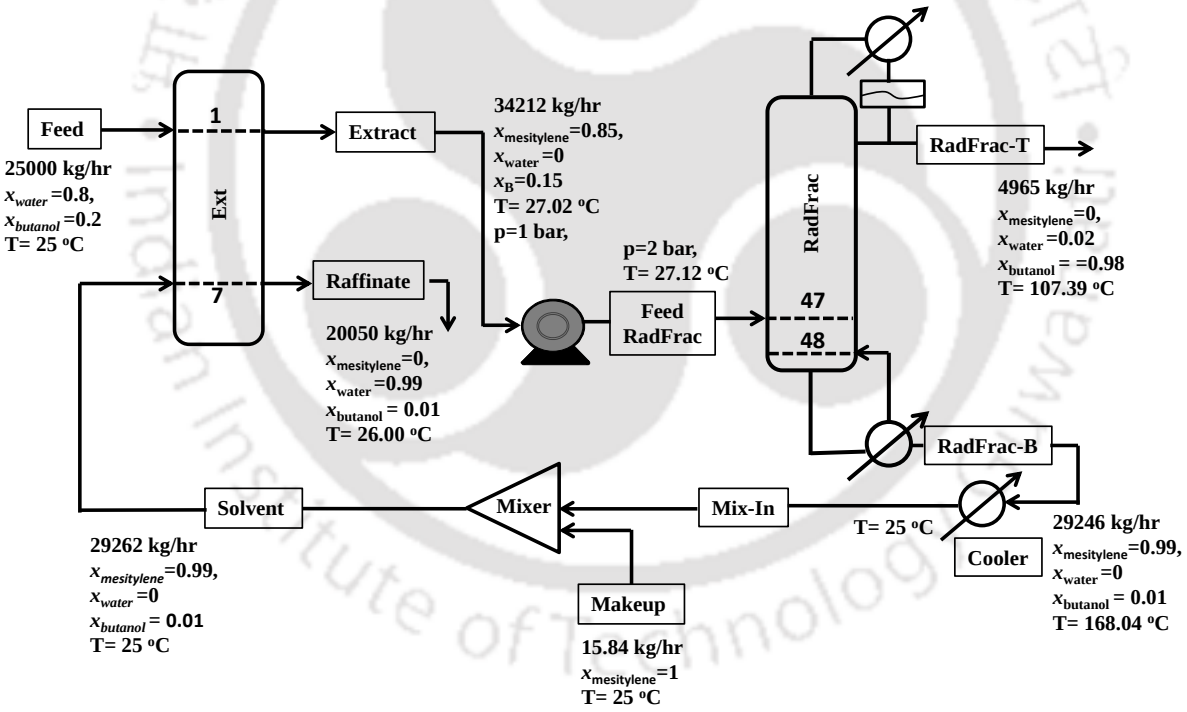

Figure 4.7: Hybrid Extraction-Distillation Process flow sheet for the separation of 1-butanol from aqueous mixture

Table 4.2 shows the mass as well as energy balance for the complete process flow sheet. It shows the extraction as well as solvent recovery section for the production of 1-butanol at 5000 kg/h using mesitylene as a solvent. Presently ~98% of 1-butanol recovery is possible from

the distillation column, while at the same time 99.97% 1-butanol is recovered from the extractor by using an optimum amount of solvent. Overall the total number of stages is kept as seven in the extractor and forty eight in the distillation column. A reflux ratio 2.458 is obtained via individual optimization of extractor (section 4.4.4) and distillation column (section 4.4.5). While a reflux ratio at 2.460 is obtained in case of entire hybrid extraction distillation system together with recycle Solvent Stream

Table 4.2: Stream Report for the entire Hybrid Extraction System using Mesitylene as Solvent

Stream Name*	Feed	Solvent	Extract	Raffinate	Feed-RADFRAC	RADFRAC-T	RADFRAC-B	Make-Up	Mix-In
$N_{Extractor}$ = 7, $N_{Distillation}$ = 48, RR = 2.46 $D_{Distillation}$ = 2.05 meter									
From		Mixer	EXT	EXT	Pump	RADFRAC	RADFRAC		Cooler
To	EXT	EXT	Pump		RADFRAC		Cooler	Mixer	Mixer
Phase:	Liquid	Liquid	Liquid	Liquid	Liquid	Liquid	Liquid	Liquid	Liquid
Component Mass Flow (kg/h)									
Mesitylene	0	28970.11	28969.06	1.05	28969.06	14.71	28954.35	15.84	28954.35
WATER	20000	0.01	109.44	19890.57	109.44	109.43	0.01	0.00	0.01
1-Butanol	5000	292.47	5133.96	158.50	5133.96	4841.50	292.47	0.00	292.47
Component Mass Fraction									
Mesitylene	0	0.99	0.85	0.00	0.85	0.00	0.99	1.00	0.99
Water	0.8	0.00	0.00	0.99	0.00	0.02	0.00	0.00	0.00
1-Butanol	0.2	0.01	0.15	0.01	0.15	0.98	0.01	0.00	0.01
Volume Flow (lpm)	435.24	566.02	668.69	337.05	668.75	113.41	667.29	0.31	565.72
T (°C)	25.00	25.00	27.02	26.00	27.12	107.39	168.04	25.00	25.00
P (bar)	1.01	1.01	1.01	1.01	2.00	1.01	1.34	1.01	1.01
Molar Enthalpy (cal/mol)	-68755	-16126	-29736	-68259	-29731	-73194	-7973	-15122	-16127
Molar Entropy (cal/mol-k)	-43.99	-133.82	-130.56	-39.06	-130.54	-112.08	-111.83	-134.00	-133.82
Mass Density (gm/cc)	0.96	0.86	0.85	0.99	0.85	0.73	0.73	0.86	0.86

* Stream Name as per Figure 4.7; $N_{Extractor}$ and $N_{Distillation}$: Refers to number of stages in the extractor and distillation column respectively; RR = Reflux Ratio; $D_{Distillation}$ = Diameter of Distillation Column

Figure 4.8 shows the overall total annual cost with total number of stages of distillation column. In this case, number of stages of the distillation column is varied by keeping the number of stages of extractor and feed rate constant. The overall cost is then calculated using the empirical relationships and design parameters as given in Table 4.1. The results are shown in Table 4.3. It has been observed that for an overall optimum cost (i.e for a complete process), the optimum number of stages in extractor is eight while the number of stages of the distillation column is 50. This reason is due to the fact that initially we have optimized the extractor cost on the basis of 100% recovery of 1-butanol which shall require a very high solvent mass flow rate (~60,000 kg/hr as per Figure 4.5b). In order to compromise on the yield but save on the huge solvent cost, we have adopted an optimum amount of solvent flow rate (~30,000 kg/hr) from the sensitivity analysis (Figure 4.5c).This corresponds to a yield of 97.5% 1-butanol. With this we have conducted the overall TAC as given in Figure 4.8 for a complete process setup. Table 4.3 reports the itemized equipment sizing and its related costs. Here the number of stages in the extractor has been varied while keeping the total number of stages in the distillation column as 48 (Figure 4.6b and Figure 4.6c).

Table 4.3: Itemized Equipment Sizing and Costs (N_T:No of stages in extractor)

N_T Extractor column	6	7	8
Distillation Column D (m)	2.176	2.134	2.121
Distillation Column H (m)	33.672	33.672	33.672
Condenser duty Qc (MW)	2.840	2.994	3.163
Reboiler duty Qr (MW)	5.705	5.528	5.480
Reflux Ratio RR	2.351	2.481	2.638
Condenser area A_c (m^2)	440.391	449.890	461.139
Reboiler area A_r (m^2)	472.057	447.172	433.482
Shell cost ($\times 10^6$ \$)	0.678	0.664	0.660
HX cost ($\times 10^6$ \$)	0.781	0.772	0.771
Energy ($\times 10^6$/yr)	0.846	0.819	0.812
Make up cost ($\times 10^3$ \$/yr)	20.599	16.478	12.525
Extraction capital cost ($\times 10^3$ \$/yr)	40.070	42.264	44.723
Pump capital cost ($\times 10^3$ \$/yr)"	13.500	13.500	13.500
Pump energy cost,($\times 10^3$ \$/yr)	0.264	0.264	0.264
Cooling water cost: ($\times 10^3$ \$/yr)	11.715	11.715	11.715
Overall TAC ($\times 10^5$ \$/yr)	14.180	13.824	13.718

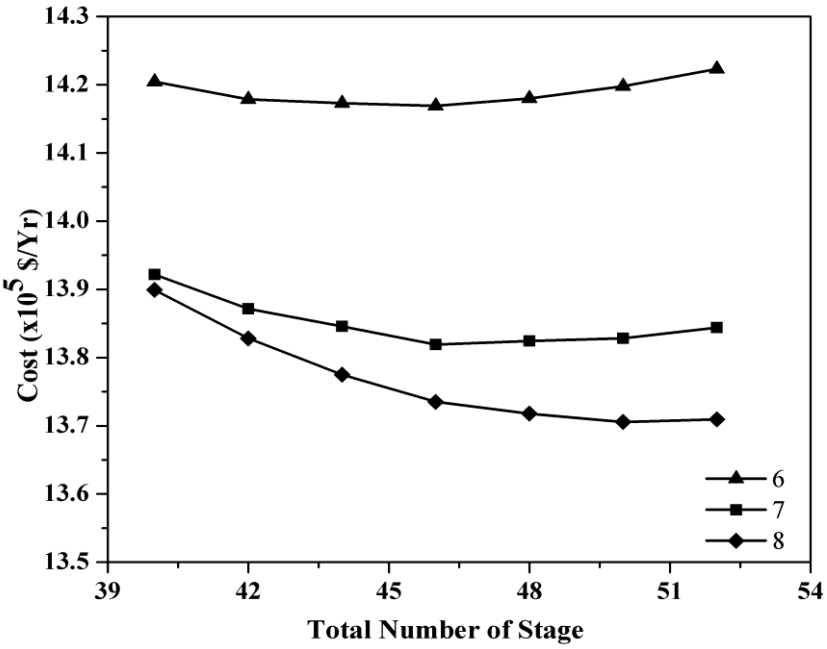

Figure 4.8: Effect of Extractor and Distillation stages with overall TAC

4.5. Hybrid Extraction-Distillation Unit for DES

As discussed in our earlier section 4.1, separation of lower chain alcohols is considered difficult because of azeotrope formation which is the reason that a hybrid extraction-distillation (distillation column coupled with liquid-liquid extraction) was adopted. In order to evaluate the economic feasibility of these DES, an economic analysis needs to be performed. In our earlier chapter 3, we have already measured the LLE of DES with lower alcohols and water. The encouraging results have prompted us to now measure its practical effectiveness. From the LLE results the hydrophobic organic solvents or DES have shown to possess high affinity for 1-butanol and low solubility with water.

In the ASPEN Plus simulation, DES here is defined with PSEUDOCOMPONENT as per ASPENone definition [21]. DES will here act as a solvent for the separation of Butnaol + Water system in the extractor column. As explained in Appendix 4.1, the sigma profile obtained by COSMO-SAC is used for the simulation. Similar to mesitylene, ASPEN simulation shall include optimization of the extractor and distillation unit and then coupling it to get the solvent recovery by recycling the DES to extractor [12, 22, 23].

4.5.1. Use of Sigma Profile in COSMO-ASPEN model

As discussed in Chapter 2 (Section 2.5) for generation of sigma profile, COSMO files are necessary. The first step therefore refers to geometry optimization with Gaussian 09 [24] at B3LYP/6-31G* from at least three initial geometries of component. The geometries were drawn by Gauss View 5.0 [25] visualization package. Frequency analysis was carried out on each complex at the same level of theory. An absence of imaginary vibrational frequencies determined the true energy minimum structures.

Thereafter COSMO file generation was performed using BVP86 [26] level of Density Functional Theory (DFT). Here the SVP [27] basis set is used in combination with density fitting basis set DGA1[28].The COSMO files once generated, were then used to generate the sigma profile [29-32] of the molecules, which shall now be used as input for ASPEN particularly for DES. The information contained inside the cosmo file is converted to a probabilistic form histograms. The entire number of segments in the cosmo file is thus reduced to 60 histograms ranging from -0.03 e/ $Å^2$ to +0.03 e/ $Å^2$. This form of histogram is already given in Figure 2.30 or 2.31 and are known as sigma profile. For DES, the sigma profile of HBA and HBD are multiplied with their respective mole fraction (Eq. 3.16 of chapter 3) to get the sigma profile of DES, The sigma profile divides the entire screening charge in 60 histograms ranging from -0.03 e/ $Å^2$ to +0.03 e/ $Å^2$ with each histogram having width of 0.001 e/ $Å^2$. The 60 histograms are then divided into five sets of 12 histograms and then inserted in the ASPEN database as user input. Once this is done ASPEN performs the simulation using DES as a single component (Appendix 4.1).

4.6. Hybrid Extraction-Distillation with DES-1

Figure 4.9 shows the hybrid downstream process for the production of 1-butanol at the rate 5000 kg/h (4.38×10^4 ton/yr.). Feed stream containing 0.2 w/w 1-butanol with a flow rate of 25000 kg/hr is used for the flowsheet. In the hybrid system, the optimized flow rates from both extractor and distillation column has been connected as per flow diagram explained in Figure 4.2. The results for the sequential optimization scheme is done in a similar manner as per mesitylene (Figures 4.5-4.7 or Table 4.2) and sections (4.4.3-4.4.5).This has been done so as to compare the performance and economic efficiency for conventional and DES solvents. The extraction column here contains seven equilibrium stages while the distillation column had 44 stages. DES has been added as a make-up solvent for the material balance. As discussed earlier COSMO-SAC thermodynamic model has been

used in the ASPEN Plus V8.8® professional simulator (Bedford, Massachusetts) using the *PSEUDOCOMPONENT* input so as to define the DES. Further COSMO-ASPEN model has also been used to predict the tie lines as discussed in chapter 3.

Figure 4.10 shows the sensitivity result i.e. 1-butanol recovery with solvent flow rate in the extract stream. It has been observed that for a 100 % recovery of 1-butanol, around 3000 kg/h flow rate of DES-1 is required. To save the solvent rate, the optimal solvent (DES) was used as 2,500 kg/h for a recovery of 0.999 wt/wt 1-butanol (Figure 4.10). This is as per the necessary requirement i.e. without compromising on the yield of butanol significantly (i.e. 1.0 vs 0.999)

As discussed earlier in section 4.3.4, lesser the number of stages, higher the reboiler heat duty which in turn increases the column diameter and heat exchanger area. For DES also, *DESIGN SPEC* has been used by fixing the mass fraction of 1-butanol in the distillate at 0.862 as this was the maximum possible recovery of 1-butanol after convergence in case of DES-1. Thereafter the distillate rate and reflux ratio was varied as per established procedure for optimizing the distillation column. A minimum number of stages ($N_{Distillation}$) of 44 have been obtained for this case with a reflux ratio of 2.01 after optimization of distillation column. The diameter of the column obtained ($D_{Distillation}$) was 1.68 meter.

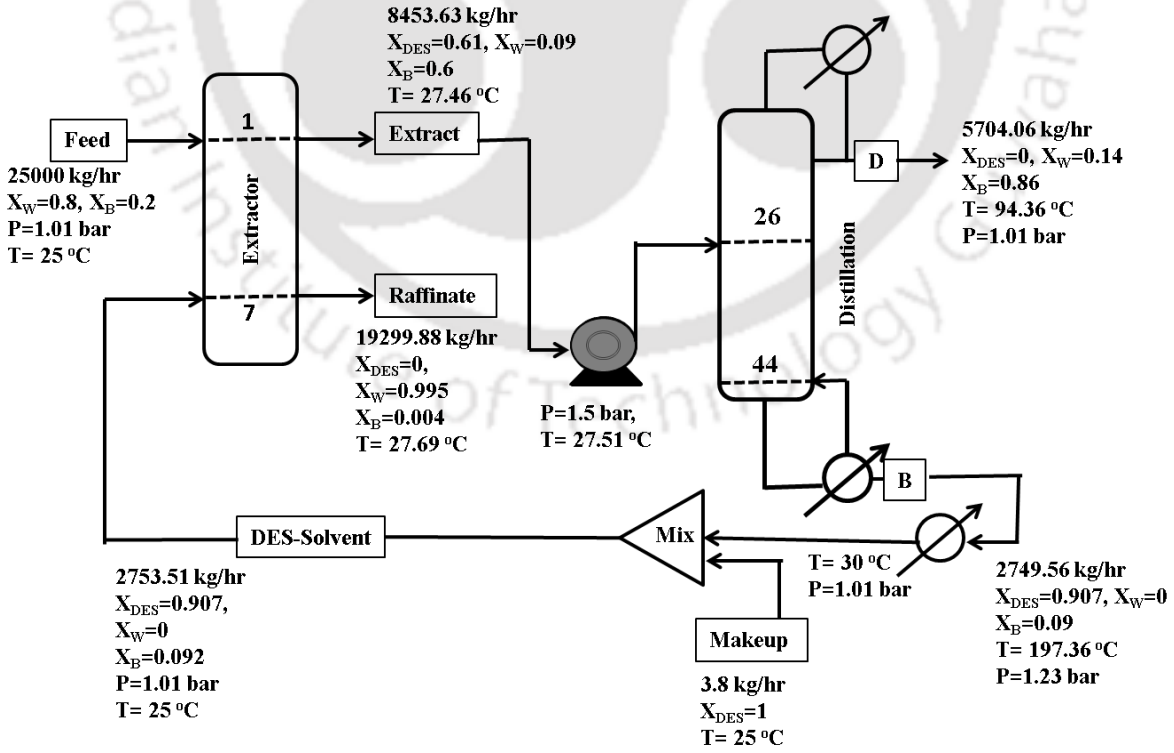

Figure 4.9: Hybrid Extraction-Distillation Process flow sheet for the separation of 1-butanol from aqueous mixture using DES-1 as a solvent

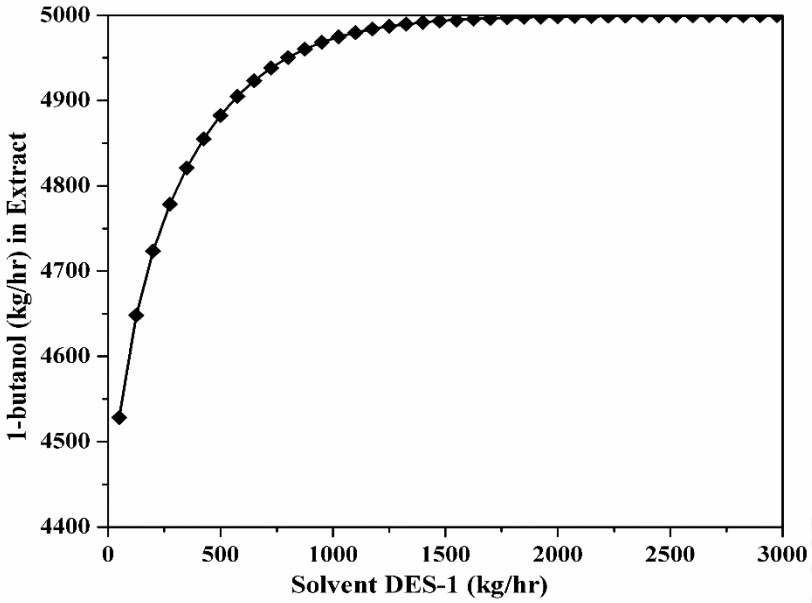

Figure 4.10: LLE of 1-butanol using sensitivity analysis for obtaining the optimum DES-1 (solvent) flow rate

Table 4.4 shows 1-butanol recovery results for the different streams as obtained from the ASPEN process sheet (Figure 4.9). It can be seen that the raffinate phase (in extractor) is dominated by water which is in line with our experimental results (Figure 3.9, Table 3.8 Chapter 3), while the extract phase after solvent separation (via Distillation) consists mainly 1-butanol.

Table 4.4: Stream Results as obtained using DES-1 as solvent

Stream Name*	Feed	DES-Solvent	Extract	Raffinate	D	B	Make-Up
Component Mass Flow (Kg/h)							
DES	0.00	2498.92	2494.98	3.94	0.00	2494.98	3.80
1-Butanol	5000.00	254.59	5171.49	83.10	4916.91	254.59	0.00
Water	20000.00	0.00	787.16	19212.84	787.16	0.00	0.00
Component Mass Fraction							
DES	0.000	0.908	0.295	0.000	0.000	0.907	1.000
1-Butanol	0.200	0.092	0.612	0.004	0.862	0.093	0.000
Water	0.800	0.000	0.093	0.995	0.138	0.000	0.000
Mass flow (kg/h)	25000.00	2753.51	8453.63	19299.88	5704.07	2749.57	3.80
Volume flow (lpm)	435.24	55.25	180.53	324.79	123.26	65.46	0.07
T (°C)	25.00	25.00	27.46	27.69	94.36	197.36	25.00
P (bar)	1.01	1.01	1.01	1.01	1.01	1.23	1.01
Molar Enthalpy (cal/mol)	-68782.20	-54806.00	-71397.80	-68222.90	-71453.60	-40922.10	-49312.80
Molar Entropy (cal/mol-K)	-44.13	-205.94	-110.06	-38.90	-86.34	-170.34	-223.41

Optimal Results:

Extractor Column: P = 1 atm, T = 25 ^{o}C, $N_{Extractor}$= 7,

Distillation Column: $N_{Distillation}$=44, N_{feed}=26, Distillate rate: 5704.07 kg/h, Reflux ratio: 2.01, $D_{Distillation}$: 1.68 meter

4.7. Hybrid Extraction-Distillation with DES-2

Figure 4.11 depicts the hybrid downstream process for the production of 1-butanol at the rate 5000 kg/h (4.38×10^4 ton/yr). The entire process is similar as discussed in section 4.6. As per the optimization scheme outlined in the previous section, the extraction column here contains seven equilibrium stages and the distillation column possess fifty four stages. DES-2 has been added as a make-up solvent for the material balance which is on the similar lines as per section 4.6. The total number of stage in extractor has been taken as seven (section 4.4.4) while the operating conditions for the extractor column used was p=1 atm. and T=30 ^{o}C. As defined earlier, the sensitivity analysis shall provide us information with respect to 1-butanol recovery and solvent (DES) flow rate for a fixed total number of stages in extractor. Figure 4.12 shows the sensitivity result i.e. 1-butanol recovery with solvent flow rate in the extract stream. It has been observed that for a 100 % recovery of 1-butanol, an amount of 6,850 kg/h of DES-2 is required. Further the optimal solvent (DES) found was 2,500 kg/h for the recovery of 0.999 wt/wt 1-butanol from extractor (Figure 4.12).

In this case also *DESIGN SPEC* has been used for maintaining the mass fraction of 1-butanol in the distillate at 0.86. This is a similar procedure as followed in section 4.4.5. A minimum number of stages ($N_{Distillation}$ 54) have been obtained for a reflux ratio of 2.26 after the rigorous optimization of distillation column. The diameter of the column obtained is ($D_{Distillation}$) is found to be 1.7 meter.

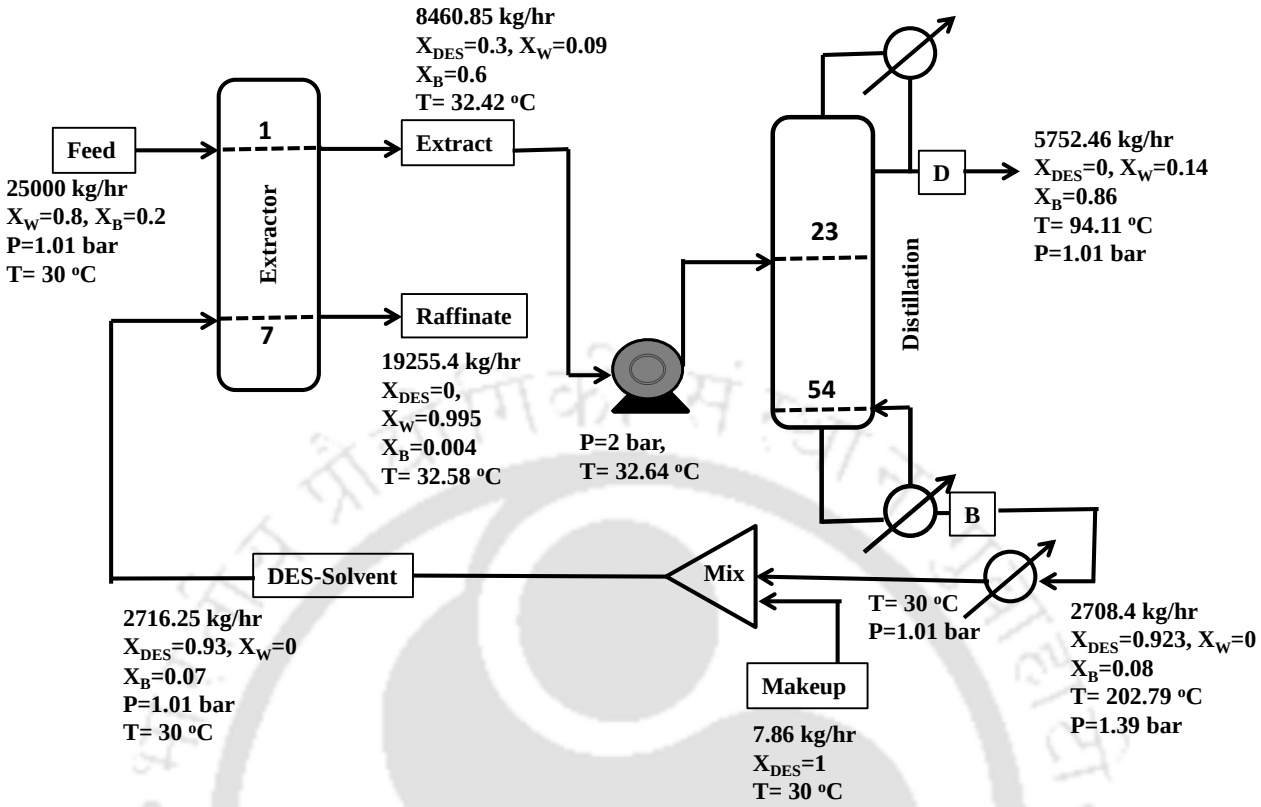

Figure 4.11: Hybrid Extraction-Distillation Process flow sheet for the separation of 1-butanol from aqueous mixture using DES-2 as a solvent

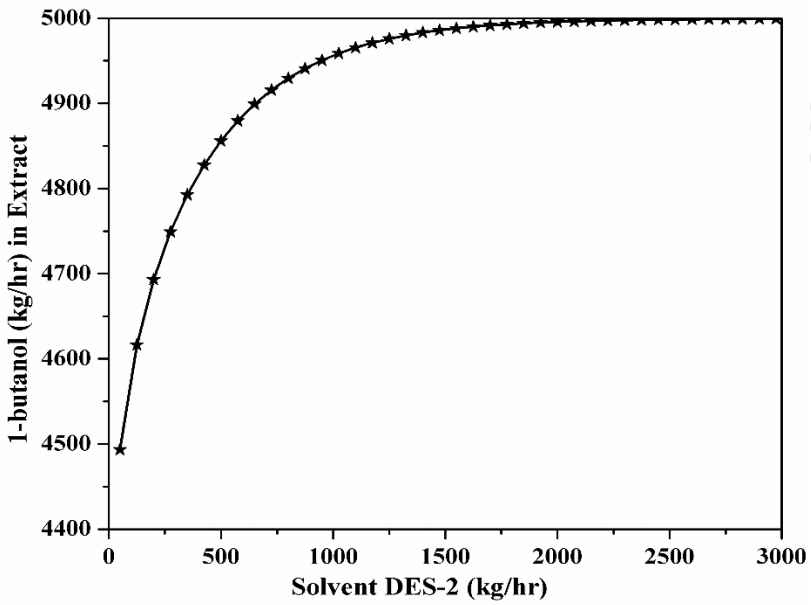

Figure 4.12: Extraction of 1-butanol using sensitivity analysis for optimum DES flow rate

Table 4.5 shows the 1-butanol recovery results for the different streams. More than 99.99% w/w 1-butanol was extracted using DES-2 as a solvent from extractor along with a weight fraction at ~0.86 w/w from distillation column. 1-butanol is recovered as a distillate product from the distillation column after the separation of the solvent by distillation. A total condenser as before has been used in the distillation column. The separated solvent from the distillation is recycled back to the extractor after cooling it to 25 ^{o}C. The final purity after convergence for 1-butanol from the distillate has been obtained as ~0.86 w/w, when using a fixed distillate and feed rate. As observed (Table 4.5), with DES1, the raffinate phase (in extractor) is again dominated by water which is in line with our experimental results while the extract phase after solvent separation (via Distillation), consists mainly 1-butanol.

Table 4.5: Stream Results for 1-butanol recovery using DES-2 as a solvent

Stream* Name	Feed	DES-Solvent	Extract	Raffinate	D	B	Make-Up
Component Mass Flow (Kg/h)							
DES	0.00	2509.73	2501.87	7.85	0.00	2501.87	7.85
1-Butanol	5000.00	206.52	5124.86	81.65	4918.35	206.52	0.00
Water	20000.00	0.00	834.11	19165.90	834.11	0.00	0.00
Component Mass Fraction							
DES	0.000	0.924	0.296	0.000	0.000	0.924	1.00
1-Butanol	0.200	0.076	0.606	0.004	0.855	0.076	0.00
Water	0.800	0.000	0.099	0.995	0.145	0.000	0.00
Mass flow (kg/h)	25000.0	2716.2	8460.8	19255.4	5752.4	2708.3	7.8
Volume flow (lpm)	437.61	53.83	178.17	325.64	124.05	63.67	0.15
T (°C)	30.0	30.0	32.4	32.5	94.1	202.1	30.0
P (bar)	1.01	1.01	1.01	1.01	1.01	1.38	1.01
Molar Enthalpy (cal/mol)	-68681.9	-55259.5	-71357.5	-68135.1	-71352.7	-40841.3	-50866.1
Molar Entropy (cal/mol-K)	-43.80	-214.03	-108.24	-38.61	-85.16	-177.92	-230.59

Optimal Results:

Extractor Column: P = 1 atm, T = 30 ^{o}C, $N_{Extractor}$= 7,

Distillation Column: $N_{Distillation}$=54, N_{feed}=23, Distillate rate: 5752.46 kg/h, Reflux ratio: 2.26, $D_{Distillation}$: 1.7 meter

4.8. Hybrid Extraction-Distillation with DES-3

Figure 4.13 here depicts the hybrid downstream process for the production of 1-butanol at the rate at 5000 kg/h (4.38×10^4 ton/yr) which is similar as discussed in the section 4.7. As before after optimization, the extraction column contains seven equilibrium stages while the distillation column possess 55 stages. DES has been added as a make-up solvent for the material balance similar to section 4.7. Figure 4.14 shows the sensitivity result i.e. 1-butanol recovery with solvent flow rate in the extract stream. It has been observed for a 100 % recovery of 1-butanol, 5000 kg/h flow rate of DES-3 is required. The optimal solvent (DES) rate was chosen to be 3,500 kg/h for a recovery of 0.999 wt/wt 1-butanol from extractor (Figure 4.14).

After the application of *DESIGN SPEC* the minimum number of stages ($N_{Distillation}$) was 55 corresponding to a reflux ratio of 7.24. The diameter of the column obtained ($D_{Distillation}$) was found to be 1.68 meter.

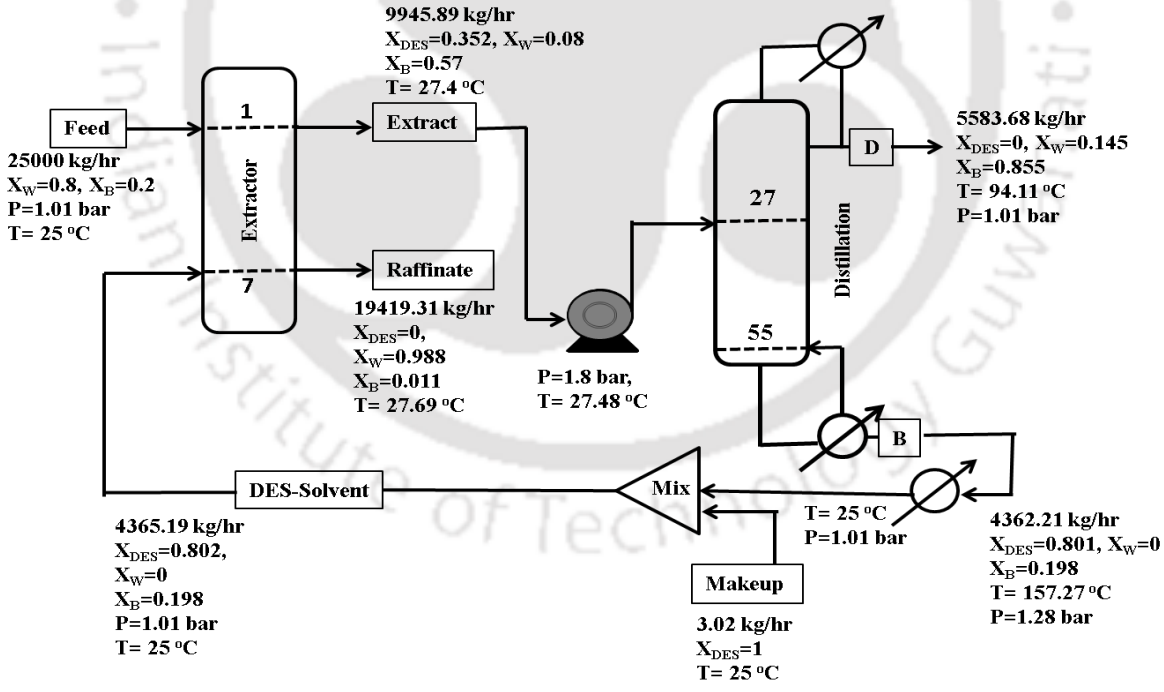

Figure 4.13: Hybrid Extraction-Distillation Process flow sheet for the separation of 1-butanol using DES-3 as a solvent

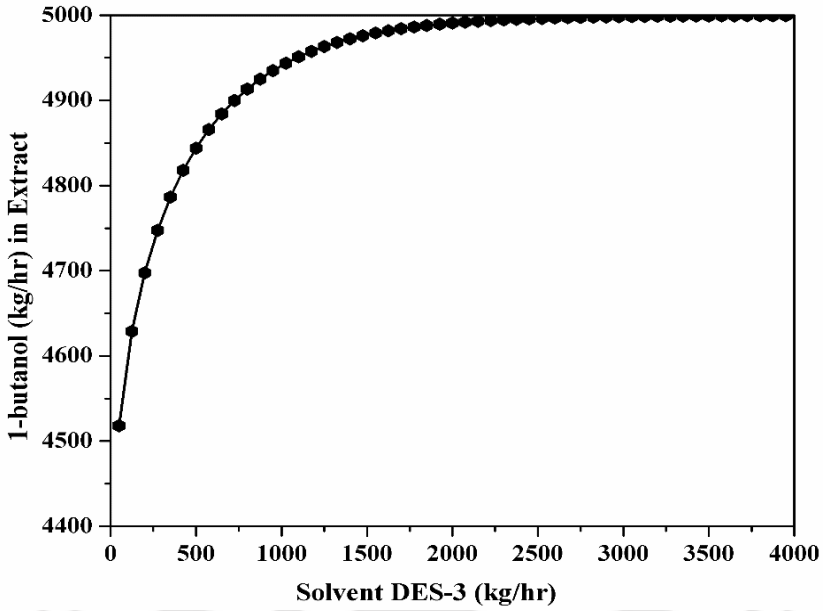

Figure 4.14: Optimized DES-3 flow rate using 1-butanol yield as per Sensitivity Analysis

Table 4.6 shows the 1-butanol recovery results of the different streams. Around 99.99% w/w 1-butanol was extracted using DES-3 as a solvent with a weight fraction at ~0.855 w/w from the distillation column. 1-butanol is recovered as a distillate product from the distillation column after the separation of the solvent by distillation. It can be seen that the raffinate phase (in extractor) is dominated by water which is in line with our experimental results (Table 4.6), while the extract phase after solvent separation (via Distillation), consists mainly 1-butanol.

Table 4.6: Stream Results as obtained using DES-3 as a solvent

Stream Name*	Feed	DES-Solvent	Extract	Raffinate	D	B	Make-Up
Component Mass Flow (Kg/h)							
DES	0.00	3500.00	3496.98	3.02	0.00	3496.98	3.02
1-Butanol	5000.00	865.19	5639.27	225.92	4774.05	865.23	0.00
Water	20000.00	0.00	809.63	19190.37	809.63	0.00	0.00
Component Mass Fraction							
DES	0.000	0.802	0.352	0.000	0.000	0.802	1.000
1-Butanol	0.200	0.198	0.567	0.012	0.855	0.198	0.000
Water	0.800	0.000	0.081	0.988	0.145	0.000	0.000
Mass flow (kg/h)	25000.00	4365.20	9945.89	19419.31	5583.68	4362.21	3.02
Volume flow (lpm)	435.24	89.74	208.75	327.08	120.41	102.03	0.06
T (°C)	25.00	25.00	27.40	27.15	94.11	157.29	25.00
P (bar)	1.01	1.01	1.01	1.01	1.01	1.28	1.01
Molar Enthalpy (cal/mol)	-68782.21	-60382.88	-70904.08	-68248.24	-71352.67	-50572.44	-50078.41
Molar Entropy (cal/mol-K)	-44.13	-193.15	-115.33	-39.08	-85.16	-167.10	-229.32

Optimal Results:
Extractor Column: P = 1 atm, T = 25 ^{o}C, $N_{Extractor}$= 7,
Distillation Column: $N_{Distillation}$=55, N_{feed}=27, Distillate rate: 5583.68 kg/h, Reflux ratio: 7.24, $D_{Distillation}$: 1.68 meter, Reboiler heat duty 11773.68 KW

4.9. Hybrid Extraction-Distillation with DES-4

Figure 4.15 shows the corresponding flowsheet for the production of 1-butanol at the rate 5000 kg/h (4.38×10^4 ton/yr) using DES-4. After the sequential optimization, the extraction column contains seven equilibrium stages while the distillation column possess 60 stages. Figure 4.16 shows the sensitivity result i.e. 1-butanol recovery with solvent flow rate in the extract stream. It has been observed for a 100 % recovery of 1-butanol, 8000 kg/h flow rate of DES-3 is required. The optimal solvent (DES) rate was chosen 6000 kg/h for a recovery of 0.999 wt/wt 1-butanol from extractor (Figure 4.16).

In this case also, *DESIGN SPEC* has been used by keeping the mass fraction of 1-butanol in the distillate as 0.852. This is due to the strict convergence criteria adopted in the extractor design. A minimum number of stages ($N_{Distillation}$) of 60 along with a reflux ratio of 7.97 was obtained after the rigorous optimization of distillation column. The diameter of the column (2.93 m) obtained here is much larger when compared to other DES.

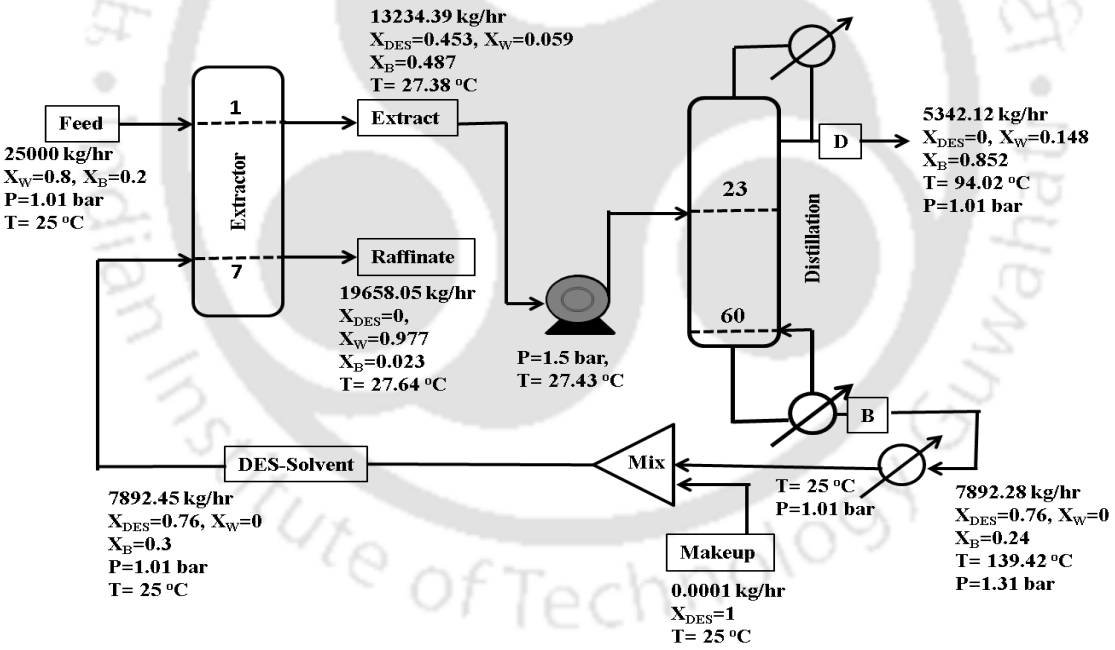

Figure 4.15: Hybrid Extraction-Distillation Process flow sheet for the separation of 1-butanol using DES-4 as a solvent.

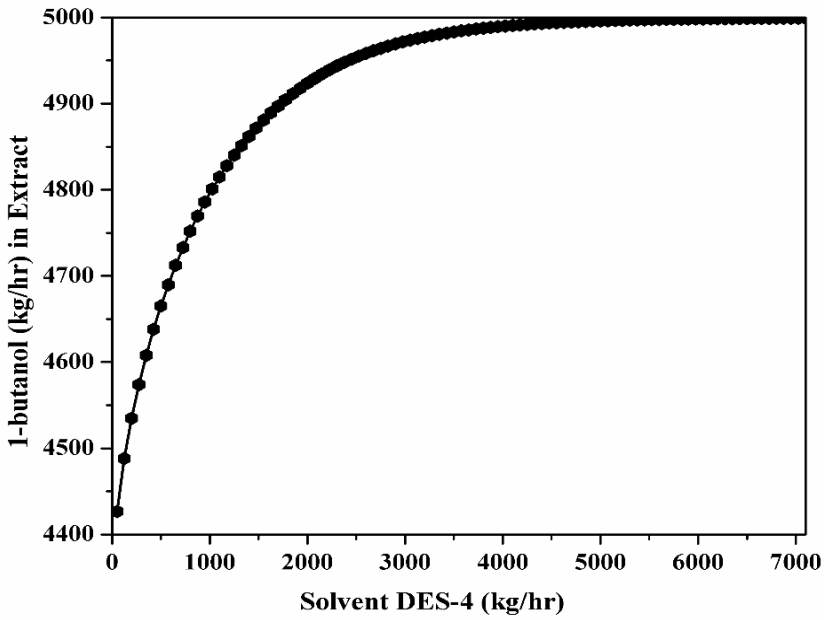

Figure 4.16: Optimal DES-4 solvent flowrate using 1-butanol via *Sensitivity Analysis*

Table 4.7 shows 1-butanol recovery results for different streams. More than 99.99% w/w 1-butanol was extracted using DES-4 as a solvent with a weight fraction at ~0.852 w/w. Similar to other DES, it can be seen (Table 4.7) that the raffinate phase (in extractor) is dominated by water which is in line with our experimental results while the extract phase after solvent separation (via Distillation), consists mainly 1-butanol.

Table 4.7: Stream Results for 1-Butanol Recovery using DES-4 as a solvent

Stream Name*	Feed	DES-Solvent	Extract	Raffinate	D	B	Make-Up
Component Mass Flow (Kg/h)							
DES	0.00	5999.96	5999.95	0.00	0.00	5999.95	0.00
1-Butanol	5000.00	1892.49	6443.81	448.68	4551.48	1892.33	0.00
Water	20000.00	0.00	790.63	19209.37	790.63	0.00	0.00
Component Mass Fraction							
DES	0.000	0.760	0.453	0.000	0.000	0.760	1.000
1-Butanol	0.200	0.240	0.487	0.023	0.852	0.240	0.000
Water	0.800	0.000	0.060	0.977	0.148	0.000	0.000
Mass flow (kg/h)	25000.00	7892.45	13234.39	19658.05	5342.12	7892.28	0.00
Volume flow (lpm)	435.24	161.85	276.63	331.62	115.10	181.20	0.00
T (°C)	25.00	25.00	27.38	26.64	94.02	139.44	25.00
P (bar)	1.01	1.01	1.01	1.01	1.01	1.31	1.01
Molar Enthalpy (cal/mol)	-68782.21	-58142.78	-68038.05	-68282.04	-71310.05	-50167.95	-43900.69
Molar Entropy (cal/mol-K)	-44.13	-180.03	-124.57	-39.35	-84.66	-158.09	-214.16

Optimal Results:

Extractor Column: P = 1 atm, T = 25 ^{o}C, $N_{Extractor}$= 7,

Distillation Column: $N_{Distillation}$=60, N_{feed}=23, Distillate rate: 5342.11 kg/h, Reflux ratio: 7.97, $D_{Distillation}$: 2.93 meter, Reboiler heat duty =12488.44 KW

4.10. Comparison of DES and Conventional solvent

Table 4.8 shows the comparison of all the solvent (DES1, DES2, DES3 and DES4) for the same feed 25000 kg/hr [Water= 0.8, BtOH=0.2 w/w] and the same number of extractor stages 7. It has been observed that DES-1 is the most effective in terms of solvent requirement. It only required a flow of 2499 kg/h with a reflux ratio at 2.01 and a reboiler duty of 4733.21 KW. This is almost one tenth than required for mesitylene. Further the number of stages in the distillation column is also the least at 44. Hence economically DES-1 or Menthol with a lower organic acid chain length (decanoic acid) is the preferred solvent for the extraction of the lower alcohols. In terms of TAC also it can be termed as the most efficient as the cost is lower than both the remaining DES and mesitylene.

Table 4.8: Overall Comparison of DESs as well as Mesitylene for the extraction of 1-butanol

Solvent Name	**Mesitylene**	**DES-1**	**DES-2**	**DES-3**	**DES-4**
Feed Flow [kg/hr] [W= 0.8, Bt=0.2 w/w]	25000	25000	25000	25000	25000
Solvent Required [kg/hr]	30,000	2499	2500	3500	6000
RR	2.46	2.01	2.26	7.24	7.97
N_T extractor	7	7	7	7	7
N_T Dist. Col.	48	44	54	55	60
N_F Dist. Col.	47	26	23	27	23
D(m) Dist. Col.	2.05	1.68	1.7	1.68	2.93
Recovered BuOH $_{Dist\ Col.}$[kg/hr]	4866.0	4916.9	4918.35	4774.05	4551.48
Solvent$_{Dist.Col.}$ [kg/hr]	14.71	0	0	0	0
Reboiler duty (kw)	5673.23	4733.21	5135.79	11773.68	12488.44
Energy (10^3 $/year)	760.25	634.28	688.23	1577.75	1673.53
Capital (10^3 $/year)	1380.56	987.57	1115.90	1756.65	2206.29
$TAC_{Dist-Col}$* (10^6 $/year)	1.220	0.963	1.0600	2.163	2.408
$TAC_{Ext-Col}$** (10^3 $/year)	13.746	8.768	8.752	9.286	9.925
Pump capital cost*** (10^3 $/year)	8.585	9.577	8.585	8.306	7.803
Pump energy cost*** (10^3 $/year)	2.692	0.525	1.008	0.909	0.678
Cooling water cost*** (10^3 $/year)	11.715	1.518	1.475	1.853	2.907
TAC overall**** (10^3 $/year)	1.257	0.984	1.080	2.184	2.430

Based on the methodology given by *Luyben [1]; **Seider et al. [13]; ***Pathak et al. [18]; ****Chen et al. [12]

4.11. Summary

The current chapter reports the scale up study that has been carried out using ASPEN Plus v8.8 with various solvents. A Hybrid extraction-distillation system was proposed so as to effectively separate 1-butanol from aqueous stream. An economic consideration with respect to Total Annual Cost (TAC) was also attempted. An optimized 1-butanol recovery of ~ 98% w/w was obtained for a solvent/feed ratio of 1.16 using mesitylene as a solvent. Once the conventional solvents were predicted, the DESs as solvents were also attempted in the flowsheet. Overall the raffinate phase from the experiment and simulation was found to comprise mainly water with mass composition as high as 99.99% w/w. For DES-1 an optimized 1-butanol recovery of ~ 86.2% w/w was obtained for a solvent/feed ratio of 0.1. Among all the DES, it required the least solvent flow rate of 2499 kg/h with a reflux ratio of 2.01. Thus DES-1 was found to be the best for the extraction of the lower alcohols among DES and mesitylene. Thus the current work provided a perfect example of experimental data generated in laboratory scale to process scale-up along with the Total Annual Cost (TAC).

References

1. W.L. Luyben: Distillation design and control using Aspen simulation, John Wiley & Sons (2013)
2. R.B. Eldridge, A.F. Seibert, S. Robinson, J. Rogers: Hybrid separations/distillation technology. Research opportunities for energy and emissions reduction, Univ. of Texas, Austin, TX (United States) (2005)
3. S. Ishii, M. Taya, T. Kobayashi: Production of butanol by Clostridium acetobutylicum in extractive fermentation system. Journal of chemical engineering of Japan 18 (1985) 125-130
4. A. Oudshoorn, L.A. van der Wielen, A.J. Straathof: Assessment of options for selective 1-butanol recovery from aqueous solution. Ind. Eng. Chem. Res. 48 (2009) 7325-7336
5. W. Groot, R. Van der Lans, K.C.A. Luyben: Technologies for butanol recovery integrated with fermentations. Process Biochemistry 27 (1992) 61-75

6. N. Qureshi, I. Maddox: Reduction in butanol inhibition by perstraction: utilization of concentrated lactose/whey permeate by Clostridium acetobutylicum to enhance butanol fermentation economics. Food Bioprod. Process. 83 (2005) 43-52
7. G. Liu, L. Gan, S. Liu, H. Zhou, W. Wei, W. Jin: PDMS/ceramic composite membrane for pervaporation separation of acetone–butanol–ethanol (ABE) aqueous solutions and its application in intensification of ABE fermentation process. Chem. Eng. Process. 86 (2014) 162-172
8. W.M. Haynes: CRC handbook of chemistry and physics, CRC press (2014)
9. A. Pereiro, J. Araújo, J. Esperança, I. Marrucho, L. Rebelo: Ionic liquids in separations of azeotropic systems–A review. J. Chem. Thermodyn. 46 (2012) 2-28
10. D. Rabari, T. Banerjee: Biobutanol and n-propanol recovery using a low density phosphonium based ionic liquid at T= 298.15 K and p= 1atm. Fluid Phase Equilib. 355 (2013) 26-33
11. S. Pierucci, G.B. Ferraris: 20 European Symposium on Computer Aided Process Engineering. Comput.-Aided Chem. Eng. 28 (2010) 1-1342
12. Y.C. Chen, K.L. Li, C.L. Chen, I.L. Chien: Design and Control of a Hybrid Extraction–Distillation System for the Separation of Pyridine and Water. Ind. Eng. Chem. Res. 54 (2015) 7715-7727
13. W.D. Seider, J. Seader, D.R. Lewin, S. Widagdo: Product and Process Design Principles: Synthesis, Analysis and Evaluation, Wiley (2010)
14. I. Díaz, J. Palomar, M. Rodríguez, J. de Riva, V. Ferro, E.J. González: Ionic liquids as entrainers for the separation of aromatic–aliphatic hydrocarbon mixtures by extractive distillation. Chem. Eng. Res. Des. 115 (2016) 382-393
15. F.M.F. Vallana, L.A. Holland, K.R. Seddon: A New Technique for Studying Vapour–liquid Equilibria of Multi-Component Systems. Aust. J. Chem. 69 (2016) 1240-1246
16. K.I. Al-Malah: Aspen Plus: Chemical Engineering Applications, John Wiley & Sons (2016)
17. R. Turton, R.C. Bailie, W.B. Whiting, J.A. Shaeiwitz: Analysis, synthesis and design of chemical processes, Pearson Education (2008)

18. A.S. Pathak, S. Agarwal, V. Gera, N. Kaistha: Design and control of a vapor-phase conventional process and reactive distillation process for cumene production. Ind. Eng. Chem. Res. 50 (2011) 3312-3326
19. W.L. Luyben, I.-L. Chien: Design and control of distillation systems for separating azeotropes, John Wiley & Sons (2011)
20. R.E. Treybal: Mass transfer operations. McGraw-Hill (1980)
21. J. De Riva, V. Ferro, D. Moreno, I. Diaz, J. Palomar: Aspen Plus supported conceptual design of the aromatic–aliphatic separation from low aromatic content naphtha using 4-methyl-N-butylpyridinium tetrafluoroborate ionic liquid. Fuel Process. Technol. 146 (2016) 29-38
22. S. Nandi, Y. Badhe, J. Lonari, U. Sridevi, B. Rao, S.S. Tambe, B.D. Kulkarni: Hybrid process modeling and optimization strategies integrating neural networks/support vector regression and genetic algorithms: study of benzene isopropylation on Hbeta catalyst. Chem. Eng. J. 97 (2004) 115-129
23. V. Ferro, J. De Riva, D. Sanchez, E. Ruiz, J. Palomar: Conceptual design of unit operations to separate aromatic hydrocarbons from naphtha using ionic liquids. COSMO-based process simulations with multi-component “real” mixture feed. Chem. Eng. Res. Des. 94 (2015) 632-647
24. M. Frisch, G.W. Trucks, H.B. Schlegel, G.E. Scuseria, Robb M. A., J.R. Cheeseman, G. Scalmani, V. Barone, B. Mennucci, G.A. Petersson, H. Nakatsuji, M. Caricato, X. Li, H.P. Hratchian, A.F. Izmaylov, J. Bloino, G. Zheng, J.L. Sonnenberg, M. Hada, M. Ehara, K. Toyota, R. Fukuda, J. Hasegawa, M. Ishida, T. Nakajima, Y. Honda, O. Kitao, H. Nakai, M.T. Vreven, J.J. A, J.E. Peralta, F. Ogliaro, M. Bearpark, J.J. Heyd, E. Brothers, K.N. Kudin, V.N. Staroverov, T. Keith, R. Kobayashi, J. Normand, K. Raghavachari, A. Rendell, J.C. Burant, S.S. Iyengar, J. Tomasi, M. Cossi, N. Rega, J.M. Millam, M. Klene, J.E. Knox, J.B. Cross, V. Bakken, C. Adamo, J. Jaramillo, R. Gomperts, R.E. Stratmann, O. Yazyev, A.J. Austin, R. Cammi, C. Pomelli, J.W. Ochterski, R.L. Martin, K. Morokuma, V.G. Zakrzewski, G.A. Voth, P. Salvador, J.J. Dannenberg, S. Dapprich, A.D. Daniels, O. Farkas, J.B. Foresman, J.V. Ortiz, J. Cioslowski, D.J. Fox Gaussian 09 Revision B. 01, Gaussian, Inc, Wallingford, CT, DOI. (2010)

25. R. Dennington, T. Keith, J. Millam: GaussView, version 5. Semichem Inc., Shawnee Mission, KS (2009)
26. R. Biswas, A. Malviya, T. Banerjee, P. Ghosh, S.M. Ali: Alkali Metal Ion Partitioning with Calix [4] arene-benzo-crown-6 Ionophore in Acidic Medium: Insights from Experiments, Statistical Mechanical Framework, and Molecular Dynamics Simulations. J. Phys. Chem. B 122 (2018) 2102-2112
27. A. Schäfer, H. Horn, R. Ahlrichs: Fully optimized contracted Gaussian basis sets for atoms Li to Kr. The Journal of Chemical Physics 97 (1992) 2571-2577
28. C. Sosa, J. Andzelm, B.C. Elkin, E. Wimmer, K.D. Dobbs, D.A. Dixon: A local density functional study of the structure and vibrational frequencies of molecular transition-metal compounds. J. Phys. Chem. 96 (1992) 6630-6636
29. D. Kundu, T. Banerjee: Multicomponent vapor–liquid–liquid equilibrium prediction using an a priori segment based model. Ind. Eng. Chem. Res. 50 (2011) 14090-14096
30. A. Bharti, D. Kundu, D. Rabari, T. Banerjee: Phase Equilibria in Ionic Liquid Facilitated Liquid–Liquid Extractions, CRC Press (2017)
31. A. Klamt: Conductor-like Screening Model for Real Solvents: A New Approach to the Quantitative Calculation of Solvation Phenomena. J. Phys. Chem. 99 (1995) 2224-2235
32. S.-T. Lin, S.I. Sandler: A priori phase equilibrium prediction from a segment contribution solvation model. Ind. Eng. Chem. Res. 41 (2002) 899-913

Chapter 5

Conclusions and Future Directions

5.1. Conclusions

Dwindling supply of fossil fuel have spurred efforts towards enhancing the production of lower alcohols from bio-resources. The main aim of this thesis was to explore new solvent (DES) for the economical and effective extraction of lower alcohols so that it can be scaled to an industrial level. The experiments started with the search for hydrophobic DESs which remained as liquid at room temperature. In the present study four hydrophobic DESs (DL-menthol and organic acids) as well as conventional solvents (mesitylene and oleyl alcohol) have been used as an azeotrope breaker for lower alcohol and water. Initially the COSMO-SAC model has then been used to predict the eutectic points for the mixture of HBA and HBD at an appropriate molar ratio. Thereafter once the ratio are known, the synthesis was carried out. Here DL-menthol has been used as HBA and organic acids such as decanoic, lauric, myristric, palmitic as HBD. All the synthesized DESs were found to be hydrophobic and lighter in density as compared to water. They remained as liquid in room temperature. ^{1}H NMR was used to check the hydrophobicity of DESs after washing multiple times with water.

Initially the LLE measurement were reported and compared with conventional solvents namely: water (1) + 1-butanol (2) + mesitylene (3) and water (1) + butanol (2) + oleyl alcohol (3). Overall the NRTL, UNIQUAC and COSMO-ASPEN models gave %RMSD values as (0.21, 0.34 and 1.34); and (0.16, 0.21 and 0.83) using mesitylene and oleyl alcohol respectively. Further once the DES were synthesized, the LLE for the ternary systems (water (1) + ethanol/1-propanol/1-butanol (2) + DES (3)) were measured and ternary plots were obtained. They were also correlated by NRTL, UNIQUAC and COSMO-SAC models. The NRTL and UNIQUAC models gave RMSD values less than unity for all systems indicating an excellent fit. The average RMSD for predictions using COSMO-ASPEN were as follows: DES-1: 0.053, 0.01, 0.008; DES-2: 0.036, 0.025, 0.022; DES-3: 0.05, 0.01, 0.008; DES-4: 0.005, 0.016, 0.021 for ethanol, 1-propanol and 1-butanol, respectively. Improved mass transfer rates coupled with high separation efficiency was observed with DES-1 for the separation of 1-butanol-water mixtures. Larger values of selectivity indicated easier separation of 1-butanol from water. The raffinate phase from the experiment and simulation for all the DES were found to comprise mainly water with mole composition as high as 99%. The slopes of the tie lines and the spread of two-phase region

indicated greater separation. A butanol recovery of ~ 99% was found for all DES. Larger values of 1-butanol distribution coefficient for all the DES indicated a lesser solvent requirement for butanol-water separation. It should be noted that the overall concentration of 1-butanol is found to be almost six times higher than ethanol in ABE fermentation broth, hence the results can be used for the selective extraction of butanol using optimized hybrid fermentation-extraction process. Acetone is highly volatile and can be evaporated easily from fermentation products, hence it has not been considered for extraction. Thus, DL-menthol and organic acid based DESs are proposed as solvents for extraction of 1-butanol and ethanol from the aqueous solution.

The final chapter includes the scale-up for the commercial level production of 1-butanol using ASPEN Plus V8.8. A Hybrid extraction-distillation system was proposed so as to effectively separate 1-butanol from aqueous stream. An economic consideration with respect to Total Annual Cost (TAC) was also attempted. An optimized 1-butanol recovery of ~ 98% w/w was obtained for a solvent/feed ratio of 1.16 using mesitylene as a solvent. Once the overall performance of the conventional solvents were predicted, the DESs as solvents were also attempted in the flowsheet. Overall the raffinate phase from the experiment and simulation was found to comprise mainly water with mass composition as high as 99.99% w/w. For DES-1, an optimized 1-butanol recovery of ~ 86.2% w/w was obtained for a solvent/feed ratio of 0.1.Among all the DES, it required the least solvent flow rate of 2499 kg/h along with a reflux ratio of 2.01. Thus DES-1 was found to be the best for the extraction of the lower alcohols among all used DES and mesitylene.Overall menthol based Deep Eutectic Solvent having a shorter organic acid chain length is recommended for lower alcohol extraction.

5.2. Future Directions

The following are the probable future work which holds good using DES as solvents.

a. A Pilot plant study can be envisaged with DES-1 (i.e. decanoic acid based acid) as solvent due to its superior performance in terms of selectivity and solute distribution ratio. Further ASPEN plus simulation has also provided encouraging results as DES1 had the least TAC among all the solvents.

b. Molecular Dynamic and Quantum Chemical Calculations can also provide insight or explain the higher effectiveness of lower chain acid as compared to longer chain organic acids.

c. Liquid-Liquid Equilibria can be measured for multicomponent mixtures such as ethanol + 1-butanol + 1-propanol + water or acetone + 1-butanol + ethanol + water (ABE fermentation product) along with DES. This will give us selective extraction criteria of the DES for a particular lower alcohol.

d. The optimization of the cost function can be formulated by combining the multistage extractor with acetone distillation unit and solvent (DES) recovery unit.

Appendix

1. Method to Define DES as a Pseudo Component in Aspen Plus:

For defining an unknown compound such as DES in ASPEN we shall be requiring the following properties: average molecular weight, density, normal boiling point, COSMO volume and sigma profile. While the first three are pure component properties obtained from literature, the latter two are derived from our inhouse COSMO-SAC model. Let us discuss them briefly.

1.1. Average Molecular weight of DESs

Eq. 4A.1 shows the method to calculate the average molecular weight of the DES which is the mixture of hydrogen bond donor (HBD) and the hydrogen bond acceptor (HBA) in different molar ratio.

$$Avg.Mol.wt_{DES} = f_{HBA} Mol.wt_{HBA} + f_{HBD} Mol.wt_{HBD} \quad (4A.1)$$

Here f_{HBA} and f_{HBD} are the mole ratio's, namely the HBD and HBA that have been adopted in the experimental work as per chapter 2 Table 4A.1 shows the average molecular weight of all the DES used in the present study as calculated using Eq. 4A.1.

Table 4A.1: Average Molecular weight of the synthesized DES-1 to DES-4

Name of DES	Average Molecular weight (gm/mol)
DES-1	164.27
DES-2	170.95
DES-3	170.69
DES-4	163.97

1.2 Density and Viscosity of DES-2

Table 4A.2 shows the density and viscosity of synthesized DESs in the temperature range 20-85°C.The density of the all the solvents is measured by a DMA 4500M densitometer (Anton Paar Make).The viscosity of DES was measured by an interfacial

rheometer (Model: Physica MCR301, Anton-Paar Make) with a relative expanded uncertainty of 0.033.

Table 4A.2: The Experimental Density and Viscosity Data of Pure DES at Atmospheric Pressure (p = 1 atm.) and Different Temperatures[a]

Temperature (K)	Density (g cm^{-3})[b]		Viscosity (mPa)[b]	
	Present work	Literature[1]	Present work	Literature[1]
293.15	0.8971	0.9002	21.810	29.689
303.15	0.8898	0.8930	12.500	16.957
313.15	0.8826	0.8857	7.657	10.527
323.15	0.8753	0.8780	5.112	7.057
333.15	0.8678	0.8703	3.623	4.872
343.15	0.8603	0.8631	2.670	3.599
353.15	0.8526	0.8549	2.088	2.650

[a]The standard uncertainty u are $u\ (T)$ = 0.1 K, $u\ (p)$ = 1 kPa, [b] the relative expanded uncertainty U are $U_r(\rho)$ = 0.003, and $U_r(\eta)$ = 0.033

1.3. Sigma Profiles

For the sigma profile calculation of DES, a molar ratio was used for DL-menthol (HBA) and organic Acid (HBD) molecule respectively. The screening charge distribution for such a DES will then be the algebraic sum of the sigma profiles calculated separately [2]. It takes the form:

$$p_{DES}(\sigma) = p_{HBA}(\sigma) + p_{HBD}(\sigma) = f_{HBA}p_{HBA}(\sigma) + f_{HBD}p_{HBD}(\sigma) \qquad (4A.2)$$

Here $p_{HBA}(\sigma)$ and $p_{HBD}(\sigma)$ are the sigma profile of the components of DES, namely the HBA and HBD respectively. f_{HBA} and f_{HBD} are the mole ratio's that have been adopted in the experimental work as per chapter 2. The sigma profiles for all the components as obtained through our inhouse COSMO-SAC code are given in Table 4A.3.

Table 4A.3: Sigma Profile of Lower Alcohols and Synthesized DES

Screening charge density, σ (e/ Å^2)	Sigma profile p^x (σ)						
	Ethanol	**Propanol**	**butanol**	**DES-1**	**DES-2**	**DES-3**	**DES-4**
-0.03	0	0	0	0	0	0	0
-0.029	0	0	0	0	0	0	0
-0.028	0	0	0	0	0	0	0
-0.027	0	0	0	0	0	0	0
-0.026	0	0	0	0	0	0	0
-0.025	0	0	0	0	0	0	0
-0.024	0	0	0	0	0	0	0
-0.023	0	0	0	0	0	0	0
-0.022	0	0	0	0	0	0	0
-0.021	0	0	0	0	0	0	0
-0.02	0	0	0	0	0.948	0	0
-0.019	0	0	0	0	0.705	0	0
-0.018	0	0	0	0.948	1.626	0	0
-0.017	0	0	0	0.579	1.641	0.637	0.948
-0.016	0	1.586	1.654	1.435	2.164	2.594	4.343
-0.015	1.102	0.934	0.579	2.751	3.878	11.318	21.439
-0.014	1.172	1.493	1.793	1.428	3.035	7.487	14.592
-0.013	1.108	1.091	1.016	1.501	2.308	5.758	10.756
-0.012	0.557	0.801	0.562	1.549	2.494	8.623	14.679
-0.011	1.091	0.186	0.437	1.818	1.833	4.407	9.220
-0.01	0.424	0.528	1.079	1.928	2.837	6.845	11.583
-0.009	0.513	0.916	0.837	0.417	1.389	3.506	5.595
-0.008	0.520	1.175	0.318	1.055	3.130	6.928	12.638
-0.007	1.894	0.589	0.493	1.979	3.343	4.709	8.410
-0.006	1.320	0.206	0.769	4.176	8.504	13.029	18.750
-0.005	0.333	0.025	0.356	5.757	3.687	10.354	11.978
-0.004	1.835	2.663	1.594	7.928	12.946	24.455	41.090
-0.003	11.655	16.096	17.986	30.161	61.631	126.074	238.826
-0.002	11.682	18.586	22.086	73.963	113.504	260.949	483.138
-0.001	13.556	10.640	17.766	96.388	145.360	346.324	633.353
0	10.646	13.160	14.874	73.668	88.154	222.167	392.263
0.001	7.338	10.173	13.751	60.335	85.922	198.126	352.076
0.002	4.649	11.960	10.162	50.257	77.636	172.763	316.469
0.003	1.286	1.276	6.444	20.799	56.694	116.763	232.580
0.004	0.980	0.689	1.277	4.808	5.675	14.011	26.075
0.005	0.966	1.390	1.301	4.787	4.807	13.228	24.343
0.006	1.899	0.284	0.905	2.822	4.465	8.160	14.633
0.007	1.137	1.094	0.243	3.328	4.353	12.435	22.020
0.008	0.956	1.033	1.935	5.130	6.175	8.908	16.808
0.009	1.323	1.137	0.578	3.005	2.186	5.756	8.131
0.01	1.709	0.690	1.190	6.030	8.786	11.387	20.065
0.011	0.590	1.558	0.667	4.431	10.600	17.988	29.145
0.012	1.649	0.432	1.291	6.095	5.277	10.234	13.878
0.013	0.822	1.557	1.146	2.117	5.908	11.823	19.084
0.014	2.344	1.065	1.513	0.975	3.598	6.295	12.633
0.015	1.829	2.085	1.033	1.045	2.538	6.272	12.544

0.016	0	1.852	2.827	0.843	1.687	5.060	10.120
0.017	0	1.049	0.678	0.776	1.551	4.653	9.306
0.018	0	0	0	0	0	0	0
0.019	0	0	0	0	0	0	0
0.02	0	0	0	0	0	0	0
0.021	0	0	0	0	0	0	0
0.022	0	0	0	0	0	0	0
0.023	0	0	0	0	0	0	0
0.024	0	0	0	0	0	0	0
0.025	0	0	0	0	0	0	0
0.026	0	0	0	0	0	0	0
0.027	0	0	0	0	0	0	0
0.028	0	0	0	0	0	0	0
0.029	0	0	0	0	0	0	0
0.03	0	0	0	0	0	0	0

1.4 Normal Boiling Temperature

The boiling point of the DES can be calculated by the method given by Lydersen−Joback−Reid (LJR) [3]. The equations proposed for calculating the normal boiling point is given as:

$$T_b = 198.2 + \sum n_i \Delta T_{bMi} \tag{4A.3}$$

Here T_b is the normal boiling temperature (K), $n_i$is the frequency of appearance of the i^{th} group of atoms in the molecule and ΔT_{bMi} is their contribution to the normal boiling temperature (K).

Table 4A.4: Estimated normal boiling temperature of synthesized DES-1 to DES-4 [3, 4]

Name of DES	Normal boiling point (K)
DES-1	561.56
DES-2	566.44
DES-3	561.20
DES-4	545.80

1.5 COSMO Volume

Table 4A.5 shows COSMO file details of the molecules used in the present study as generated by Gaussian09. The COSMO file of the molecule gives information about the number of segments ('nps') with their corresponding cavity areas ($Å^2$), volume ($Å^3$) and screening charges. The area and volume refers within the conductor which has an infinite dielectric constant. One such abridged form of COSMO file of DL-menthol is given in Table 4A.6

Table 4A.5: COSMO File Details

Molecule	**Number of segments(nps)**	**Cavity Area within conductor* ($Å^2$)**	**Cavity Volume Within conductor* ($Å^3$)**
DL-menthol	1737	797.91	1436.24
Decanoic acid	2318	947.55	1594.8
Lauric acid	2714	1093.09	1861.49
Myristic acid	3132	1247.72	2145.18
Palmitic acid	3532	1400.76	2421.21

*The cavity surface area and volume are output of our inhouse generated COSMO File

Table 4A.6: Abridged COSMO file for DL-menthol **(red portion as input)**

Gaussian COSMO output

$cosmo_data;fepsi =1;
nps= 1737;
area =797.91;
volume=1436.24

#atom	x	y	z	element	radius	area	COSMO	sigma
1	4.395	-0.428	-0.529	6.000	[A]	3.431	charge	0.001
2	2.949	-2.667	0.606	6.000	2.000	8.605	0.002	0.002
3	0.183	-2.739	-0.253	6.000	2.000	7.000	0.015	0.001
4	0.112	-3.090	-2.299	1.000	2.000	6.520	0.010	-0.001
5	-0.755	-4.349	0.634	1.000	1.300	5.421	-0.009	-0.002
6	-1.279	-0.289	0.363	6.000	1.300	2.202	-0.012	0.001
7	0.184	1.938	-0.805	6.000	2.000	3.844	0.003	0.000
8	0.127	1.707	-2.875	1.000	2.000	6.568	-0.001	-0.002
9	2.951	2.019	0.048	6.000	1.300	7.506	-0.012	0.001
10	2.994	2.397	2.087	1.000	2.000	6.507	0.007	-0.002
11	3.894	3.627	-0.867	1.000	1.300	6.525	-0.010	-0.003
12	3.885	-4.446	0.102	1.000	1.300	6.491	-0.017	-0.002
13	3.024	-2.540	2.678	1.000	1.300	6.523	-0.013	-0.001
14	4.431	-0.680	-2.593	1.000	1.300	6.538	-0.009	-0.002
15	-1.238	-0.038	2.426	1.000	1.300	6.293	-0.010	-0.001
16	7.131	-0.304	0.401	6.000	1.300	16.984	-0.008	0.002
17	8.160	-2.041	-0.051	1.000	2.000	6.467	0.037	-0.002
18	7.210	-0.051	2.454	1.000	1.300	6.480	-0.014	-0.002
19	8.157	1.272	-0.461	1.000	1.300	6.469	-0.012	-0.002
20	-4.107	-0.349	-0.483	6.000	1.300	3.050	-0.015	0.002
21	-4.170	0.329	-2.445	1.000	2.000	6.267	0.006	-0.001
22	-5.295	-3.001	-0.456	6.000	1.300	14.870	-0.008	0.002
23	-4.375	-4.316	-1.755	1.000	2.000	5.822	0.036	-0.002
24	-7.283	-2.883	-1.012	1.000	1.300	6.445	-0.013	-0.002
25	-5.244	-3.840	1.436	1.000	1.300	6.485	-0.013	-0.002
26	-5.755	1.423	1.125	6.000	1.300	16.015	-0.011	0.003
27	-5.029	3.346	1.130	1.000	2.000	4.341	0.052	0.000
28	-5.832	0.760	3.087	1.000	1.300	6.493	0.002	-0.001
29	-7.698	1.456	0.413	1.000	1.300	6.474	-0.008	-0.002
30	-1.053	4.264	-0.164	8.000	1.300	12.630	-0.010	0.012
31	-0.096	5.646	-0.873	1.000	1.720	8.172	0.146	-0.013
					1.300		-0.109	

$coord_car;!BIOSYM archive 3;PBC=OFF;coordinates from GAUSSIAN/COSMO calculation

C1	2.326	-0.226	-0.280	GAUS	1	C	C	0
C2	1.560	-1.411	0.321	GAUS	1	C	C	0
C3	0.097	-1.449	-0.134	GAUS	1	C	C	0
H4	0.060	-1.635	-1.216	GAUS	1	H	H	0
H5	-0.399	-2.302	0.335	GAUS	1	H	H	0
C6	-0.677	-0.153	0.192	GAUS	1	C	C	0
C7	0.097	1.026	-0.426	GAUS	1	C	C	0
H8	0.067	0.903	-1.521	GAUS	1	H	H	0
C9	1.562	1.068	0.025	GAUS	1	C	C	0
H10	1.584	1.269	1.104	GAUS	1	H	H	0
H11	2.061	1.920	-0.459	GAUS	1	H	H	0
H12	2.056	-2.353	0.054	GAUS	1	H	H	0
H13	1.600	-1.344	1.417	GAUS	1	H	H	0
H14	2.345	-0.360	-1.372	GAUS	1	H	H	0
H15	-0.655	-0.020	1.284	GAUS	1	H	H	0
C16	3.774	-0.161	0.212	GAUS	1	C	C	0
H17	4.318	-1.080	-0.027	GAUS	1	H	H	0
H18	3.816	-0.027	1.299	GAUS	1	H	H	0
H19	4.316	0.673	-0.244	GAUS	1	H	H	0
C20	-2.173	-0.185	-0.256	GAUS	1	C	C	0
H21	-2.207	0.174	-1.294	GAUS	1	H	H	0
C22	-2.802	-1.588	-0.242	GAUS	1	C	C	0
H23	-2.315	-2.284	-0.929	GAUS	1	H	H	0
H24	-3.854	-1.526	-0.536	GAUS	1	H	H	0
H25	-2.775	-2.032	0.760	GAUS	1	H	H	0
C26	-3.046	0.753	0.595	GAUS	1	C	C	0
H27	-2.661	1.771	0.598	GAUS	1	H	H	0
H28	-3.086	0.402	1.633	GAUS	1	H	H	0
H29	-4.074	0.771	0.219	GAUS	1	H	H	0
O30	-0.557	2.257	-0.087	GAUS	1	O	O	0

H31 end	-0.051	2.988	-0.462	GAUS	1	H	H	0	
$screening_charge; cosmo=-0.03418; correction=0.034181; total=0; $cosmo_energy; Total energy corrected [a.u.] = -468.082 Dielectric energy corr. [a.u.] = -0.00785; $segment_information; #n-segmentnumber; #atom-atom associated with segment n # position – segment coordinates [a.u.]; # charge – segment charge (corrected); # area – segment area [A**2] # potential - solute potential on segment (A length scale)									
#	nps	atom	position	X	Y	Z)	charge	area	charge/area
	1 2 3 4 5	27 27 27 27 27	-6.143 -5.336 -5.498 -4.229 -4.400	5.054 4.743 5.517 4.164 5.026	2.500 3.128 2.181 3.304 2.809	0.000 0.000 0.000 0.000 0.000	0.060 0.051 0.168 0.008 0.258	0.000 0.000 -0.002 -0.001 -0.001	-0.045 -0.051 -0.045 -0.064 -0.060

	1736 1737	1 1	6.567 6.540	0.528 1.193	-3.471 -3.185	0.000 0.000	0.093 0.051	0.000 0.002	0.012 0.011

Now using the information of sigma profile (Table 4A.3) and cavity volume (Table 4A.6) we are in a position to complete the PSEUDOCOMPONENT definition.

1.6 Method for Insertion using PSEUDOCOMPONENT Tool

Step 1: Specify DES as a PSEUDOCOMPONENT in ASPEN Plus

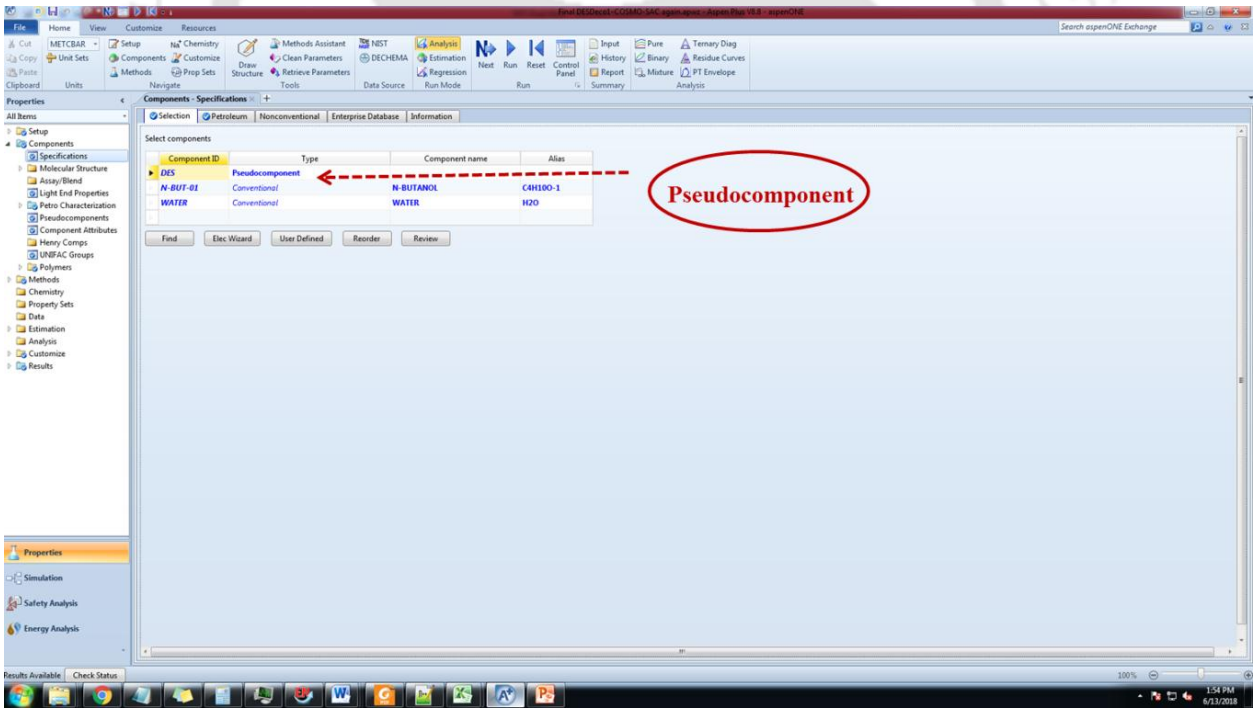

Step 2: Insert the properties of the PSEUDOCOMPONENT such as density (Table 4A.1),average molecular weight (Table 4A.2) and normal boiling point (Table 4A.4)

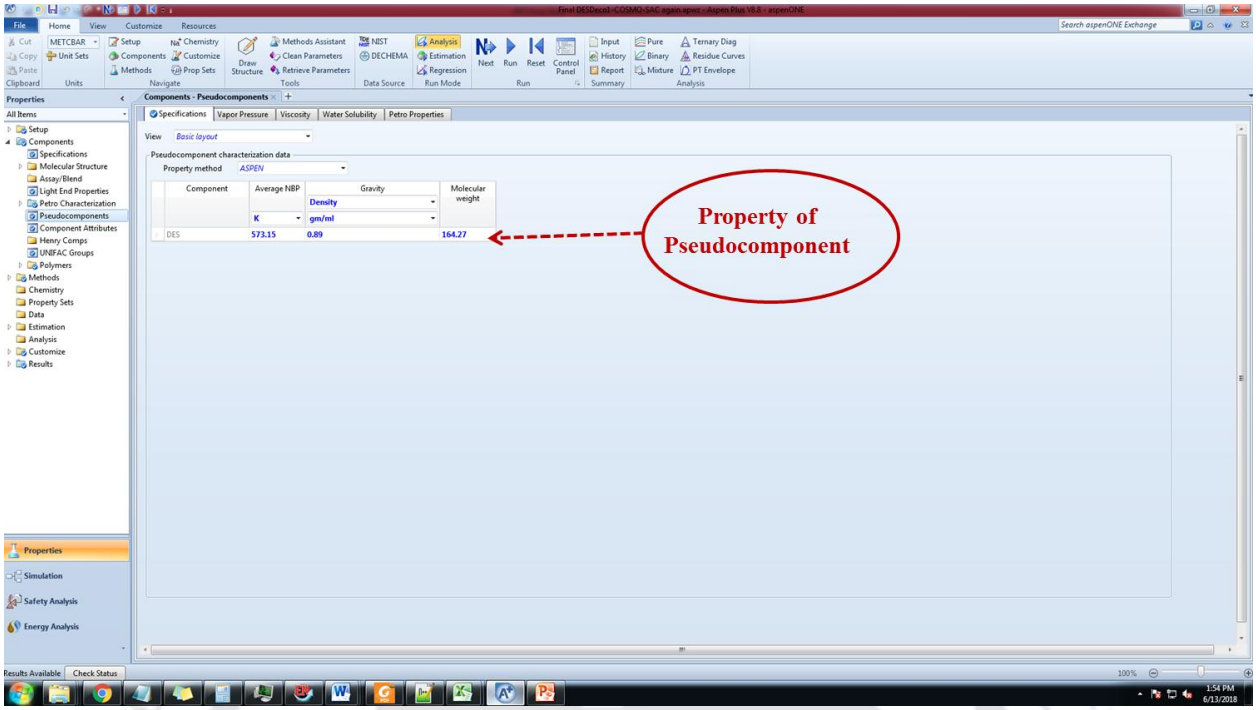

Step 3: Invoke COSMO-SAC Thermodynamic Model

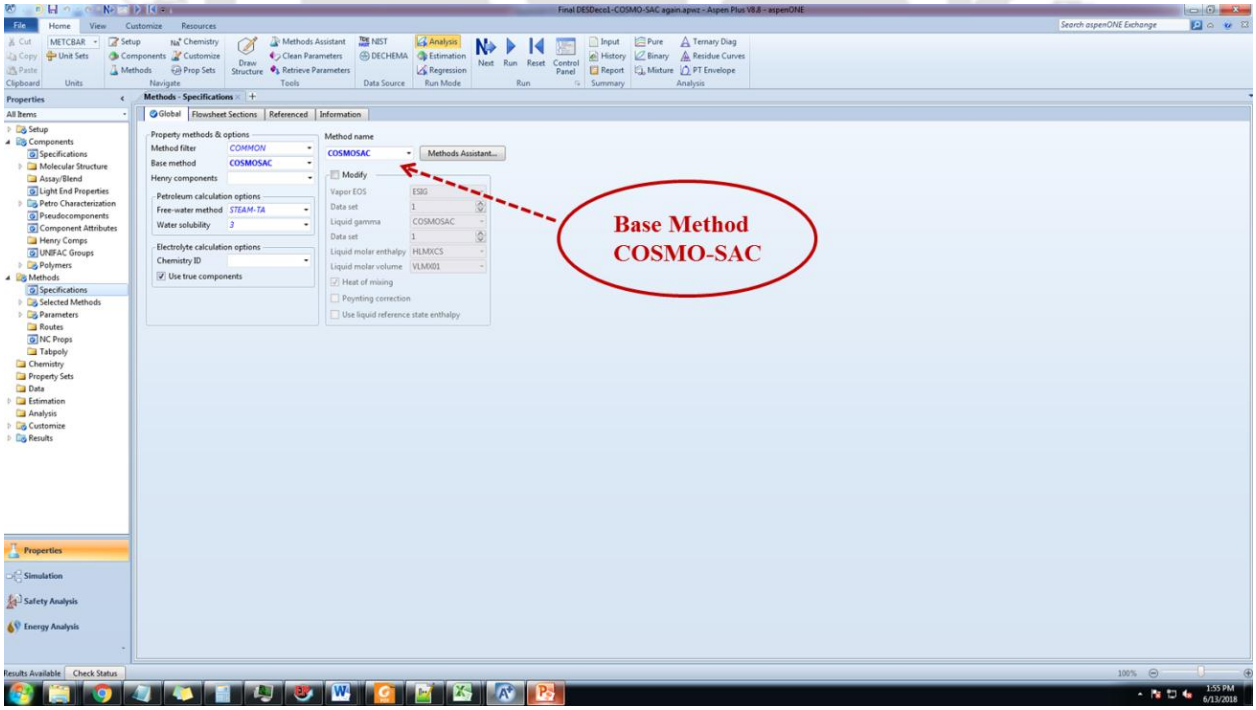

Step 4: Insert the Viscosity and Temperature of PSEUDOCOMPONENT

Figure 4A.1 shows the variation of experimental viscosity with inverse of temperature (As per data of Table 4A.2). The coefficients A and B are obtained from an exponential fit. A and B values are then used as input in the next step within ASPEN.

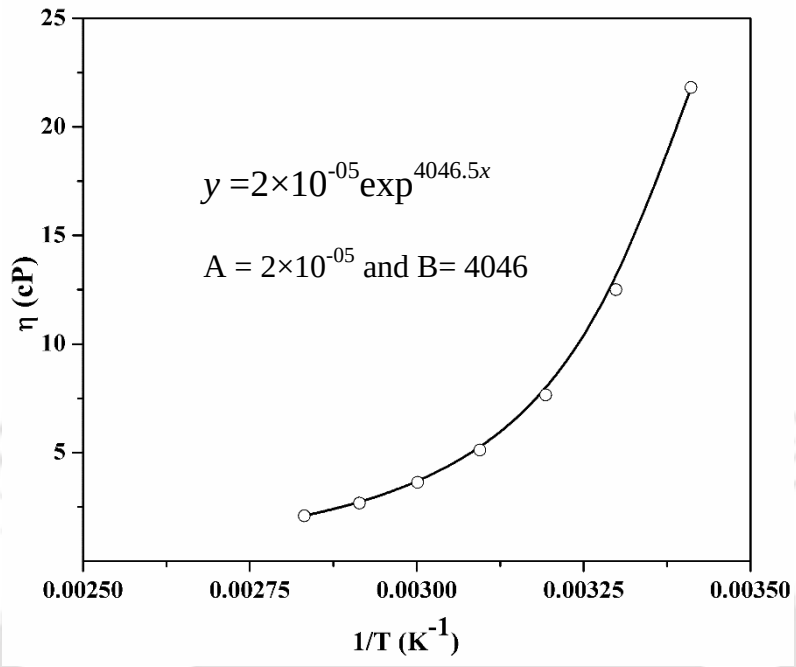

Figure: 4A.1: Variation of viscosity vs. inverse of temperature

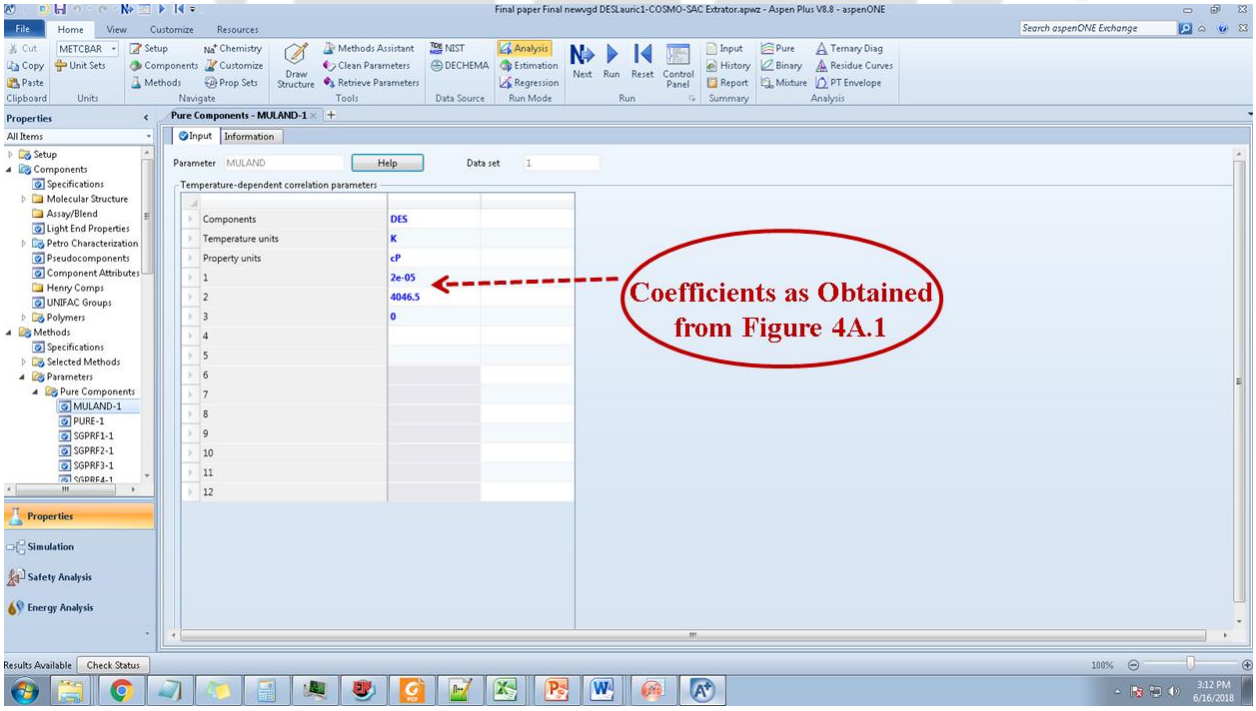

Step 5: Insert the COSMO Cavity Volume as per Table 4A.6.

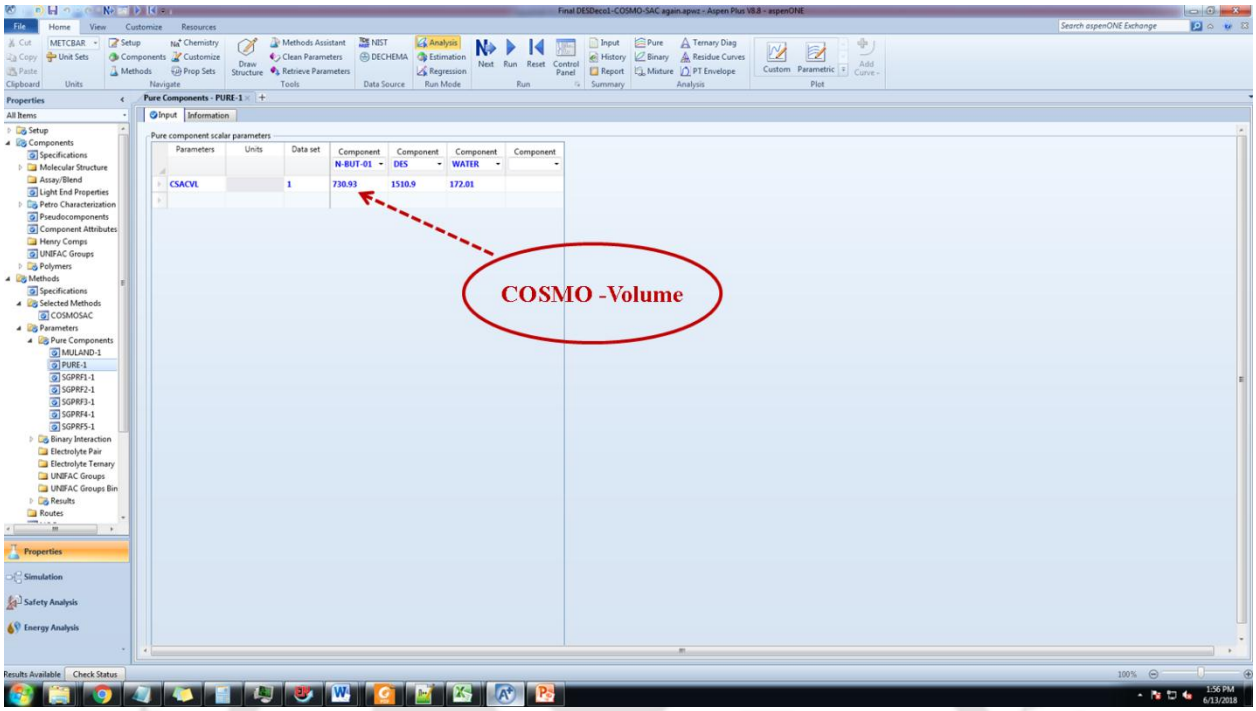

Step.6 Insertion of Sigma Profile:

Step: 6-a: Divide the entire 60 histograms in five equal division each having 12 segments. These are termed in ASPEN from SGPRF1-1 to SGPRF5-1. Kindly note we have to paste the actual histogram (or sigma profile) and not the normalized profile.

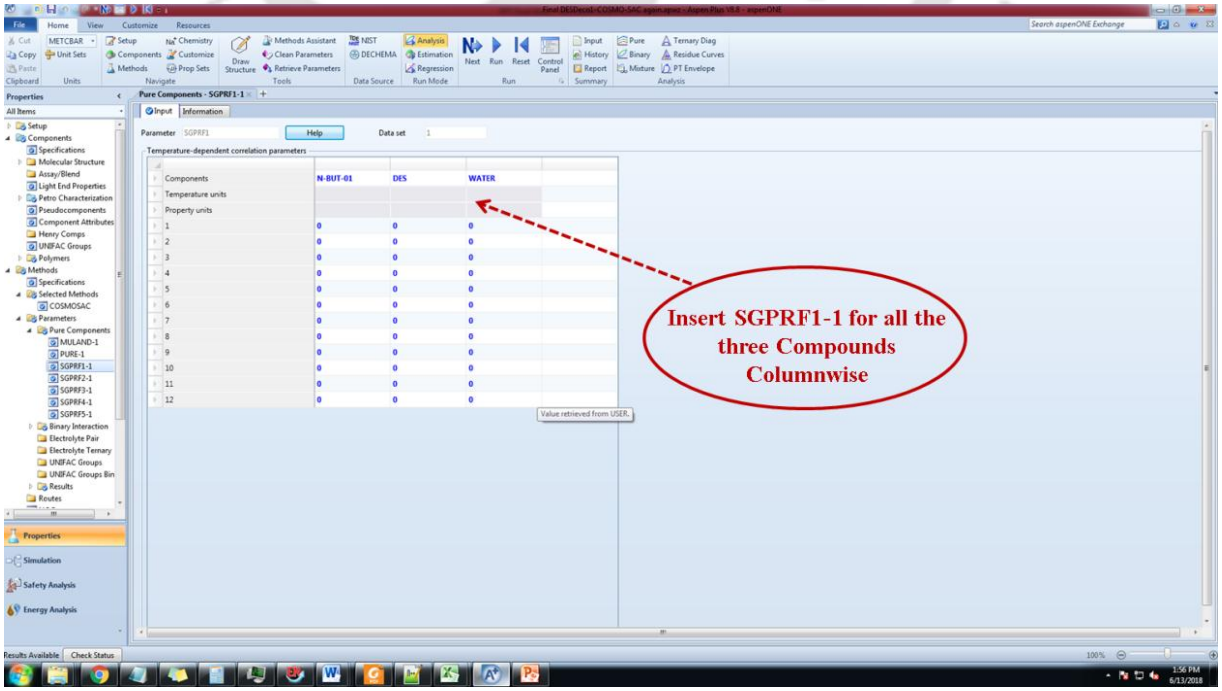

Step: 6-b

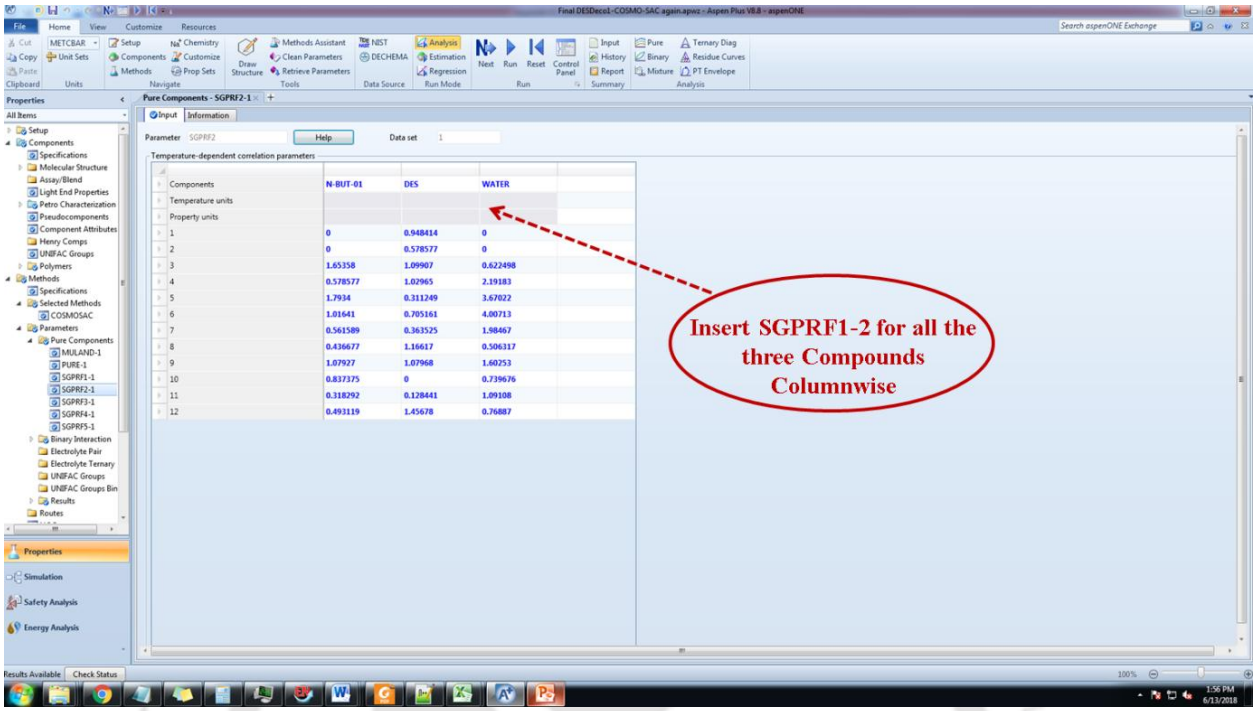

Step: 6-c

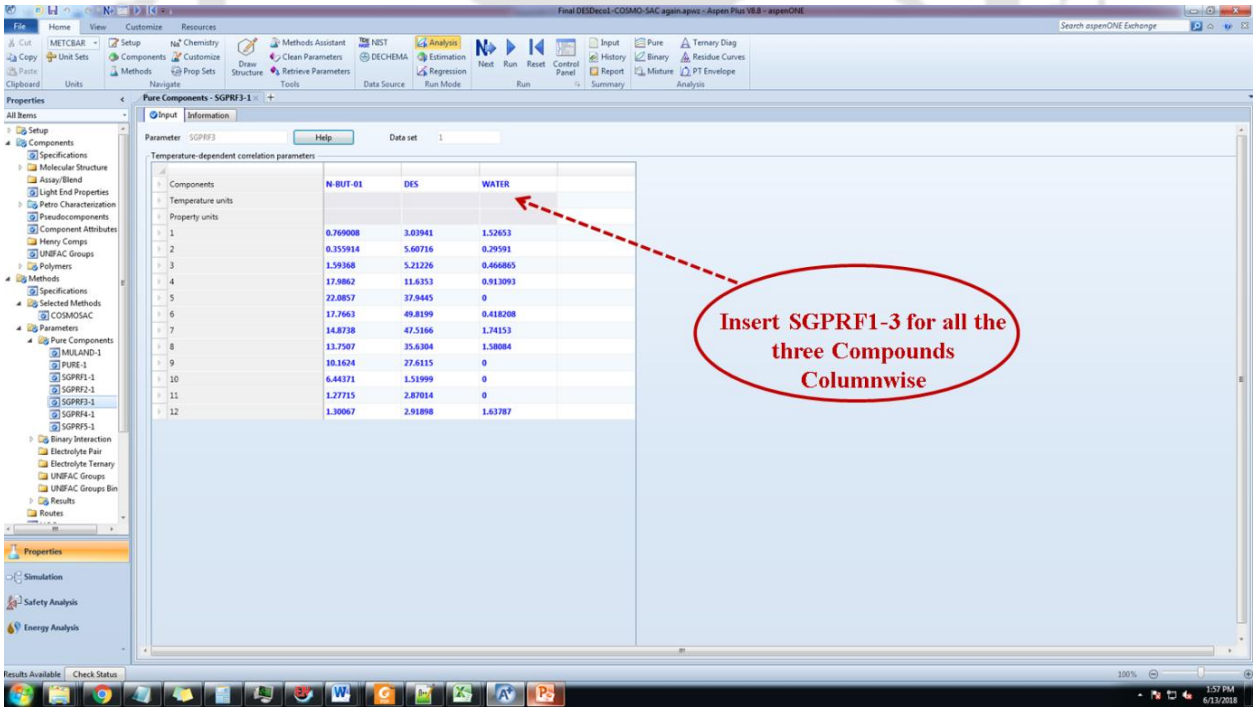

Step: 6-d

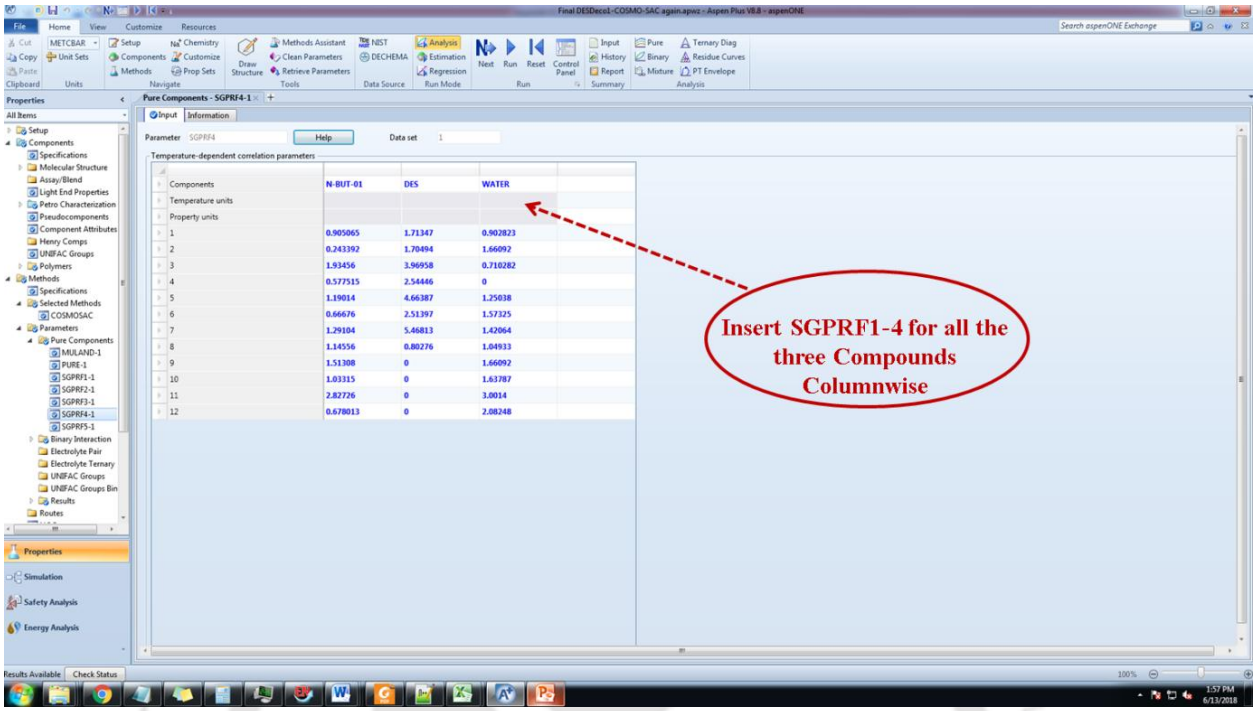

Step: 6-e

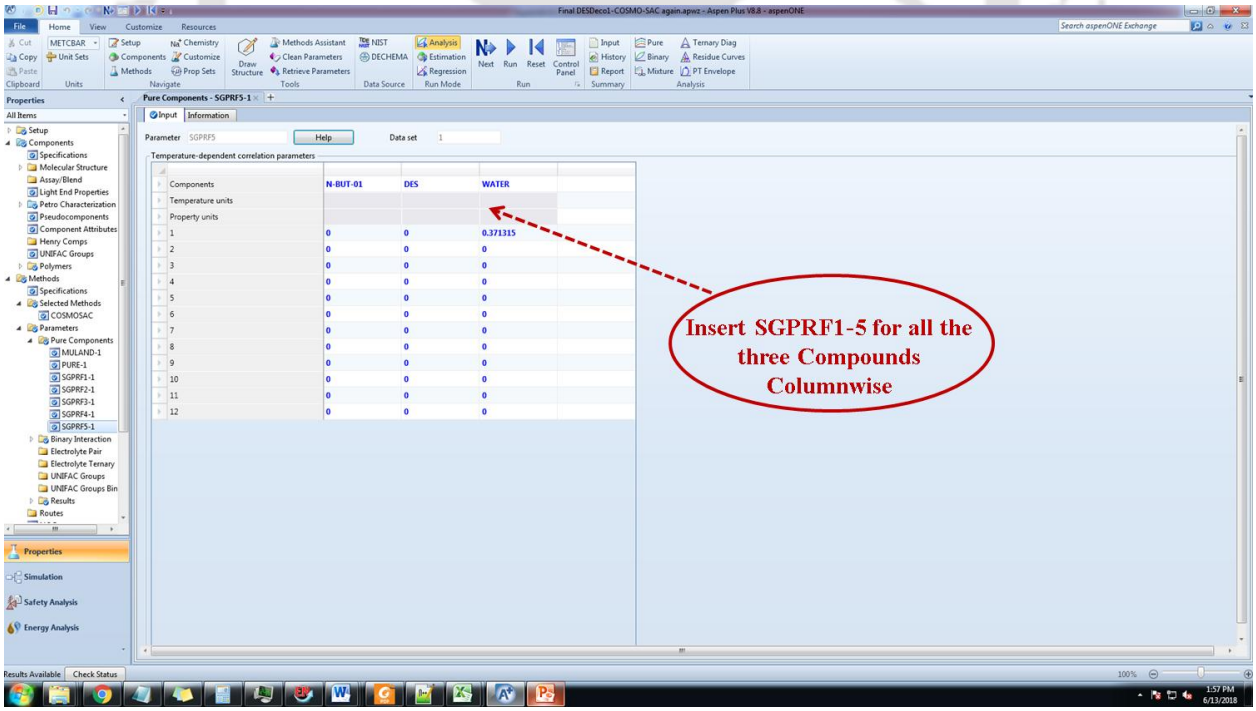

Once all the sigma profile i.e SGPRF1-1 to SGPRF1-5 are inserted, we are now ready for any process simulation.

References

1. B.D. Ribeiro, C. Florindo, L.C. Iff, M.A. Coelho, I.M. Marrucho: Menthol-based eutectic mixtures: hydrophobic low viscosity solvents. ACS Sustainable Chem. Eng. 3 (2015) 2469-2477.

2. T. Banerjee, K.K. Verma, A. Khanna: Liquid–liquid equilibrium for ionic liquid systems using COSMO-RS: Effect of cation and anion dissociation. AIChE journal 54 (2008) 1874-1885.

3. K.G. Joback, R.C. Reid: Estimation of pure-component properties from group-contributions. Chemical Engineering Communications 57 (1987) 233-243.

4. N.R. Mirza, N.J. Nicholas, Y. Wu, S. Kentish, G.W. Stevens: Estimation of normal boiling temperatures, critical properties, and acentric factors of deep eutectic solvents. J. Chem. Eng. Data 60 (2015) 1844-1854

Research Output

List of Publications

1. **Rupesh Verma,** Mood Mohan* and Tamal Banerjee, Operational Strategies and Comprehensive Evaluation of Menthol Based Deep Eutectic Solvent for the Extraction of Lower Alcohols from Aqueous Media. (accepted, ACS Sustainable Chemistry & Engineering, DOI: 10.1021/acssuschemeng.8b04255, Nov., 2018)

2. **Rupesh Verma,** Pyarimohan Dehury, Anand Bharti and Tamal Banerjee. Liquid-Liquid Extraction, COSMO-SAC Predictions and Process Flow sheeting of 1-Butanol Enhancement using Mesitylene and Oleyl Alcohol. *Journal of Molecular Liquids* 265 (2018) 824-839

3. **Rupesh Verma** and Tamal Banerjee. Liquid–Liquid Extraction of Lower Alcohols Using Menthol-Based Hydrophobic Deep Eutectic Solvent: Experiments and COSMO-SAC Predictions. *Industrial Engineering Chemistry Research* 57 (2018) 3371−3381

4. Anand Bharti, **Rupesh Verma,** Prerna, Sarvesh Namdeo, Abhigyan Malviya, Tamal Banerjee and Stanley I. Sandler. Liquid-liquid equilibria and COSMO-SAC modeling of organic solvent/ionic liquid - hydroxyacetone - water mixtures. *Fluid Phase Equilibria.* 62 (2018) 73-84

5. **Rupesh Verma,** Ismael Diaz and Tamal Banerjee, Extraction of Lower Alcohols using Novel Hydrophobic Deep Eutectic Mixtures: Synthesis, COSMO-SAC Predictions, Phase Equilibria and Process Economics. (submitted in "Chemical Engineering Research and Design" Journal, Nov., 2018)

6. **Rupesh Verma,** Diaz and Tamal Banerjee, Synthesis, Liquid-liquid equilibria, COSMO-SAC modeling of Lower Alcohols and Process Flow sheeting of 1-Butanol Enhancement using Menthol + Myristic acid based Deep Eutectic Solvent. (Manuscript under preparation)

7. **Rupesh Verma** and Tamal Banerjee, Synthesis, Liquid-liquid equilibria, COSMO-SAC modeling of lower alcohols and Process Flow sheeting of 1-Butanol Enhancement using Menthol + Palmitic acid based new hydrophobic Deep Eutectic Solvent. (Manuscript under preparation)

Conference Proceedings

1. National: (BIOPROCESSING INDIA 2017, BPI-2017)

Liquid-Liquid Extraction and Process Flow sheeting of bio-butanol Enhancement using Mesitylene and Oleyl Alcohol, Bioprocessing India 2017 [**Rupesh Verma,** Anand Bharti, Pyarimohan Dehury and Tamal Banerjee]

2. International: (Indo-Japan Bilateral Symposium, IJBS-17)

Liquid-Liquid Extraction and COSMO-SAC prediction of lower alcohols Enhancement using Deep Eutectic Solvent [DES] [**Rupesh Verma** and Tamal Banerjee]

Award/Prize

Won, **100 Euro** for the best poster presentation award in the International conference: (**Indo-Japan Bilateral Symposium, IJBS-17**). Springer International Publishing Company U.S.A.

ACS Sustainable Chemistry & Engineering

Article

Operational Strategies and Comprehensive Evaluation of Menthol Based Deep Eutectic Solvent for the Extraction of Lower Alcohols from Aqueous Media

Rupesh Verma, Mood Mohan, Vaibhav V. Goud, and Tamal Banerjee

ACS Sustainable Chem. Eng., **Just Accepted Manuscript** • DOI: 10.1021/acssuschemeng.8b04255 • Publication Date (Web): 11 Nov 2018

ACS Publications

is published by the American Chemical Society. 1155 Sixteenth Street N.W., Washington, DC 20036

Journal of Molecular Liquids 265 (2018) 824–839

Contents lists available at ScienceDirect

Journal of Molecular Liquids

journal homepage: www.elsevier.com/locate/molliq

Liquid-liquid extraction, COSMO-SAC predictions and process flow sheeting of 1-butanol enhancement using mesitylene and oleyl alcohol

Rupesh Verma [a], Pyarimohan Dehury [a], Anand Bharti [b], Tamal Banerjee [a,*]

[a] Department of Chemical Engineering, Indian Institute of Technology Guwahati, Guwahati, Assam 781039, India
[b] Birla Institute Of Technology Mesra, Ranchi, Jharkhand 835215, India

ARTICLE INFO

Article history:
Received 1 February 2018
Received in revised form 1 June 2018
Accepted 21 June 2018
Available online 26 June 2018

Keywords:
Mesitylene
Oleyl alcohol
NRTL
UNIQUAC
COSMO-SAC
1-butanol
Aspen Plus

ABSTRACT

The current work reports the extraction of 1-butanol from aqueous streams using low density solvents namely, mesitylene ($\rho = 0.864$ g/cm^3) and oleyl alcohol ($\rho = 0.849$ g/cm^3). The ternary Liquid-Liquid Equilibrium (LLE) studies for mesitylene (1) + 1-butanol (2) + water (3) and oleyl alcohol (1) + 1-butanol (2) + water (3) were conducted to explain the effectiveness of the two solvents. A type-I phase behavior with a large immiscible region was observed at $T = 298.15$ K and $p = 0.1$ MPa. High values of selectivity ranging from 400 to 2500 for mesitylene and 750–6500 oleyl alcohol were observed. Distribution coefficient values higher than unity indicated an easier diffusion of 1-butanol from aqueous phase to extract phase. It also confirmed a lower solvent to feed ratio for separation of 1-butanol from water. ^{1}H NMR spectra indicated an aqueous rich phase free of solvent and while the contrary was observed in the solvent rich phase. Non-random two liquid (NRTL) and UNIversal QUAsichemical (UNIQUAC) models gave root mean square deviation (RMSD) in the range of 0.1–0.5% for both the systems. Further the predictions of the tie lines were also confirmed though the quantum chemical based COnductor like Screening MOdel Segment Activity Coefficients (COSMO-SAC) which gave RMSD in the range of 5%. Based on the selectivity values of 1-butanol at lower concentration, mesitylene was chosen as the recommended solvent for extraction. Thereafter a hybrid extraction process using Aspen Plus V8.8® was designed to carry out an optimized flowsheet concerning the recovery and recycle of butanol and mesitylene respectively.

1. Introduction

The increasing demand of energy in the developing countries has led to the depletion of fossil fuels at a high rate. The primary energy consumption has increased worldwide by 1% in 2016 following a growth of 0.9% in 2015 as well as 1% in 2014 [1]. In the present scenario fossil fuels such as oil, natural gas and coal are the world's leading energy sources. The excess consumption of these fossil fuels further creates greenhouse gas emission and poses threat to human life. Thus it becomes a challenge for governments, engineers, scientists and economists so as to mitigate the ill effects of these gases. To overcome these challenges lower alcohols such as 1-butanol as an alternative fuel is gaining importance [2].

Butanol is conventionally produced through the ABE (Acetone-Butanol-Ethanol) fermentation where bacteria like clostridium acetobutylicum and clostridium bjerinkci ferment biomass under anaerobic conditions thereby producing acetone, butanol, and ethanol with a proportion of 3:6:1 [3–5]. Bio-butanol obtained by ABE fermentation process is now considered as a potential biofuel. Bio-butanol like 1-butanol have similar properties as 1-butanol obtained from petroleum products. It has a higher calorific value (29.2 MJ/dm^3) as compared to ethanol (19.6 MJ/dm^3) and has a lesser flammability and lower hydrophilicity values. The RON and MON numbers of butanol are also close to petrol while at the same time less corrosive than ethanol. All these features make 1-butanol as a useful additive to gasoline and as biofuels [3, 5–7]. However the separation of lower chain alcohols such as 1-butanol is difficult as it forms azeotropic mixtures with water [8–10]. Hence it becomes essential to separate 1-butanol from water, so as to lessen the effect of azeotrope formation.

It should be noted that a high concentration of 1-butanol inhibits the growth of microbes and bacterial cell in the fermentation broth. Hence a systematic removal of this compound is essential [3, 11]. Methods such as extraction, adsorption, pervaporation, gas striping and membrane separation have been conventionally used for the separation of 1-butanol during fermentation broth [3, 12–18]. Membrane separation and pervaporation are expensive due to its low mass transfer rates and requirement of low pressure. Adsorbents for butanol have low capacity which discourages its use in industrial or semi-industrial plant. On the other hand membrane reactors immobilizes the microorganisms, but in industrial scale the cell immobilized technique possess more disadvantages due to poor mechanical strength and an increase in mass

* Corresponding author.
E-mail address: tamalb@iitg.ernet.in (T. Banerjee).

https://doi.org/10.1016/j.molliq.2018.06.088
0167-7322/

I&EC research
Industrial & Engineering Chemistry Research

Article

Cite This: Ind. Eng. Chem. Res. 2018, 57, 3371−3381

pubs.acs.org/IECR

Liquid−Liquid Extraction of Lower Alcohols Using Menthol-Based Hydrophobic Deep Eutectic Solvent: Experiments and COSMO-SAC Predictions

Rupesh Verma and Tamal Banerjee*

Department of Chemical Engineering, Indian Institute of Technology Guwahati, Guwahati, Assam 781039, India

Supporting Information

ABSTRACT: The lower alcohols tend to form azeotropic solution with water which makes the separation challenging. The current work primarily focuses on the synthesis and application of a menthol-based hydrophobic deep eutectic solvent (DES) for the removal of lower alcohols from its aqueous solutions. The DES is synthesized by the addition of DL-menthol and lauric acid (dodecanoic acid) with a molar ratio of 2:1. Liquid−liquid equilibria (LLE) experiments are then performed to evaluate the performance of the synthesized DES for the extraction of lower alcohols such as ethanol, 1-propanol, and 1-butanol. LLE corresponding to the pseudo ternary systems of lower alcohols (1-butanol, ethanol, and 1-propanol) + hydrophobic DES + water are measured at T = 303.15 K and p = 1 atm. The composition of the tie lines were evaluated using ^{1}H NMR analysis for both extract and raffinate phases. Thereafter, the extraction efficiency of the DES is analyzed and compared by determining the solute distribution coefficients and the selectivity values. Finally, the experimental LLE data for the systems were regressed using the excess Gibbs free energy model, namely the Non Random Two Liquid (NRTL). Further the predictions of the tie lines were also confirmed through the COnductor like Screening MOdel Segment Activity Coefficients (COSMO-SAC) model. The average root-mean-square deviations (RMSD) obtained were 0.01 and 0.07 for NRTL and COSMO-SAC model, respectively.

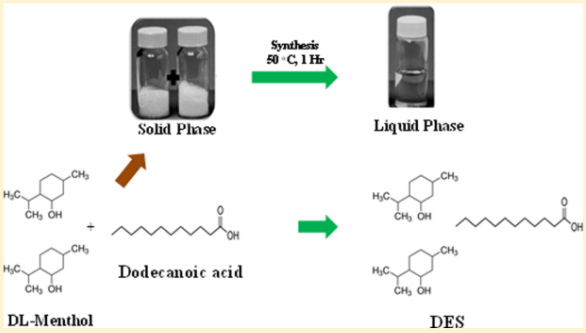

INTRODUCTION

The demand for energy is increasing proportionally with the current population. In such a scenario, energy generation is the key to sustain such a fast pace development. Currently fossil fuel replenishes nearly 80% of the energy demand globally. Hence, there is a dire need to explore alternate energy sources in order to lessen the dependency on the nonrenewable fossil fuel which are limited.[1−4] Lower alcohols are considered a potential replacement for conventional fuels. Lower alcohols such as ethanol, 1-propanol, and 1-butanol are vital and are potential renewable energy sources. 1-Butanol has higher calorific value, higher hydrophobicity, and lesser flammability than other alcohol fuels.[5] Qureshi et al.[4,6] described that 1-butanol with a lower vapor pressure and higher flash point is less corrosive. Lower alcohols have also shown properties similar to gasoline. Lower alcohols hence can be used as a renewable biofuel with little or no modification to the engine. One of the sources of lower alcohols is the acetone-butanol-ethanol (ABE) fermentation where alcohols exist as an azeotrope having a water-rich phase. Hence its extraction from aqueous phase is essential.

In the chemical process, industrial separation of azeotropic mixtures is of great importance. Methods such as extraction, adsorption, pervaporation, gas stripping, and membrane separation have been used conventionally for separation of lower alcohols from the fermentation broth. Membrane separation and pervaporation are expensive due to low mass transfer rates and requirement of low pressure.[1,7−10] Typically, removal of lower alcohols from fermentation broth by adsorption from the liquid phase can only be used in laboratory scale due to the small-capacity of adsorbents. The other option for removal of lower alcohols can be used, such as membrane reactors where the immobilization of microorganisms occurs in the membrane. On industrial scale, cell immobilized technique gives more disadvantages due to poor mechanical strength and an increase in mass transfer resistance.[2]

One normally switches to liquid−liquid extraction when component separation (from a mixture of many components) cannot be achieved economically by other mass transfer operations such as distillation, evaporation, and crystallization. Azeotropic distillation, extractive distillation, and liquid−liquid extraction, which are three of the most important industrial separation techniques for azeotrope breaking, involve the use of an extracting agent. In such a scenario, solvent extraction is a suitable operation particularly when the solvents possess

Received: December 21, 2017
Revised: February 6, 2018
Accepted: February 12, 2018
Published: February 12, 2018

DOI: 10.1021/acs.iecr.7b05270
Ind. Eng. Chem. Res. 2018, 57, 3371−3381

Fluid Phase Equilibria 462 (2018) 73–84

Contents lists available at ScienceDirect

Fluid Phase Equilibria

journal homepage: www.elsevier.com/locate/fluid

Liquid-liquid equilibria and COSMO-SAC modeling of organic solvent/ionic liquid - hydroxyacetone - water mixtures

Anand Bharti [a], Rupesh Verma [a], Prerna [b], Sarvesh Namdeo [a], Abhigyan Malviya [a], Tamal Banerjee [a, *], Stanley I. Sandler [c]

[a] Department of Chemical Engineering, Indian Institute of Technology Guwahati, Guwahati, Assam 781039, India
[b] Department of Chemical Engineering, Birla Institute of Technology, Mesra, Ranchi, Jharkhand 835215, India
[c] Department of Chemical and Biomolecular Engineering, University of Delaware, Newark DE 19716, USA

ARTICLE INFO

Article history:
Received 21 June 2017
Received in revised form
12 January 2018
Accepted 23 January 2018
Available online 2 February 2018

Keywords:
Hydroxyacetone
Ionic liquid
Organic solvent
LLE
COSMO-SAC

ABSTRACT

In this work conventional organic solvents (ethyl acetate, *n*-propyl acetate, *n*-butyl acetate, chloroform) as well as ionic liquids, 1-ethyl-3-methylimidazolium bis(trifluoromethylsulfonyl)imide ([EMIM][Tf_2N]) and 1-butyl-3-methylimidazolium bis(trifluoromethylsulfonyl)imide ([BMIM][Tf_2N]), were investigated for the extraction of hydroxyacetone from aqueous solution. The liquid–liquid equilibrium (LLE) data for the ternary systems were experimentally determined at $T = 298.15$ K and atmospheric pressure. In terms of the distribution coefficient and selectivity, [EMIM][Tf_2N] and [BMIM][Tf_2N] were found to be the most effective solvents for the extraction of hydroxyacetone from aqueous solution, and the composition of ionic liquids in the raffinate phase was found to be negligible. The experimental results were correlated with the NRTL and UNIQUAC models. The root mean square deviations (RMSD) obtained between the NRTL and UNIQUAC correlations for all the systems were in the range of 0.19–5.18%. COSMO-SAC was then used to make a first principles prediction of the phase equilibria of the systems studied. For the organic solvent-based systems, the deviations between predicted and experimental values were in the range of 3.49–8.00% (% RMSD) whereas for the ionic liquid systems, the deviations were in the range of 16.81–18.53%.

1. Introduction

The changing global climate and the depletion of fossil resources are major issues for the current generation. Consequently, the development of alternative renewable energy resources has been intensely promoted. Compared to other renewable energy sources, biomass has the potential to replace a large fraction of fossil fuels as feedstocks and thus capable of meeting the energy, chemicals and materials requirement of mankind. Biorefineries are manufacturing facilities that produce biofuels and biochemicals from various biomass feedstocks. Conceptually, this is analogous to current petroleum refinery that produces fuels and chemicals from crude oil [1–8].

In order to convert biomass into valuable products within a biorefinery, several processes are needed. These can be divided into four groups: physical, biochemical, thermo-chemical and chemical processes. Among them, fast pyrolysis is a thermo-chemical process for the production of liquid fuel and chemicals from biomass. Bio-oil is the main product of fast pyrolysis and depending on the biomass source, the oxygen content will be in the range of 35–40 wt% due to several oxygen-containing components (acetic acid: 0.5–12 wt%, glycolaldehyde: 0.9–13 wt%, hydroxyacetone: 0.7–7.4 wt %, and furfural alcohol:0.1–5.2 wt %). A higher oxygen content is responsible for a lower heating value of bio-oil. However, the high concentration of oxygen-containing compounds makes bio-oil a good raw material for the production of various chemicals [3,9–16].

The first step in the recovery of chemicals from bio-oil usually involves fractionation using water that results in two fractions-an aqueous top phase enriched in carbohydrate-derived chemicals (acetic acid, glycolaldehyde, hydroxyacetone) and an organic bottom phase containing lignin-containing fractions. Both phases can be processed separately to extract the valuable chemicals. Several studies have been reported for the extraction of bio-oil chemicals including acetic acid [17,18], levoglucosan [19], sugar/sugar

* Corresponding author.
E-mail address: tamalb@iitg.ernet.in (T. Banerjee).

https://doi.org/10.1016/j.fluid.2018.01.026
0378-3812/